LOCAL PRESSURES IN THE HUMAN HIP JOINT IN VIVO, CORRELATED WITH MOTION KINEMATICS AND EXTERNAL FORCES

by

KJIRSTE LYNN CARLSON
B.S. Mech. Eng., Massachusetts Institute of Technology
(1984)

SUBMITTED TO THE DEPARTMENT OF
MECHANICAL ENGINEERING
IN PARTIAL FULFILLMENT OF THE REQUIREMENTS
FOR THE DEGREE OF

MASTER OF SCIENCE IN MECHANICAL ENGINEERING

at the

MASSACHUSETTS INSTITUTE OF TECHNOLOGY
December 13, 1985

© Massachusetts Institute of Technology 1985

Signature of Author _____
Department of Mechanical Engineering
December 13, 1985

Certified by _____
Robert W. Mann, Sc. D.
Thesis Supervisor

Accepted by _____
Chairman, Departmental Commitee on Graduate Studies

Archives
MASSACHUSETTS INSTITUTE OF TECHNOLOGY
APR 28 1986
LIBRARIES

LOCAL PRESSURES IN THE HUMAN HIP JOINT IN VIVO, CORRELATED WITH MOTION KINEMATICS AND EXTERNAL FORCES

by

KJIRSTE LYNN CARLSON

Submitted to the Department of Mechanical Engineering on December 13, 1985 in partial fulfillment of the requirements for the Degree of Master of Science in Mechanical Engineering

ABSTRACT

Local pressures at 10 sites in a human hip joint have been measured and evaluated in vivo. Data were obtained at a frame-rate of 254 hz. from an instrumented endoprosthesis implanted in a 73-year-old woman. Concurrently, movement kinematics of the relevant body segments and foot-floor external forces were recorded. These results were compared to in vivo and in vitro data and estimates published by other investigators. Pressures and rates of loading in vivo present profiles similar to the external force characteristics; differences occurred in the relative magnitude and timing of pressure and force peaks. Muscle forces acting across the hip, including co-contraction, have a significant role in determining local pressures in the joint. The greatest in vivo pressure observed was 18 M-Pa which occurred 1 year post-implantation while the subject was rising from a chair.

Thesis Supervisor: Robert W. Mann, Sc. D.
Title: Whitaker Professor of Biomedical Engineering
Department of Mechanical Engineering

Acknowledgements

As is usually the case in research, this thesis would have been impossible to complete without the contributions made by many other people. I am particularly indebted to Professor R. W. Mann, my thesis supervisor, for trusting me to work on this project.[*] His perception in the guidance of research and the continuity he fosters in work on biomechanics at M.I.T. are remarkable.

My gratitude to Dr. Andrew Hodge at M.G.H. for his time and effort and for a medical perspective of this work. Others connected to the Biomotion lab at M.G.H., in particular Dr. W.H. Harris, also had much influence on the direction of this investigation. The facilities at the M.G.H. Gait Lab have been used extensively for data acquisition, processing, and display.

The hip project at M.I.T. has a long history; many people no longer at M.I.T. did the important early work which I was fortunate to inherit. In particular, Bob Fijan did much work on the in vivo hip project, both prior to my arrival and during his year at M.G.H., and was very helpful throughout my work.

Special thanks to Liz Brodbine for putting up with my harried schedule changes and for the effort she puts into keeping the lab afloat.

I am grateful to everyone in the M.I.T. biomechanics lab.; the camaraderie in the lab makes it more than an office or place to work. I was surprised by how much I enjoyed being a graduate student; the friendship, support, and assistance of folks in the lab made an enormous difference.

The care of friends both in outside of M.I.T. was greatly appreciated. I particularly thank those who fed me and kept me going through the final traumatic stages of this project. Sometimes the best thing to do is take a break; Amy, thanks for saving me from "terminal" illness.

Finally, my gratitude to my two best teachers is immeasureable. Thank you, Mom and Dad, for your encouragement in all my endeavors. I love you both very much.

---

[*] This research was funded through a subcontract from the National Institute of Handicapped Research - Department of Education.

Table of Contents

I. Introduction

The focus of this thesis is the distribution and variation of pressures found in life in the human hip joint. As such, it is a part of the effort to apply principles of physical science and engineering to the human body. Medical knowledge benefits greatly from advances in understanding of the mechanical, chemical and electrical forces at work in living tissue. However, progress is slow in this area and high-quality data is scarce. The results presented in this thesis are unique; completely new information gathered from a living human being without risk or discomfort to that person. These data have been compared with in vitro and in vivo information on hip joint characteristics obtained by other means. The mechanics of synovial joint function are further illuminated through consideration of these results.

The in vivo hip data acquired at the Massachusetts General Hospital (M.G.H.) and Massachusetts Institute of Technology (M.I.T.) movement facilities and presented here consists of 10 local pressure readings in the hip joint, spatial locations and orientations of three leg segments and the pelvis, and foot-floor interaction forces. Other information - body segment velocity, rate of pressure change, position of the transducers in the hip joint - can be derived from this set of measurements.

The pressure distribution in the acetabulum provides information on areas of the joint cartilage which experience the most severe load conditions and areas not involved in load transmission. The magnitude and rate of loading, as well as the cartilage surface location of highly-loaded areas,

can help define the type of loading regime that cartilage experiences and thus guide the direction of future research. Knowledge of the speed of load application and the change of pressures with time should benefit comprehension of joint lubrication studies [81].

Pressure information may eventually contribute to establishing the magnitude and direction of the force vector at the hip with higher confidence. Greater accuracy in this calculation will be permitted through inclusion of forces across the joint due to muscular contraction and co-contraction. The distribution of pressures and timing of changes relative to related foot-floor interaction forces gives an indication of the importance of muscle forces in determining the loading environment of the hip. This data may illuminate endoprosthesis failure mechanisms, especially protrusion through the acetabulum.

In vivo pressure data may provide a basis for evaluation of rehabilitation procedures. The information gathered from the in vivo prosthesis will also be useful in evaluating joint model simulators.

These areas of study are part of the general accumulation of knowledge about joint mechanics. This information is needed for a more complete understanding of the manner in which the parts of the joint function and the development of a mathmatical model of the hip joint [37]. Advancement in understanding of the forces the hip experiences may enhance prosthesis design and hip replacement functional requirements [78]. Furthermore, the initiating events leading to mechanical failure of the natural hip joint and other hip joints may be clarified [81].

A. Outline of Work

The equipment used to obtain data was designed and built through earlier work by many others in the Eric P. and Evelyn E. Laboratory for Biomechanics and Human Rehabilitation at the Massachusetts Institute of Technology. Information about previous work may be found in the background section of this paper and in references.

In June 1984 a femoral head replacement developed at MIT was implanted in a 73- year-old woman who had sustained a displaced fracture of the right femoral neck. The prosthesis design replicates the function of an Austin-type prosthesis (Figure I-1 from [21]). The structure includes 14 pressure transducers, each in a well which was machined into the inner wall of the prosthesis head. This integrates a pressure-sensitive diaphragm into the spherical prosthetic femoral head surface [21]. Diaphragm deflection is used to bend cantilever beams equipped with strain gages. The electronic circuitry in the femoral head is connected to an antenna on the distal end of the prosthesis (Figure I-2). Output from the transducers is transmitted through this antenna via radio-telemetry in the FM mega-cycle frequency spectrum; power is supplied also through radio-frequency (100 KHz) coupling through a primary coil that fits like a garter onto the subject's leg. The same garter-coil accepts the pulse-amplitude modulated FM signal from the 14 transducers at a frame rate of 254 Hertz. Without this garter attachment the instrumented prosthesis is virtually indistinguishable from the standard prosthesis.

Data was gathered from the prosthesis during the two weeks immediately

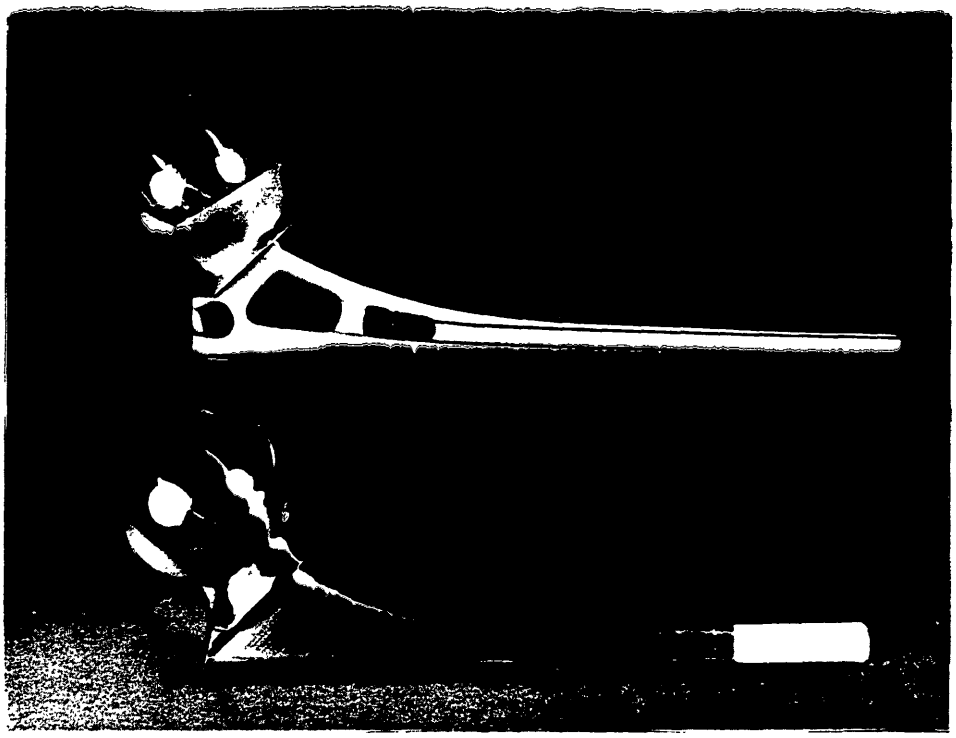

Figure I-1: Standard and Instrumented Prostheses

From Carlson [2]

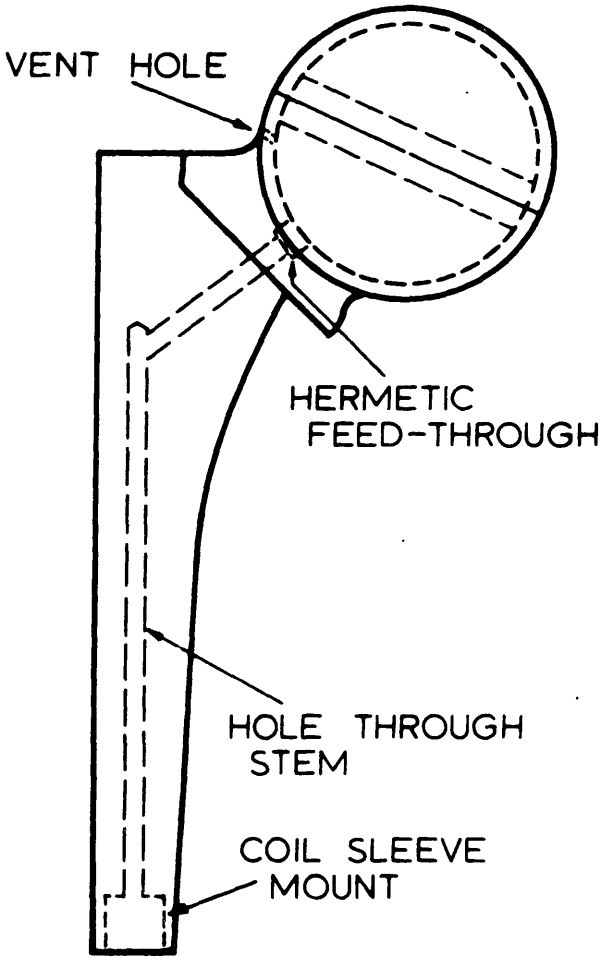

SIDE VIEW OF MODIFIED PROSTHESIS
(POWER INDUCTION COIL NOT SHOWN).

Figure I-2

From [21].

after implantation in June 1984, and in December 1984, May, June, August, and September 1985. Reception of pressure signals was normal at the most recent data collection session and data will be obtained in the future.

The performance of the transducers was evaluated at body temperature prior to implantation. The readings from 10 transducers displayed a linear relationship with applied pressure [31] (Figure I-3). The other 4 transducers were essentially unresponsive to increases in pressure on the order of physiological forces. After implantation the linearly behaving transducers were re-calibrated periodically by unloading the joint; traction was applied to the subject's leg to remove the prosthetic femoral head from contact with the acetabulum.

Transducer readings were converted to pressure values, then related to simultaneously acquired kinematic and forceplate data through software [3]. The ability to acquire at high speed the 3-D positions and rotations of the leg and pelvis body segments allowed transformation of transducer pressures from positions on the femoral head to the corresponding instantaneous acetabulum locations (Figure I-4). A set of programs was developed to permit manipulation and display of the prosthesis data. Among the available options are:

1. Display of pressure vs. time;

2. Frequency analysis of pressure data;

3. Filtering of pressure data;

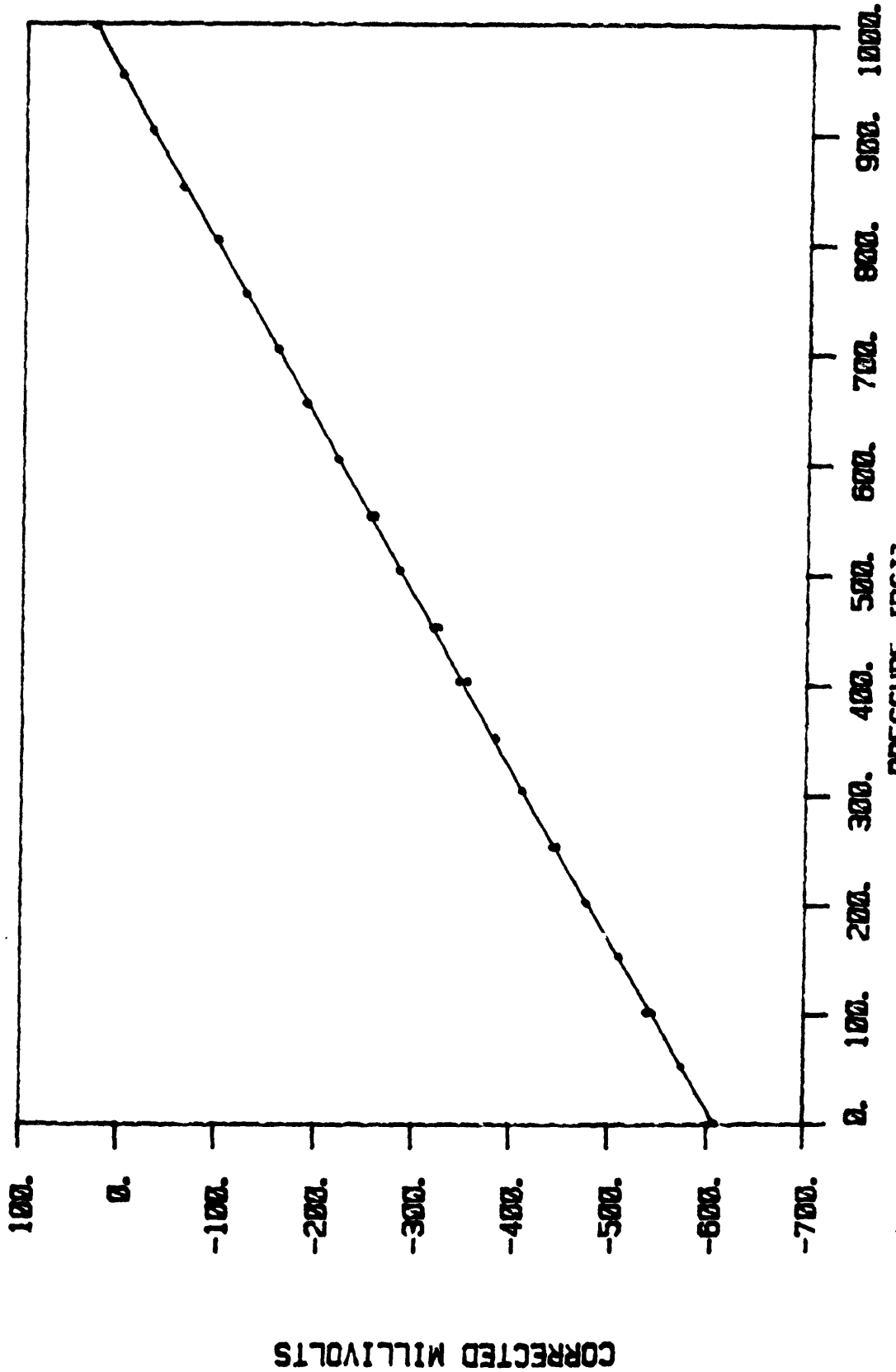

Figure I-3: Calibration Measurements, transducer 5
From [31]

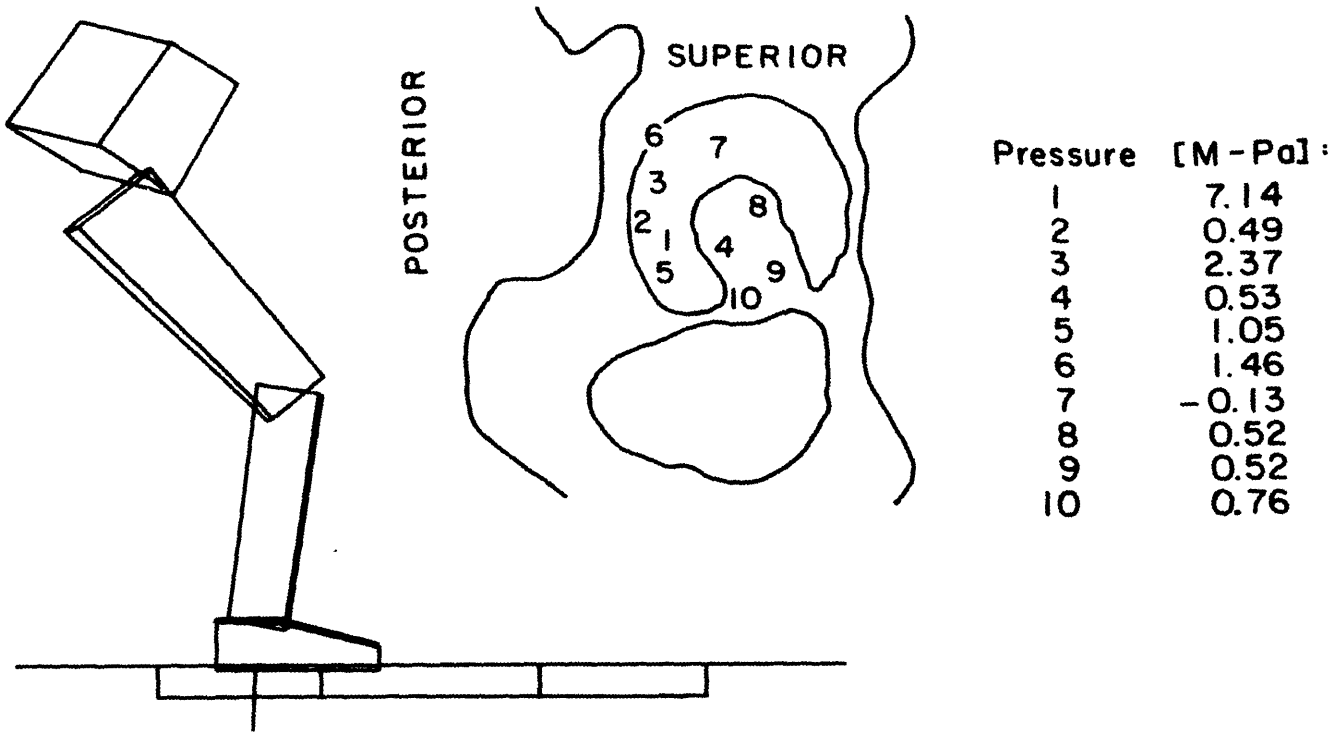

Figure I-4: Display of leg segment positions and of pressure locations in the acetabulum. Kinematic display developed by Bob Fijan and Pete Loan at MIT and MGH.

From [108].

4. Display of pressures at acetabulum locations (3-D or 2-D projection);

5. Display of transducer path over the acetabulum;

6. Display of forceplate data vs. time;

7. Concurrent display of pressure and forceplate data;

8. Numerical differentiation and double differentiation of the pressure data with repect to time and display of the results;

9. Assessment of pressure load rate and external force rate of increase.

Transducer histories have been compiled to allow assessment of transducer performance over the range of test dates. The issue of reproducibility of data has been approached through comparison over several tests of transducer readings for a single dynamic loading situation. A gait cycle was chosen as the most readily obtained, frequently examined, and representative test. Some transducers are in inappropriate locations during a gait cycle and have been evaluated in various other loading conditions. After normalization with respect to time the pressure vs. time and force vs. time data were superimposed. Visually, data presents very similar profiles for all gait cycles, with some variance from sample to sample.

B. Overview of Results

The data obtained is rich in information, only some of which has been extracted thus far. The maximum pressure found at the hip joint after filtering was 18 M-Pa. This occurred in May 1985, 11 months after implantation of the prosthesis, while the subject rose from a chair. Maximum pressures from filtered gait cycle data ranged from 5 to 6 M-Pa after the subject's recovery and were located in the dome of the acetabulum at 30 percent of the stance phase. The maximum load rates of change at the hip were produced in sitting-to-standing tests and the greatest observed was 107 M-Pa/sec while the subject rose from a seated position 45 cm above the floor.

Pressure contours and force vectors proved difficult to establish accurately using few simultaneous data points; further investigation may prove fruitful.

Of the 10 working transducers, 6 consistently produced reproducible and meaningful results. The outer ring of transducers was less often subjected to significant loads and more frequently was rotated out of contact with the acetabular cartilage and thus provides less valuable data about cartilage behavior. The location of tranducers on the femoral head surface of future instrumented prostheses should be reexamined.

The in vivo results confirm some prior findings; in other ways they are surprising. The irregular pressure contours observed by Rushfeldt in earlier in vitro tests were apparent for in vivo data. The pressures found

at discrete locations in the joint were high in comparison to previous estimates and also higher than local pressures found in in vitro studies [78,86,89,90]. The rate of loading at the hip joint seemed surprisingly high in some cases. Others have ventured [78] that the femoral load rate might be 47 kN/sec during gait. Pressure rates of change that could indicate changes of joint force of similar magnitude were observed after full recovery of the subject. Comparison of the information from the instrumented prosthesis with simultaneous forceplate data points out the importance of the role of muscles acting across the hip in movement.

II. Background

A. Hip Joint anatomy

1. Structure and purpose

A major synovial joint, in size as well as function, the hip must satisfy many requirements. Stability at the interface between trunk and leg is necessary for upright stance, but mobility at the hip is also needed to provide adequate range of motion of the lower limbs. Much of the body weight is borne across the hip joint, particularly when only one leg is in contact with the ground as during the stance phase of gait. The deep ball and socket arrangement of the joint is very stable and, unlike the knee and ankle, allows a wide range of rotational motions. The structure of the hip joint is shown in Figure II-1.

The distal portion of the joint is the femoral head, a cartilage- covered ball, nearly spherical in shape. Estimates of the deviation from sphericity of the femoral head range from 200 μm [100] to 1.4 mm [23,24]. The neck connecting the femoral head to the upper part of the femur is narrower than the head, minimizing restiction of rotation of the ball in the acetabular socket.

The socket is a cup formed by the three components of the innominate bone, the ilium, ishium, and pubis and is termed the acetabulum. The shape of the socket is less spherical than that of the femoral head [19,86], but may

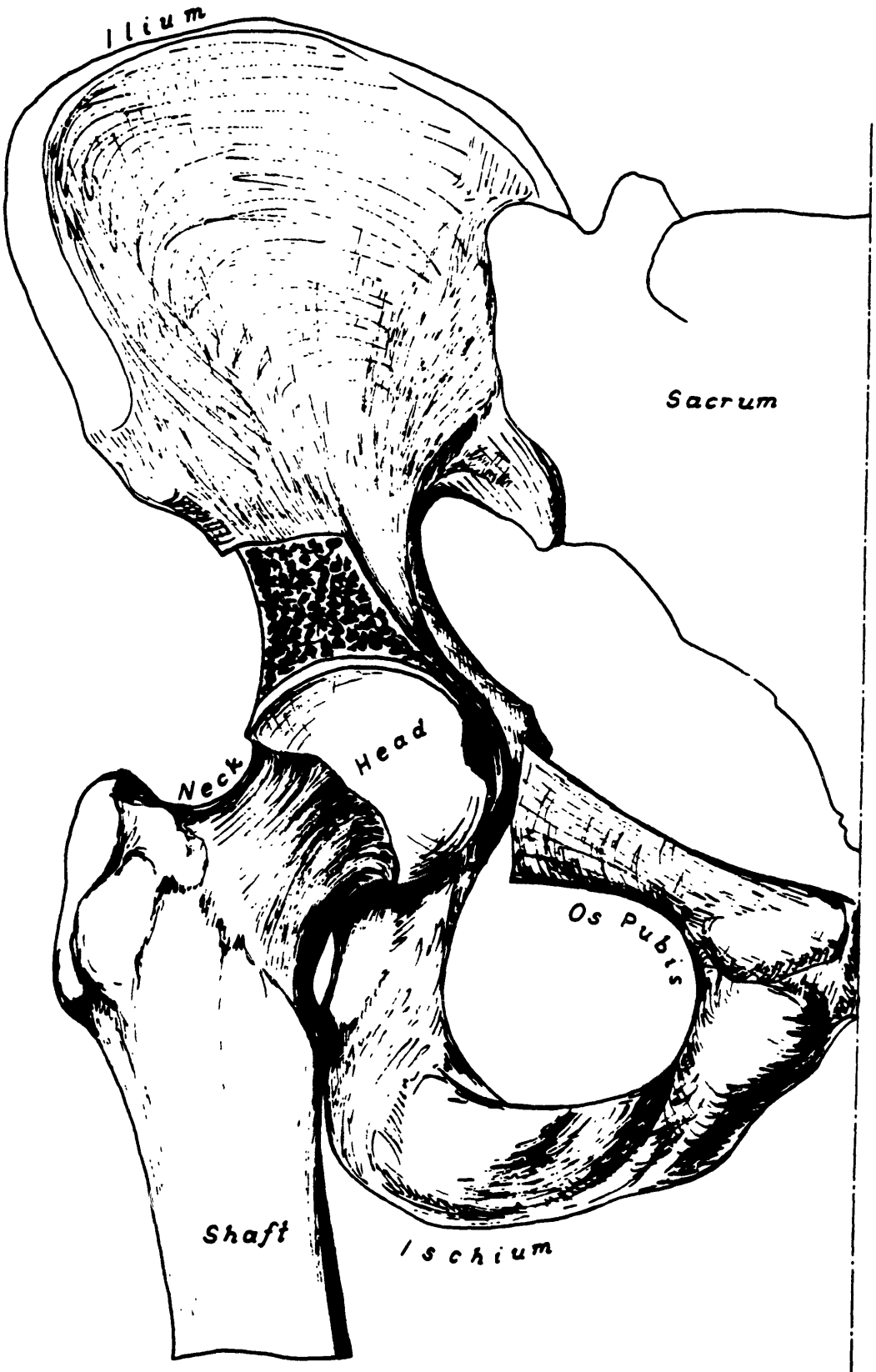

Figure II-1: Hip Joint - Frontal plane

become more nearly spherical with age and load [40,41]. The bony parts of both sides of the joint are primarily covered with articular cartilage. The cartilage in the acetabulum forms a horseshoe shape, the central and inferior region covered with fat pads and synovial membrane (Figure II-2). A central region on the femur is also free of cartilage; the ligamentum teres femoris attaches in this location. A rim of cartilage, the labrum, deepens the acetabular cavity and encloses the femoral head more completely.

The joint is sheathed in the synovial membrane which retains fluid in the joint, outside of it is the articular capsule formed of ligaments and collagenous fibers.

2. Musculature and Motions

There are a number of muscles acting across the hip. Posterior to the joint is the gluteal maximus muscle; this is the chief extensor and lateral rotator. Under the gluteus maximus are several small lateral rotator muscles. Laterally on the ilium are the powerful hip abductor muscles, gluteus medius and minimus which also act in medial rotation. On the thigh are the hamstring flexor muscles which act in extension and rotation of the thigh. The anterior portion of the thigh is the location of several large muscles; of these the sartorius, rectus, femoris, and iliopsoias flex the hip and the iliopsoias also acts in medial rotation. The three adductor muscles on the medial region of the thigh act in both adduction and lateral rotation of the hip.

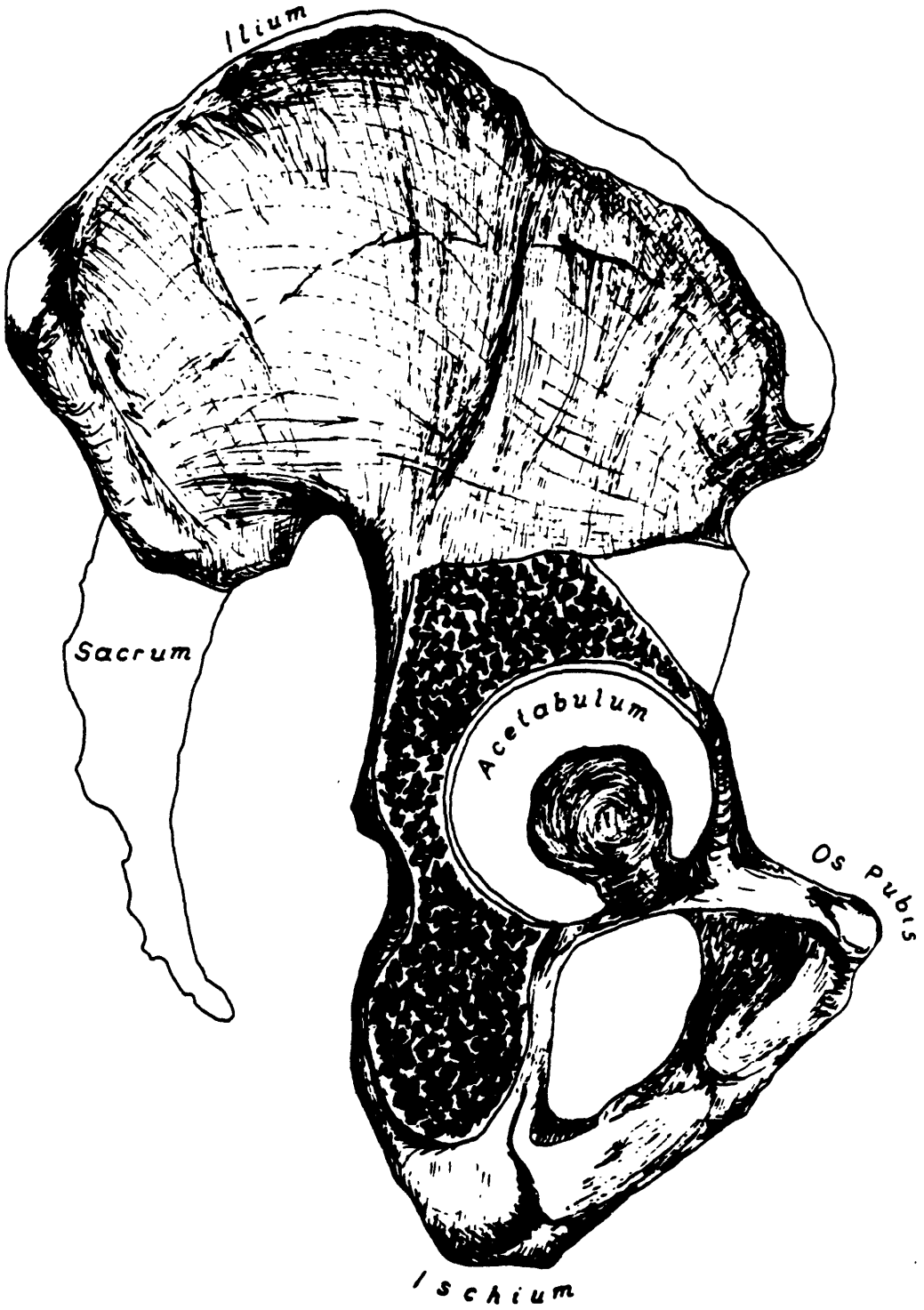

Figure II-2: Acetabulum - Side view

Average ranges of motion for the hip are 120 degrees in flexion (raising the thigh with respect to the body), 30 degrees in adduction, 50 degrees in abduction, and about 30 degrees for internal and external rotation. Figure II-3 illustrates the definitions of hip motions.

3. Cartilage

Articular, hyaline, cartilage is a poroelastic material that covers all joint surfaces participating in articulation. Its structure consists of an extracellular matrix formed of collagen fibers, and a carbohydrate-protein-water substrate, apparently formed and upkept by a small number of chondrocytes unevenly distributed in the cartilage [7,74]. It is thought that the chondrocytes may be responsible for the degradation of cartilage as well as its formation [64]. The mechanical properties of the joint are dictated by the matrix and subchondral structure of the joint. Lubrication appears to be influenced by the matrix as well, and by the fit of opposing joint surfaces.

There are four zones in articular cartilage, distinguished by depth from the articulating surface (Figure II-4). The relative amounts of chondrocyte and matrix components and the orientation of collagen fibers vary between zones. Under the joint surface is a region containing tightly packed collagen fibers parallel to the surface. Deeper zones consist of randomly distributed fibers and more chondrocyte cells. The deepest region contains large collagen fibers oriented perpendicular to the articular surface. There are fewer chondrocytes in this area.

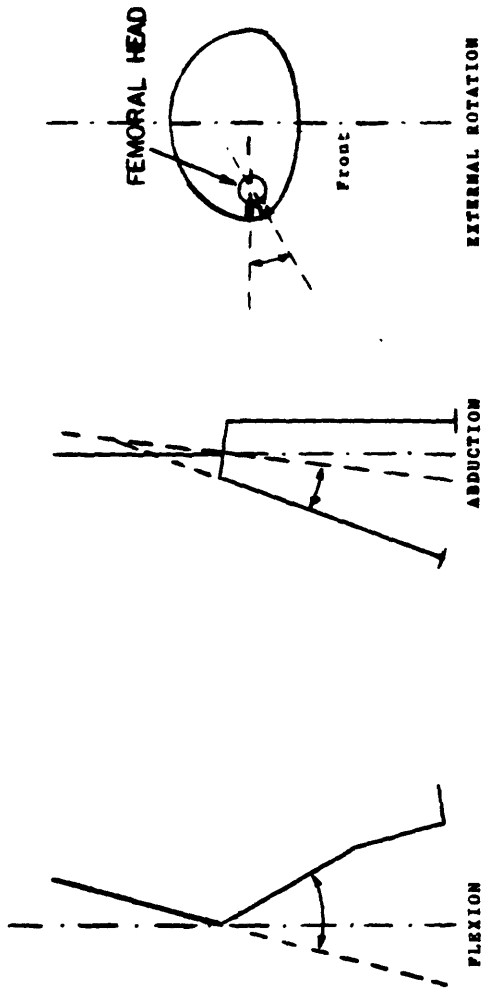

Figure IX-3: Definition of hip joint angles

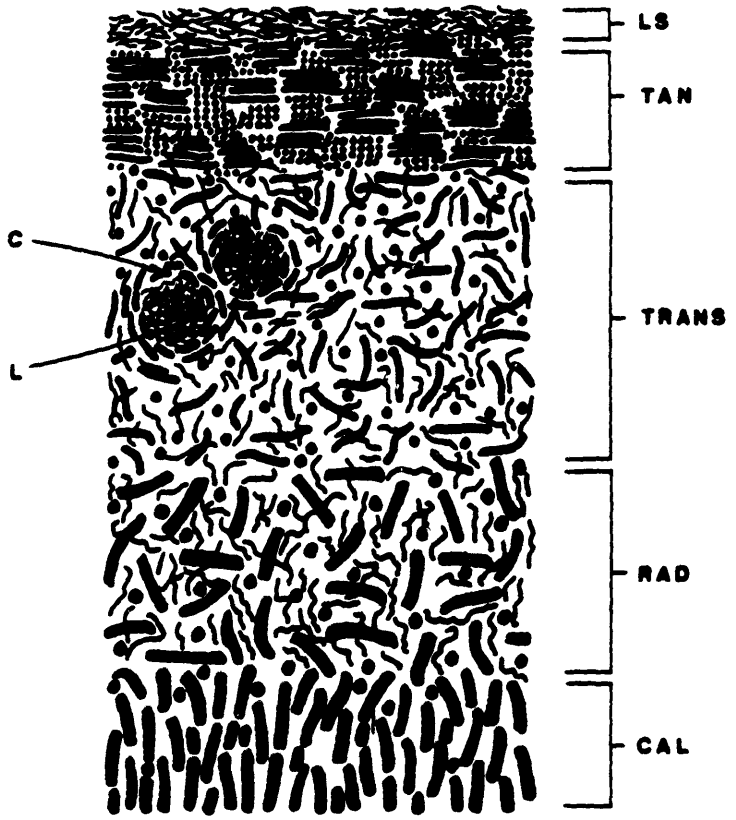

Figure II-4 FIBROUS ARCHITECTURE OF ADULT ARTICULAR CARTILAGE

From Halcomb [44]

The fluid content of articular cartilage is important in maintenance of its excellent lubricating properties. Tests performed by Linn [61] on cartilage allowed to dry out and then re-immersed exhibited a coefficient of friction for a plug of cartilage that was 200 times higher for dry cartilage than wet.

a. Properties of Articular Cartilage; The mechanical properties of cartilage have been studied extensively in vitro, primarily through the use of segments of cartilage removed from the joint. In vivo tests are rarely possible, but in vivo properties are likely to be different from those determined in vitro due to interaction between all components of the joint. In cartilage itself, the extracellular matrix has a dominant effect on cartilage mechanical properties. Fluid flow through cartilage is determined mostly by the proteoglycan gel. Compressive behavior of cartilage depends on both the fibers and the proteoglycan-water mix. The collagen fiber matrix establishes the cartilage tensile strength and maintains the basic structure.

Flow of synovial fluid is accomplished by deformation of tissue or by hydraulic pressure gradients [60,71]. The motion of water through cartilage is influenced by frictional interactions with both collagen and proteoglycan molecules [67]. Cartilage is most permeable slightly below the articulating surface and decreases in permeability with depth. When a compressive load is applied to cartilage the fluid flows from the loaded to the unloaded regions. Consolidation of cartilage occurs if the load is maintained [86]. Loading starts fluid flow across the surface of the joint, and through cartilage in a direction parallel to the articulating

surface. Radial flow equilibrium appears to be dominated by high resistance at the articular surface layer [58,63]. However, radial flow may also occur, and it has been shown that under high pressures cartilage "weeps" fluid into the joint space [67]. McCutchen and Maroudas [67] have proposed that the permeability in the radial direction is essentially the same as that in the tangential direction at a given depth in the tissue.

Compression characteristics of cartilage have been studied through indentation tests [56,57]. It has been found that cartilage exhibits two time-differentiated behaviors in compression. An initial, "instantaneous", elastic deformation is followed by a creep response. Upon load removal, recovery also consists of elastic and time-dependant phases. This result was also established by Rushfeldt [86] in consolidation tests carried out over a 20 min. time period with human acetabula and a prosthesis in a hip simulator.

In tension, the stiffness and fracture stress of cartilage are dependant on the relationship between collagen fiber orientation and the direction of tension. The tensile elastic modulus and fracture stress decreases with depth into cartilage, and with age [5]. The fracture strength of cartilage is dependant on collagen content as well as orientation [57].

Fatigue behavior of cartilage has been investigated by Weightman [110] and was found to vary widely; the general pattern of behavior was typical of other materials, fatigue stress to failure decreases with increased numbers of loading cycles.

b. Functions; The primary purposes of articular cartilage are to distribute load in the joint and act as a low-friction bearing surface. Both funtions are related to the pressure magnitude and gradient obtained at the articulating surface.

Estimation of the contribution of joint constituents in carrying load in the joint has found that fluid pressure supports 90 percent of the load [63]. Stress in the cartilage matrix found from models based on experimentally-determined joint parameters did not exceed 0.3 M-Pa [63]. Rushfeldt [88,86] and Tepic et al [100] have found that boney surface irregularities affect the pressure gradients formed at the joint. The distribution of pressure in the joint is very sensitive to the direction of the load vector relative to the acetabular cartilage as well [63]. The pressure distribution indicates which portions of the joint are involved in load transmission for a particular motion.

As a bearing, articular cartilage performs better than most man-made substances. Charnley [25] found the coefficient of friction in normal joints to be on the order of .005 to .023. In comparison, Teflon™ on Teflon™ exhibits a coefficient of friction of .04. The reasons behind this phenomenal ability of cartilage have been the source of much academic discussion. Several theories of joint lubrication mechanisms have been proposed. The pressure distribution, magnitude, and gradient should illuminate the lubrication processes active in the joint for a given load and action. The lubrication mechanisms that exist under low pressures may be different from those in high pressure regions.

Discussion of lubrication possibilities centers around the thickness and means of maintenance of the fluid film between the articulating surfaces. If the film is extremely thin, pure fluid lubrication will not occur, boundary lubrication, in which each bearing surface is coated with molecules which slide rather than shear off the substrate, may occur (Figure II-5 from [82]). A thicker film would allow one or more pure fluid lubrication modes. Squeeze film lubrication may occur as joint surfaces approach and generate a pressure field in fluid trapped by surface irregularities. Hydrodynamic lubrication, in which relative motion of the surfaces permits formation of a wedge of fluid that keeps the surfaces separated, has been suggested [69]. Elastohydrodynamic lubrication is similar to the hydrodynamic mode, but notes that the elasticity of joint surfaces allows asperities to be depressed and remain out of contact [98]. Any of these mechanisms may have a place in joint motion. More complexity is introduced in the question of the direction of flow of fluid in the joint. Noting that cartilage exudes fluid from surface pores under pressure, McCutchen [70] has suggested a type of hydrostatic "weeping" lubrication in which fluid is squeezed from cartilage into the joint space (Figure II-6). Alternatively, Longfield,Dowson, Walker and Wright [62] have put forth an idea calling for fluid flow out of the contact region through these same cartilage pores. This mechanism relies on pore size restricting the flow of larger solute molecules from the contact region, supposedly concentrating the lubricating factor in synovial fluid in the region of contact (Figure II-7).

Boundary lubrication may occur with the presence of a gycoprotein component of the joint fluid which binds to the cartilage surface and resists

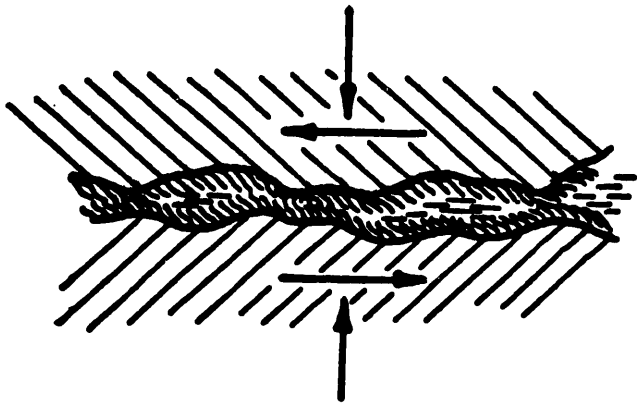

Figure II-5: Boundary lubrication
Figure from Radin et al [71]

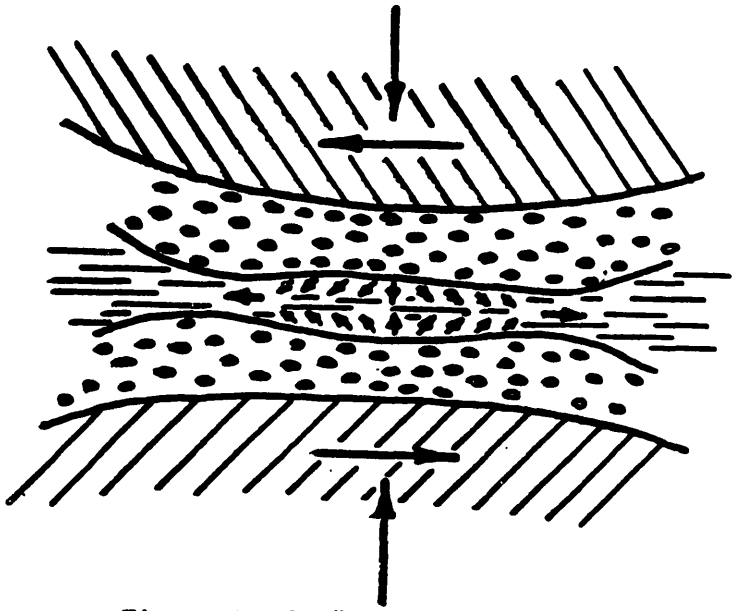

Figure II-6: "Weeping" lubrication
Figure from Radin et al [71]

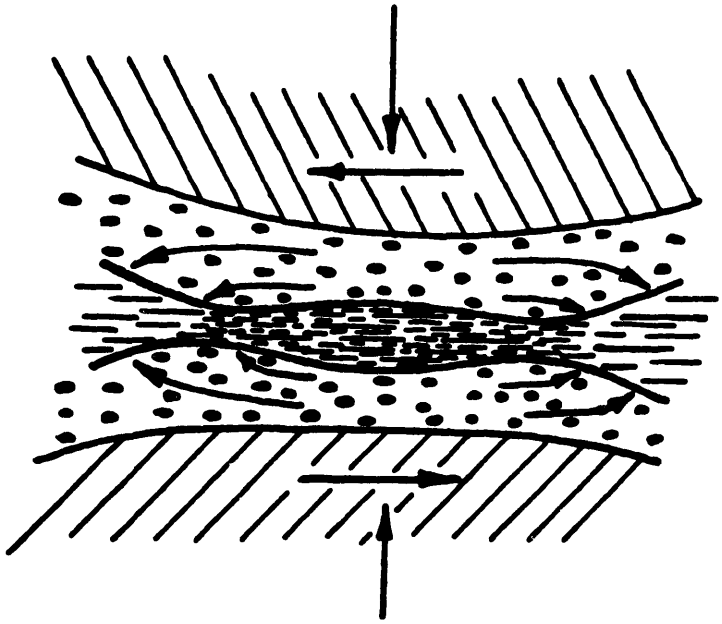

Figure II-7: "Boosted" lubrication
Figure from Radin et al [71]

shearing [61]. It has been shown that the coefficient of friction of cartilage increases more if these molecules are destroyed than if other synovial fluid constituents are missing [80]. At low pressures the behavior of cartilage and this glycoprotein suggests that boundary lubrication does take place.

At high pressures the lubrication is probably a squeeze film type. This may occur with cartilage fluid expression on the edges of the contact area, where pressures are lower and fluid is more likely to flow. This effect may be assisted by cartilage elasticity, which may provide some degree of elastohydrodynamic lubrication as well.

4. Osteoarthritis

Osteoarthritis is a "non-inflammatory disorder of moveable joints characterized by deterioration and abrasion of articular cartilage" [97]. The degradation of cartilage may lead to pain and severe restriction of mobility. The causes of osteoarthritis are not fully understood. Abnormal hip structure, metabolic problems, trauma, and bone infarcation all may lead to destruction of articular cartilage [36]. Osteoarthritis often arises in joints apparently free of the above factors; in these cases the cause is unknown. A view held by many is that:

"Wear and tear or repetitive trauma is frequently to be held responsible for the degenerative breakdown of articular cartilage. However, no direct evidence has yet been put forward to implicate local stress of this type." [38]

Studies exist which appear to indicate that the joint areas not frequently loaded are most likely to undergo osteoarthritic changes [20].

B. Prosthesis Development

The implanted prosthesis was manufactured in 1980. This device was similar to the prototype designed by Carlson at the MIT Biomechanics Laboratory [21,22]. The original design was altered slightly, after tests under high pressure indicated that the structural integrity of the prosthesis head material, specifically in the diaphragm area, was insufficient for in vivo use. Essential information on the prosthesis will be included here, refer to Carlson [21] for more detailed information.

Major issues in the design of the instrumented prosthesis were 1) Subject safety; 2) Performance characteristics identical or better than normal prostheses; 3) High data accuracy; 4)Adequately high frequency response to capture temporal frequencies occurring during motion; 5) Absence of patient encumberment during data acquisition; 6)Sufficiently high number of pressure data points in the joint; 7) Prosthesis data-taking ability for more than two years. Not all of these need apply to in vitro testing, however, human implantation of the prosthesis was a goal of this project from the initial stages onward.

A block diagram of the prosthesis/data system established to meet these requirements is presented in Figure II-9. The physical prosthesis design is shown in Figure II-10. This instrument is similar in structure to an Austin-Moore prosthesis. (Figure II-1). However, the instrumented prosthesis includes 14 pressure transducers located in the upper medial region of the prosthesis head. These transducers are powered and read through a radio-telemetry system contained in the prosthesis. External to

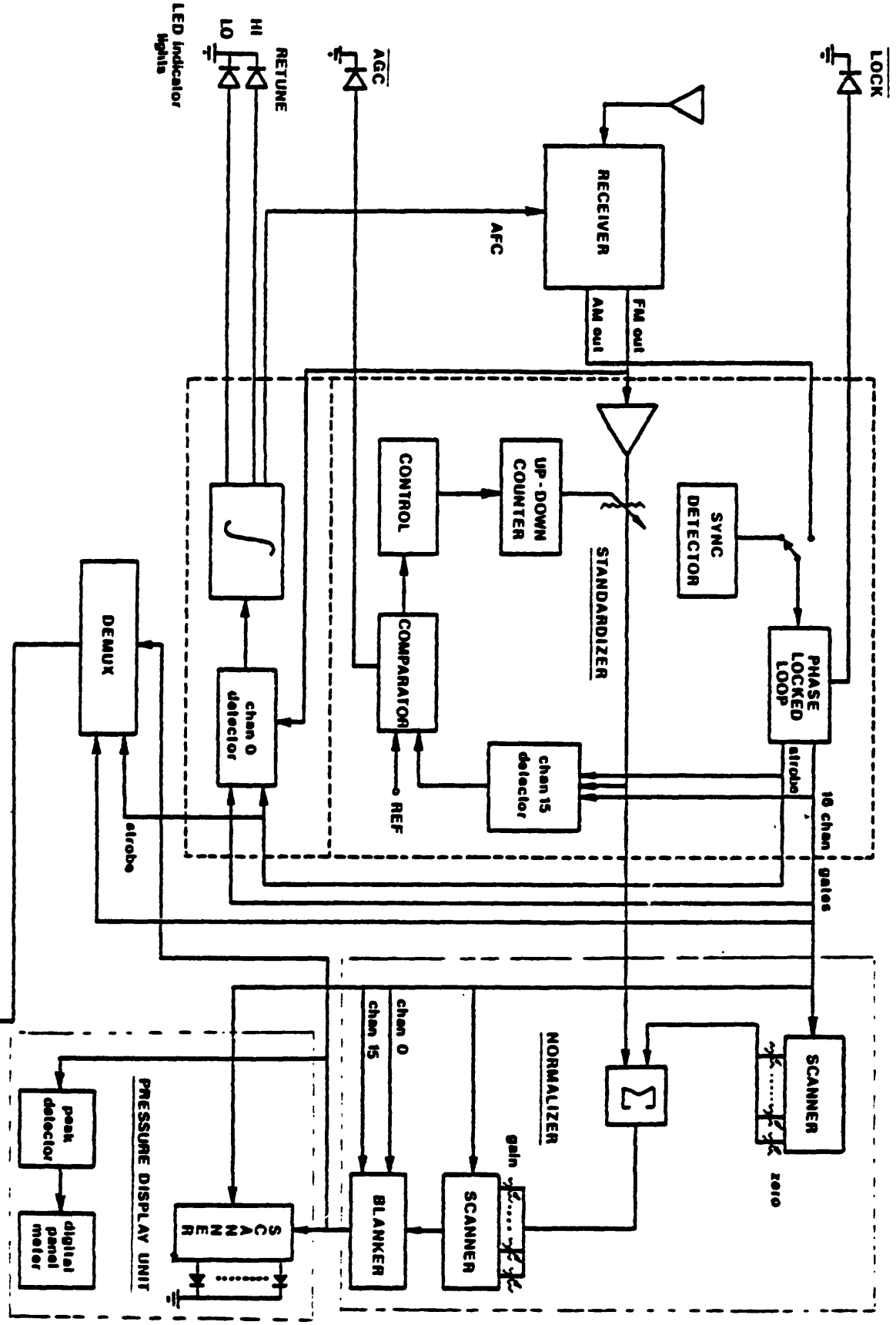

Figure II-9: Block diagram of data collection system for instrumented prosthesis. From Mann [65].

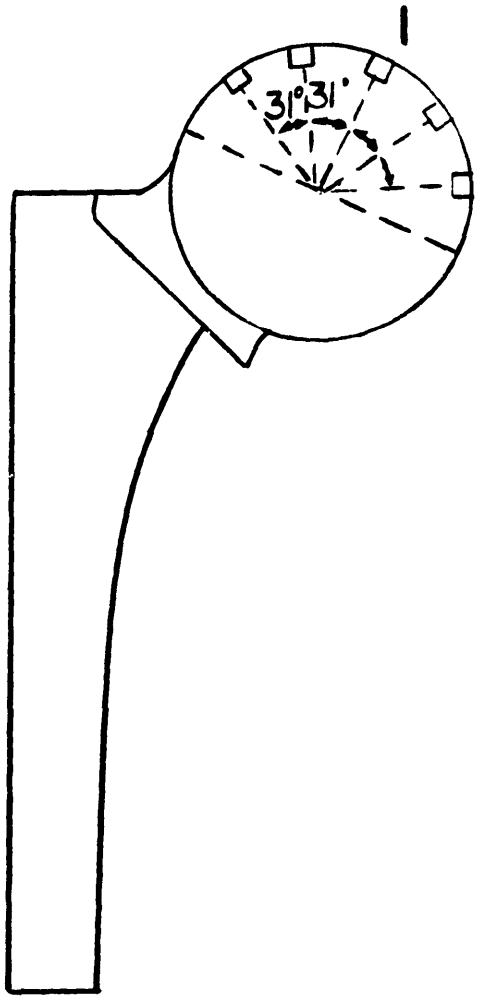

Figure II-10: Prosthesis with transducer positions shown

the subject and prosthesis are the power supply and signal receiver. A garter about the subject's leg (or the prosthesis stem) and an FM tuner suffice for signal transmission and reception (Figure II-11). The analog signal from the prosthesis (Figure II-12) is converted to a digital set of numbers which are stored on a computer and interpreted in software programs.

The mechanical portion of the transducer system is shown in Figure II-13. Deflection of the surface of a well on the inner prosthesis shell is transmitted to a cantilever beam. Strain gages on the cantilever beam are used to generate a signal proportional to the shell deflection. The 14 transducers are set in the prosthesis head, in the arrangement shown in Figure II-14 and II-10. The electronic circuits are sequentially powered through the radio-telemetry system, so that one analog output signal contains information from all 14 transducers serially. In addition, this signal carries a sample at 1 V. and at 0 V. at the start of each sampling sequence. These are used in calibration of each transducer output magnitude. Each transducer is sampled at 254 Hz. This frequency is considered more than adequate to capture the range of physiological frequencies [78,4]. The natural frequency of these transducers is 12 kHz.

The hermetically sealed single-unit structure of the prosthesis ensures protection of the subject from electronic materials. The risk of infection during data-acquisition is non-existent. The integrity of the prosthesis structure also protects the electronic instrumentation and is expected to prolong the life and accuracy of the transducer assembly. To the subject the prosthesis is indistinguishable from a normal Austin-Moore prosthesis.

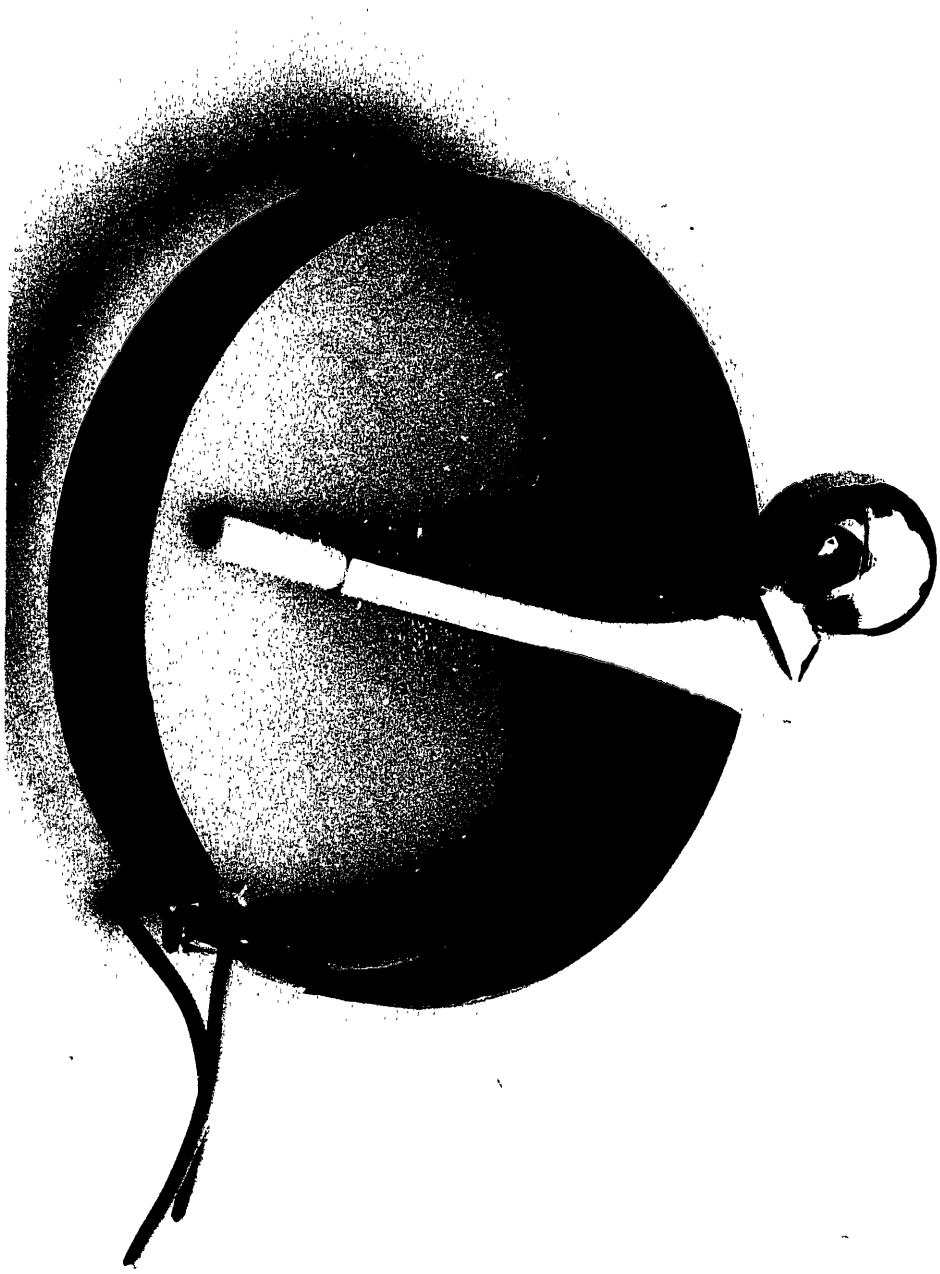

Figure II-11: Equipment used in data collection

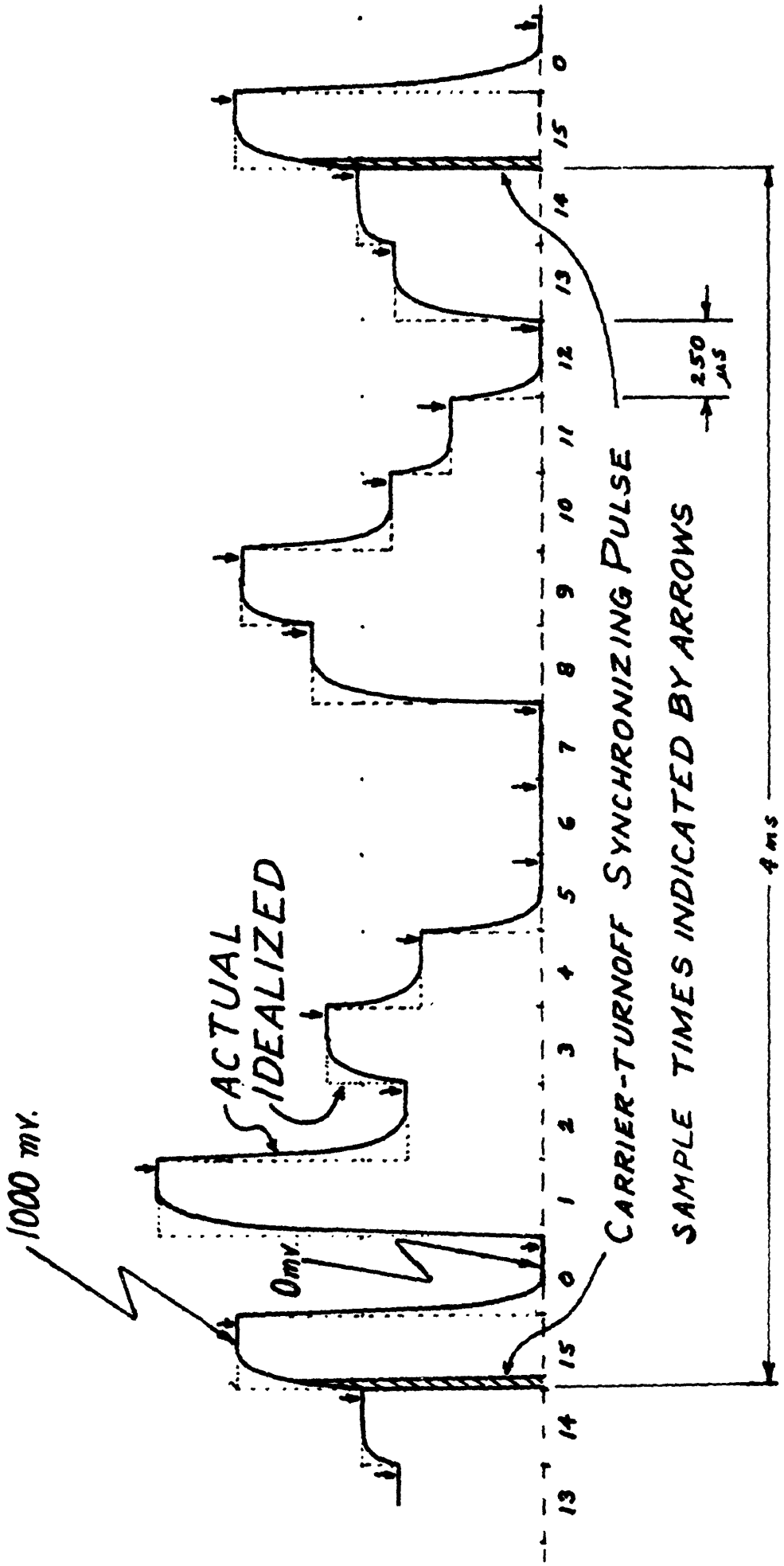

Figure II-12: Prosthesis output signal

From R. Burgess.

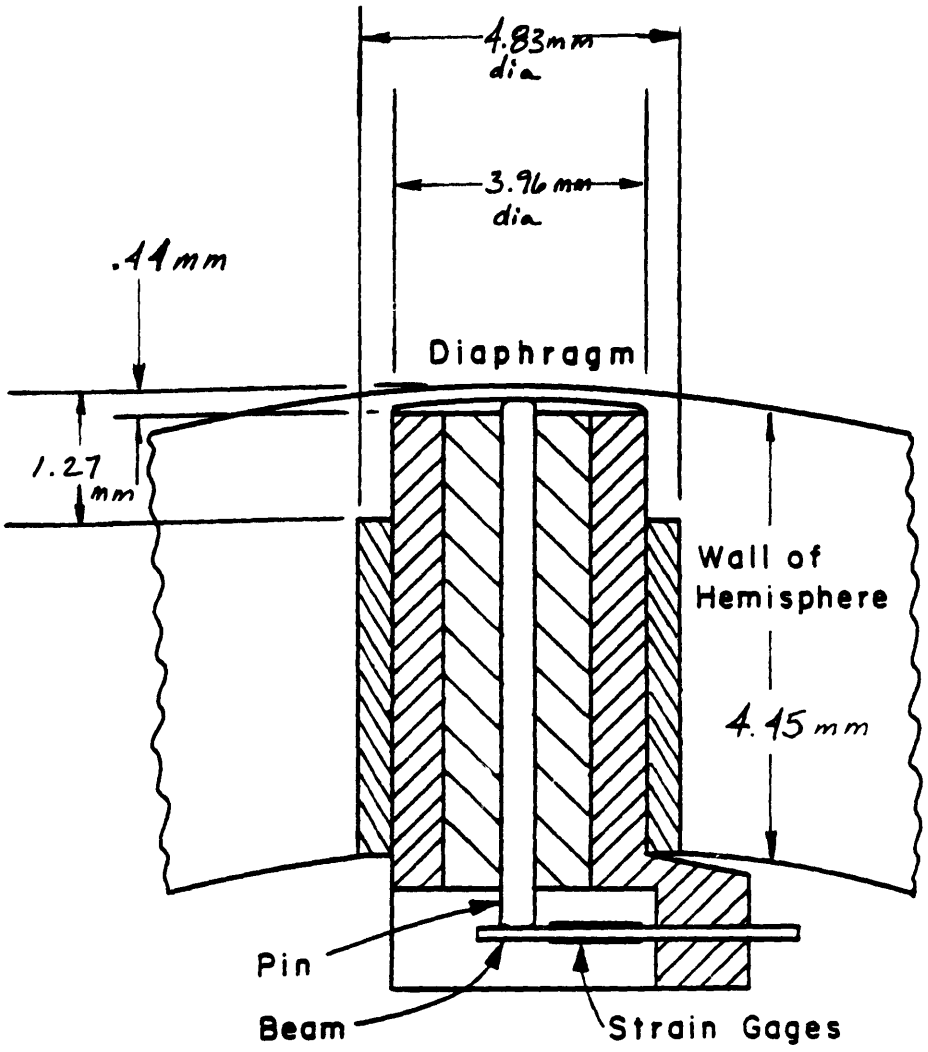

Figure II-13: Pressure transducer, mechanical construction.

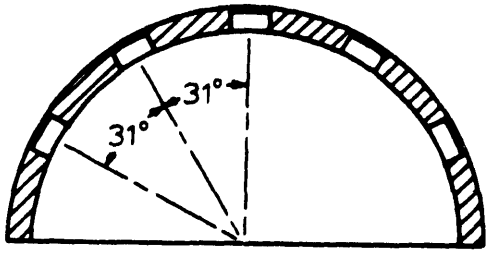

side view

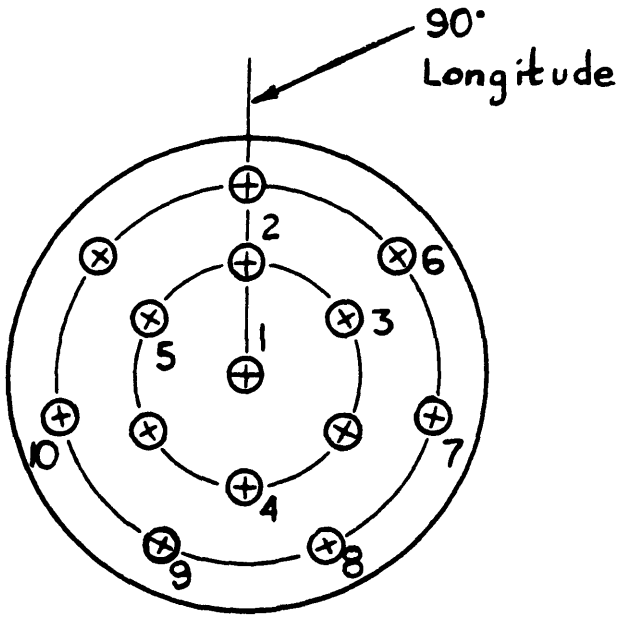

Figure II-14: Transducer positions on prosthesis surface looking from center of femoral head toward inner surface. Non-working transducers have not been numbered.

From Carlson [21] in part

Accuracy of data transmitted from the prosthesis is addressed in Chapters 3 and 5. The slope of the relationship between transducer reading and applied pressure remained constant from the initial calibration of the prosthesis until implantation and is expected to remain constant indefinitely. The zero-pressure readings of the transducers have shown a tendency to change slightly with time, recalibration is done at each data-taking session through application of traction to the subject's leg, thereby establishing a zero-pressure state. Previous values for the accuracy of the system, acquired in hydrostatic tests, show an overall error of less than 7.4% [31].

The number of transducers set in the prosthesis is the maximum possible for the available space. Unfortunately, 4 of the transducers in the implanted prosthesis are not usable; they display non-linear performance characteristics. The ten remaining transducers (Figure II-14) give information adequate for an interesting global and local view of load on the hip joint, however, they are not sufficient for the confident prediction of hip constant pressure contours and force vector direction and magnitude [23].

C. Previous Studies

The most common approach to the problem of estimating joint forces and load distribution has been analytical, with experimental basis in kinematic data, kinetic data, or electromyographic data. Some studies have considered the results of in vitro tests or used data reported by Rydell [90]. Although such examinations of the loading environment provide

essential insight and are powerful in determining fruitful areas of research, many simplifying assumptions are necessary to reduce the problem to a manageable size. Lacking complete information even as to material parameters, the validity of these simplifications must be questioned. The analytical approach allows consideration of the normal joint, whereas taking data on joint tissue involves extraction of pieces of tissue from the joint environment, replacement of one or both parts of the joint, or introduction of other foreign material into the region. However, all estimates produced analytically fail to consider co-contraction muscle forces across the joint, which will undoubtedly act to increase the load experienced at the joint.

Among those attempting analysis of the hip joint have been Inman [55], and Blount [14]. Both of these early studies concentrated on a subject standing on one leg. Only forces in the frontal plane were considered in either study. Inman calculated forces of 2.4 to 2.6 times body-weight acting against the femoral head. Blount found the femoral load to be about 3.4 times body-weight.

Williams and Svensson [103] analyzed a 3-D model of the hip joint for static one-legged stance and calculated femoral head loads of about 6 times body-weight. This model was updated and reevaluated in a 1977 report by Goel and Svensson [37], with the use of e.m.g. measurements. They presented estimates of forces in the ligaments and muscles at the joint.

Paul [77] assessed the forces at hip and knee joints in a series of experiments in which forceplate, photographic, and e.m.g. data were taken

and used to solve the inverse dynamic equations (excluding that about the long axis of the femur). Forceplate data was taken for one foot. Motions of body segments were recorded from the front and side with 16 mm cameras operating at 50 Hz. Myoelectric signals were retreived from surface electrodes attached to the skin over muscle groups expected to be active. The average peak values were 3.29 and 3.88 times body-weight; occuring at approximately 7 and 47 percent of the gait cycle as calculated by starting at heel-strike and setting stance phase duration to 60 percent of the cycle. In 1976 Paul reported results for other actions utilizing the same experimental methods. The actions he considered at that time included ramp and stair ascent and descent, in addition to fast, slow, and normal walking. He reported averaged maximum hip joint forces of 4.9 times body-weight for slow and normal walking speeds, and 7.6 times body-weight for fast walking (Figure II-15 from [78]). In stair ascent the averaged peak was 7.2 times body-weight; the greatest force in descent was 7.1 times body-weight. Walking up and down a ramp resulted in joint forces of 5.9 and 5.1 times body-weight respectively.

Seireg and Arvikar [93] developed another mathematical model incorporating muscle sharing and predicted maximum joint forces of 5.4 times body-weight for quasistatic level walking. The muscle forces predicted showed close time correlation with e.m.g. measurements.

Crowninshield and others [28] investigated the load condition at the hip for level walking, stair-climbing, and rising from a chair. Photography of LEDs was used to obtain kinematic data, a forceplatform established kinetic data, and e.m.g. data was taken in an attempt to estimate the force vector

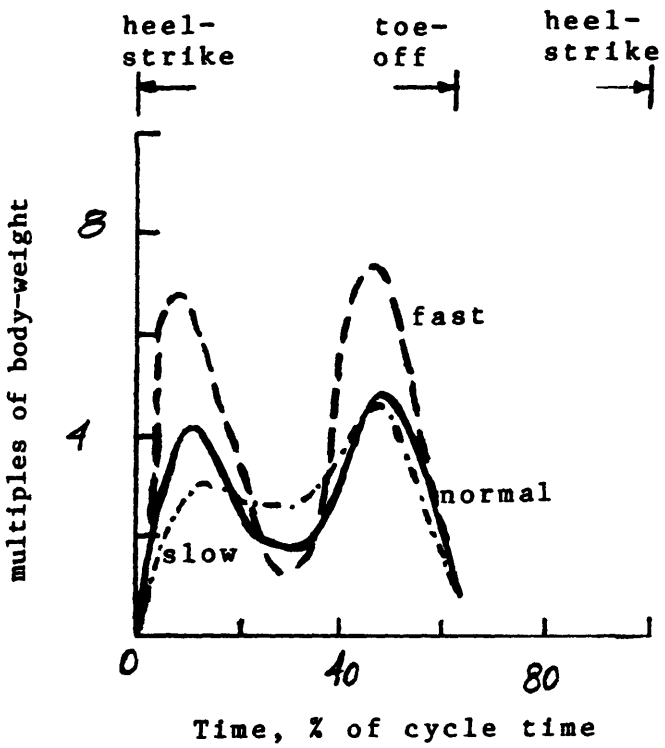

Figure II-15: Hip joint forces estimated by Paul in slow, normal, and fast walking.

Reproduced from Paul [76]

magnitude and direction at the hip. Magnitudes of peak forces estimated for walking were 5 times body-weight. In stair-climbing a peak resultant force of over 7 times body-weight was determined.

Finite-element analysis methods have recently been applied to solution of the forces and stress distribution on the hip joint [18]. Through specification of displacement of the acetabulum with respect to the femoral head, Brown and DiGioma obtained contact stress patterns and used these to calculate the resultant load. The results of this procedure have as yet only been reported for a two dimensional cross-section of the joint.

In vitro studies have also been done on the hip joint, most have focussed on the surface pressure distribution rather than directly attempting to determine the force vector. Most researchers pursueing this direction of progress have measured the surface pressure at only a few locations and then inferred a uniform or axisymmetric sinusoidal pressure distribution. Greenwald and O'Connor [40] evaluated the contact area-external load magnitude relationship in cadaverous hips and suggested that at large loads a uniform pressure distribution is found in the hip. Ahmed and others [1] used bursting capsules of different color dyes, organized by the pressure at which the capsules would break, and sheets of conductive paint inserted between the two joint surfaces in attempts to measure the pressures on intact joints. Day et al [29] divided the acetabulum into three concentric rings and calculated the pressures on each from compression data.

Cristel and coworkers [26] implanted pressure transducers in vitro in the pelvic subchondral bone and dynamically stressed the pelvis and femurs in

an electro-mechanical device that simulated walking loads and motions. Comparisons were made for each pelvis activated with Moore prostheses in place of one of the femoral heads as well. Measurements were made at only three locations on each hip, and it is not known how stress in the subchondral bone relates to acetabular pressures. However, the relationship between prosthetic and normal hips is an important issue.

Direct in vitro surface pressure measurements have been made by Rushfeldt and collegues [86,88]. These experiments were done using the instrumented endoprosthesis developed by Carlson and others [21,22] and a hip simulator. Results from this work demonstrated that non-uniform, steep spatial pressure gradients exist in the hip joint, and that local pressures exceed those assumed previously. This data also indicated the importance of correct fit between prosthesis and acetabular socket.

Brown [111] reported pressure distributions very similar to those found through in vitro experiments and simulations at the MIT biomechanics lab. [86,88,63]. His technique involved machining of recesses in the cartilage surface layer on the femoral head and insertion of piezoresistive pressure transducers. The joint was then loaded in a number of orientations.

Modelling of the synovial joint stress distribution based on experimentally measured geometry and poroelastic constitutive properites was done by Macirowski [63] to predict the surface boundary conditions governing interarticular fluid flow. Among the findings in this investigation were the concentration of stress in the joint fluid, 0.3 M-PA solid stress at most was carried by the cartilage matrix, even after 20 minutes of loading.

In vivo measurements of force transmission at the hip were reported by Rydell [90]. This study employed a strain-gage instrumented Austin-Moore prosthesis implanted in two subjects. The degree of recovery of the subjects at the time data was taken (6 mo. post-operative) may not have been complete. The maximum joint force recorded was 4.3 times body-weight for running. The greatest force recorded in walking was 3.3 times body-weight.

An in vivo study incorporating femoral prostheses instrumented with strain-gaged necks and telemetric output was reported by English and Kilvington [107]. The greatest stance phase load reported was 2.7 times body-weight, however, the subject had a total hip replacement, thus neither part of the joint was normal.

Few authors have considered the loading rate conditions experienced by the hip.[*] Paul [78] has estimated the maximum hip load rate to be 47 kN/sec.

---

* Radin [83] estimates pressures of 40 to 70 kg/(cm)**2, and loading of 70 to 1000 kg/(cm**2 * sec). Since these units are not physically consistent one cannot be sure whether he may have meant force rather than mass.

III. Data Acquisition

A. Pressure Measurements

1. Pressure Transducer

The basic structure of the instrumented prosthesis was presented in the last chapter. This section will repeat some of that information, with an emphasis on the transmission of data signals. The mechanical parts and dimensions of the current transducer system were shown in Figure II-13; the original design was developed by Carlson [21] and later changed to meet more stringent stress requirements [65]. Each transducer consists of a thinned portion of the prosthesis shell coupled by a sliding pin to a cantilever beam. Deflection of the diaphragm surface pushes the pin and thereby deflects the free end of the silicon crystal cantilever beam. Semiconductor strain gages in a Wheatstone bridge circuit on the cantilever beam generate a signal proportional to the shell deflection, which is determined by the pressure on the surface. The actual deflection of the shell is negligible and does not unduly influence the measurement of pressure. The natural frequency of the transducers is 12 kHZ.

2. External communication

a. Telemetry Device; As with the other data acquisition system components, this unit is thoroughly described in another source, in this case Dr. C. Carlson's thesis [21]. The Wheatstone bridge outputs from the transducers are sequentially transmitted through a radio-telemetry

system, so that one analog output signal contains information from all 14 transducers. The telemetry device, a 16 channel, time-multiplexed system shown in Figure III-1, is completely contained in the hermetically sealed endoprosthesis head except for a single part; a small induction coil is mounted on the end of the prosthesis stem. Each transducer is sampled at about 250 Hz, which should be more than adequate for the expected frequency content of the pressure signal (0 to 50 Hz [78,4]). The amplitude of the signal transmitted by the telemetry device for each transducer is proportional to the amplitude of the transducer output, and thus to the pressure on the diaphragm surface. A sweep through the channels, referred to as a frame of data, includes two channels used for synchronization and scaling of the transducer outputs. Channel 1 carries a sample at 1 V. and channel 2 is set to 0 V. The difference between channels 1 and 2 is used to scale the transducer outputs for all prostheses made at MIT. This process will be described in Chapter IV.

The electronic circuitry of the device isolates each transducer output and amplifies the pulse-amplitude-modulated (PAM) signal in an operational amplification stage. The amplified signal is used to frequency modulate a 100 MHz oscillator. The resulting FM signal is transmitted to the external receiver through the coil on the prosthesis stem.

b. Power Induction Link; The signal collection and transmission system of the prosthesis is powered externally through a magnetic power induction link. There are three components active in power transmission: 1) a 100 kHz power oscillator (Hewlett-Packard Model 20SAH); 2) a primary coil contained in either a teflon sleeve which fits over the prosthesis

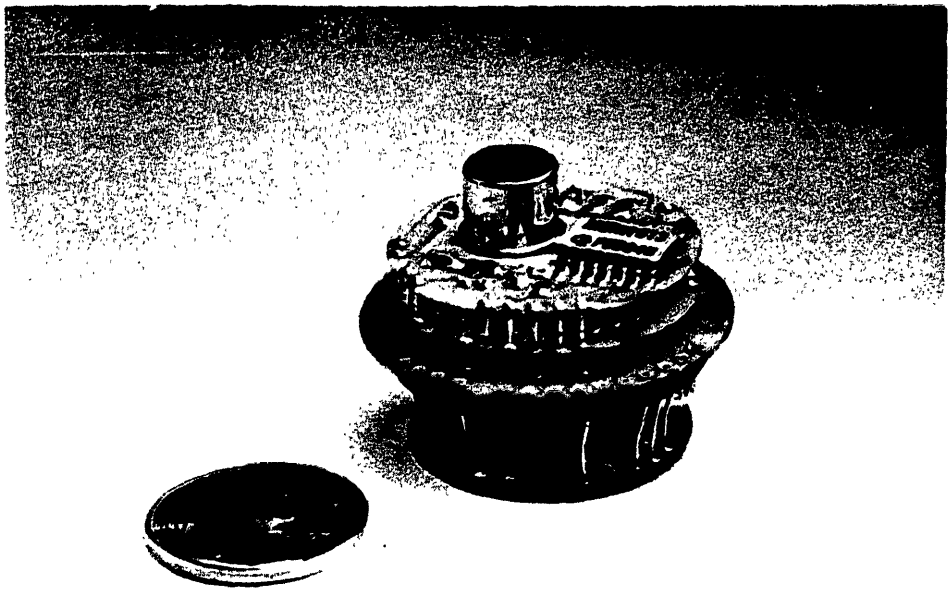

Figure III-1: Sixteen - Channel Radio Telemetry Device from Carlson [21]

stem or a garter fitting over the subject's leg; 3) a secondary coil inside che Teflon™ tip of the prosthesis stem, the same coil which acts as the PAM/FM transmitting antenna. Approximately 500mW are delivered to the telemetry system through the power system.

The primary coil used for in vivo tests, the "garter", was tested by Ralph Burgess and Bob Fijan in the MIT biomechanics lab, because of concern that difficulties in positioning and tuning would arise in the use of this device. Tests in which the prosthesis was mounted in a 8 inch diamenter plastic tank filled with saline solution at 37 C indicated that the garter would be no more difficult to tune than the more closely fitting Teflon™ sleeve used for in vitro tests and that the radial placement of the prosthesis with respect to the garter did not affect data signal transmission to the FM receiver. The axial distance between the primary coil and the secondary coil did affect signal tuning; the allowable distance between the coils was about 2 1/2 inches. With an increase in power to the primary coil it was possible to increase this distance.

During in vivo tests it has in fact been found that some precision is required in garter placement. Tests that require the subject to make abrupt motions, or that involve large ranges of motion tend to shift the garter with respect to the prosthesis stem. An example is data taken while the subject rises from a chair. However, care in securing the garter allows acquisition of this type of data.

3. Signal Recovery and Initial Processing

The external receiver for the PAM-FM signal output by the prosthesis is a Heathkit FM tuner (Model AJ15). Additional circuitry was needed to recover the output signal. Ralph Burgess, a Research Engineer at M.I.T., designed and built the multiplex signal recovery system that has been combined with the FM tuner to standardize and normalize the multiplex signal. A block diagram of the signal recovery and initial processing steps is shown in Figure III-2.

The FM tuner outputs 4 analog signals, one of which is the pressure data at 4000 Hz (16 channels at 250 Hz). For the in vivo prosthesis the other analog channels contain; 1) A frame start/synchronization pulse; 2) A channel synchronization pulse which indicates to the computer A/D converter when the pressure analog signal should be sampled; 3) A signal indicating whether the prosthesis signal is tuned or not. The frame start pulse is used to determine which sample of the 4000 Hz. pressure signal corresponds to a given transducer. The channel pulse is necessary because the analog signal is not perfectly square (Figure II-12). The prosthesis signal should be sampled near the end of the time period for transmitting the output of a particular transducer.

Knowledge of the tuning status of the signal is necessary to determine whether data is valid and whether the garter position needs adjustment.

4. Data Storage

The raw data is stored on a digital computer by direct memory access. After acquisition is complete, this data may be processed. The processing

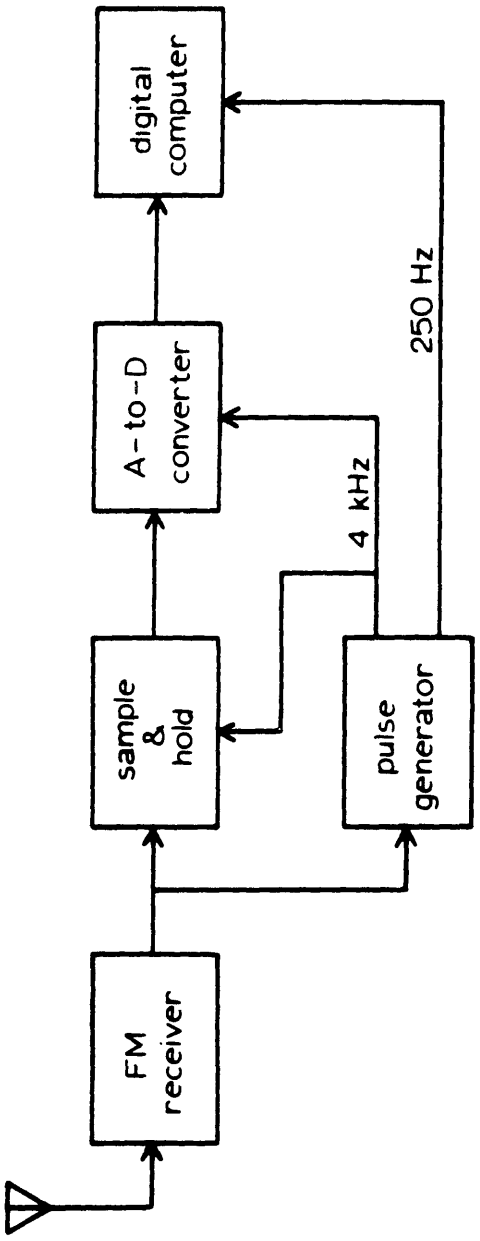

Figure III-2: Block diagram of signal recovery and initial processing for prosthesis.

From [217].

will be discussed in Chapter IV. After processing several files are stored for each test, one each for pressure, kinematic, forceplate, body-segment length, and transducer position data. Each file has the same name and different types of data are distinguished by the file extension.

The format of the pressure data file is that each record carries a sample from each of the 16 prosthesis output channels as well as the outputs from the other 3 analog channels as described above. Programs requiring unfiltered pressure measurements read these files and calculate pressures based on the values of the first two channels. Filtered pressure data already in pressure units is also stored at times.

B. Three-Dimensional Motion Data

The MIT and MGH Gait labs have very similar kinematic data acquisition systems. The two labs differ in a few respects. Most data reported here was acquired at MGH. The basic structure of this system, labelled TRACK was developed at MIT in the Biomechanics Laboratory by Frank Conati and Eric Antonsson [3]. The system is described in slightly greater detail in Appendix 1. A block diagram of the kinematic data acquisition system is shown in Figure III-3. The system obtains data through two opto-electronic Selspot cameras and a Kistler forceplate (two forceplates at M.G.H.). Kinematic data is acquired as the locations of up to 30 infra-red light emitting diodes in the laboratory reference frame. These LEDs have been mounted in rigid arrays of known dimensions on the subject's leg segments. The location and rotation of each LED fitted body segment is computed by hardware and software in the TRACK system. Kinematic data is stored in

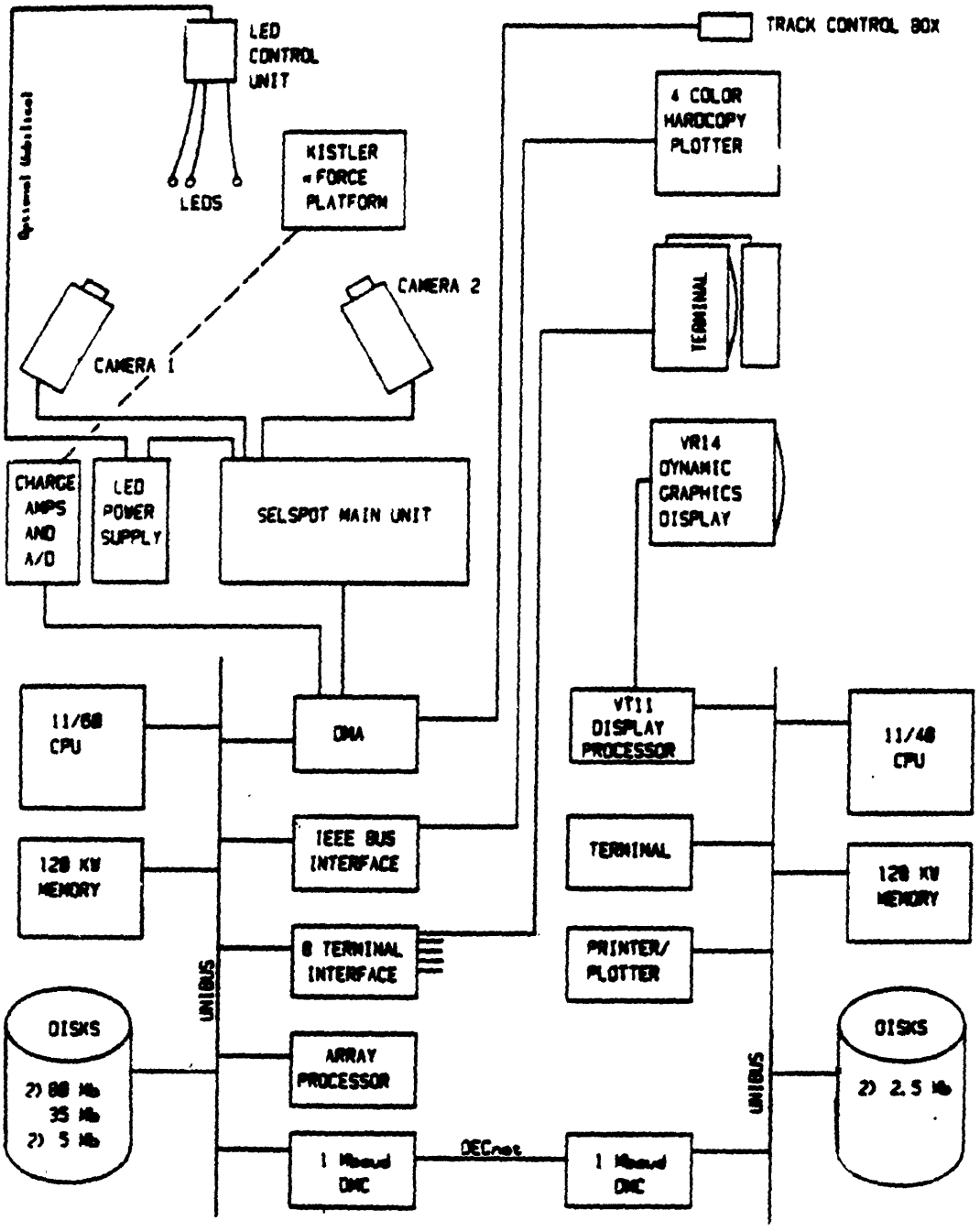

Figure III-3: Block diagram of kinematic data collection system.

From Antonsson [3]

final form as 3-D location and orientation of coordinate systems fixed to each body segment. The three components of forceplate data are also saved. Forceplate and kinematic data are acquired simultaneously at the same rate. The frequency of data acquisition used for kinematic and kinetic data taken with instrumented prosthesis data has varied between 315 and 153 Hz. Most kinematic data presented in this paper was acquired at 153 Hz.

C. Test Description

1. General

The overall process followed in acquiring data is diagrammed in Figure III-4. The subject puts body segment molds and LED arrays on her right leg. The molds are made of plastic and are molded for the subject's body to achieve maximum fidelity between limb segment movement and LED array movement. The garter that provides the external power link to the prosthesis is placed around the subject's thigh and fastened with Velcro™ to the hip segment mold. The TRACK system is made ready to acquire data. The prosthesis is powered just prior to taking data. The FM tuner locks onto the output multiplex signal in about 10 seconds if the garter is well placed. At this time, programs are run to acquire and store kinematic, forceplate, and pressure data. The subject is asked to perform a specific movement and practices the action a few times. When she is ready a trigger is activated by one of the observers. Data is taken for a length of time specified when starting the data acquisition programs; during this time one person monitors the prosthesis tuning indicators on the FM receiver. The prosthesis is not powered between tests. At M.G.H.

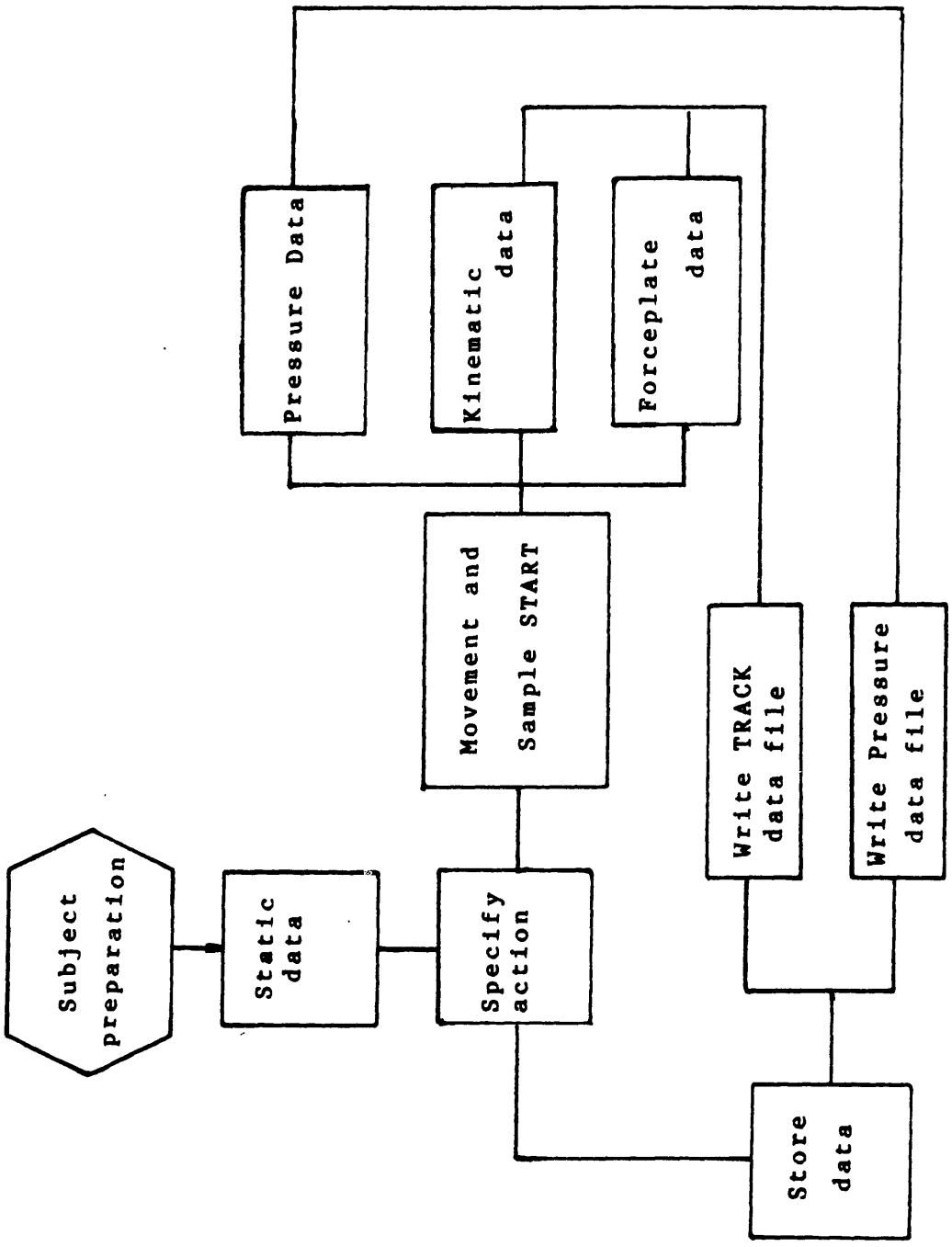

Figure III-4: General procedure followed in data acquisition

the forceplate data and the prosthesis tuning signal are immediately displayed on a Megatek graphics terminal. This display allows the computer operator to determine whether the prosthesis signal was tuned during the test. In many tests the forceplate signal provides an indication of whether the data stored included the desired action. On the basis of these displays the operator decides whether the test should be saved or repeated. Data is stored on the computer system and is not completely processed until after the data acquisition session.

2. Specific Tests and Test Descriptions

A large number of different tests have been performed by the subject since implantation of the prosthesis on June 20, 1984. Test descriptions and information on the number and dates of trials are presented in Table III-1. Data taken in June and July 1984, except July 5, 1984, was acquired at 10 Hz. This rate is insufficient to capture signal frequencies above 5 Hz, but most of the data taken during this time (the 2 weeks immediately post-operative) was under static conditions for which 5 Hz may be a sufficiently high frequency. On July 5th data was taken at a higher frequency, 254 Hz., for the first time. All data has been taken at this frequency since July 1984. Data was taken approximately six months post-operative, in December 1984, and again in May, June, August, and September 1985. Data will be taken well into the future; the use of an external power source allows this possibility.

a. Calibration data; Traction, in which the subject's femoral head was pulled out of contact with the acetabulum, was applied on July 3rd

Table III-1: Test Descriptions and Date of trials

Test Description	No. of Trials during months after implantation					
	0	6	11	12	14	15
Abduction,						
Active and Passive 0 to Max	8					
splint	1					
stance (30 degrees)		1				
Adduction,						
Active and Passive, 0 to Max	6					
Buck's traction (3, 5, 8, and 10 lb)	1					
External Rotation						
30 Degrees with 45 degrees flexion,						
20 Abduction)	1					
stance		1				
Flexion						
CPM Machine	2					
30 degrees with 30 Degrees						
Abduction (Balanced Suspension)	3					
45 Degrees, Neutral						
Abduction, Neutral Rotation	2	1				
toe-touches		1				
active and passive,0 to Max	9				1	
90 degrees		1				
Heel Bounce			6		1	
Hopping				2		
Hyper-Extension		1				
Internal Rotation						
15 degrees with 45 degrees						
flexion, 20 Abduction	1					
30 degrees, stance		1				
Isometric Abduction, Side-lying	3	1				
Isometric Adduction	2	1				
Isometric Gluteus Maximus	9	1				
Isometric Quadriceps	9					
Jogging				3		
Leg raise		1				
Lying to Sitting position in Bed	1					
Lying on Tilt Table, 0 to 45 degrees	1					
Lying on Tilt Table, 45 to 90 degrees	1					
Knee-Sling Exercise (20 Flexion,						
Resisted Extension)	2					
Neutral Flexion, Abduction, Rotation	10	1				
Onto bedpan	1					
Pedalling a Bicycle	1					
Rising from seated position	7	1	2		7	
Single-Leg Stance (Left and Right)	3	2			1	
Sitting from Standing		1				
Sitting Position	7					
straight-back		1				

Table III-1 continued

Test Description	No. of Trials during months after implantation					
	0	6	11	12	14	15
Sitting position						
slouched		2				
Slow Loading to Stance			2			
Slow Loading from Single-Leg Stance			2			
Stair-climbing						
up, Left Leg First	1					
up, Right Leg First	1	1	2		2	
down, Left Leg First	1				2	
down, Right Leg First	1	1				
Standing Position						
Walker or Crutches	4					
Unassisted or with Cane Only	4	1		1		
slouched		1				
on Tilt Table at 90 degrees	1					
Unloading Traction	3	1	1		1	1
Walking						
level,(some a single step)	6	3	2		2	
cane		2	3			
with crutches,						
foot off ground			1	2		4
two-point	1					
toe-touch			1	1		3
partial weight-bearing		1	1			3
with walker	2	1				

and July 7th 1984. The lowest average transducer reading from these two tests has been used as the zero-pressure transducer output for all data taken in June and July 1984. Similar traction data was taken at the end of each of the subsequent sessions except in June 1985. The averages obtained in these tests have been used to determine the zero-pressure transducer output for that date as will be described in Chapter 4. June 1985 data has been interpreted using the zero-pressure measurements taken in May 1985.

b. Gait tests; Walking tests were usually performed so that the subject stepped on the forceplate with the instrumented leg. When two forceplates were used tests were conducted so that the instrumented leg hit a forceplate first. No attempt was made to control the walking speed for the subject; the tempo at which she performed these tests can be obtained from the kinematic data. On each day she chose a pace which was comfortable for her. A year after surgery data was taken while she jogged. Gait tests were also done with walking supports on several occasions. Tests with a walker were carried out in July 1984, and in December 1984. Crutch-assisted walking was done in July 1984, December 1984, May and September 1985 in a variety of ways. Some tests were done in which the subject held the instrumented leg completely off the floor while others had her touching the toe of that leg to the floor but not placing weight on that leg. In some tests her whole foot was placed on the floor and bore part of her weight. Cane-assisted walking was performed with 15, 30 and 50 pounds of the subject's weight borne by the cane.

c. Sitting-to-Standing; Some variation occurred in test parameters for this type of test during the year of data acquisition. In

general, data acquisition was started as the subject sat in a chair and continued as she rose to a standing position. The height of the chair, position of the subject on the chair, and subject's strategy in rising all varied, as can be seen in the data. Early (June and July 1984) data was probably taken at too low a frequency; it was later discovered that load transfer occurs very quickly during this type of test. On all dates the seated position was about 46 cm above the floor. About 85 degrees of flexion is found at the subject's knee when she sits in a chair of this height with her tibia perpendicular to the ground. Leg position was not constrained during the movement; tests may have started while the subject had a greater or smaller joint angle.

In August 1985 data was taken as the subject rose from seated positions in chairs 38, 46, and 56 cm high.

d. Stair-climbing; The precise manner in which stair-climbing tests were done varied. Typically, data acquisition was started with the subject standing. She then stepped onto the stair with her instrumented leg first. After a set of two stairs was built, data was taken as she stepped first with her instrumented leg, placed the other leg on the next stair, then brought the instrumented leg up to the top stair. The step used for stair-climbing tests in December 1984, 6 months after implantation, was 23 cm (9 inches) high. The one used 11 months post-operative was 18 cm (7 inches) high. After 14 months of recovery time, stair-climbing was done on a set of two 18 cm high steps.

e. Heel Bounce; A test was devised in an attempt to quantify more precisely the relationship between external force timing and the pressure increase at the hip. This "heel bounce" test consisted of the subject rising onto her toes from a normal standing position on the forceplate, and then dropping abruptly back to a flat-footed stance. The change in force applied to the forceplate was expected to be visible as an abrupt increase in pressure at the joint. Tests of this type were done 11 and 14 months after surgery; several different surfaces were used in May.

IV. Data Analysis and Display

A. Overview of processing

The steps that have been followed in processing data taken from the implanted prosthesis are outlined in Figures IV-1 and IV-2. The general procedure is as follows:

Transducer outputs was first translated into pressure values by consideration of known transducer characteristics and prosthesis behavior specific to a given data acquisition session. The pressure signals were then filtered to remove high frequency electronic noise. Filtering decisions were based on the energy spectra of the signals. Next, the temporal relationship of kinematic and pressure data was used to establish prosthesis position and orientation in the hip joint over the course of each set of data. Pressures are ultimately displayed at acetabular locations for an instant of time or over a period of time.

The rate of loading at the hip has been obtained from the time variation of the filtered pressure signal. Estimates of the acetabular areas in which the greatest rates of loading occurred were made. The corresponding external load rate may be obtained from the slope of the forceplate signal over the same short period of time.

Pressure signal reproducibility over repeated tests has been examined and compared to external force variability as given by forceplate signals.

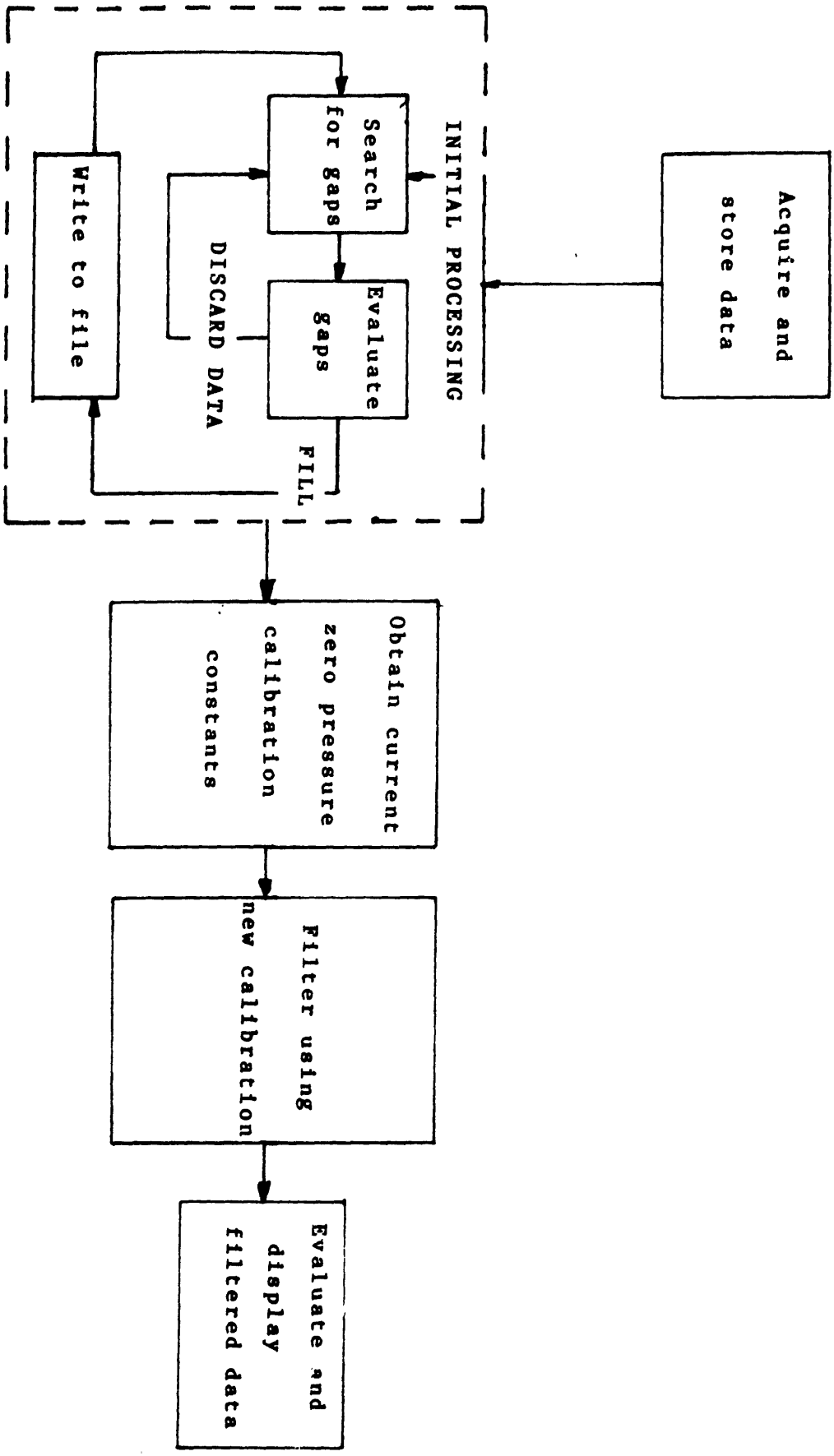

Figure IV-1: Outline of data processing procedure

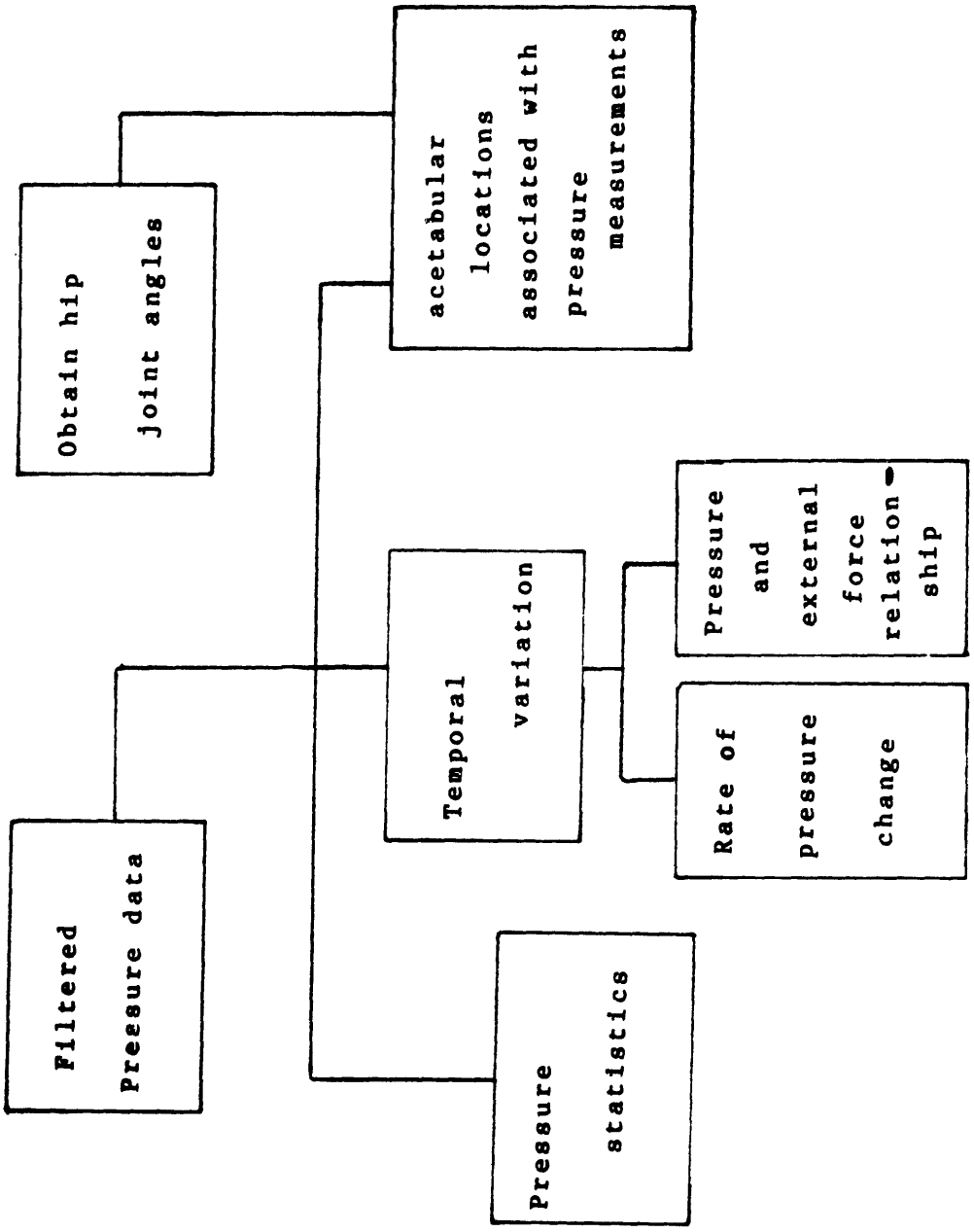

Figure IV-2: Display categories

B. Data processing

1. Determining Pressures from Prosthesis Output

Much of the basic method used to relate values stored as transducer outputs to pressure measurements was inherited from those who previously worked on the instrumented hip prosthesis project. Techniques have not changed substantially, but have been standardized and augmented.

The first stage in processing was to determine if the data was good or bad, and if bad, what portion of it should be discarded. Judgement of the worth of data was based on the tuning status transmitted by the multiplex signal recovery system. If data was untuned it was thrown out. Two frames on either side of the discarded section of data were also considered invalid because the precise time during the series of transducer signals at which the signal became untuned was not known. If a data set contained substantial information following excision of the untuned sections, values for the gap were interpolated from the series of transducer output signals on both sides of the untuned section and inserted in place of the discarded data. This permitted preservation of the time correspondence of pressure and kinematic data. If interpolation was deemed inappropriate the data was not saved. In all data sets a single frame of information was occasionally lost due to computer response speed during data conversion. This was unavoidable given the quantity of information transferred, and does not significantly diminish the value of the data. Data has sometimes been saved even if it contained a sequence of several untuned frames if this occurred during a portion of the test which was not otherwise interesting

or could be easily discarded and not replaced. Judgement of data worth occurred at two stages in processing, immediately after acquisition and just prior to final storage.

The next step in processing was conversion of the sequentially stored transducer readings to a more compact and easily accessed form. The start of the sixteen channel signal was determined and information about one sequence of transducer samples was stored in one record of a data file. Determination of the start of a sequence was made possible by reading the frame start signal from one of the channels output by the signal recovery system. The frame start signal was high at the same time that 1 V. was output by the prosthesis multiplex signal transmitter. The prosthesis data read immediately following the initial 1 volt sample was the sample at 0 V., followed by the fourteen pressure transducer outputs in numerical order. These sixteen values and the tuning status value, in that order, were then written into a record of a new data file.

The process of actually converting transducer outputs to pressures is performed in subroutines called by programs requiring unfiltered pressure data. Interpretation of each transducer signal is based on the calibration history of the corresponding transducer. Extensive calibration of the in vivo prosthesis was done prior to implantation [31] and will be discussed shortly. The results of calibration tests showed, for each of the 10 transducers which worked and behaved in a linear fashion, that the slope of the relationship of transducer output with pressure remained constant over time and for different temperatures. Data from the four non-working or nonlinear transducers has not been used, and the remaining transducers have

been numbered as if the other four transducers do not exist. The zero-pressure output for each transducer changes over time and is established for each specific test day from the most recent in vivo calibration; the method by which this is done will be discussed in the next section. The zero-pressure values change with temperature as well as time. The manner in which they vary is known for temperatures around body temperature (37 degrees C). The algorithm for determining a pressure measurement from a transducer output is to correct the transducer output for temperature, correct for the zero-pressure value, then use the slope of transducer reading with pressure to obtain a pressure at that time for that transducer. More information on transducer characteristics has been included in Appendix 2.

2. Prosthesis Calibration

An intensive six-month-long evaluation of the effect on transducers of pressure, time, and temperature was performed in the first half of 1983 by Bob Fijan [31]. The results of these tests were: 1) the slope of transducer output vs. pressure is linear for 10 transducers over 0 to 6.9 M-Pa (0 to 1000 psi); 2) The slopes are invariant with time and temperature; 3) The zero-pressure reading for each transducer changes with temperature in a specific manner; 4) The zero-pressure reading varies unpredictably with time. The manner in which these facts were determined will be outlined briefly, the decisions made regarding interpretation of transducer outputs will be discussed, and the in vivo calibration procedure will be presented.

Transducer response at constant temperature over short (5-10 sec.) time periods was investigated in a series of hydrostatic pressure tests in a tank of pressurized oil (Figure IV-3). The pressure was set to zero psi as measured with a dead-weight tester, then increased slowly in .35 MPa (50 psi) increments to 6.9 M-Pa (1000 psi). Data was also taken while the pressure was decreased in .35 M-Pa steps. At each pressure setting the 16 channels of information were recorded from the prosthesis, then it was turned off while the tank pressure was changed. Hydrostatic tests were done at room temperature, body temperature (37 C) and at 42 C. No hysteresis was evident in the transducer outputs.

Further temperature calibration tests were performed because the transducers exhibited radically different zero-pressure behavior at the three temperatures. Since the slope of the each relationship remained constant only the zero-pressure readings were required for temperature calibration corrections. Tests were done over a range of temperatures centered about 37 degrees C. One set of tests was done with the prosthesis set on an aluminum heating block as it was heated from below. The heating block had been machined to fit the prosthetic femoral head. Two sets of temperature calibrations were done in a tank of heated water. Both methods subjected the prosthesis transducers to some slight pressure - due to its weight or the water pressure - but the amount was negligible compared to pressures in a functional hip joint. Data was taken only after the prosthesis had equilibrated to the surrounding temperature. These calibration tests established data for evaluating the change in transducer zero-pressure readings with changes in temperature about 37 degrees C. likely under physiological conditions. Response of the transducer

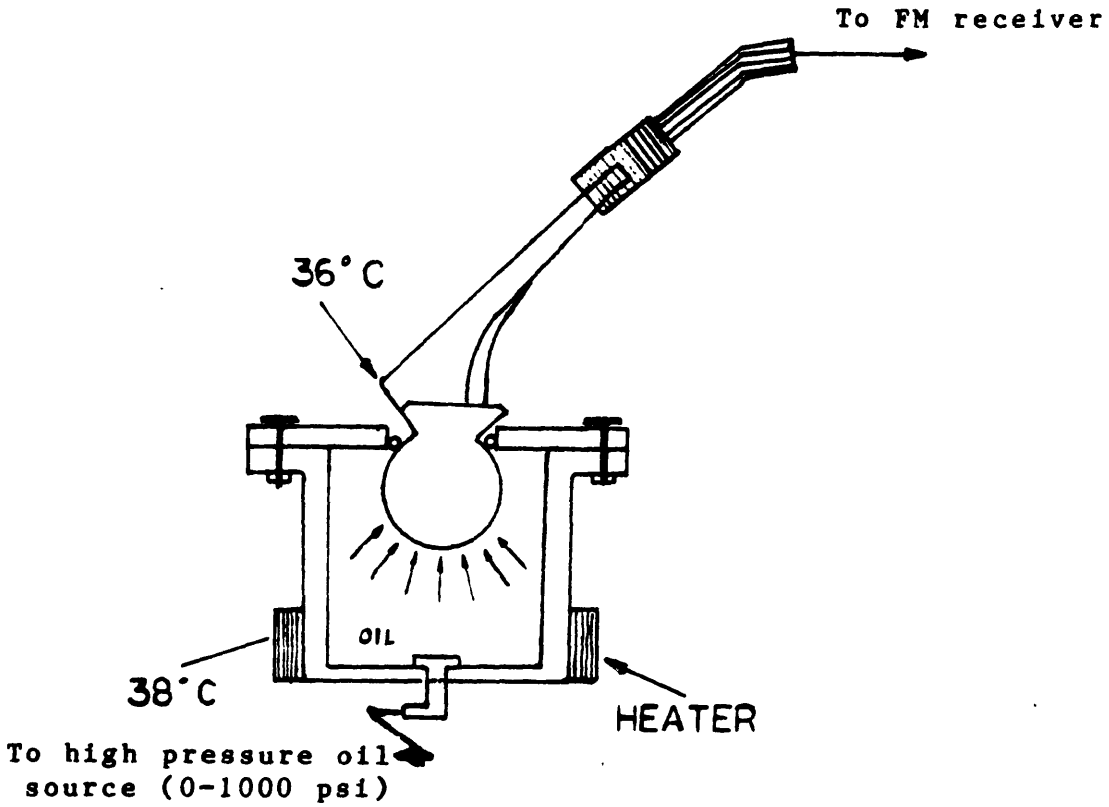

Figure IV-3: Hydrostatic calibration equipment

zero-pressure readings over time is influenced by temperature dependant changes in prosthesis behavior, since powering the prosthesis results in dissipation of some heat in the prosthesis and surroundings. Evaluation of the change in zero pressure reading over relatively long times was done by powering the prosthesis for a period of 50 minutes and recording the transducer signals at 1 sec intervals during that time. It was expected that the transducer readings would change initially but eventually achieve a steady-state value at which time the power generation in the electronics would equal the dissipation to surroundings. This was not seen to occur. In some tests a given transducer unloaded reading would converge to a steady-state value, in others the zero-pressure readings obtained from the same transducer would not converge. It was speculated that the behavior is unpredictable because the power actually delivered to the prosthesis varies. No means of fully accounting for power-up time dependant changes was found; the alternative to attempting to reach thermal equilibrium under power-up conditions was to recommend that data be acquired during brief periods of prosthesis powering.

Peak-to-peak noise measurements were made during tests of 1 sec. duration, with prosthesis data collected at 250 Hz. Transducer noise was about 25 mv in amplitude for all transducers, which translates to a somewhat different pressure range for each transducer but generally in the range of 30-50 psi, or .2 to .35 M-Pa. The noise is random and occurs at a high frequency, with energy spectrum peaks at 50 Hz. for most transducers (Figures IV-4 and IV-5). Since human motion-related frequencies are below 20 Hz. it was possible to filter out the electronic noise.

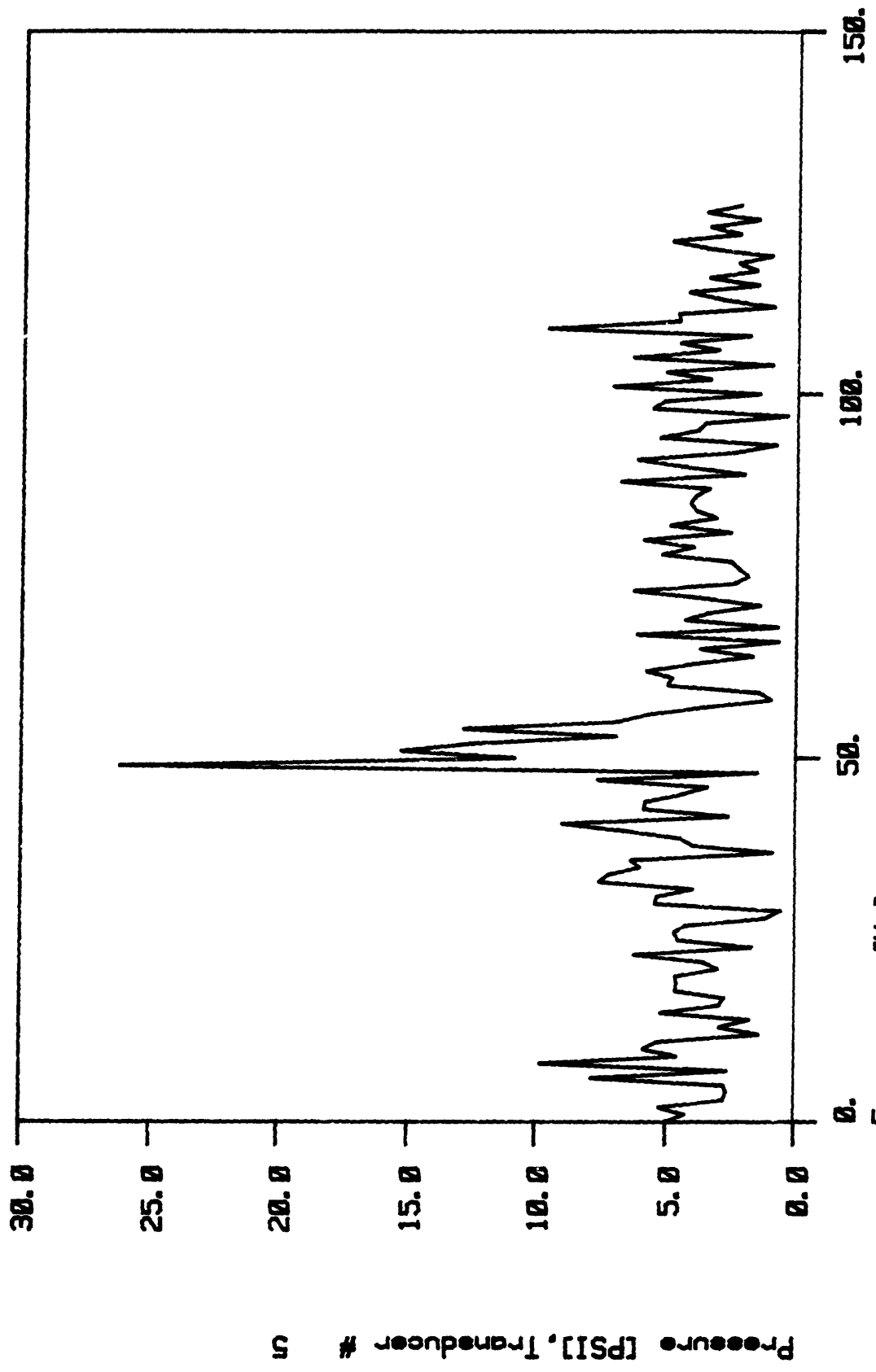

Figure IV-4: Energy spectrum for pressure data from a calibration test.

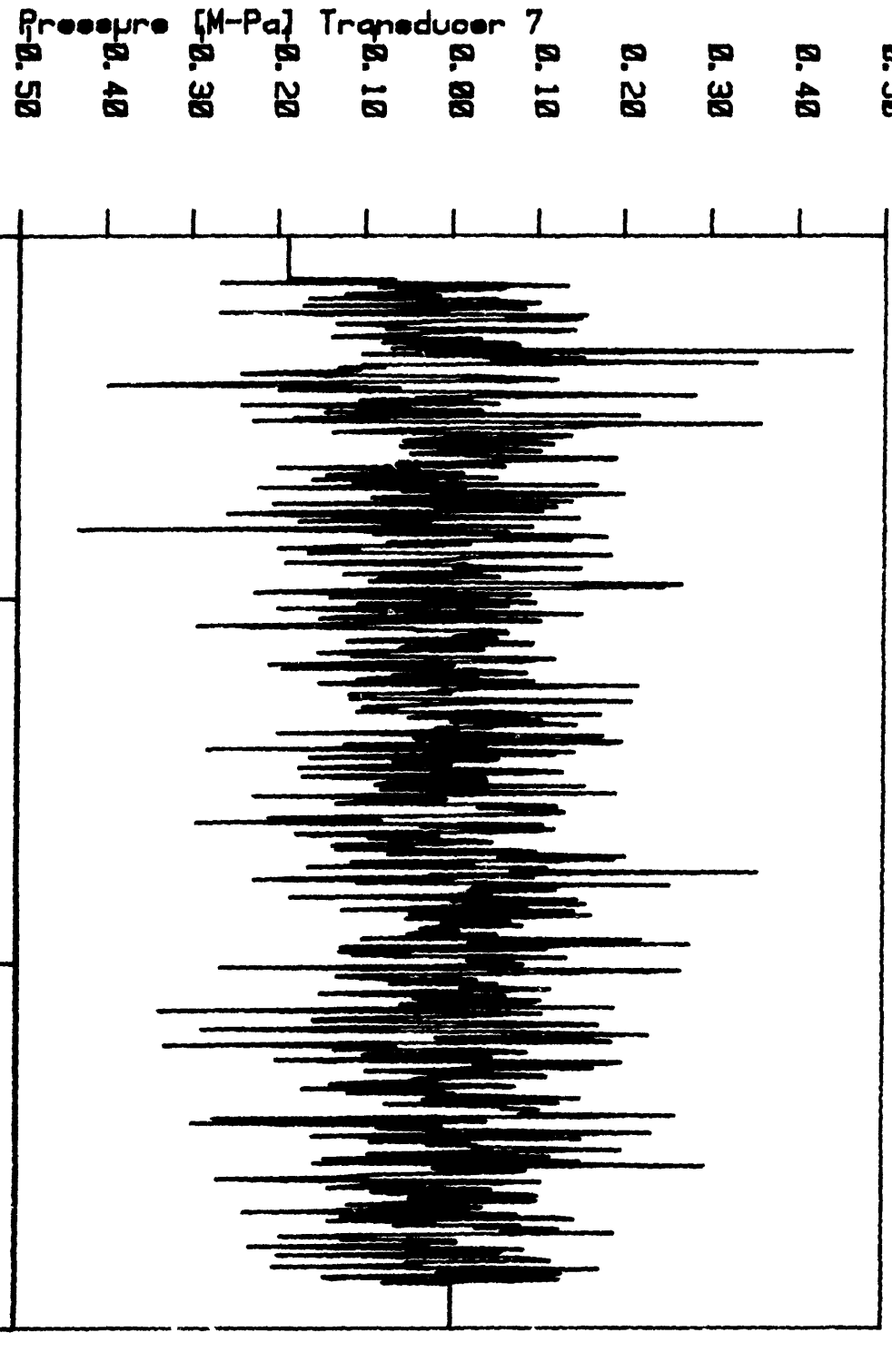

Figure IV-5: Typical transducer output during calibration test

After calibration tests the decisions made were: 1) The prosthesis should be powered only for short time periods; 2) The slopes derived from hydrostatic calibration tests may be used with all data; 3) The temperature calibration corrections for body temperature tests may be used for temperatures around 37 degrees C.; 4) A method of in vivo evaluation of zero pressure transducer readings is required; 5) Filtering of data so as to preserve the signal below 50 Hz may be necessary.

3. In vivo Calibration

a. Basis; Not only do the transducer zero-pressure outputs vary with time, but the absence of load on the femoral head probably produces something other than zero hydrostatic pressure on the prosthesis. The prosthesis was again calibrated in the operating room during implantation, but the prosthesis temperature control was impossible at that time, and thus these calibration values are difficult to interpret. It was decided that after the subject had recovered zero pressure recordings would be determined from data taken while unloading traction was applied to the subject's leg, essentially pulling the femoral head out of contact with acetabulum cartilage. Even if the values so obtained were not true zeroes, they represent pressures as close to the unloaded condition as are likely to be experienced in the body. These values were then used to scale pressures found in other tests, and at worst led to underestimation of the actual condition. Given the elapse of time between days on which data was collected and the need for accurate data, it was decided to try to perform an unloading traction test at each follow-up data session.

b. Methods; In vivo calibration was done in the following manner; the subject's leg was gently pulled at the ankle away from her body while she was lying relaxed on a couch, her shoulders restrained. The lowest pressure section, usually 1 to 3 seconds, of data from these tests was used for calibration. The data was processed as usual, and average values were found for the selected portion of the test. Averages were used rather than minimums to avoid filtering the data. The average pressure was converted back to a millivolt reading through use of the previous zero-pressure value and the slope:

newzero = Pressure * slope + oldzero

This zero reading was then associated with the date on which data was taken and input to the prosthesis parameter file used later in data interpretation.

c. Results; Transducer zero-pressure millivolt readings for in vivo calibration tests are presented in Table IV-1. The inter-test variation in Mega-Pascals is given in Table IV-2. As can be seen, some transducers have varied more over time than others. There appears to be no orderly pattern of changes in the unloaded readings obtained at any particular transducer. The acetabular locations of the transducers during calibration are shown in Figure IV-6.

The pressures obtained for static and gait tests have not varied erratically as one would expect were the in vivo calibration methods invalid. In Figure IV-7 data for one transducer over four gait cycles have

Table IV-1; In Vivo Zero-Pressure Calibration Measurements

Values are average transducer reading over lowest 1 - 2 seconds of each unloading test.

Date	July 84	Dec 84	May 85	Aug 85	Sept 85
Transducer					
1	153.25	170.95	136.91	160.98	89.33
2	981.19	1016.27	1009.36	1049.28	949.64
3	1127.99	1129.01	1133.94	1121.23	1046.93
4	640.73	641.74	669.34	666.75	617.01
5	1127.99	1429.19	1509.91	1557.13	1508.62
6	-914.37	-983.40	-990.4	-1042.18	-1077.79
7	760.98	714.94	777.63	639.94	683.85
8	732.99	832.42	847.44	903.11	810.36
9	-121.99	-129.5	-86.25	-102.86	-138.28
10	-358.8	-401.0	-403.67	-455.75	-522.31

Table IV-2; Mean In Vivo zero-pressure values

Transducer	Mean	Std. Dev.
1	142.3	32.1
2	1001.1	37.6
3	1111.8	36.6
4	647.1	21.5
5	1426.6	173.1
6	-1001.6	62.3
7	715.5	56.2
8	825.3	61.9
9	-115.8	21.0
10	-428.3	62.8

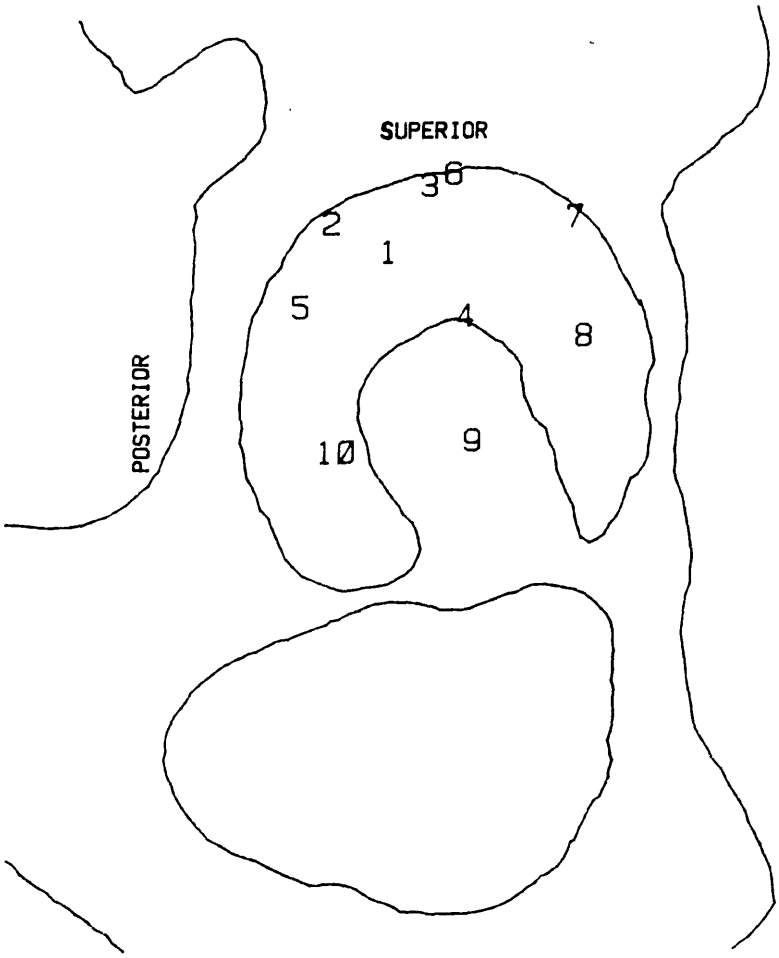

Figure IV-6: Positions at which in vivo zero pressure calibration measurements are made.

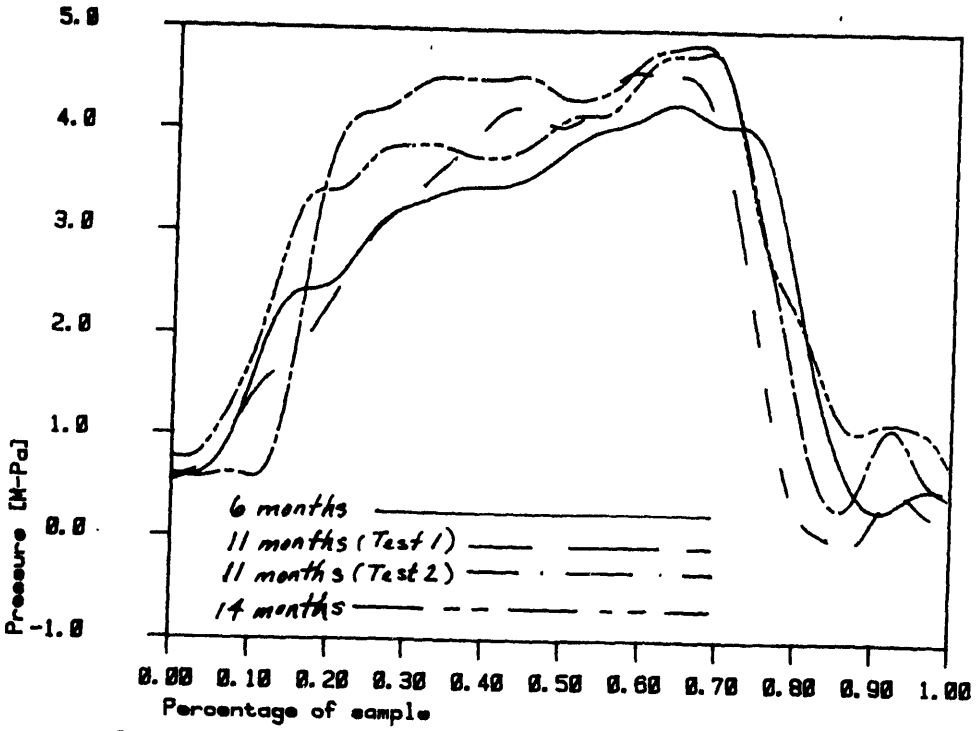

Figure IV-7: Pressure at one transducer during four walking tests performed on three test dates. Sample duration normalized by stance phase length.

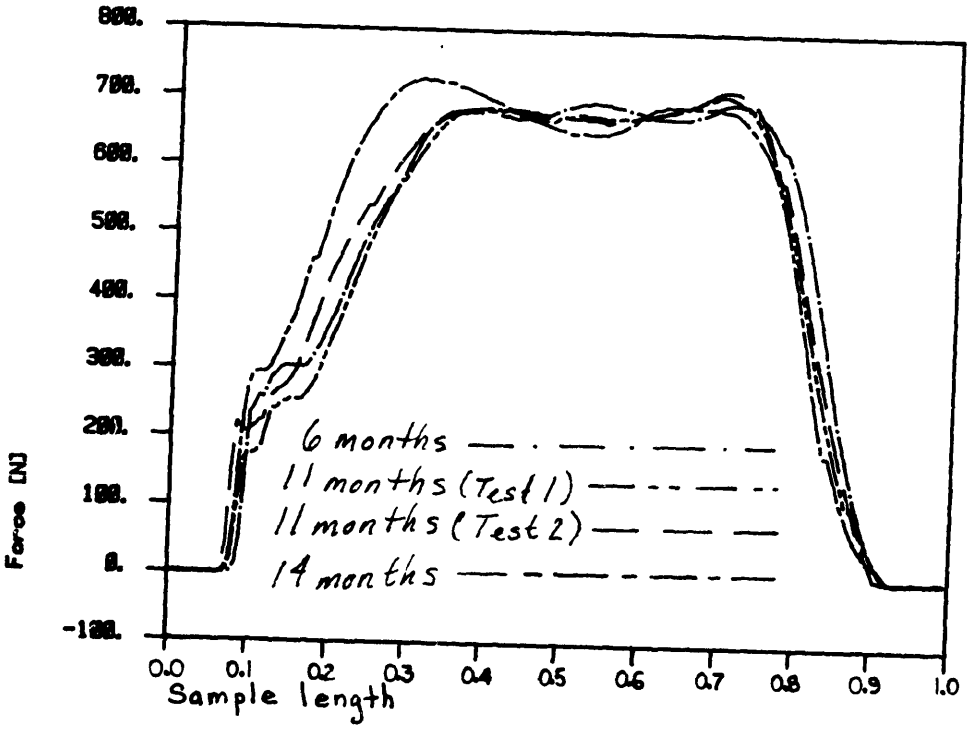

Figure IV-8: Forceplate data during four walking tests done on three test dates. Sample duration normalized by stance phase length

been plotted together. The initial and end times of samples were selected from forceplate data and sample times are normalized so that each test begins 10% of the stance phase duration before heelstrike and ends at a time 10% of stance after toe-off. One test is from six months post-operative, two from a year, and one from 14 months post-operative. There are no differences in this data which can be attributed to change in transducer characteristics alone; the forceplate recordings (which are known to be precise and time-invariant) for the same tests (Figure IV-8) show that some variations in external forces occur from cycle to cycle. Changes in limb motion while walkind undoubtedly contribute further to the inter-test variation in pressures.

4. Filtering of Pressure data

Each transducer in the instrumented endoprosthesis is sampled about 250 times per second. It was expected that this sampling rate would be more than adequate to replicate pressure variations in time since relative motion of the parts of the joint occurs at frequencies under 50 Hz. The frequency content of the external force signal in gait was previously known from the use of a forceplate [4].

The transducer noise frequency was found during calibration to be quite high. Frequency analysis of the in vivo calibration tests, when no large-scale motions or pressure changes occur, shows that seven of the ten useful transducers have a peak in their energy spectra (magnitude of the Fourier transform of the signal at a range of frequencies) at 50 Hz, of between .1 to .2 M-Pa (15 to 30 psi) in amplitude. Figure IV-5 is of one

such transducer, representative of transducers 1,2,3,5,6,9, and 10. The other three working transducers showed no obvious noise peak, however, the noise amplitude for these transducers was generally between 0 and 10 psi. This would indicate that these transducers produce less noisy signals, unfortunately 2 of these transducers rarely registered high pressures due to their acetabular locations.

It was found, through frequency analysis of motion tests and through trial and error that filtering the pressure signal at 10 hz. did not result in loss of information. Prior to filtering a given test the frequency range of the signal was determined for at least one transducer. Figure IV-9 is the energy spectrum for a typical gait test for transducer 3.

Two different filters were tried on the data. The first, a digital Butterworth filter previously used on kinematic data, seemed to give inaccurate replication of pressures in some tests. "Ringing", referring to filter-induced oscillations in the data at approximately the cutoff frequency of the filter, is an unfortunate characteristic of Butterworth filters which appears near abrupt changes in the data. Some pressure data contained variations which caused this phenomenon to be seen. A "finite-impulse-duration-reponse" filter implemented by Ted Milner and Mansoor Ijaz out of Stearns [112] was tried as well in hopes of replicating abrupt changes more accurately. The energy spectrum after filtering with the FIDR filter is shown in Figure IV-10.

The FIDR filter did seem to reduce ringing and reproduce "corners" in some of the data better than the Butterworth filter. For most data, however,

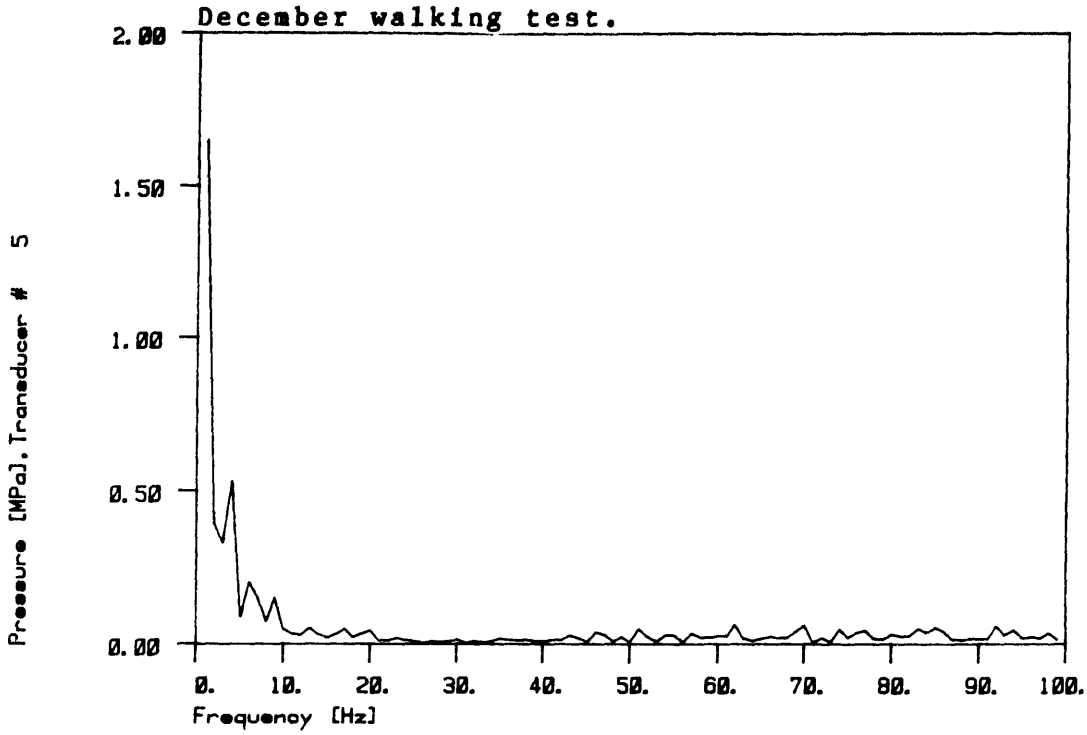

Figure IV-9: Energy Spectrum for unfiltered pressure data

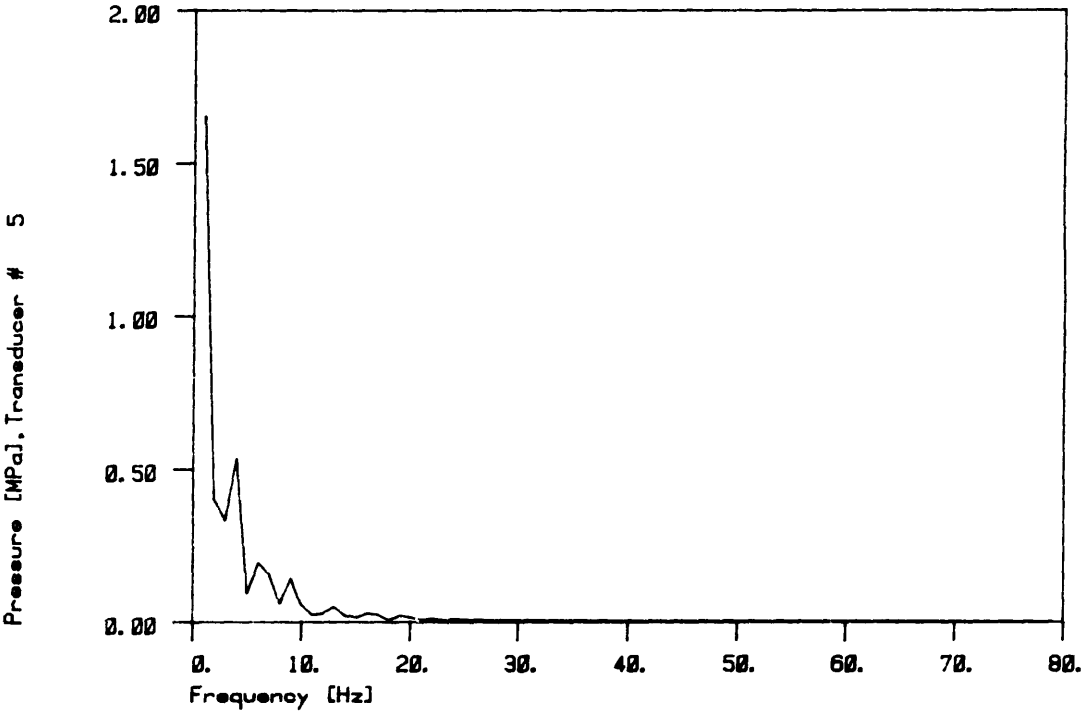

Figure IV-10: Energy Spectrum for filtered pressure.

there was no observable difference in the results of the two filters. Figure IV-11 shows one set of data filtered at 10 Hz by each filter. In Figure IV-12 the same set of data is filtered at 10 and 25 hz. by the FIDR filter, as can be seen, little difference is apparent. For the data presented in this thesis, the FIDR filter was normally used, usually with a cut-off frequency of 10 Hz. Deviations from this policy have been noted where they occur.

C. Coordination of Kinematic, Forceplate and Pressure data

One of the most significant aspects of the in vivo pressure data obtained at MIT and MGH is the ability to relate these pressures to kinematic and forceplate data. The kinematic data gathered via the TRACK system is unique in its accuracy [3,32]. The following facts are relevent to this section:

1. The 3-D position and orientation of the subject's foot, shank, thigh, and pelvis are known in the inertial reference frame and can be obtained with respect to one another.

2. The necessary body segment dimensions are established.

3. Forceplate data is available for X,Y,Z, components, as are the moments about these axes and the X-Z center of pressure on the forceplate.

4. The frequency of data acquisition is known and recorded with the

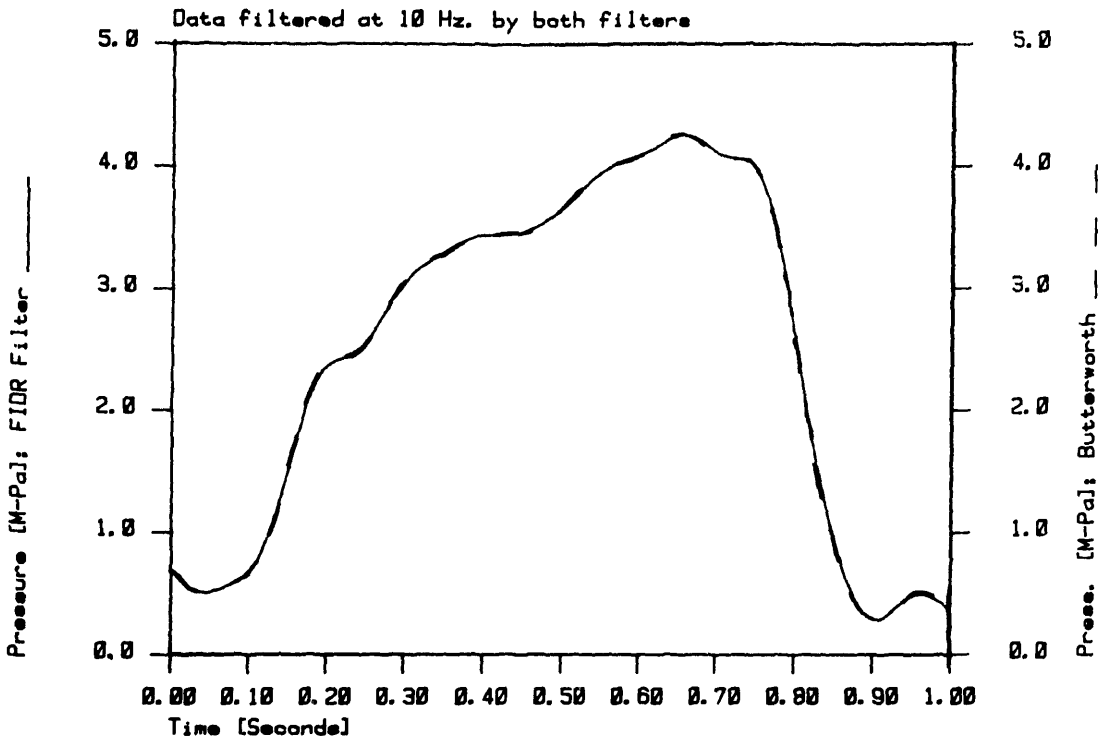

Figure IV-11: Comparison of filters

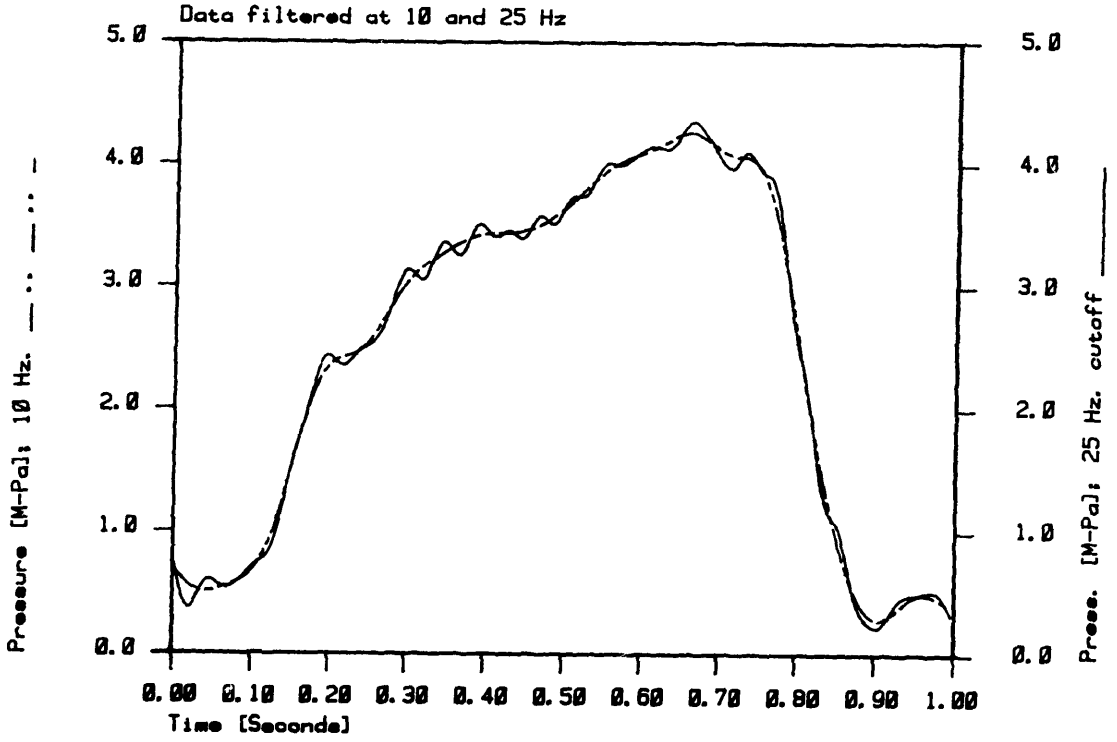

Figure IV-12: Level walking data

data.

1. Temporal Relationship of TRACK and Pressure data

The frequency of data acquisition is known for TRACK, forceplate, and pressure data. TRACK/forceplate data taken after December 1984 was acquired at 153 Hz. Pressure data has been taken 254 Hz, except during the two weeks immediately after prosthesis implantation. At that time one day of data was was taken at 254 Hz, but most was taken at 10 Hz. Data acquisition is started simultaneously for all systems. As a result of the high frequency of data acquisition and the simultaneity of data it is convenient to consider both pressure and kinematic data as continuous in time. It is then possible to choose a particular time in a data set and read the appropriate kinematic, pressure, and forceplate information for the selected time. Display programs have been developed for both the M.I.T. and M.G.H. graphics systems to display pressure and forceplate data individually or concurrently. Hip angles may also be displayed in a graph of degree vs. time. Kinematic information appears to be most helpful when it most closely resembles a human form and is thus usually displayed in the "quadrahedron" form, as developed by Bob Fijan [33]. The precise time in a data set at which something of interest occurs may be easily determined at M.G.H. on the graphics terminal by user selection of a cursor position relative to the pressure or forceplate graph displays, or reading the information output to the terminal by the kinematic display programs. At MIT the process is somewhat more laborius, involving either estimation of time from graphs or narrowing down the range of time for

which data is displayed. The entire data file is initially shown (at M.I.T.), the operator specifies initial and final times, the data is displayed for this range of time, and the process is iterated until the user is satisfied. This allows accurate determination of the time at which data of interest occurs but is not as simple as pointing to a part of the data and allowing the computer to calculate time, as may be done on a graphics terminal.

2. Coordination of Kinematic and Pressure data

An evaluation of pressures, contact area, or force, in the hip can focus on one or both of the joint components. In the present research the existence of accurate kinematic data makes it appropriate to look at the pressure distribution on the acetabulum surface rather than the femoral head. This option is attractive because;(1) The pelvis changes orientation in the inertial reference frame to a smaller degree than the femoral head; (2)Pressure can in principle be sensed at any location on the acetabulum but only at discrete locations on the femoral head;(3) It has been found [90] that the force vector excursions at the hip assume limited directions with respect to the femoral head;(4) The data may more easily be compared to that obtained with similar prostheses from in vitro experiments; (5) Finally, other research efforts at M.I.T. are addressing the role of cartilage in synovial joint mechanics and osteoarthritis and therefore the response of natural cartilage in vivo is of intense interest. This section will give an overview of the procedure used to accomplish the coordination of data, followed by a more in-depth evaluation of some of the methods. Much of the implementation was done by Bob Fijan.

a. Overview; The positions at which pressures occur are known on the femoral head, since the transducer locations are fixed. It seems a simple task to transpose these pressures onto the locations at which they occur on the other side of the joint surface, the acetabulum. However simple this task may be to the human mind, it is quite impossible for a computer having no knowlege of the spatial relationships between the leg and pelvis. The nature of the data collected by the TRACK system makes it possible to attack the translation from prosthesis coordinates to acetabulum coordinates in a somewhat more roundabout manner. Figures IV-13, IV-14, and IV-15 provide a guide to the following outline of this method.

Pressures have been obtained at locations which are fixed and defined with respect to the prosthesis as shown in Figures IV-13 and IV-14. The relationship of the prosthesis to the femur is known from the implantation technique and X-rays. Thus it is possible to transfer from the prosthesis coordinate system (P) to one fixed with respect to the femur (F). The TRACK system provides the relationship between the femoral coordinate system and the pelvis coordinate system (H) in the form of flexion, abduction and rotation angles as defined in Figure IV-16. Given this information, estimates (made from X-rays, by Dr. A. Hodge of MGH) of the location of the acetabulum with respect to the pelvis are used to transform locations in the pelvis coordinate system to their representation in a coordinate system defined with respect to the acetabulum (A). This coordinate system has been arranged so that a surface defined by unit radius and the lines of longitude and latitude (as shown in Figure IV-17) coincides approximately with the acetabular surface. The mathematical

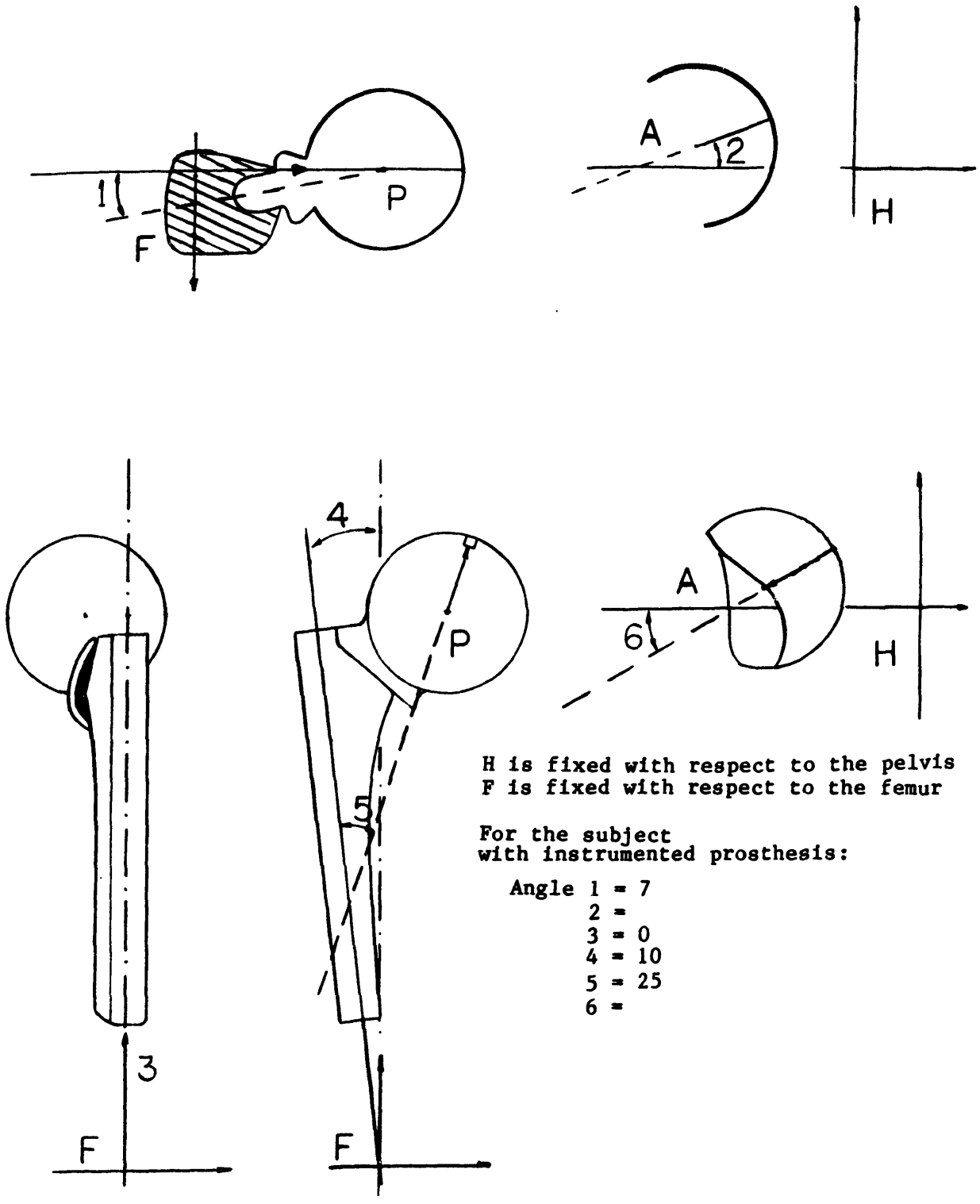

H is fixed with respect to the pelvis
F is fixed with respect to the femur

For the subject
with instrumented prosthesis:

Angle 1 = 7
2 =
3 = 0
4 = 10
5 = 25
6 =

Figure IV-13: Diagram of coordinate systems used in transformation from prosthesis to acetabulum coordinates.

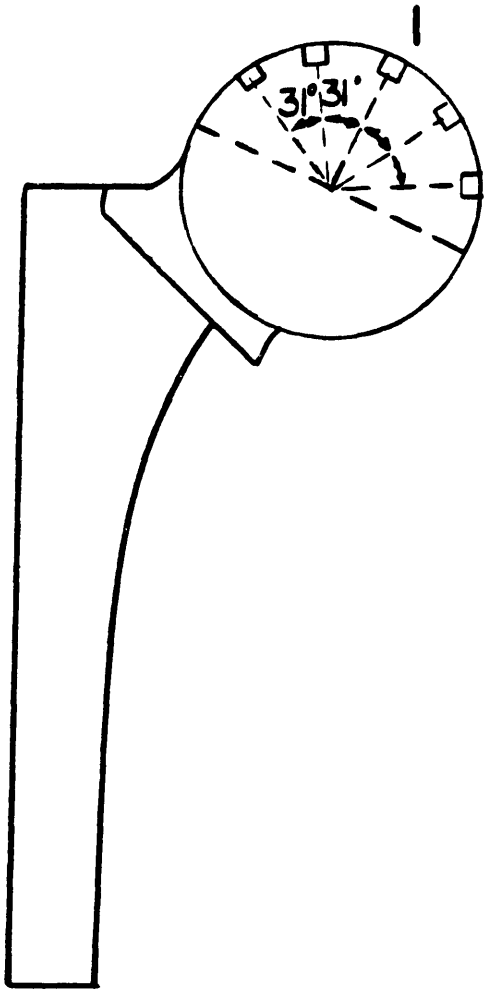

Figure IV-14: Positions of transducer 1 and inner and outer rings of transducers relative to prosthesis stem.

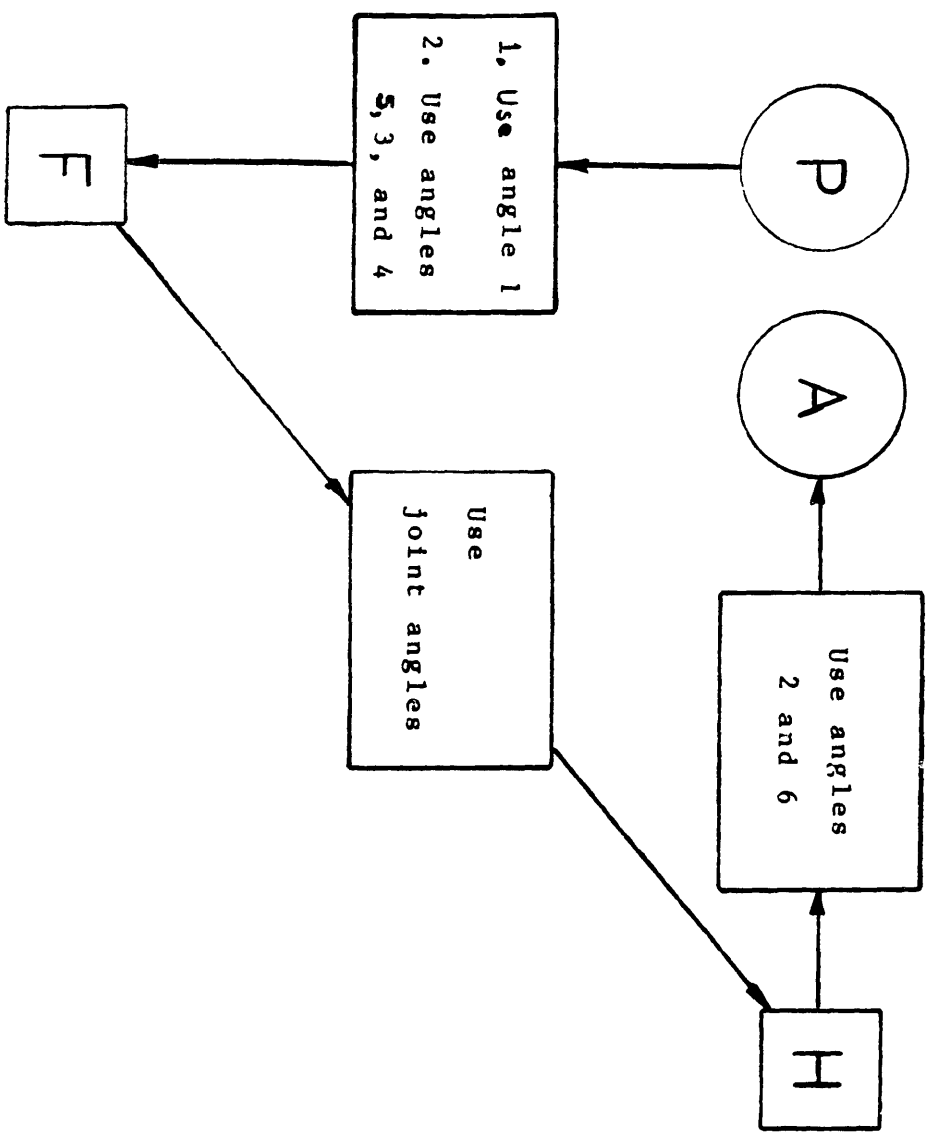

Figure IV-15: Outline of transformation

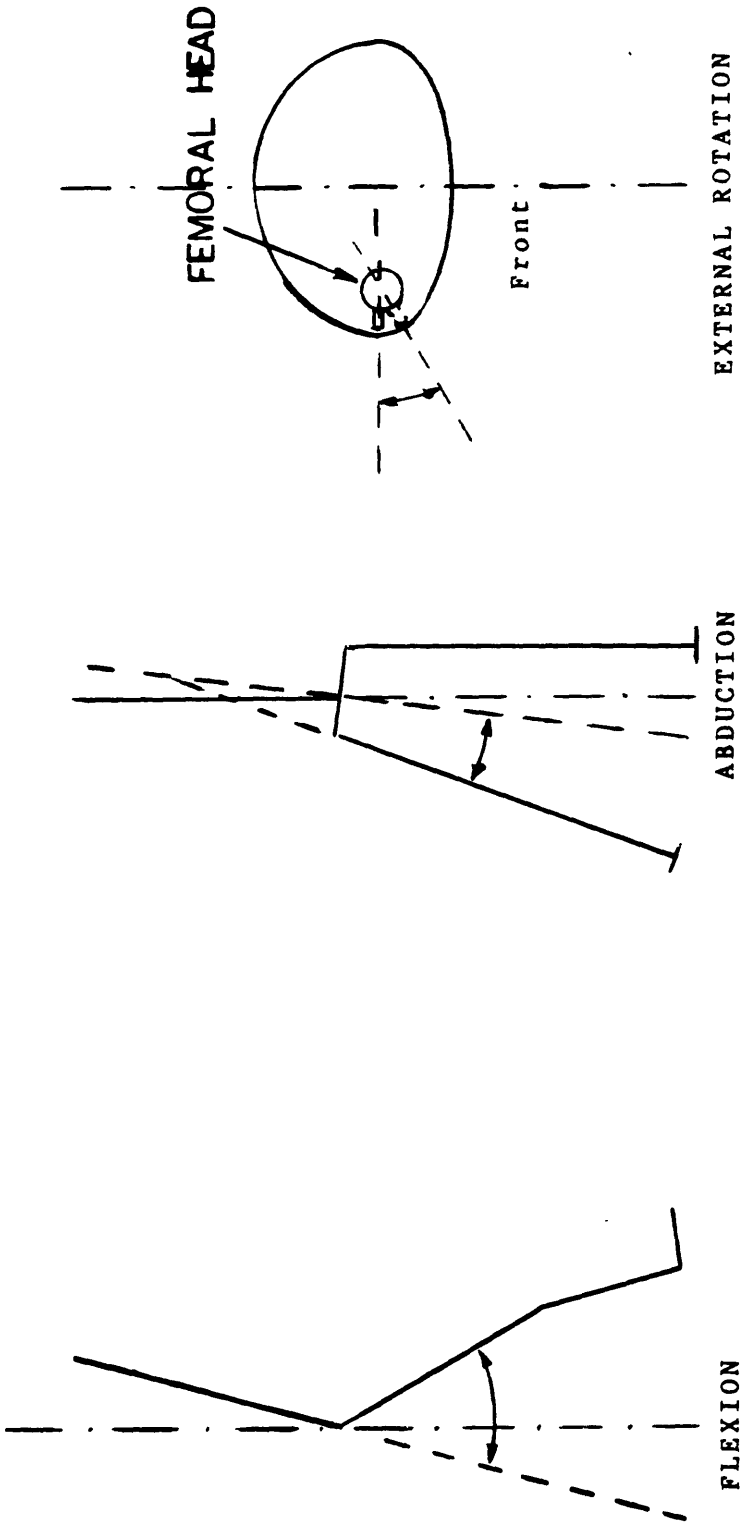

Figure IV-15: Definition of hip joint angles

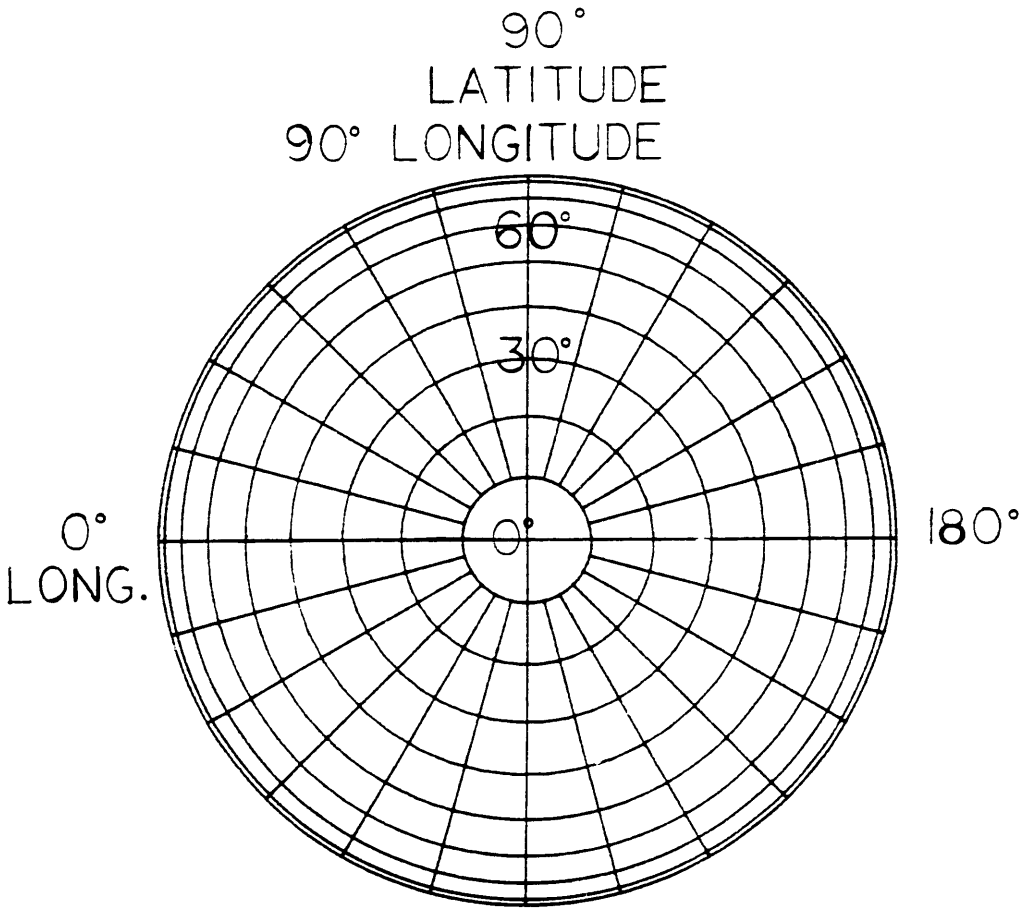

Figure IV-17: Latitude and Longitude on the surface of the joint looking in a lateral direction along the acetabular outward normal.

formulas used in the transformation of coordinate systems are presented in Appendix 3.

The location of all transducers in acetabular coordinates is stored in the form of longitude and latitude for each transducer. Fewer numbers could be stored, positions for two transducers would be sufficient to give location and rotation of the femoral head in the acetabulum, but computation time while running display programs would be increased. Programs requiring locational information read files containing transducer positions and extract the information germaine to the problem at hand. The TRACK data acquisition frequency must be known when getting this information since the kinematic data is used to obtain the positions. However, the speed of data acquisition for both pressure and kinematic data is sufficiently high that no quantifiable error is introduced by assuming both are continuous in time, as mentioned in the previous section.

The joint angles used in transformation from femoral to pelvic coordinates are known within error bounds of +/- 2.5 degrees. All three angles affect the acetabular latitude and longitude obtained. The position at which pressures have been measured is known within the region of the joint surface dictated by kinematic error limits. Description of this region in terms of acetabular latitude and longitude is not done because the same size region will have different latitude and longitude limits depending on the latitude of the original position. Distance on the surface of the sphere which fits the joint is a more general measurement, and has been used in presentation of acetabular position accuracy and change of location during the time period over which loading rate was calculated.

Joint-surface distance has been calculated and presented as a percentage of the acetabular sphere circumference.

The coordination of kinematic and pressure data does not end with the calculation of acetabular positions. The numerical value associated with transducer locations is not very helpful to a human attempting to comprehend the pressure environment at the joint. Thus a final step involved is the return to a visual display of information. This has been attempted through two separate displays, a two-dimensional projection, and one simulating three dimensions.

i. Two-Dimensional Acetabular Display

For the display of locations on the acetabulum the latitude and longitude associated with each transducer at a selected instant in time are converted to an orthogonal coordinate system with origin coincident to that of the spherical coordinate system, with assumed unit radius. The X and Y values for each transducer are then scaled appropriately and displayed on a graphics terminal or plotter. For reference, the equator of the sphere may be displayed. It was found that comprehension of locations was facilitated by the presence of physiological landmarks drawn in correct position relative to the data. Thus the display shown in Figure IV-18 was developed.[*] The position and orientation of the freeform acetabulum drawn

---

* Used a drawing program on a Megatek graphics terminal, stored points in file and reconstituted on any given available graphics plotter.

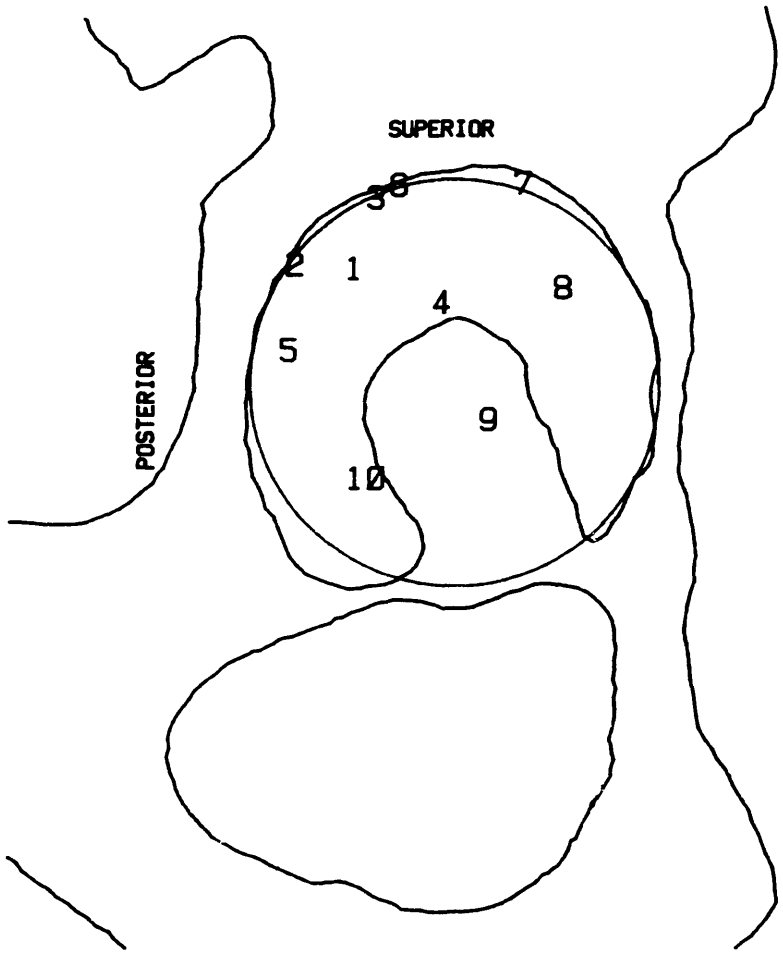

Figure IV-18: Display of transducer locations in hip joint. View is into socket with the acetabulum outward normal (Fig. IV-13 and IV-14) perpendicular to the plane of the figure. Equatorial line of spherical joint surface is shown.

in Figure IV-18 approximates that of the equator of the "acetabular" sphere as is also demonstrated in Figure IV-18. Figure IV-19 displays the relationship between acetabular latitude and longitude as defined in Figure IV-16 and the pelvis/acetabular drawing. Figure IV-19 displays the latitudes 0, 45, and 90 degrees and indicates longitudes of 0, 90 and 180 degrees.

ii. Hemisphere Display

The display in Figure IV-20 simulates three dimensions by adding the circles of latitude and longitude on an acetabular hemisphere and drawing pressures as vectors with length proportional to pressure emanating from their location on the hemisphere. The view in this figure is looking through the bone toward the back surface of the acetabulum, from a position forward and above the acetabulum. Although not a traditional physiological reference position, this view is made comprehensible by the addition of a pelvic outline as it appears from this position. The acetabular hemisphere representation is accomplished by defining selected lines of latitude and longitude in the acetabular coordinate system (Figure IV-16). All points on this hemisphere are then transformed to a new coordinate system using Euler angles. The precise method employed is given in Appendix 3. After this conversion, the 2-D projection of the results is drawn on the terminal, points having a negative Z value (the Z axis being normal to the graphics terminal surface) are not displayed. The pressure "vectors" are defined and rotated in an identical manner, but are drawn even if their Z coordinate is negative. Vectors beginning on a hidden surface of the hemisphere are drawn in a different color or line type until past the

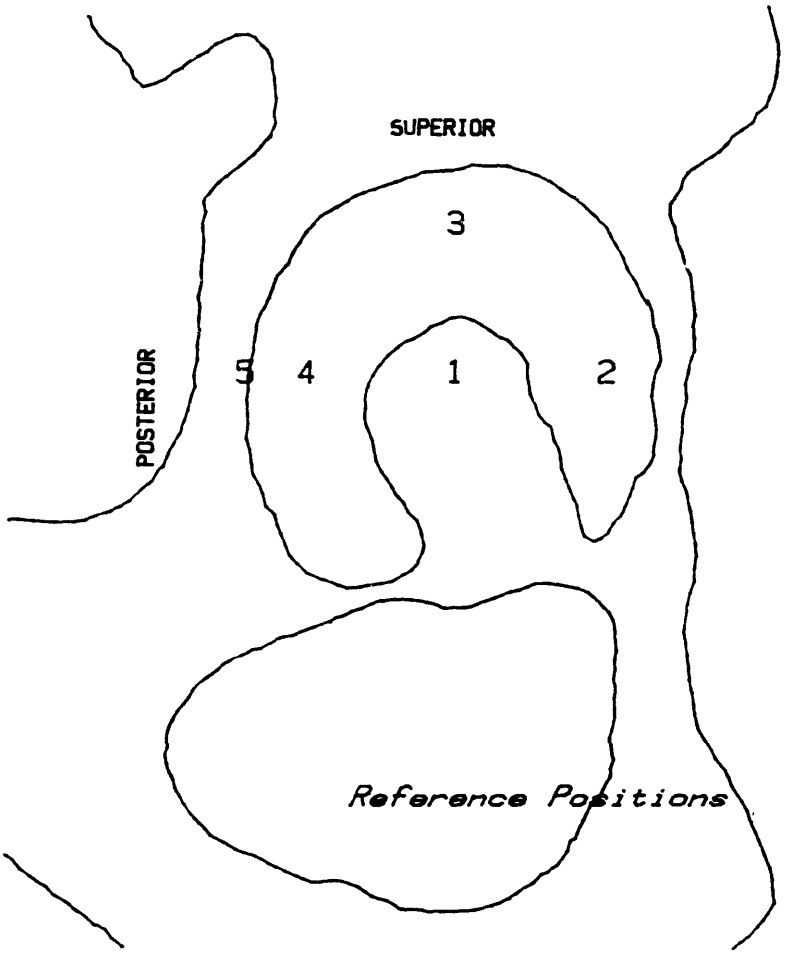

Figure IV-19: Positions in acetabular display corresponding to longitudes of 0, 90, and 180 degrees and latitudes of 0, 45, and 90 degrees.

POINT	Lat.	Long.
1	0	0
2	45	0
3	45	90
4	45	180
5	90	180

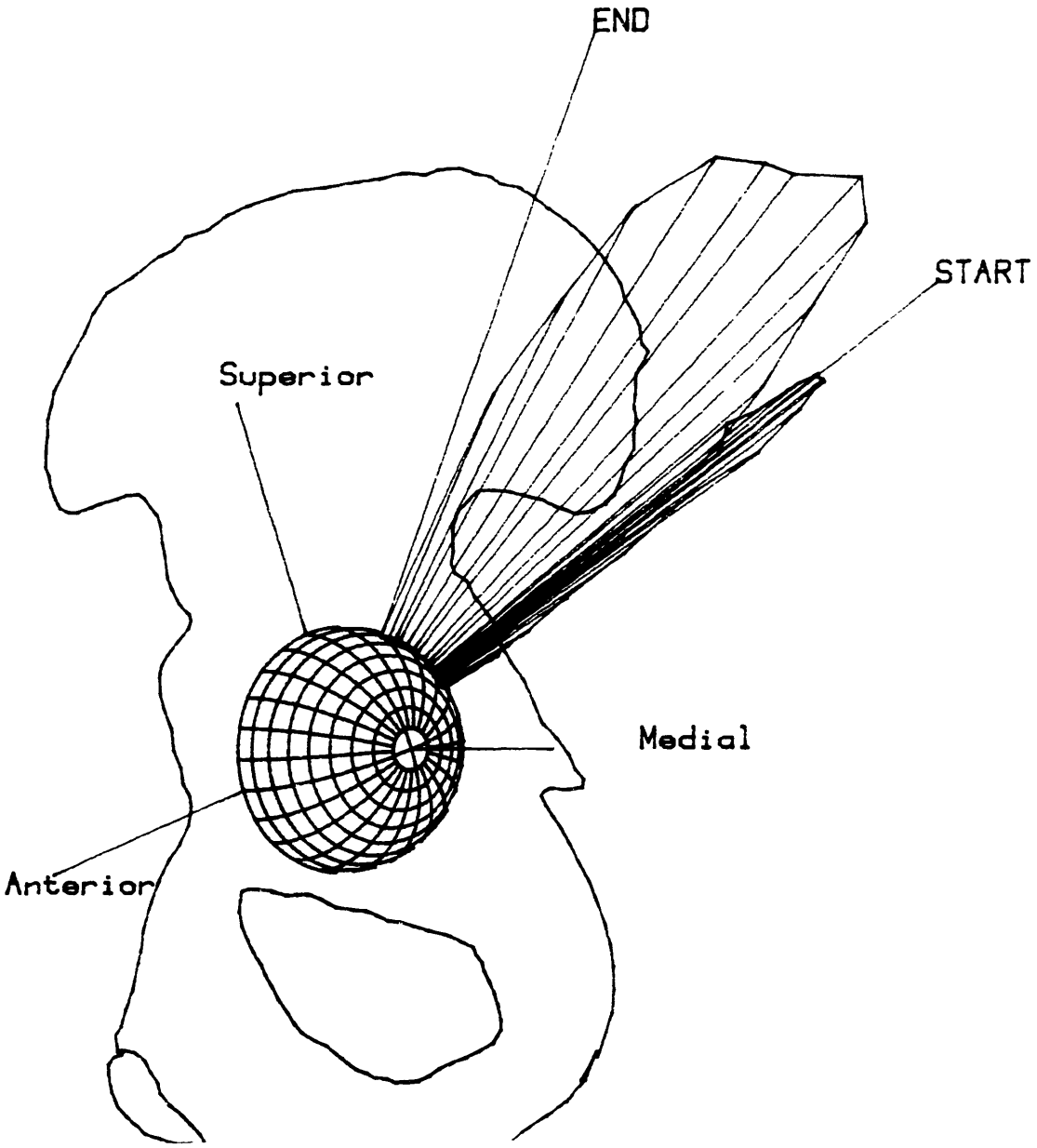

Figure IV-20: Hemisphere display of hip joint surface and pressure measurement locations over an interval of time. View is from the center of body directed through the bone backing the acetabulum.

The labelled axes are:

"Anterior" corresponds to 0 degrees longitude in acetabulum;
"Superior" is 90 deg. longitude;
"Medial" is 0 deg. latitude.

Length of lines extending from the joint surface is proportional to the instantaneous pressure measurement recorded at that location.

ouline of the hemisphere. Vector scaling may be done automatically, or through user-input values.

This form of display is appropriate for the presentation of data over a period of time, allowing a more complete depiction of the evolution of the loading condition during a given test.

D. Obtaining Isobaric Contours from Individual Transducer Locations

It was hoped that the in vivo pressures at points on the joint surface could be interpolated over the surface to obtain a distribution of pressures on the surface, through which iso-pressure contours could be drawn. Integration of the pressure distribution would give a resultant force vector at the joint. Rushfeldt [86,88] used this method for in vitro studies, with results such as that shown in Figure IV-21. However, he had available measurements at 256 locations on the joint surface. This was possible because the experiments were not performed on living tissue, could be carefully controlled, and the available orientations for the prosthesis were not limited by muscle and ligament tissue. The interpolations were thus quite accurate, and could be compared with the measured magnitude and direction of the force applied to the joint [86].

With an implanted prosthesis the possibility of carefully controlled rotations under known forces does not exist. It is thus not possible to determine the accuracy of pressure contours and force vector estimation in vivo with this prosthesis. There are pressure measurements at only 10 femoral locations for a given external force vector as measured at the

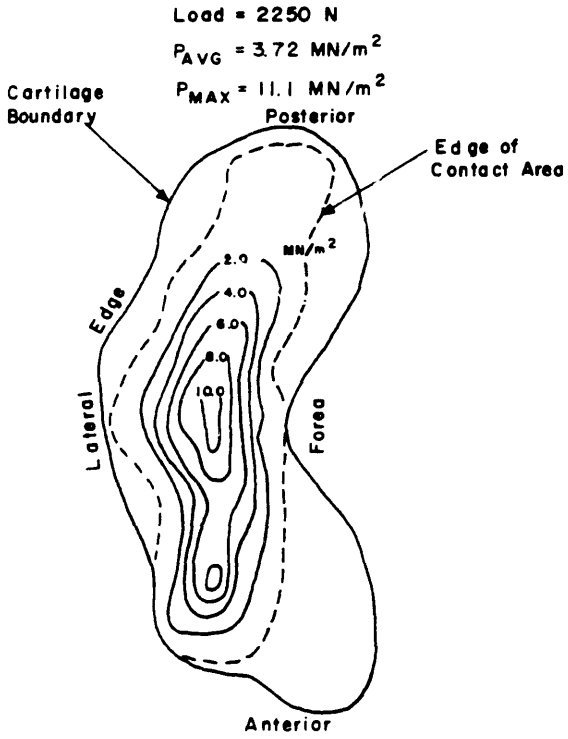

Figure IV-21: Isobar contours from Rushfeldt [78]

force-plate. These differences between in vitro and in vivo experiments were expected to greatly decrease the potential accuracy of in vivo data interpolation. Carvajal [106] used portions of Rushfeldt's in vitro data in an attempt to determine the accuracy of linear and quadratic interpolations using 10 points.

Contours and force vector estimates would be reasonably accurate were there a uniform or simple pressure distribution over the joint surface. However, Rushfeldt [86,87] has shown that the pressure distribution is complex and certainly non-uniform. The in vivo data presented in this paper supports the in vitro findings. Furthermore, for many actions, or femoral head positions, the number oftransducers actually in contact with the acetabulum is fewer than 10. (This has been shown by the transformation to acetabular coordinates, which allows estimation of the location of the foveal notch and the rim of the acetabulum.)

As a result of Carvajal's investigation and based on the judgement of researchers associated with this project, hip iso-pressure contours and force vector estimates have not been attempted for the in vivo data at this time.

E. Load Rate at the Hip Joint

Early in vivo data indicated the presence of high rates of loading at some femoral locations during certain actions. No prior data existed on the rate of load transfer and the magnitude of pressure changes which would be involved and few estimates had been made [78]. Quantification of the rate of loading that occurred at the hip and its relationship to external force was undertaken.

The simplest method of determining the load rate at a transducer is to calculate the slope of its pressure measurements (P) over the time (t) interval of interest:

$$\text{Load rate} = \Delta P / \Delta t \quad [\text{M-PA/sec}]$$

Limitations with this method are: the time frame must be selected; the transducers must be examined individually; and the load rate is measured at a femoral location which is usually moving with respect to the acetabulum. Locations on the acetabulum at which instantaneous load rates occur can, in principle, be determined but this would involve both the coordinate system transformations already developed and adequate confidence in the interpolation of the pressure field in the interarticular space.

Numerical differentiation of the pressure magnitude over the entire test was considered and performed on a few tests. However, numerical differentiation requires very smooth data and becomes unstable around abrupt changes. The pressure data contains sharp changes and reversals

during the performance of some motions.

The method of determining maximum load rates is indicated in the flow chart of Figure IV-22. Not all transducers are examined closely for each test; a decision of which to study is based on the pressure vs. time record, as is the time interval to use. Load rate is calculated from filtered data. No loss of information results from this practice since filtering did not significantly alter the pressure variation in time. (Figure IV-12) The load rate between sequentially occurring maximum and minimum pressures during the selected time interval was also calculated. The load rates that are presented in the results section are slopes, M-Pa/sec, of pressure vs. time. The arc distance on the acetabulum over which the load transfer occurs is also given.

The maximum measurable load rate for this data acquisition system is constrained by the frequency of data acquisition and the range of the pressure transducers. Pressure changes occurring at less than 127 Hz may be measured, since pressure data is acquired at 254 Hz. The diaphragms of the pressure transducers in the implanted prosthesis will not yield at pressures below 41.35 M-Pa (6000 psi). The calibration of transducers was carried out up to 6.9 M-Pa (1000 psi) and they displayed linear behavior up to and including that point. If a maximum pressure change between frames of 6.9 M-Pa (1000 psi) is allowed and the minimum time in which this may occur is 1/127 sec then the maximum load rate is 880 M-Pa/sec (127 x 10**3 psi/sec). This is much larger than any load rates determined thus far and is not necessarily a limit since a pressure jump of more than 6.9 M-Pa (1000 psi) may occur.

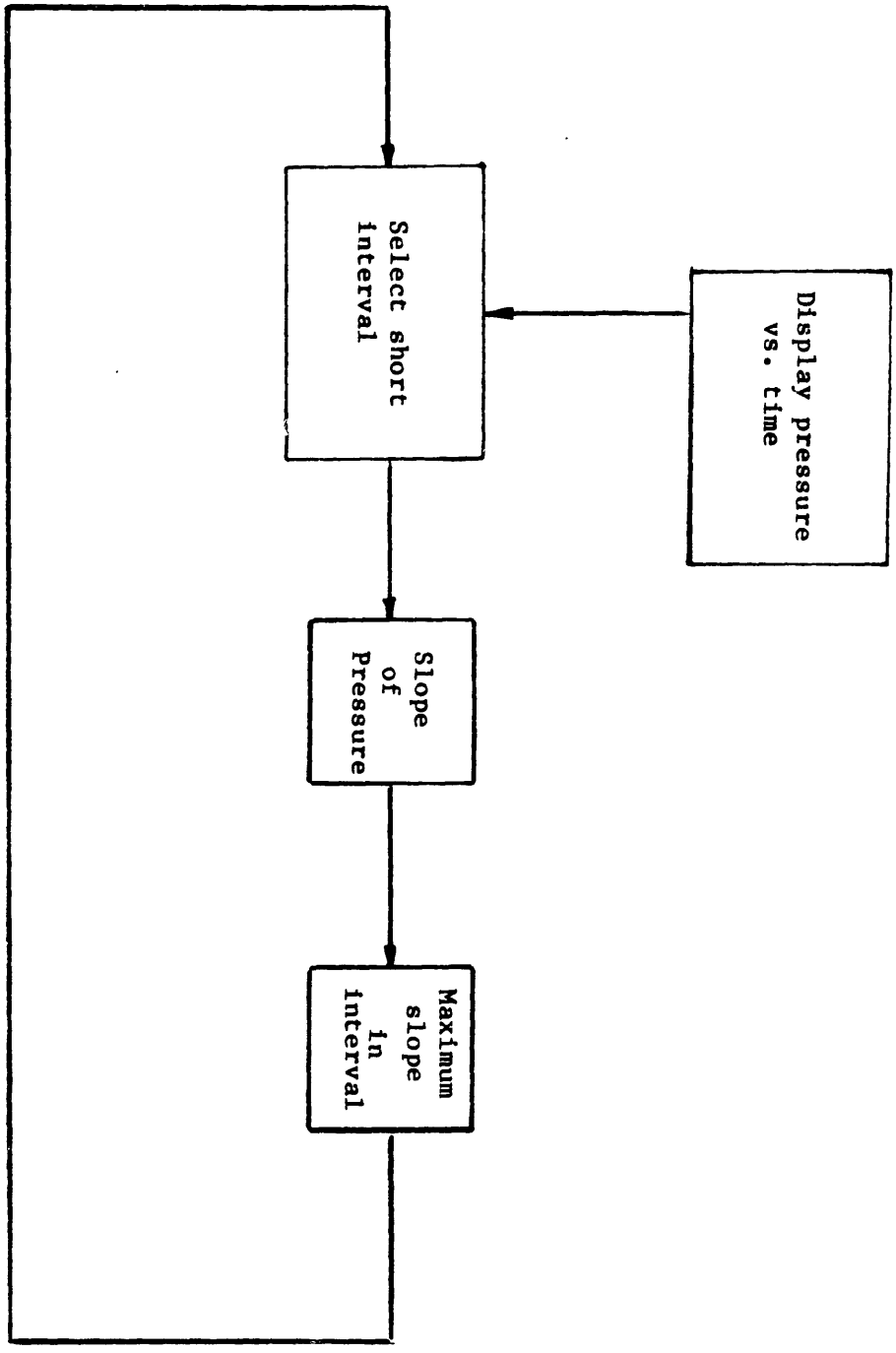

Figure IV-22: Typical procedure followed when obtaining rates of loading.

The timing of maximum pressure rate relative to external force rate of change was determined. The time of maximum increase in total external force was found and compared to the time at which the maximum pressure change occurred (at the transducer measuring the largest load rate). More than one transducer was examined if the rates of change exhibited were comparable.

F. Reproducibility of Pressure Data

The relevance of data obtained from the in vivo prosthesis is affected by three factors: 1) the degree to which the measurment system replicates the actual conditions; 2) the influence of the measuring device on the joint; 3) the ability to extrapolate general conclusions from a limited number of tests. The accuracy of measurements has already been discussed and has been assumed excellent. The replacement of the natural femoral head by a metallic ball undoubtedly changes conditions in the joint. However, even if the joint behavior is completely dissimilar to that occurring in normal hips the results from the instrumented prosthesis are applicable to joints composed of a normal acetabulum and a prosthetic femoral head, a large and much-studied sub-set of hip joints. In addition, the original decision to employ the endoprosthesis approach for both the in vivo and in vitro experiments of the M.I.T/M.G.H hip research was (and is) based on the following argument.

The femoral head and acetabulum unloaded cartilage surfaces are known to be spherical from ultrasound measurements. Conceptually there is a spherical surface which bisects the interarticular space in the loaded and unloaded

joints. If a rigid endoprosthesis of this diameter replaces the natural femoral head the surface of the endoprosthesis becomes the bisecting spherical surface and the acetabular cartilage response will be similar to that of the natural joint. This is one of the reasons for care in fitting the correct diameter instrumented prosthesis. The division of a two-component system along a common surface and the substitution of a "half-space" for the absent component is very common in physics and engineering.

Use of test results to describe or predict load conditions at the hip is affected by the repeatability of measurements under a set of specified parameters. Pressures of approximately the same magnitude were expected to occur in each region of the acetabulum as the subject repeated actions. The presence of inexplicable, large, deviations from standard results for a particular test would have caused concern regarding the propriety of assuming pressure data followed predictable patterns.

Precise repetition of the loading environment at the hip was not expected for any specific action by the subject. Even on a single day, given one set of instructions, variation can arise from changing external situations (floor roughness, illumination level), small changes in body segment placement, or fatigue. Changes in the muscles used to complete a motion will lead to different pressure magnitudes and distributions for repeated tests. Whether the range of values which occur is acceptable must be assessed in some manner. Variation is known to be inevitable in the kinematic and forceplate data obtained in gait analysis. Electromyographic (EMG) data indicates that timing of muscle contraction varies in repeated

trials of dynamic tests.

A number of ways of determining the reproducibility of data were formulated and tried. The average pressure for each transducer during repeated static (90 deg. flexion, one-legged stance, etc.) tests was compared. Examination of the maximum and minimum pressures obtained at each transducer during static or dynamic tests may convince one of the repeatability of measurements. Data was also searched for a set of times at which hip angles and external forces were comparable, and the behavior of the pressure data for those instants in time was investigated. Comparison of the relative timing and magnitude of pressure changes throughout dynamic tests is desirable; this was accomplished through examination of pressure and forceplate data from several tests containing the same actions. The Fourier transform magnitude over a range of frequencies compresses information on both the pressure magnitude and frequency content; this was also tried as a means of comparing data from dynamic tests.

These ideas met with varied success. The most basic comparison made for all sets of data immediately after processing was tabulation of unfiltered maximum and minimum pressures at each transducer. These values were corrected for the transducer peak-to-peak noise. This method of comparison involves the least computation time and operator effort and gave an approximate indication of prosthesis behavior. After filtering maximum and minimum values were compiled for processed data.

After data has been processed and filtered kinematically similar times may

be selected. Sets of tests were searched for data in which the transducer locations in the acetabulum and the force on the forceplate were similar to those for a selected time. The increments of force and degrees in transducer latitude or longitude by which a frame was allowed to differ from the selected frame and still be considered similar were set by the computer operator. Times immediately surrounding the selected data were not considered. The computer first searched the forceplate data for times having similar external force, then compared the kinematic data by looking at the acetabular positions of two transducers during that instant of time. Times at which both force and location were within the specified tolerance were recorded and pressures were compared. A graph and basic statistical manipulations of the pressure measurements for a transducer during the comparable times were then available.

The merit of comparisons made in the fashion outlined above depends on the computer operator's judgement in selection of the original test and time, tests to search for similar data, and specification of the amount of leeway allowed for matching kinematic and forceplate data, Comparisons of, for instance, static standing tests and data from the stance phase of gait are probably not appropriate when attempting to assess the reproducibility of pressure measurements. The leeway allowed in accepting kinematic data as similar enough to compare pressures should take into account the noise and accuracy of kinematic data and the inherent variability in human motion.

The magnitude of the Fourier transform of pressure data over a range of frequencies contains information on the amplitude and frequency content of the data. Comparisons made between data sets produced unpredictable

results. An attempt to compare data sets involved calculating;

$$j = \sum_{u=1}^{127} \left(a_1(u) - a_2(u)\right)^2 / u$$

in which $a_i(u)$ are the magnitude of the Fourier transform at frequency u. This criteria, somewhat like a sum-of-error-squared performance measure, did give an indication of enormous differences. It also occasionally indicated a degree of similarity which did not exist in the time record of data.

The technique ultimately used in presentation of pressure reproducibility was comparison of transducer outputs over a selected period of time. This method relies on visual communication of information. The procedure is outlined in the flow-chart of Figure IV-23. The computer operator selects the time period for each test that will be compared on the basis of one of the three (kinematic, forceplate, and pressure) types of data. After selection of the time period the computer operator determines the transducers to examine, usually on the basis of approximate acetabular location. (For instance, transducers which may be in the foveal notch during a particular action are not likely to give information pertinent to cartilage.) The pressures registered by each selected transducer are plotted together versus the percentage of the sample time. Graphs of pressure at a transducer during one test may be plotted against pressure at the same transducer during another test; the result of this comparison will be a straight line if the tests are identical.

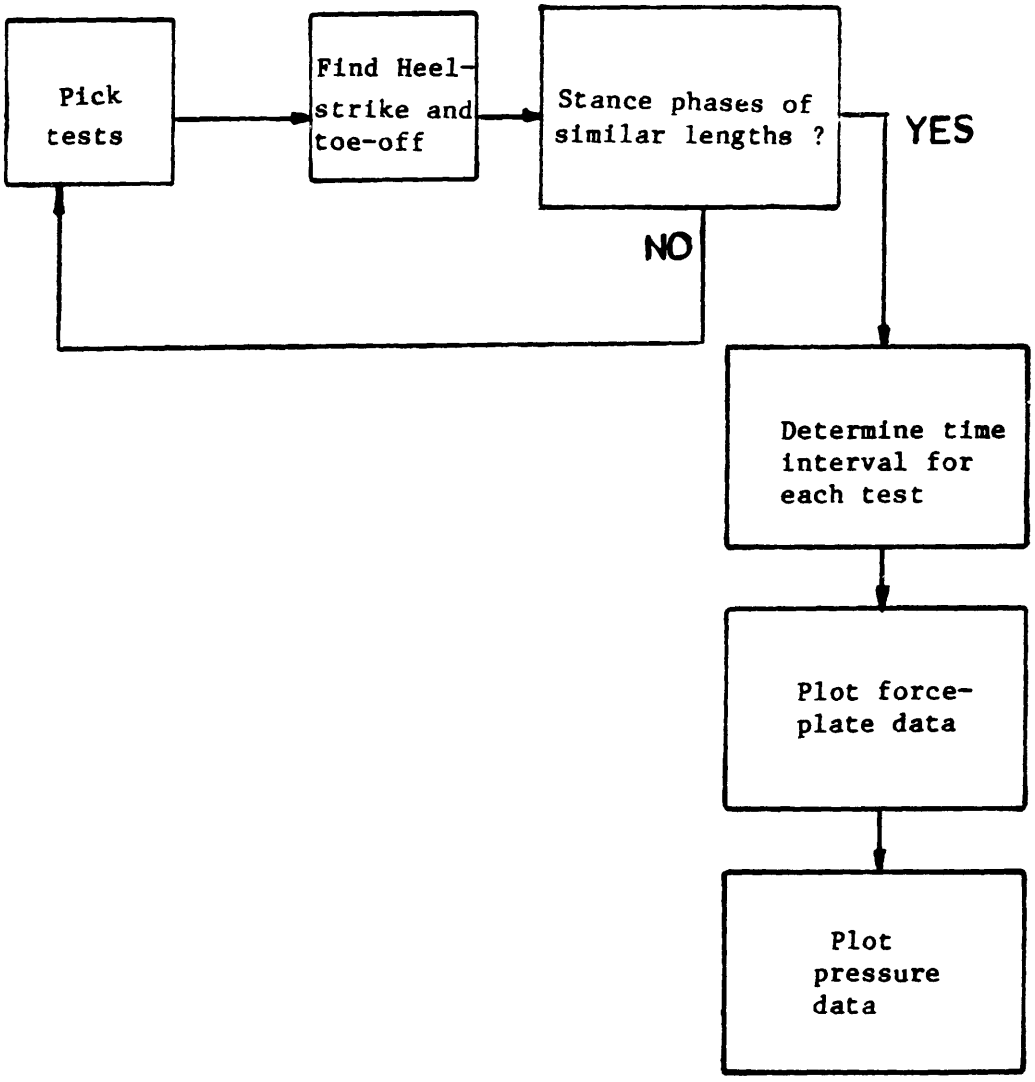

Figure IV-23: Process of assessing repeatability

The assessment of reproducibility of data made in this manner is also highly dependant on human judgement in data selection. In the course of this study samples were usually chosen on the basis of physiologically significant events, such as heel-strike on the forceplate.

The data most frequently examined through this method was from gait tests. One problem with using this data was that the subject's walking speed was much faster six-months after implantation than during the two-weeks after the operation (Figure V-11). Furthermore, her walking speed varied between days and tests after she had fully recovered; stance phase of between .7 and 1 second duration were found. The forces in the joint change with speed of locomotion [90, 78, 28]. Data for similar walking speeds was compared to assess the reproducibility of data.

Figure IV-24 compares the forceplate vertical force record for the stance phase of four gait cycles - two done in May 1985, one in December 1984, and one in August 1985. These samples were chosen to begin .1 seconds before heel strike. Figure IV-25 presents the forceplate recordings for the same four walking tests, but in this figure the samples are normalized by stance phase duration. Each set of data begins prior to heel strike, the time between the start of the data sample and heel strike is equivalent to 10% of the stance phase length. The display of each cycle ends at a time 10% of the stance phase duration after toe-off. Pressure data is displayed over the same time interval as forceplate data. Pressure data for the four cycles is shown in Figures IV-26 through IV-29. Figures 26 and 28 are for equal time periods, corresponding to Figure 24. Figures 27 and 29 are associated with Figure 25. As can be seen, the pressures in the joint were

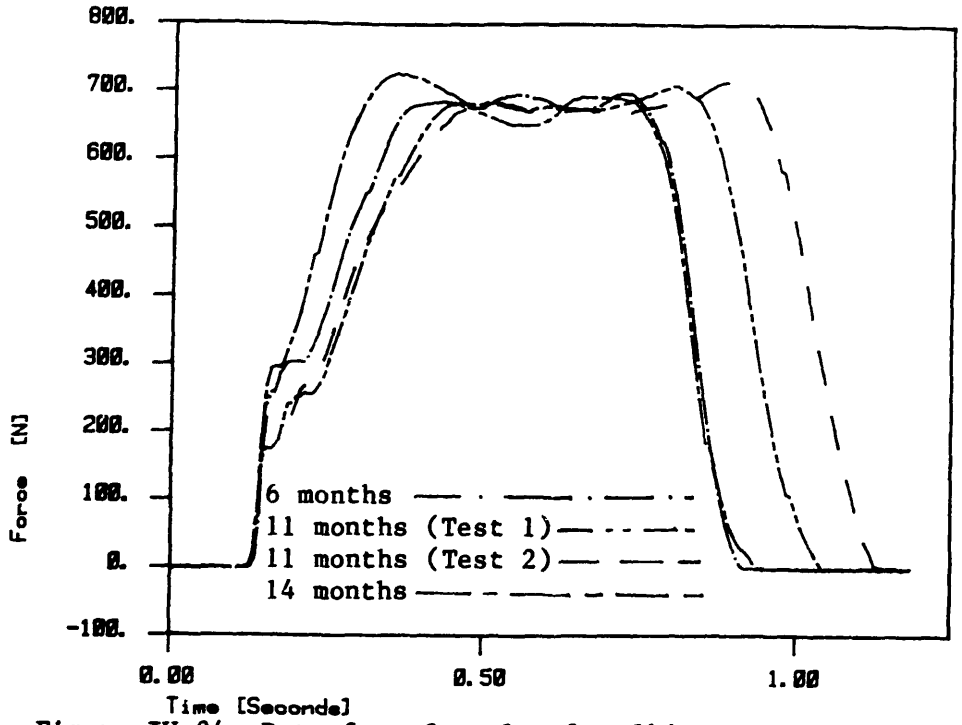

Figure IV-24: Data from four level walking test; 1.2 seconds shown for each test.

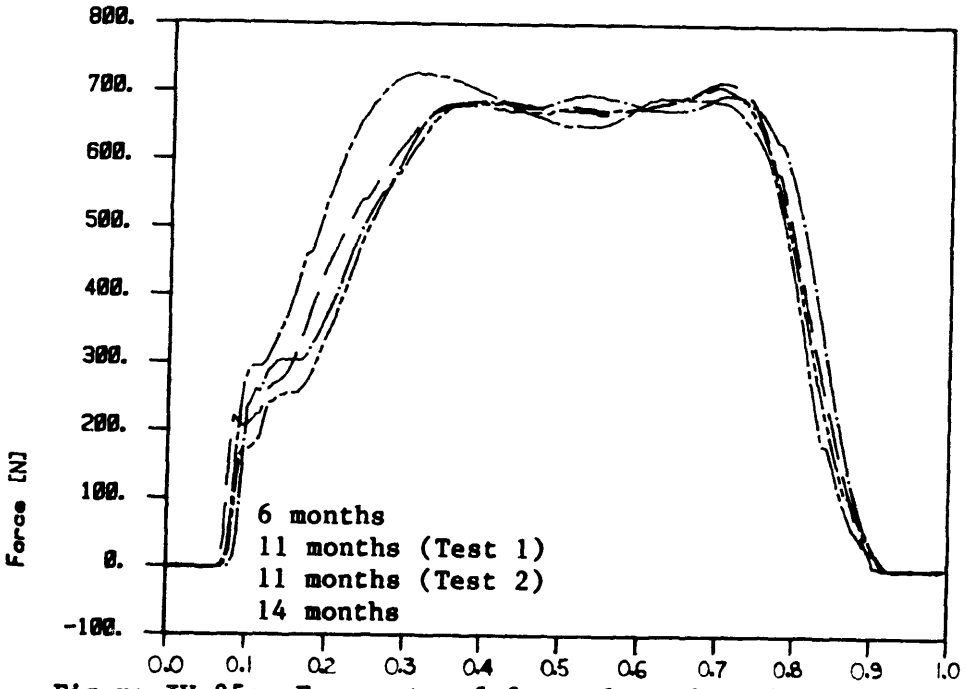

Figure IV-25: Four sets of forceplate data for walking normalized by stance phase duration. Beginning is 10 % of stance phase length before heelstrike. End is 10 % of stance phase length after toe-off.
(Same data as shown in IV-24)

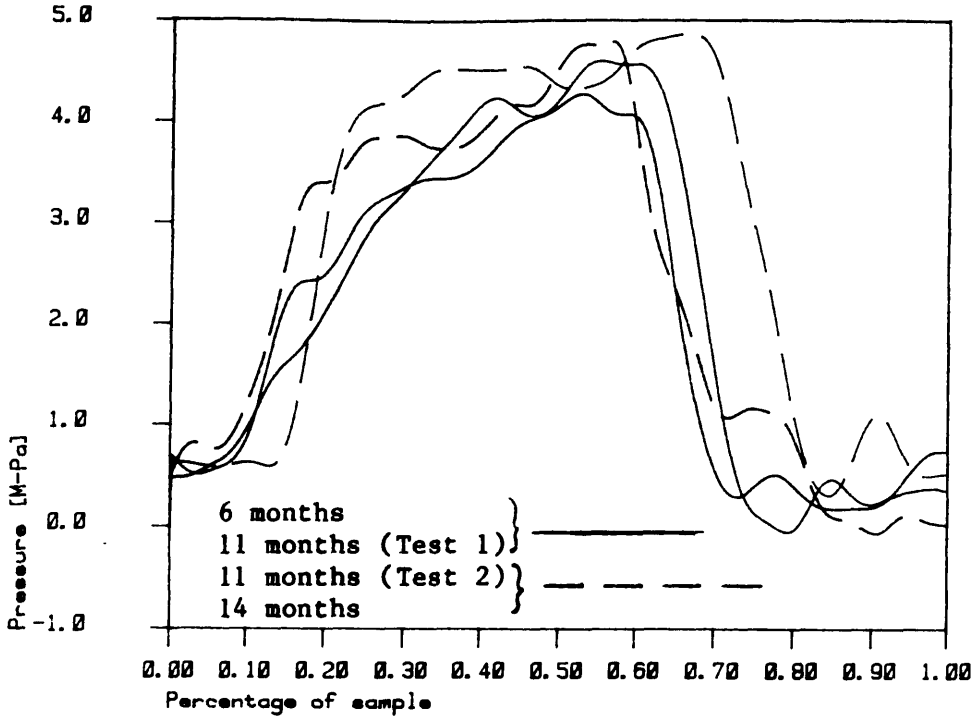

Figure IV-26: Pressure at transducer 5 associated with forceplate data shown in IV-24.

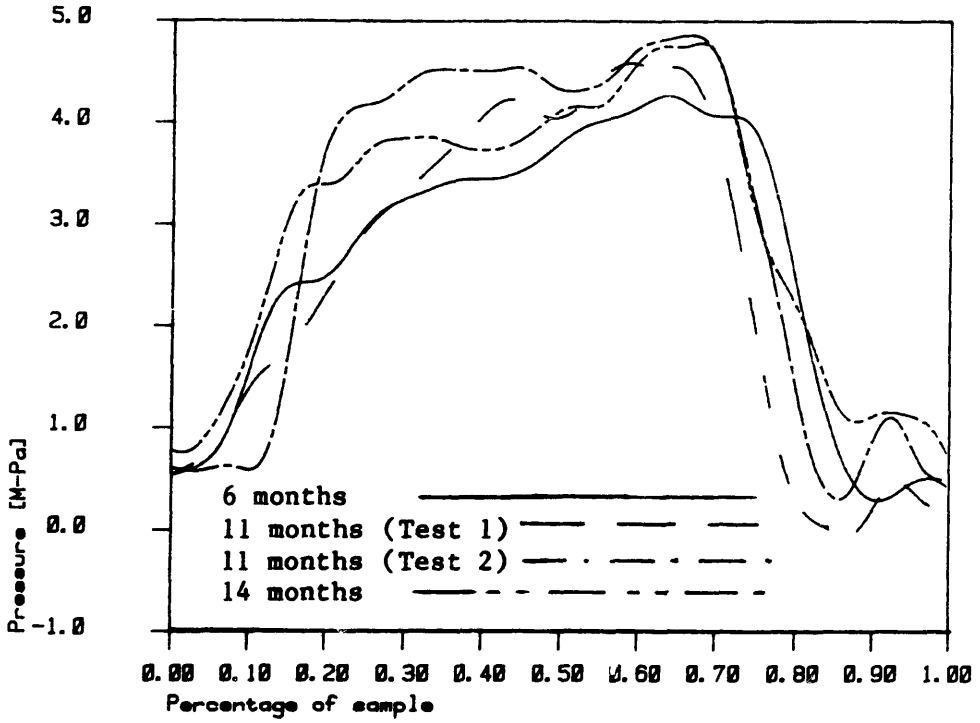

Figure IV-27: Pressure at transducer 5 associated with forceplate data shown in IV-25.

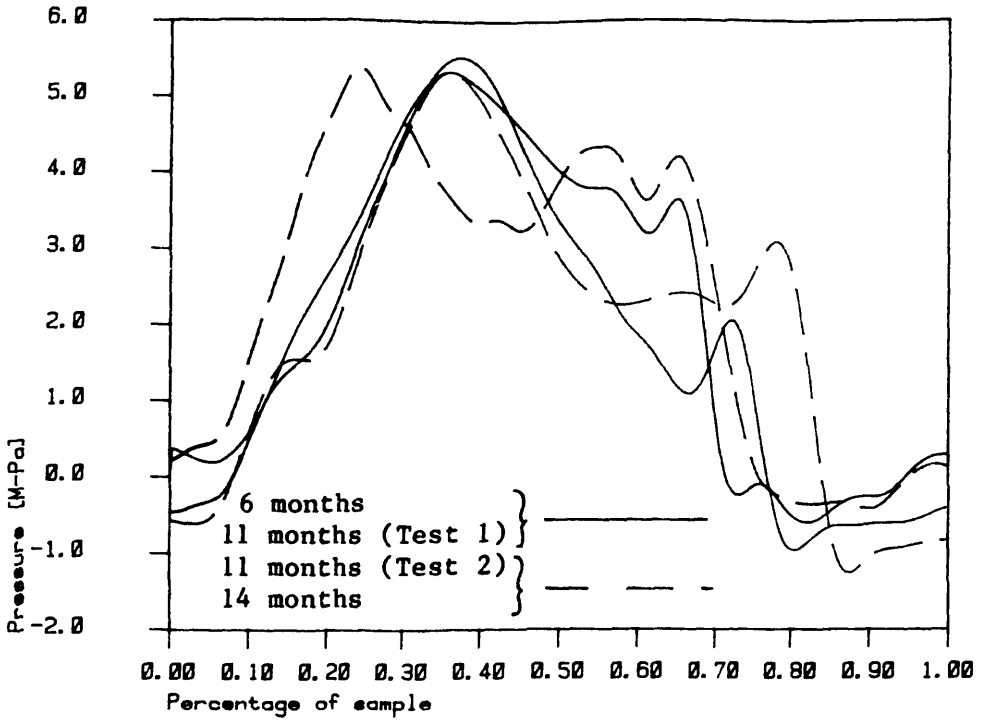

Figure IV-28: Pressure at transducer 3 associated with forceplate data shown in IV-24.

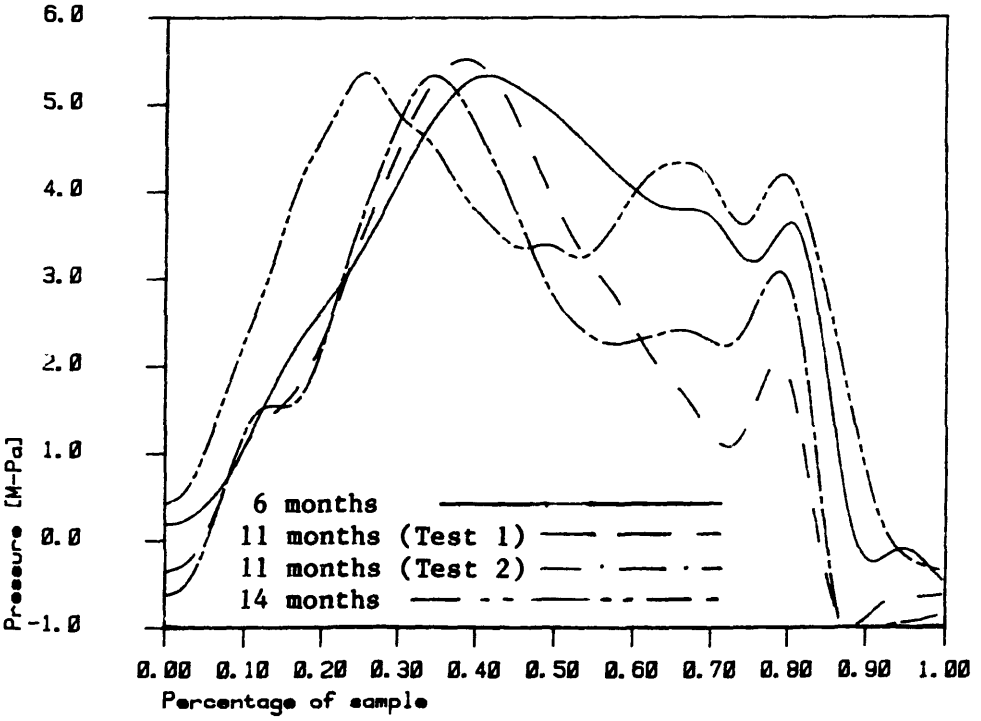

Figure IV-29: Pressure at transducer 3 associated with forceplate data shown in IV-25.

not very different from test to test. Kinematic variation, differences in the hip joint angles, contributes to the changes in pressure observed at any one transducer at a particular part of a movement. The path of the transducer presented in Figures 28 and 29 during cycles from December and August is presented in Figures IV-30 and IV-31.

Figure IV-30: Hemisphere display of pressure during stance phase for transducer 3, from data taken 6 months post-operative. Vectors drawn at about 20 Hz.

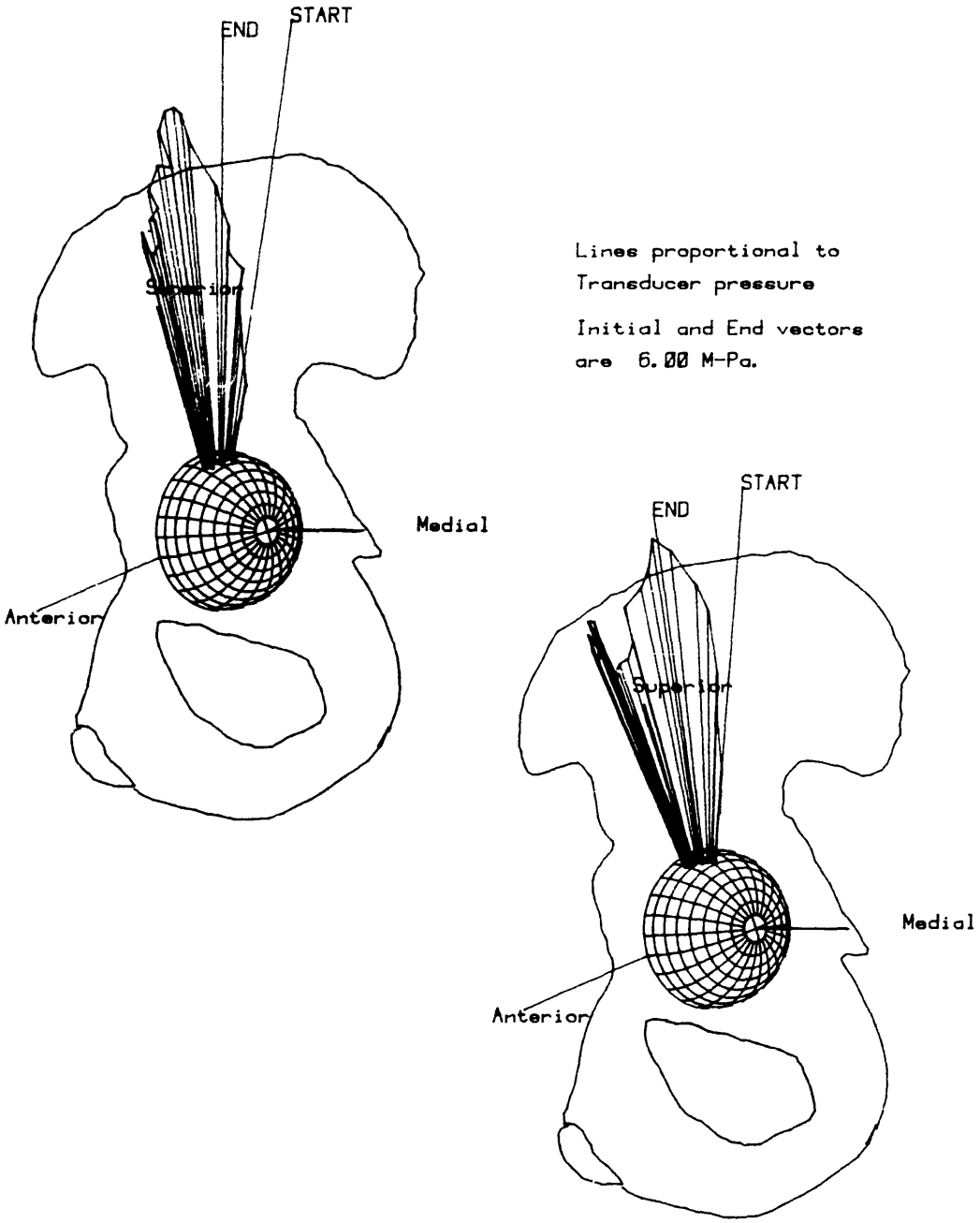

Figure IV-31: Hemisphere display of pressure during stance phase for transducer 3, from data taken 14 months post-operative. Vectors drawn at about 20 Hz.

V. Results

A. Overview

An enormous amount of data has been collected from the implanted prosthesis. A variety of displays and tabulations have been developed to facilitate access to one aspect or another of data. No all-encompassing means of communicating the extraordinary amount of information contained in the prosthesis data has been developed, nor is this likely in the future. The data presented in this section will be shown in the manner deemed most appropriate for that specific test or type of test.

The data can be divided into two categories by its time character. Data has been gathered during either posture or movement; data is either static or dynamic. Static data is that taken while the position of the subject did not change beyond the inevitable micromotion of the muscloskeletal system. Dynamic data is that in which the subject was moving, performing an action. Static data is probably adequately represented by tabulation of transducer maximum, minimum or average values, with the addition of a single view of transducer locations in the acetabulum. Dynamic data is more difficult to portray, as the position, external force, and 10 pressures all change over the course a test. Maximum pressures may be interesting, as may the record of pressure vs. time, but transmission of information on location, pressure, and pressure rate of change for 10 transducers, in addition to the external force, requires either a great many graphs and pictures or some more concise depiction. Data from dynamic tests has been displayed in numerous ways; several were found helpful and

have been used in this section. Information on load rate at the joint surface has been included for certain dynamic tests.

Dynamic data may be further differentiated by test type. Many types of dynamic tests were done, see Table III-1 for descriptions of the tests performed. Motions associated with the activities of daily living are presented here, including gait, stair-climbing, and rising from a chair. Results from jogging tests performed one year after implantation have been included. Some results from walking with supplimentary support are presented and compared with gait results. Also included are results from a test devised in the course of this project, a "heel bounce", in which the subject rose on her toes, then dropped abruptly onto the forceplate.

Another division of data may be made by the progression of time, post-operatively, over which data was taken. Included are data from two weeks, six months, and one year into the subject's rehabilitation. The prosthesis was implanted on June 20, 1984; data was taken on most of the following 16 days. December 1984 was approximately 6 months after the operation. The period from May 1985 to September 1985 was approximately a year after implantation and the post-surgery month in which data was taken is indicated in figures and tables. Comparison of data from one period with that from another must recognize the improving physical status of the subject, in fact in some activities the subject appears to be continuing to gain strength one year after the operation. The speed at which actions were performed also varied between test dates and increased as the subject recovered.

Pressure measurement locations in the acetabulum are not available for tests performed immediately after implantation, in June 1985, and in September 1985.

B. Static Data

Mostly static data was taken during the initial post-operative stage. A few of these tests were repeated at later dates. Static test descriptions and information from the initial post-operative period are given in Table III-1. Average transducer pressures for some of these tests are included in Table V-1; these averages were calculated using unfiltered data. For some frequently repeated tests the averages are composite means over all similar tests performed in the initial postoperative period.

Figure V-1 presents the positions of transducers in the acetabulum while the subject is standing in normal posture. This figure is the projection of transducer locations on the equatorial plane of the sphere fitting the joint space. The normal to the paper at the center of the acetabulum corresponds to the acetabular outward normal. Table V-2 contains the average pressure at the three highest reading transducers for static standing tests done in July and December 1984, and May 1985. The locations in the acetabulum at which these pressures were measured are presented as latitude and longitude for comparison with transducer location in dynamic tests.

In Figure V-2 the acetabular positions of transducers during single-leg stance are shown. In this test the subject stood with her weight on the

Table V-1: Average Pressures for a few early static tests.
Many other tests were performed.

Test Description	Pressure [M-Pa] at Transducer: 1	2	3	4	5	6	7	8	9	10
Abduction	-0.29	0.13	-0.19	0.06	1.36	0.50	1.57	0.21	0.13	-0.52
Flexion	0.77	0.26	0.73	0.02	0.30	-0.24	1.72	0.20	-0.08	-0.33
Active (0-90)	1.87	1.09	1.44	0.72	1.17	0.47	1.13	1.07	0.25	0.96
Passive (0-90)	1.68	1.13	1.36	0.84	1.21	0.76	0.96	1.15	0.43	1.23
Isometric Quadriceps Exercise	1.93	1.54	2.12	0.76	1.57	0.49	2.69	0.90	0.34	0.86
Neutral Position	1.06	0.94	1.02	0.70	0.89	0.41	0.61	0.78	0.28	0.72
Sitting	1.15	0.80	0.77	0.70	0.88	0.06	0.11	0.97	0.19	0.48
Standing with assistance	0.35	1.16	1.12	0.61	1.49	-0.09	0.59	0.40	0.02	0.03

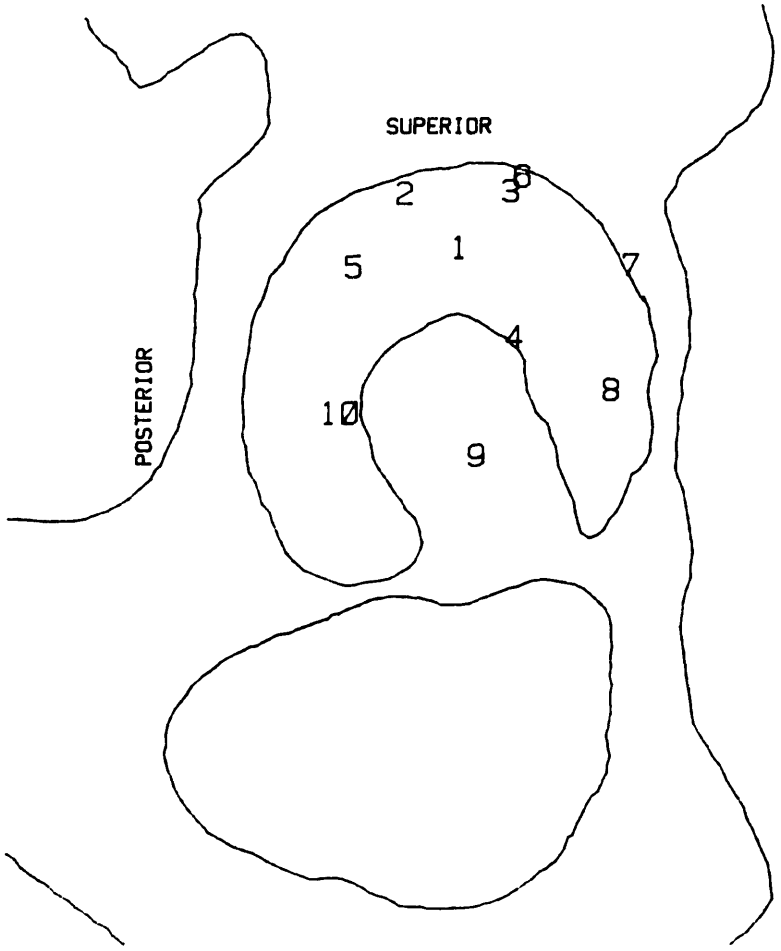

Figure V-1: Acetabular locations of transducers during normal, static stance. Transducer 6 is at a latitude greater than 90 degrees.

Table V-2; Average pressures at three highest-reading transducers during three sets of normal stance data. Location of these three transducers (2,3,and 5) in static stance also presented. Pressures in M-Pa.

Transducer	2	3	5
Time post-op			
2 weeks	1.16	1.12	1.49
6 months	1.06	1.92	1.62
11 months	.55	1.57	1.95
Location			
Latitude	70	70	50
Longitude	110	78	137

Table V-3: Maximum pressures at each transducer during single-leg stance on the instrumented leg.

	Time after implantation		
Transducer	2 weeks	6 months	14 months
1	-0.49	0.09	2.21
2	4.35	4.59	5.48
3	5.15	8.19	6.26
4	1.50	1.19	0.57
5	4.90	5.38	5.88
6	0.43	0.06	1.09
7	0.51	2.06	1.09
8	1.26	0.25	0.36
9	0.47	0.34	0.27
10	2.97	2.33	2.18

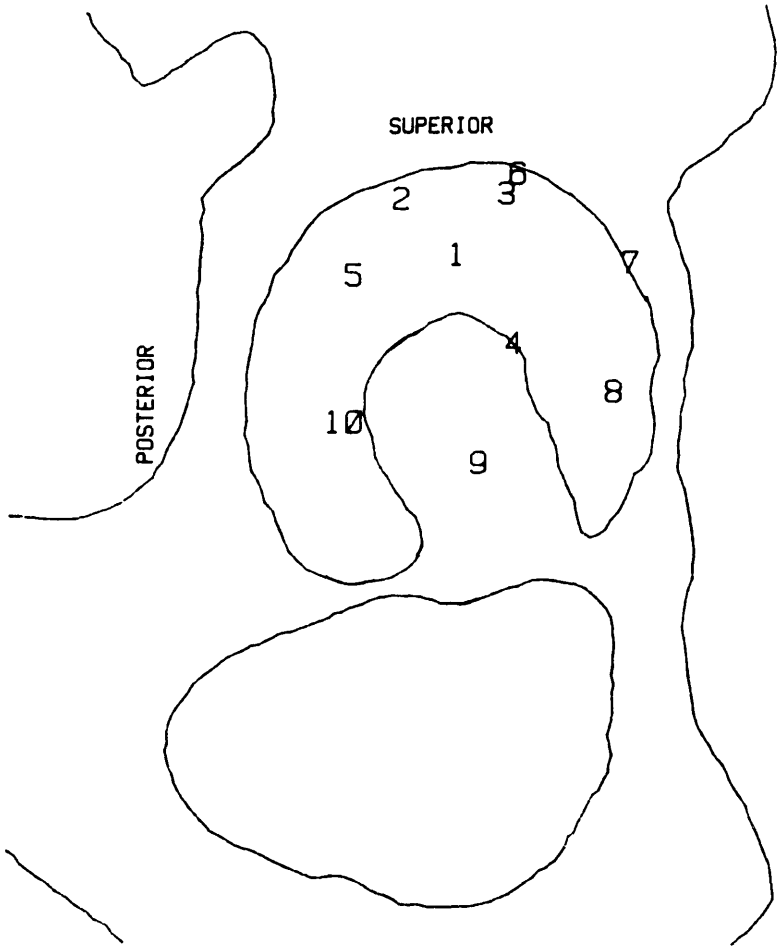

Figure V-2: Acetabular locations of transducers during single-leg stance on the instrumented leg.

instrumented leg. The average pressures obtained from this type of test can be found in Table V-3.

C. Gait Data

1. Assisted Walking

a. Walker; Tests were conducted with a walker, a four-legged stool onto which the subject transferred some body weight through her arms and hands, in June, July, and December 1984 . Data taken in the summer was acquired at 10 Hz and therefore must be viewed critically. December pressure data was acquired at 254 Hz and filtered at 10 Hz; kinematic data for December was acquired at 204 Hz. Maximum pressures for each transducer, the percentage of stance phase time at which they occurred, and the position of the transducer at that time are given in Table V-4. Figure V-3 presents one gait cycle for the transducer registering the maximum pressure in December. A 3-D display of pressure on the acetabulum for the same transducer during this gait cycle is shown in Figure V-4. The view in this figure, as described in section IV, is from a position behind the acetabulum, looking through the pelvic bone, in a posterior and downward direction.

Other transducers displayed much different behavior, as was typical of all tests. The transducers in the inner ring, as shown in Figure II-14, all tended to display higher pressures than those on the outer ring.

During the July tests the subject had not yet fully recovered; she was

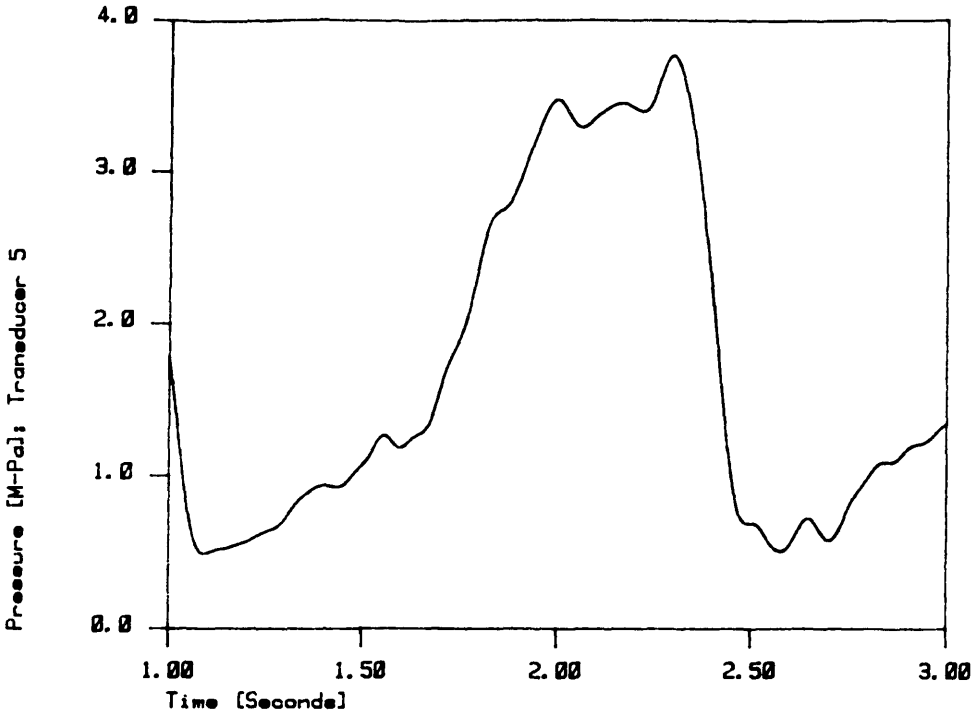

Figure V-3: Pressure at transducer 5 during a gait cycle completed with the support of a walker. Data taken 6 months after surgery.

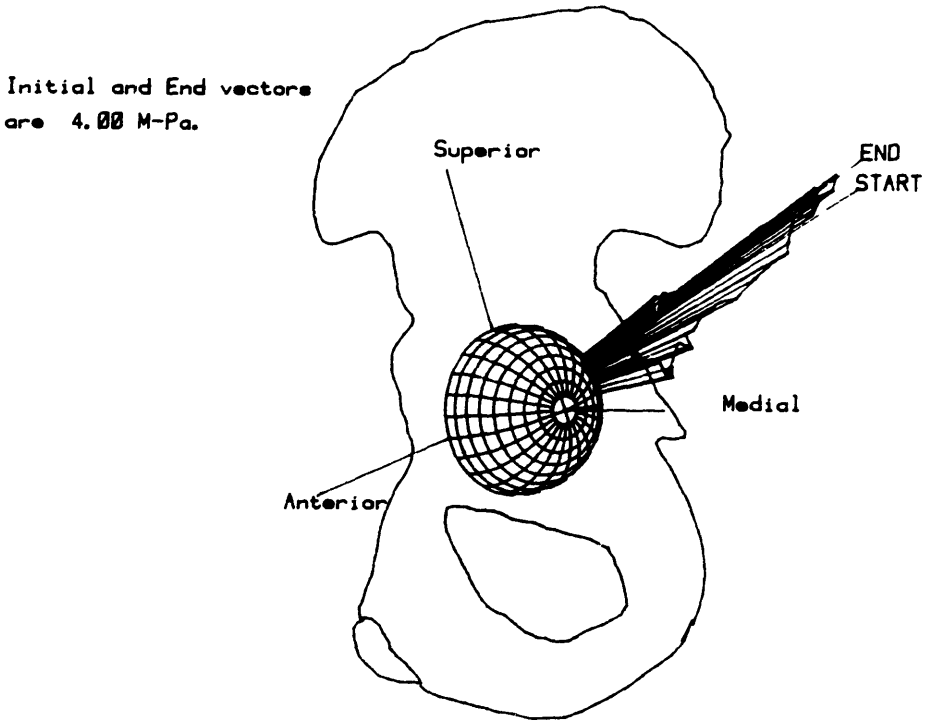

Figure V-4: Display of data from Fig. V-3 in hemisphere format. Every eigth frame of kinematic data shown.

Table V-4: Maximum pressures recorded while subject walked using a walker.

Test	Transducer	Max. Pressure [M-Pa]	Lat.	Long.
2 weeks post-operative				
Test 1	5	4.0		
Test 2	5	3.8		
6 months post-op.	5	3.8	52	152

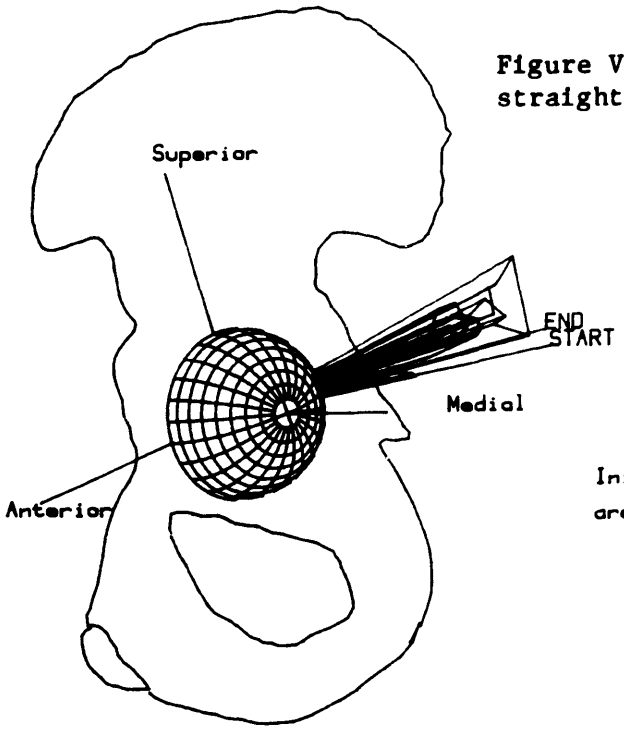

Figure V-5: Walking with crutches, knee straight and foot held off the ground.

walking slowly and needed the walker assistance. In December she was walking essentially normally and did not need a walker. Although the kinematics were different, the maximum pressure recorded 6 months post-operative was similar to pressure maximums measured early in the rehabilitation period.

b. Crutch-Support; Crutch-walking tests were done in June and July 1984 and on all later test dates. A great deal of crutch-walking pressure data was taken in September 1985, but no kinematic data was acquired at that time. The maximum pressures, location, and percentage of stance phase at which maximums occurred are presented in Table V-5. Kinematic data was taken for three categories of crutch use: 1) foot held off the ground; 2) toe touching the ground; 3) partial weight- bearing on the affected leg. The foot of the instrumented leg was held off the ground either with the knee straight and foot in front of the subject, or the knee bent and foot slightly behind the mid-line of the body. Toe-touch crutch-walking was performed for various amounts of weight on the instrumented leg. In partial weight-bearing tests, the foot of the instrumented leg was placed entirely on the ground but part of the body weight was supported by the crutches. Table V-5 is arranged by type of crutch usage, starting with full weight on two crutches, and going through partial weight-bearing modes. Figures V-5 through V-7 are hemispherical displays of the transducer registering the maximum pressure for each test. These figures show the motion of the femoral head with respect to the pelvis and acetabulum. The transducer that has been shown varies. Pressure data was filtered at 10 hz before display, and only every tenth data point is displayed as a pressure "vector".

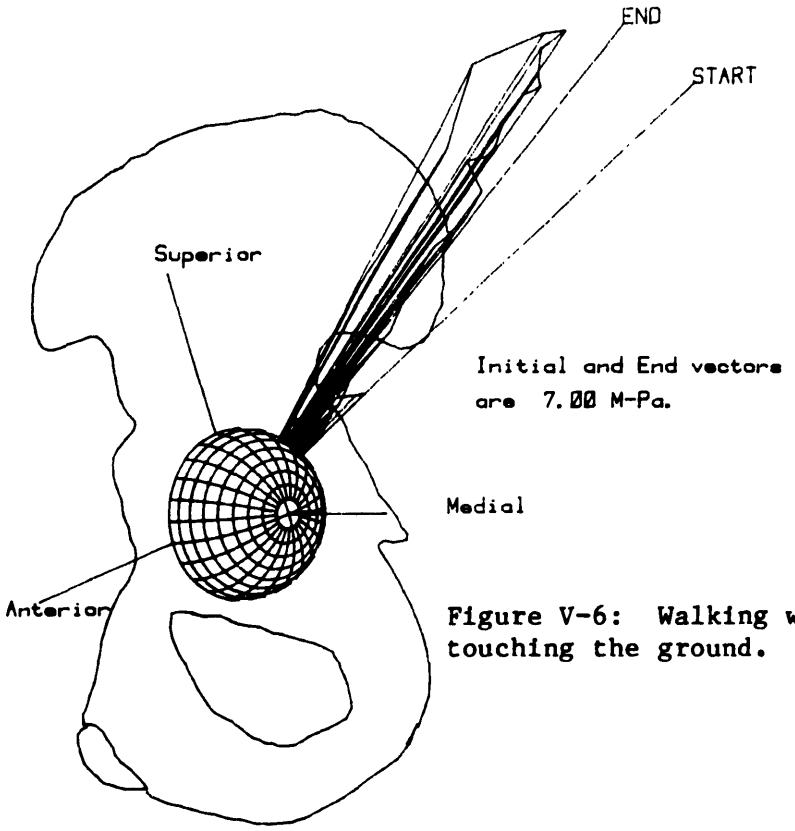

Figure V-6: Walking with crutches, toe touching the ground.

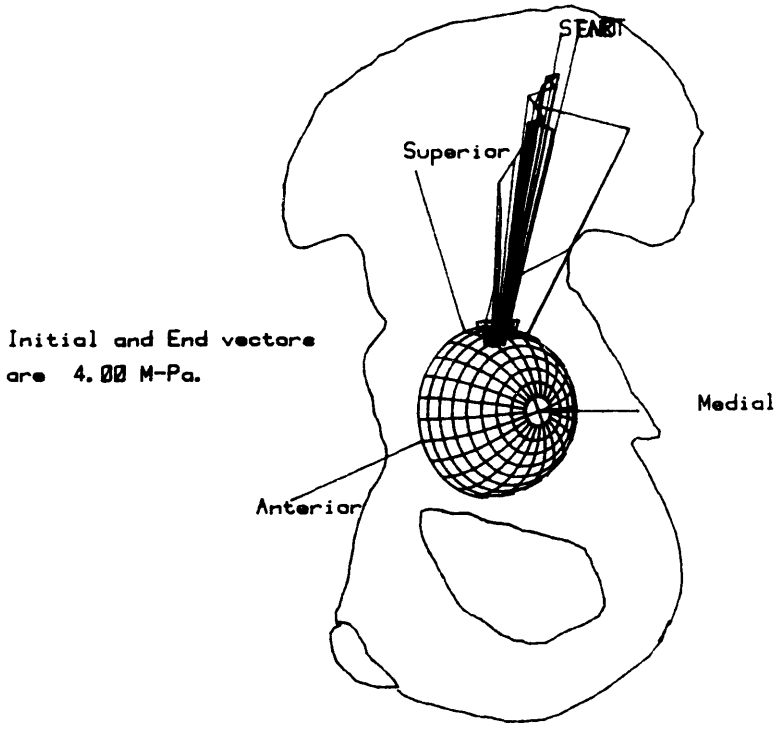

Figure V-7: Walking with crutches, partial weight-bearing.

Table V-5: Crutch-supported walking.
Divided by type of crutch usage and date

Test	Transducer	Max. Pressure [M-Pa]	% of stance phase *	Comments
Foot off ground:				
Knee bent 15 months post-op				
Test 1	7	2.4	-60 (1)	
Test 2	7	2.4	-59 (1)	
Knee straight:				
11 months	5	4.1		latitude: 40.;long. 171.
1 year post-op				
Test 1	5	3.4		
Test 2	5	3.8		
15 months post-op				
Test 1	1	5.5		
Test 1	5	3.5		
Very light toe-touch;				
15 months	2	2.5		
Light toe-touch:				
1 year	2	2.0	77	
15 months post-op				
Test 1	2	2.0	33 (1)	
Test 2	2	2.6		
Toe Touch:				
11 months	2	6.5		lat. 78.; long. 137.
Light partial weight-bearing; 15 months post-op				
Test 1	5	5.2		
Test 2	5	4.7		
Partial weight-bearing:				
2 weeks	5	2.5		
6 months	3	4.2		lat. 45.; long. 103.
15 months	5	3.5	34	

* Information on the time during stance at which high pressures occurred is presented where it was possible to ascertain. In many tests the instrumented leg did not strike the forceplate. In some tests, neither foot was placed on the forceplate.

(1) This number is stance phase time relative to stance phase of the opposite leg.

c. Cane assisted gait; Cane assisted tests were done on essentially all test dates. Results presented here are from December and May 1985. Force transmitted through the cane was also measured. Table V-6 presenting the maximums for cane assisted walking is arranged by the weight borne by the cane. The same transducer, transducer 3, produced the maximum pressure in all of these tests; this pattern is similar to that observed in normal gait tests. Figures V-8 through V-10 display the locations and pressures at all transducers at the times that maximum pressure occurred in tests where 15, 30, and 50 pounds were applied to the cane, these positions are very similar although maximum pressure occurred at widely differing times during stance phase.

2. Level Walking

Five sets of level walking data were selected for presentation. One represents level walking during the initial recovery stage, one is from six-months postoperative, and three are from data taken approximately a year post-operative.

Based on pressure, forceplate, and kinematic data the subject was walking essentially the same after one year as at six months. The maximum pressures at each transducer for each of the four tests after filtering at 10 Hz are presented in Table V-7. Table V-8 contains the overall maximum pressures for each test, the time of the gait cycle at which they occurred, time into the stance phase, and the location in the acetabulum at which they occurred. The same transducer, number 3 had the highest pressure for all gait tests except those done in the two weeks after implantation.

Table V-6: Maximum pressures during cane-assisted level walking. Time of stance phase and acetabular location also noted. All maximums presented here were recorded at transducer 3.

Arranged by amount of force on the cane

Test	Max. Pressure [M-Pa]	% of stance phase	Lat. (phi)	Long. (theta)
Light force on cane				
11 months post-op				
Test 1	5.1	43	65	95
Medium Force				
6 months post-op				
Test 1	4.8		70	91
11 months post-op				
Test 1	4.8	34	63	94
Maximum force				
11 months post-op				
Test 1	4.8	59	67	93

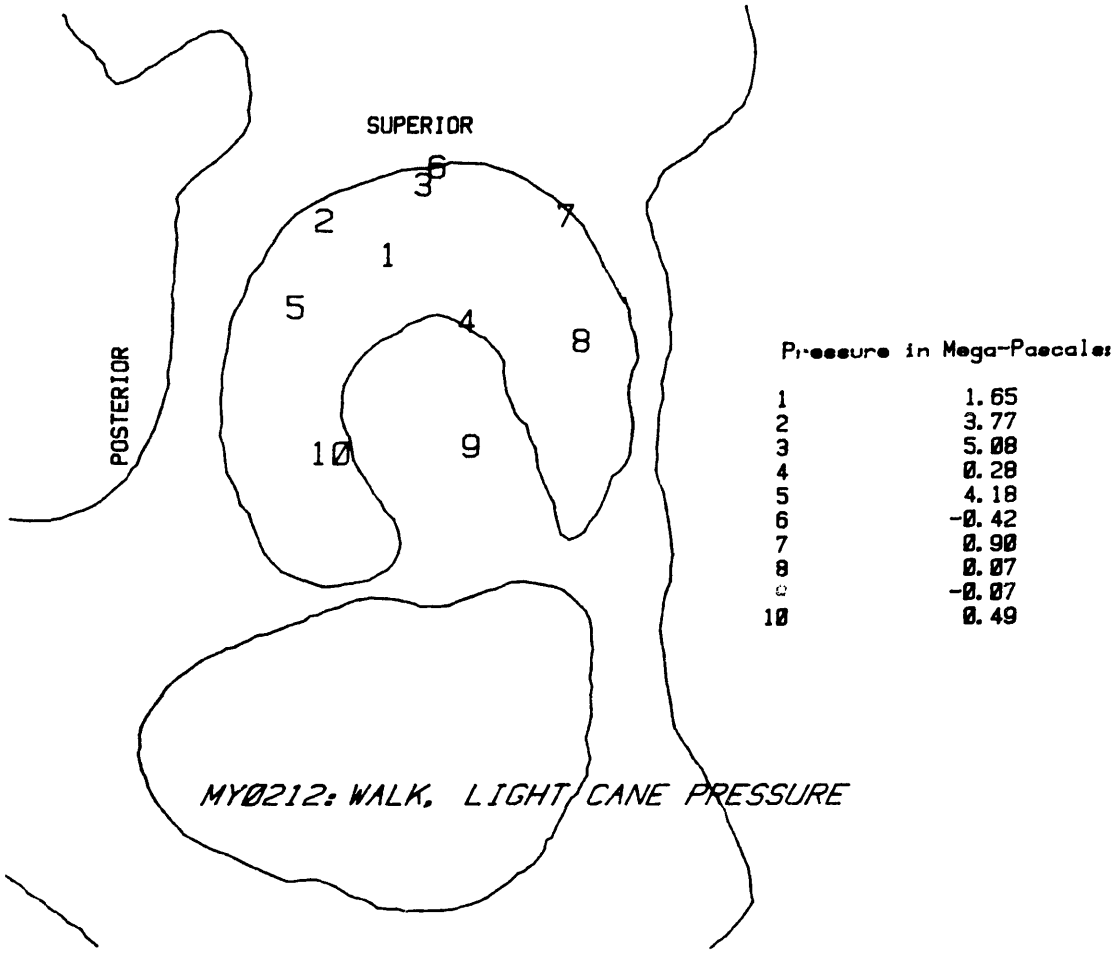

Figure V-8: Locations of all transducers in the acetabulum at time maximum pressure was recorded while walking with minimum force on a cane.

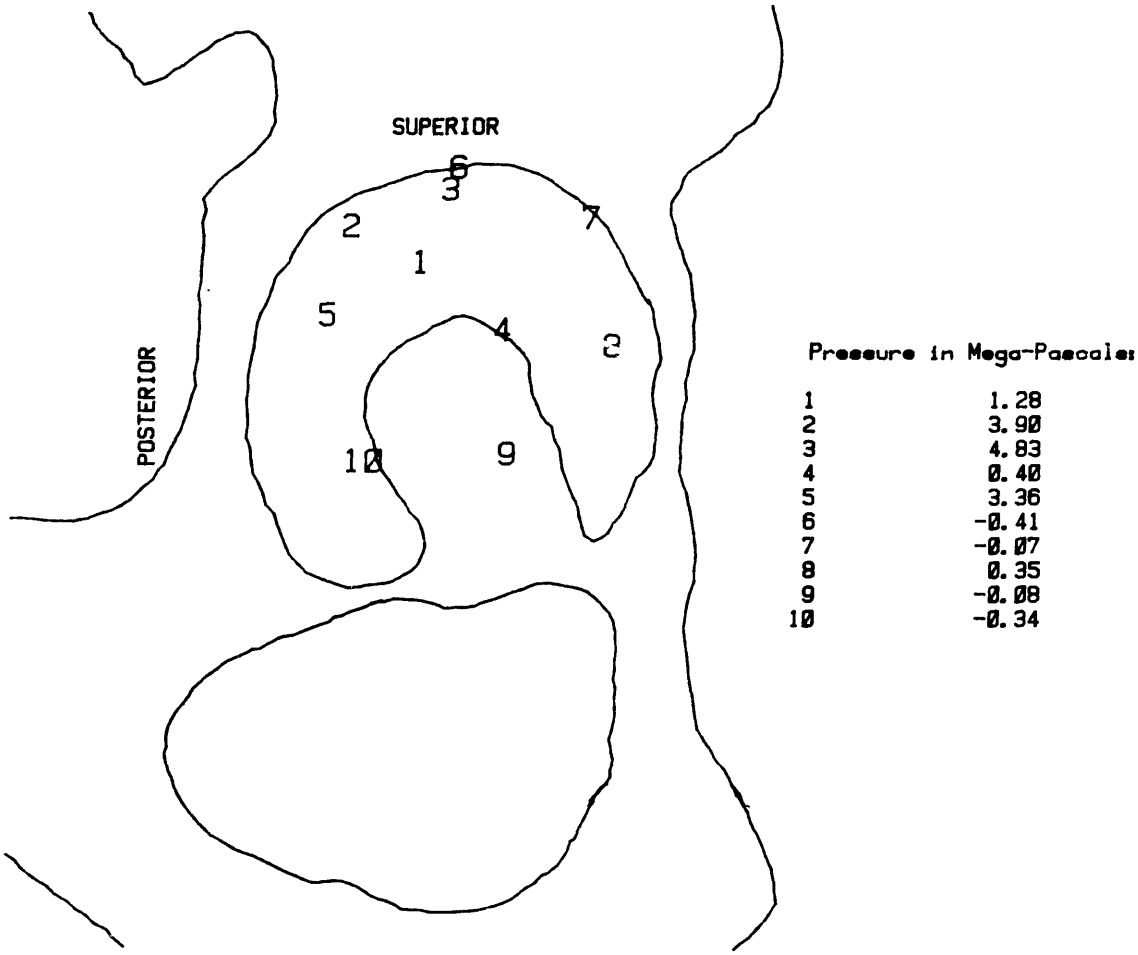

Figure V-9: Locations of all transducers in the acetabulum at time maximum pressure was recorded while walking with medium force on a cane.

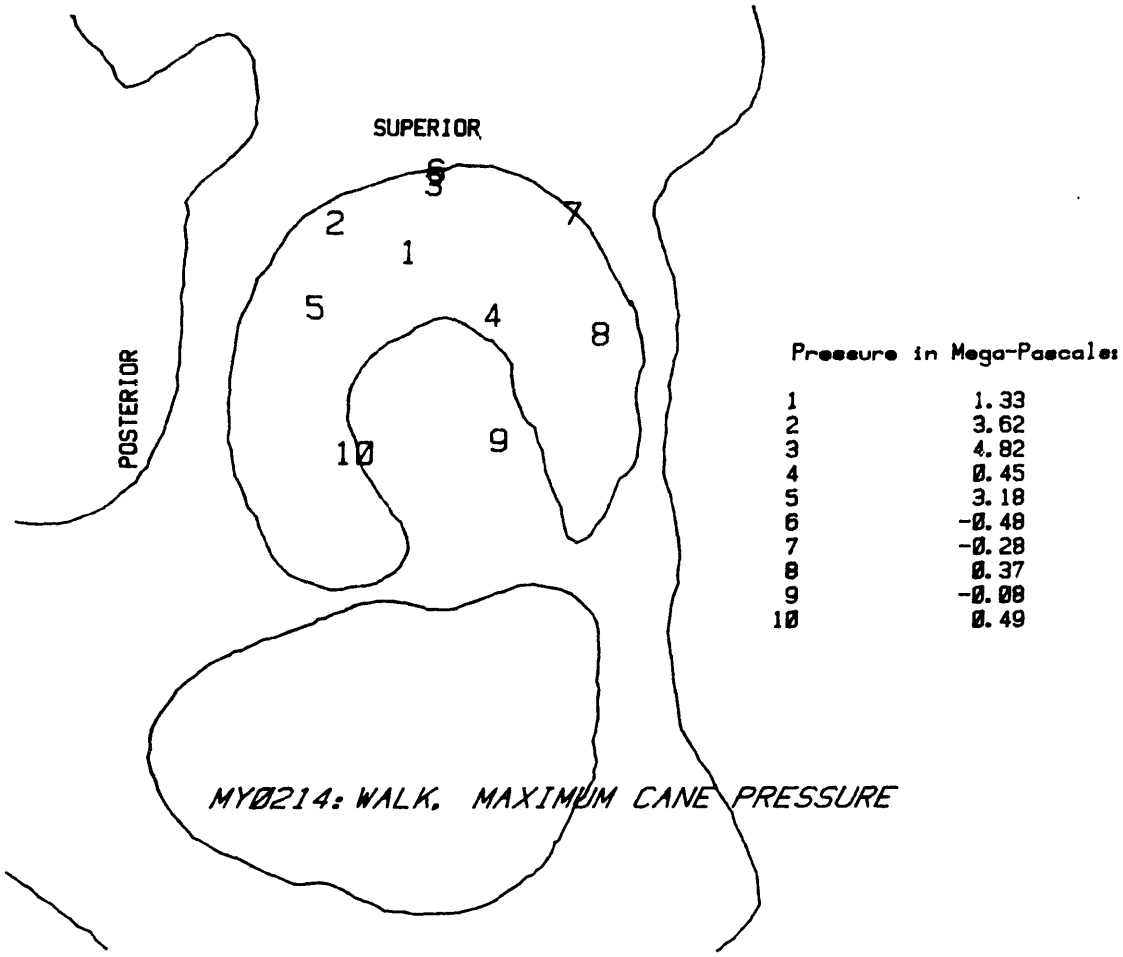

Figure V-10: Locations of all transducers in the acetabulum at time maximum pressure was recorded while walking with maximum force on a cane.

Table V-7: Maximum pressures recorded at all transducers for 5 level walking tests.

Transducer Test	1	2	3	4	5
July 84	0.46	2.61	2.78	0.54	3.33
Dec 84	2.56	4.47	5.33	0.70	4.74
May 85(1)	2.73	5.45	5.52	0.51	4.67
May 85(2)	2.73	5.21	5.34	0.67	4.86
Aug 85	2.11	5.27	5.37	0.49	4.78

Transducer Test	6	7	8	9	10
July 84	-0.08	1.20	0.78	0.37	0.05
Dec 84	0.09	0.73	0.35	0.18	2.95
May 85(1)	1.48	-0.64	0.61	0.02	1.35
May 85(2)	0.03	-0.46	0.74	0.07	1.47
Aug 85	1.35	0.55	0.39	0.25	0.80

Table V-8: Magnitude, timing, and acetabular location of maximum pressures at transducer 3(*) during level walking.

Test	Max. Pressure [M-Pa]	% of Stance at maximum pressure	% of Cycle [1]	Stance Length [sec.]	Lat. degrees	Long. degrees
July 84	2.8 *	36	22	1.44		
Dec. 84	5.3	40	24	.77	66	84
May 85(1)	5.5	36	22	.91	60	89
May 85(2)	5.3	26	16	.99	65	93
Aug. 85	5.4	20	12	.80	70	84

* Actual maximum in July 1984 was at transducer 5 (3.3 M-Pa), #3 reported here for comparison with later data.

(1) Gait cycle length was estimated by assuming the duration of stance phase 60% of the total cycle time.

Maximum pressure measurements were recorded after approximately 30 percent of the stance phase had passed. All walking tests were done at different speeds; the length of time of stance is included in Table V-7.

External force vs. time records for each of the five selected tests are shown in Figures V-11 and V-12. Figure V-11 gives only July 1984 data since the subject was walking with great difficulty at that time and the duration of stance phase was almost twice as long as at 6 months. Figure V-12 superimposes forceplate data for the other four tests. This data has been normalized by stance phase length. Forceplate data presented begins at a time that is 10% of stance phase prior to heel-strike and ends at the time corresponding to 10% of stance phase after toe-off. Heel-strike and toe-off were determined by measurement of force greater than 10 N on the forceplate. The duration of stance phase was different for all tests as noted in Table V-7. Two tests at 11 months were included because the tabulated pressure statistics indicate that one test at 11 months is similar to the test at 6 months in the timing of pressure increases and maximums, and the other test in May is like the August data. Pressure vs. time is shown for transducers 3 and 5 for July 1984 in Figures V-13 and V-14. Figures V-15 and V-16 are the corresponding displays for later test dates. Data in these figures was recorded during the same time intervals as those presented in Figures V-11 and V-12 for forceplate data.

Figure V-17 shows the stance phase of gait in the hemispherical display for transducer 3 at 11 months post-operative. Figures IV-30 and 31 present the corresponding data for 6 months and 14 months after surgery. In Figure V-18 each transducer is shown in its acetabular location at the time that

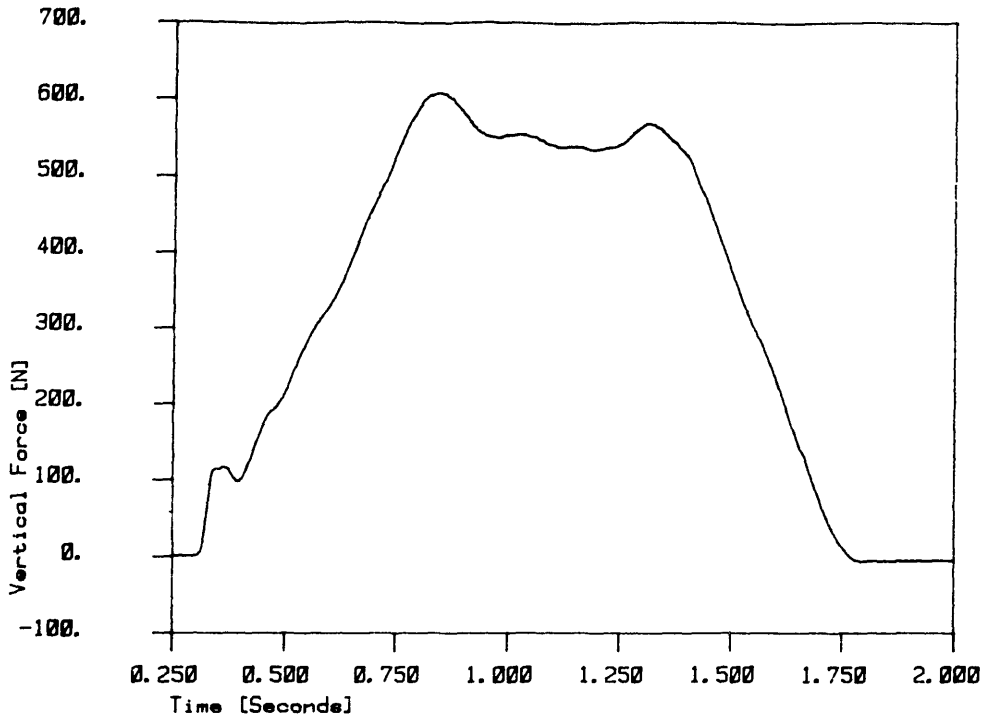

Figure V-11: Vertical force vs. time for walking 2 weeks post-operative.

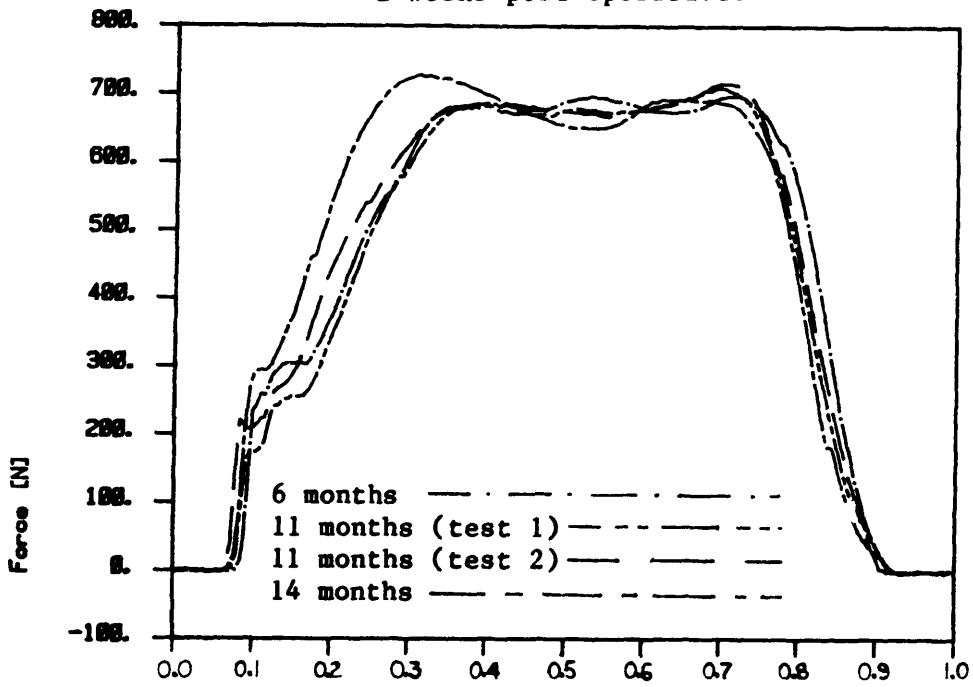

Figure V-12: Vertical force vs. time for walking 6, 11, and 14 months post-operative. Normalized by stance phase length.

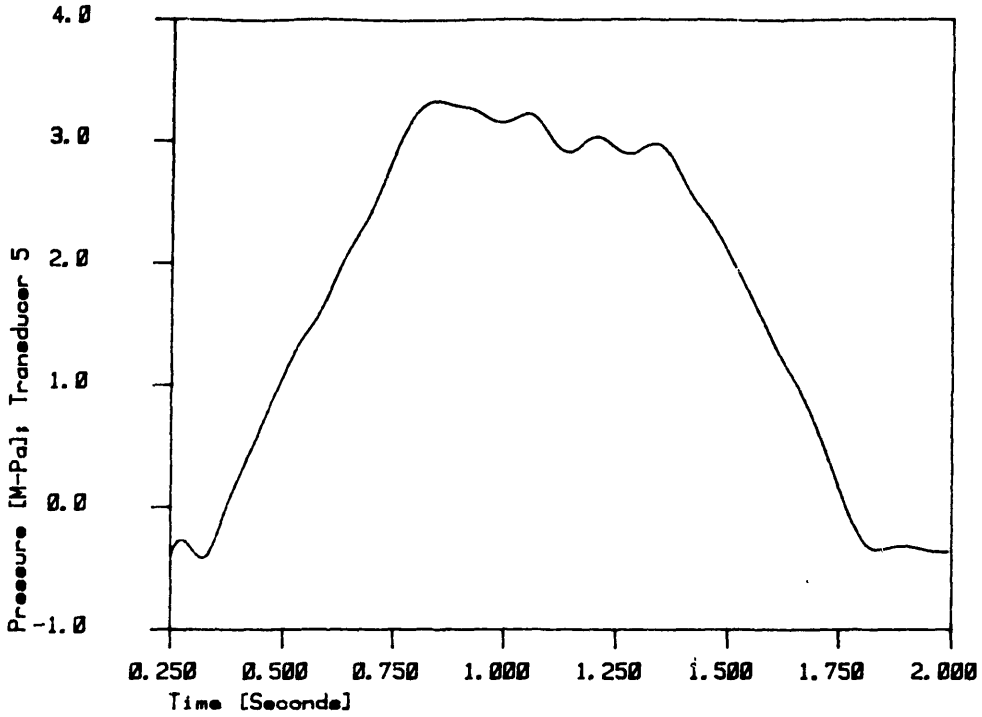

Figure V-13: Pressure vs. time recorded at transducer 3 while walking 2 weeks post-operative. Time interval same as in Figure V-11.

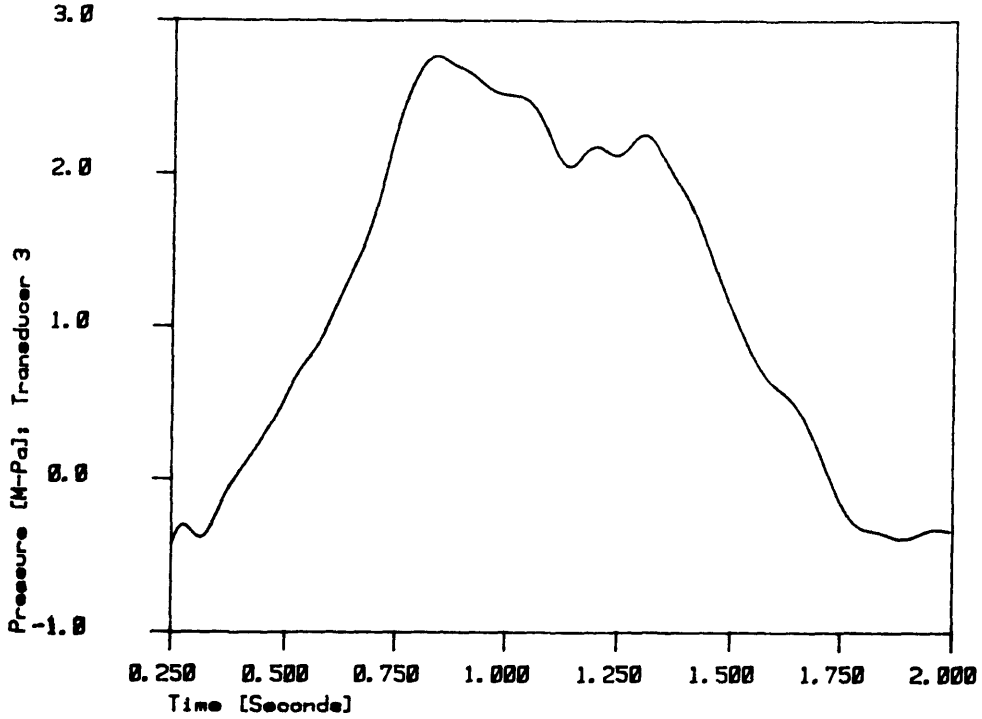

Figure V-14: Pressure vs. time recorded at transducer 5 while walking 2 weeks post-operative. Time interval same as in Figure V-11.

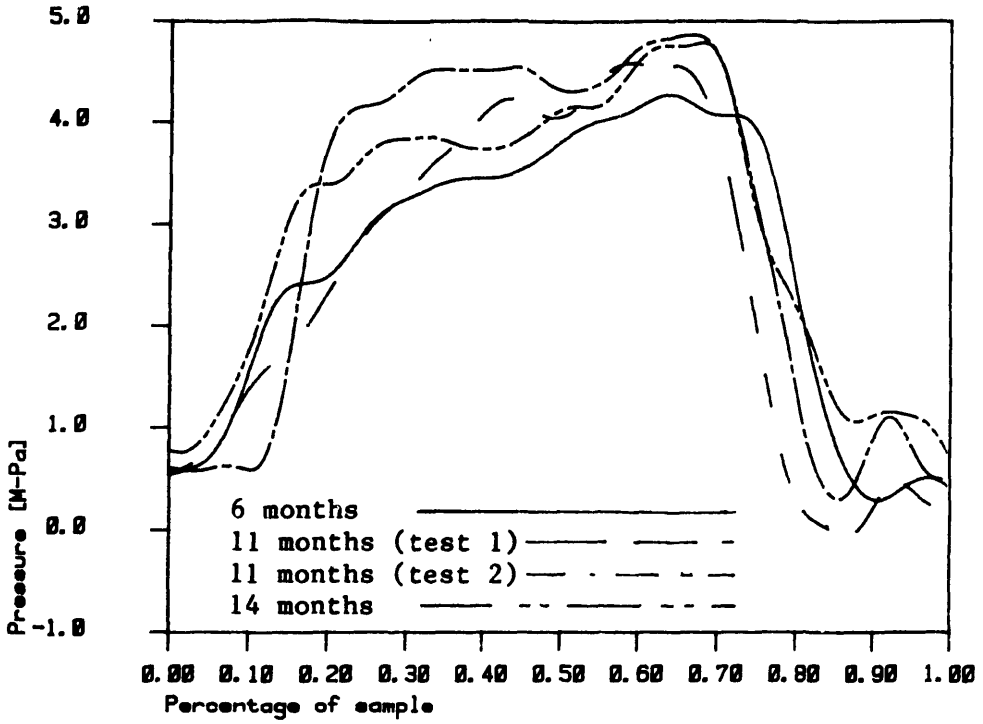

Figure V-16: Pressure vs. time recorded at transducer 5 for walking 6, 11, and 14 months post-operative. Normalized by stance phase length and corresponding to data shown in Figure V-12

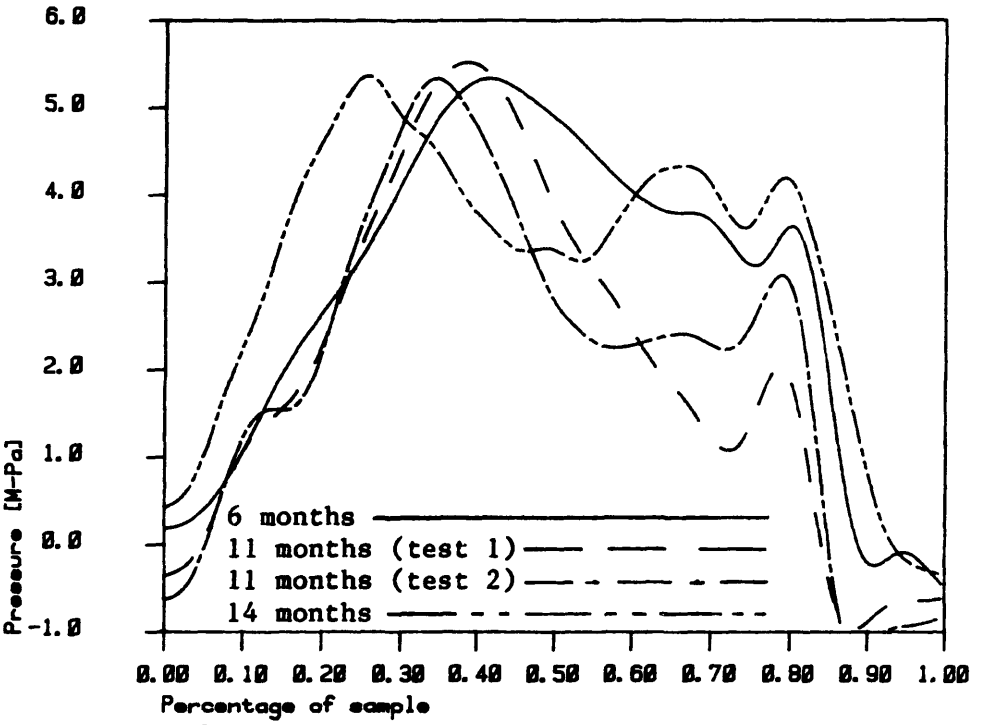

Figure V-15: Pressure vs. time recorded at transducer 3 while walking 6, 11, and 14 months post-operative. Normalized by stance phase length and corresponding to data shown in Figure V-12

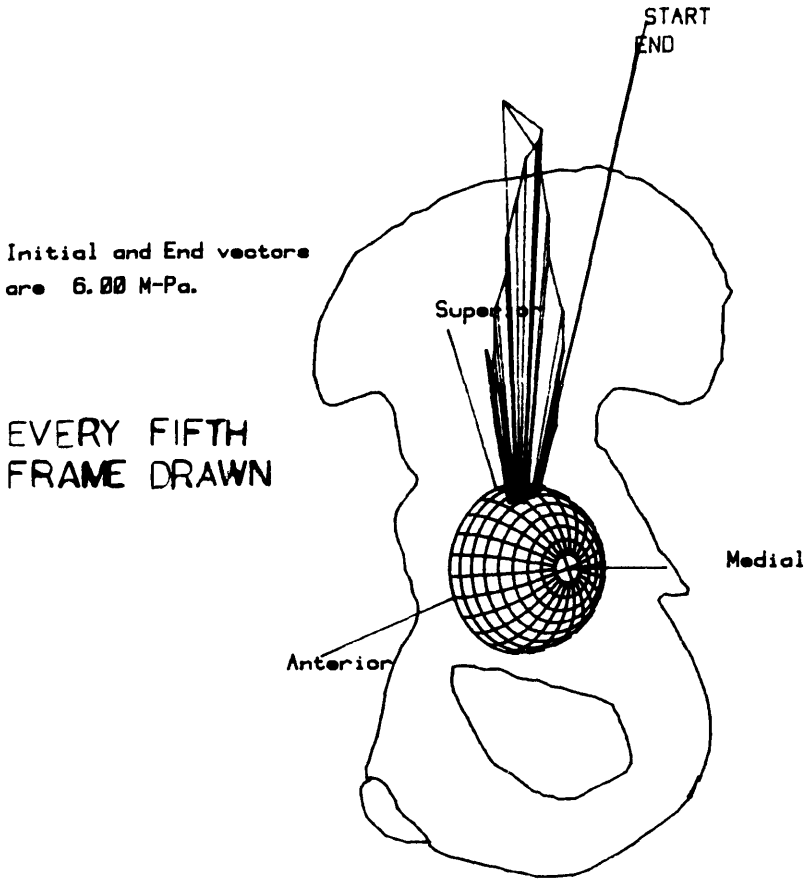

Figure V-17: Data for stance phase from 11 months after implantation. Transducer 3 shown.

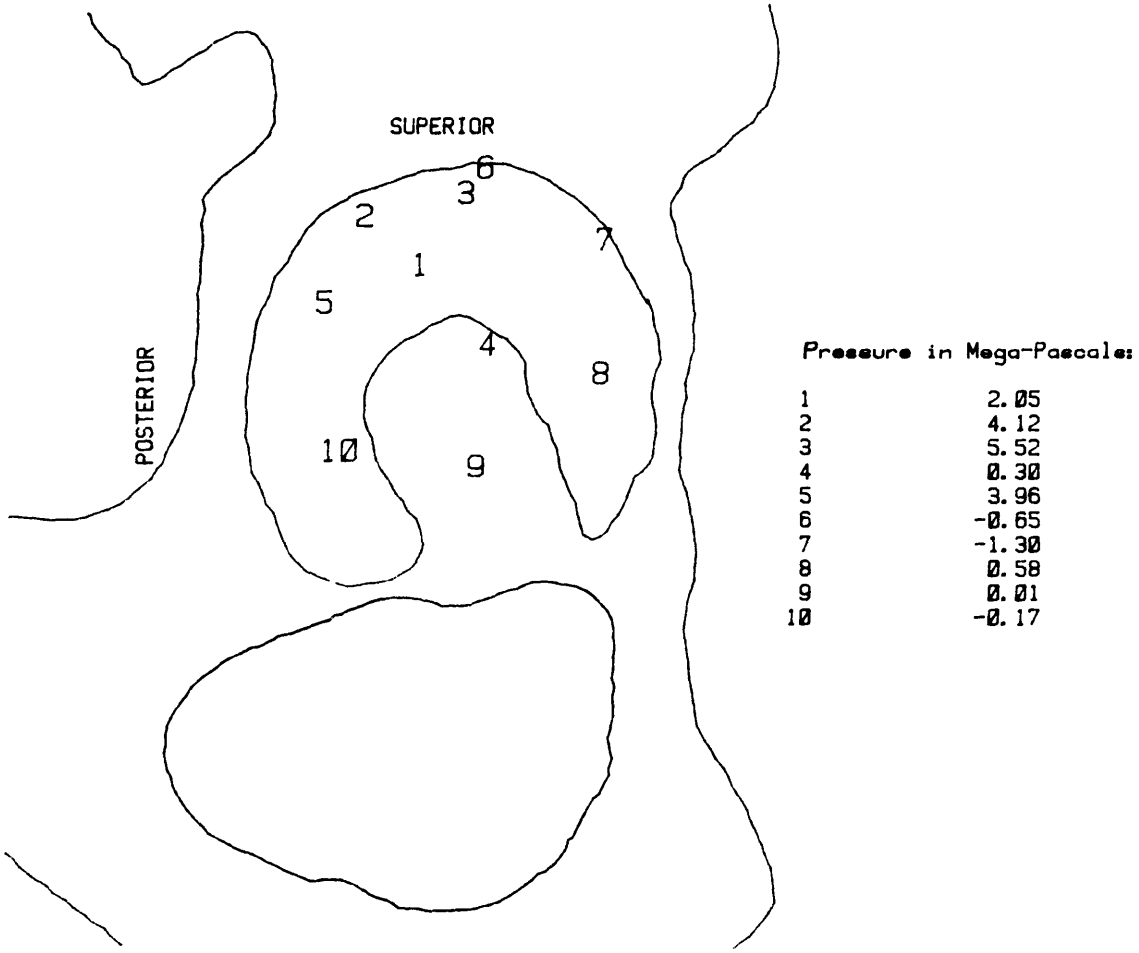

Figure V-18: Acetabular locations of transducers at time the maximum pressure was recorded in level walking in May 1985.

the maximum pressure was recorded by transducer 3 in the May gait test. Transducers other than number 3 registered comparable pressures, notably 1, 2 and 5, at different times in the gait cycle.

Positions of all transducers in the acetabulum are shown in the two-dimensional projection in Figure V-19 for heel-strike, employing May data. Figures V-18 through V-20 are from the same data set; Figure V-20 indicates transducer locations in the acetabulum immediately after toe-off.

The highest load rates of increase during level walking were found at transducers 2 and 5 after less than 5 percent of the gait cycle. The rate at which pressures decreased was slightly faster and the maximum rate of decrease occurred at transducers 3 and 5 at about 50 percent of the gait cycle, or when about 85 percent of the stance phase had passed. Table V-9 summarizes the load rate information for these transducers, including the degrees of arc in the acetabulum over which the maximum rate of load transfer occurred.

3. Jogging

In June 1985, one year after implantation, data was taken as the subject jogged across the lab floor. The maximum pressures found during these tests were about 7.5 M-Pa, at transducer 2. One other transducer, number 1, also gave a much higher reading during jogging tests than during level walking. Most other transducers registered pressures which were approximately the same during jogging as during walking. Table V-10 contains the maximums and percent of the stance phase at which they

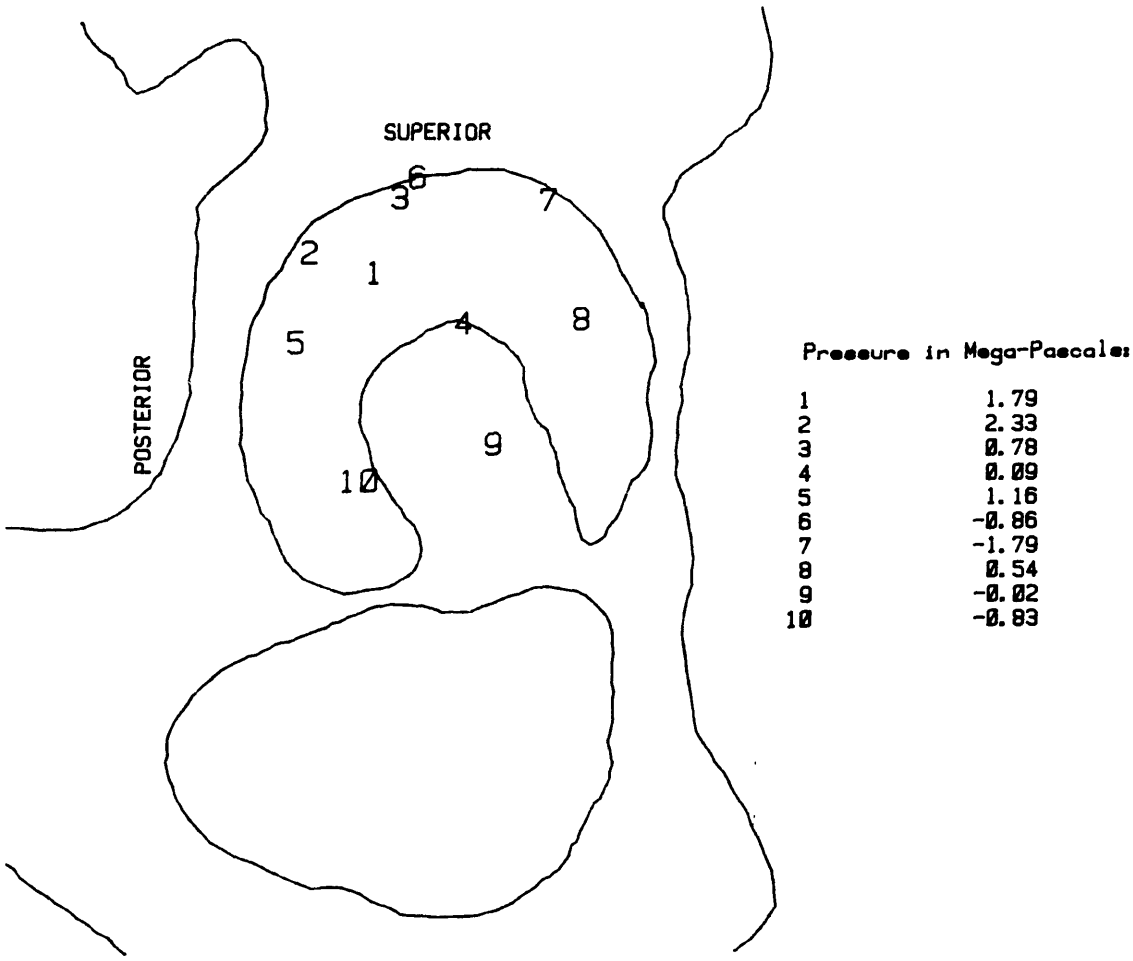

Figure V-19: Pressure measurements made at heelstrike during level walking 11 months after surgery.

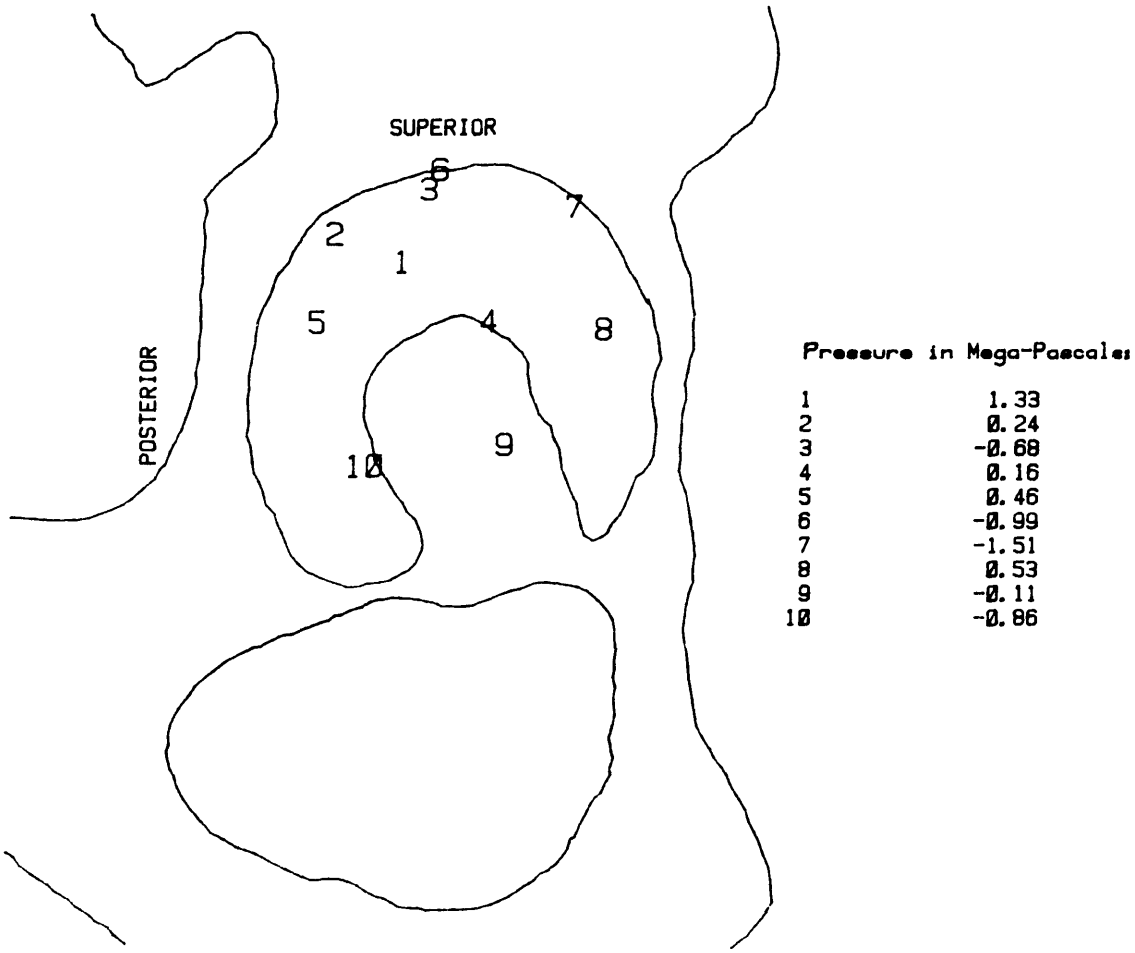

Figure V-20: Pressure measurements after toe-off for level walking. Data set same one presented in Figures V-18 and V-19

Table V-9; Maximum rates of loading during level walking

Test Transducer No.		Load Rate [M-Pa/sec]	Initial Position Lat.	Long.	Degrees of Arc	Ext. Force	% of Stance Phase
6 months post-operative							
2	+	30.2	73	132	7.9	146	3
3	-	55.6	80	84	6.1	254	92
11 months							
Test 1							
2	+	35.9	71	138	1.5	216	5
3	-	40.9	66	86	2.1	336	95
Test 2							
5	+	37.1	56	168	4.0	298	9
2	+	28.6	74	143	3.2	232	3
3	-	54.7	74	90	2.1	370	90
Aug. 85							
2	+	33.5	64	126	1.2	101	-2
3	-	38.0	73	78	2.0	152	94

Table V-10: Maximum pressures for the 4 highest reading transducers in two jogging tests.

Transducer	Maximum Pressure [M-Pa]		% of Stance	
	Test 1	Test 2	Test 1	Test 2
1	5.2	5.0	35	31
2	7.7	7.5	37	42
3	4.3	4.3	27	23
5	5.0	5.4	34	45

Table V-11: Maximum loading rates observed during jogging

Test Description		Maximum Joint Load Rate [M-Pa/sec]	Concurrent Ext. Force Rate of Change [N/sec]
Transducer No.			
Test 1			
2	+	39.2	3063.
1	-	36.8	4264.
Test 2			
2	+	44.6	15193.
2	-	46.5	5494.

occurred for 4 highest-reading transducers during these two tests. The overall maximum pressure was about 2 M-Pa higher than that for walking, and occurred at a different transducer. The acetabular location at which the maximum pressure occurred during jogging tests is not known because no kinematic data was taken. Figure V-21 shows pressure vs. time for transducers 1 and 2 in addition to the forceplate record for one of the jogging tests.

The highest rates of loading occurred at approximately the same time for all transducers during jogging tests. Table V-11 summarizes the maximum load rates found and the rate of change of external force. The greatest increase in forceplate force occurred slightly later than the maximum pressure increase in the first test, while maximum changes in both force and pressure were essentially simultaneous in the second test.

D. Stair-Climbing

Stair-climbing generated higher pressures in the hip joint than level walking or jogging. The maximum pressures occurred at completely different locations than in level walking. Information on maximum pressures at all transducers during stair climbing is given in Table V-12. Table V-13 contains the stair rise height, overall maximum pressure for each stair-climbing test, the location at which it occurred and the position of the leg at the time of occurrence. The subject appears to have been climbing stairs differently each day; changes in stair height also had an effect. Hemispherical displays of December, May and August data are given in Figures V-22, V-23,and V-24. Some differences exist between locations

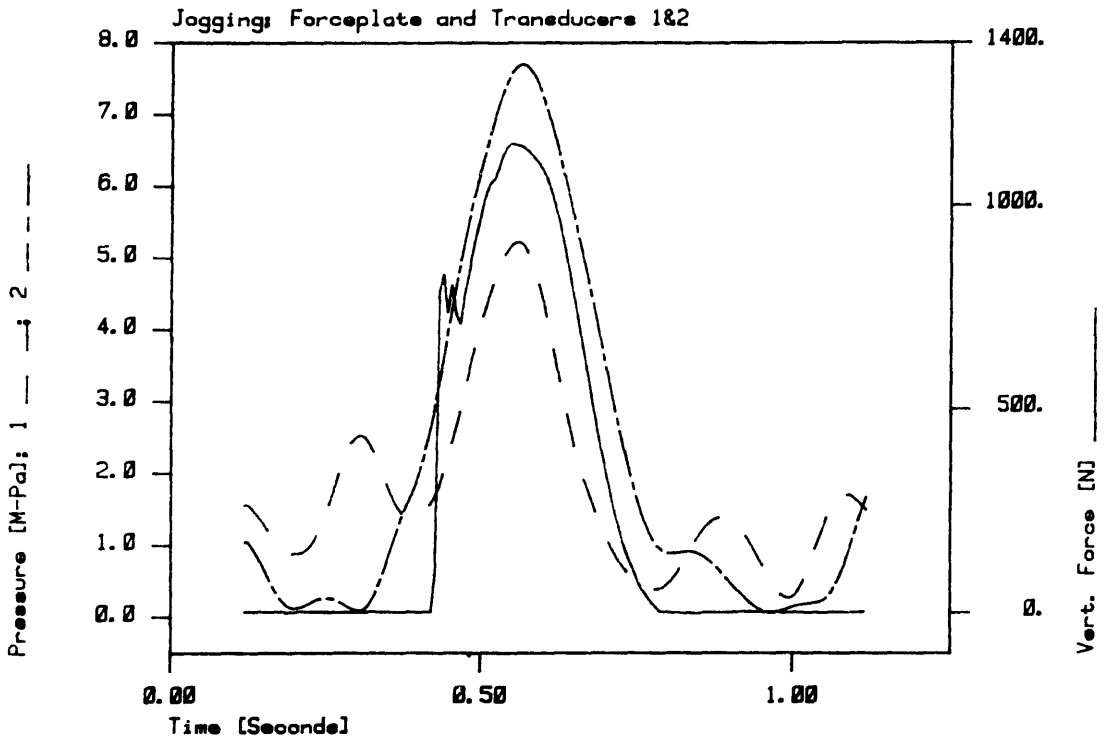

Figure V-21: Forceplate and pressure data recorded as subject jogged.

Table V-12: Maximum Pressures recorded at each transducer in stair climbing tests.

Transducer	Dec 6 months	May (1) 11 months	May (2) 11 months	Aug (1) 14 months	Aug (2) 14 months
1	6.7	9.2	10.2	7.3	7.1
2	4.5	7.7	6.2	5.2	5.7
3	5.4	7.7	7.8	7.4	7.5
4	.9	.5	.4	.6	.9
5	6.1	4.3	6.6	5.7	5.3
6	.4	.6	.1	1.6	2.0
7	4.0	.9	1.3	3.1	2.7
8	.6	.7	.7	.3	.6
9	.5	.1	.0	.3	.4
10	.5	- .4	- .5	.7	.7

Table V-13: Information on kinematic parameters and maximum recorded pressures for Stair-Climbing tests.

Test	Stair Ht. [cm]	Hip Angles [degrees] Flx.	Abd.	Rot.	Max. Pressure [M-Pa]	Lat. (phi)	Long. (theta)
6 months	23	73	2	0	6.7	46	179
11 months							
Test 1	18	66	0	3	9.2	44	168
Test 2	18	64	0	7	10.2	44	170
14 months							
Transducer 3							
Test 1	18	50	4	15	7.4	62	120
Test 2	18	57	9	12	7.5	60	116
Transducer 1							
Test 1	18	50	4	15	7.2	34	141
Test 2	18	57	9	12	7.1	36	140

* Maximum pressures in August tests were at a different transducer. Included transducer 1 info for Aug. tests too.

Figure V-22: Pressure measurements made at transducer 1 while stair-climbing 6 months after surgery.

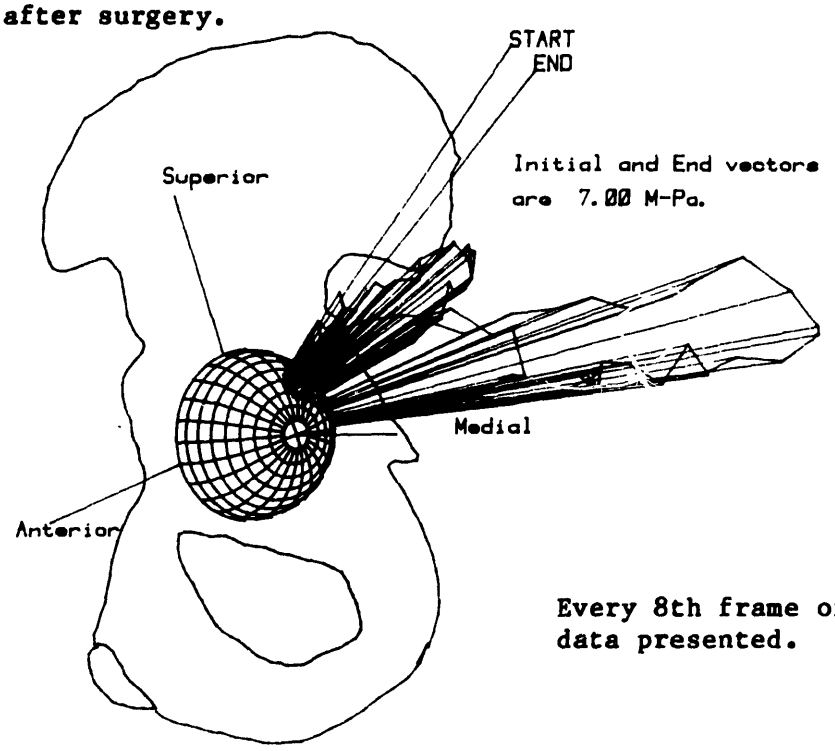

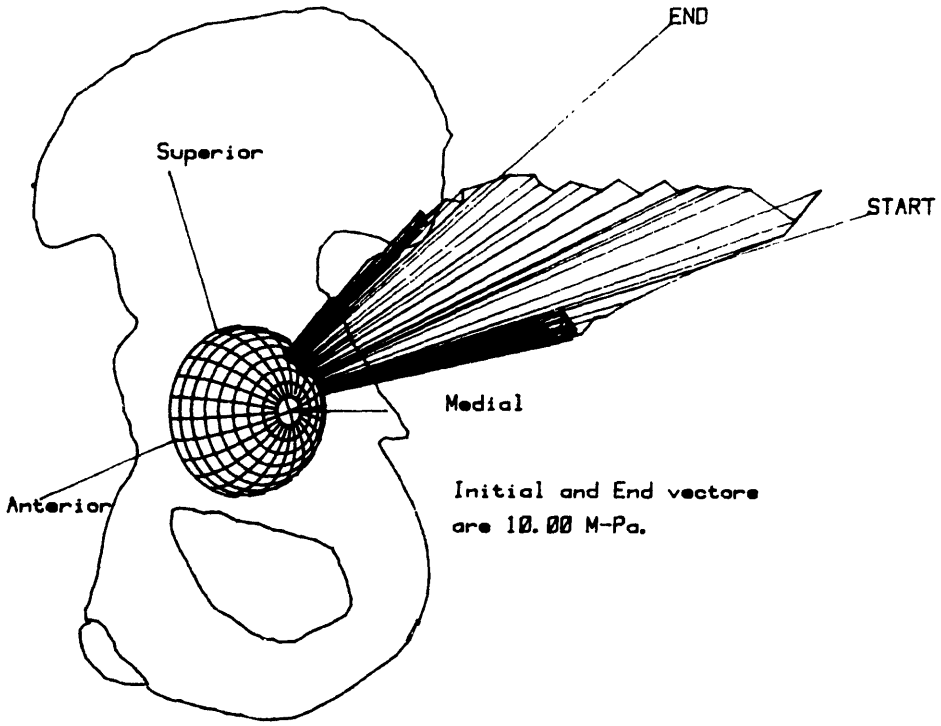

Figure V-23: Pressure measurements made at transducer 1 while stair-climbing 11 months after surgery.

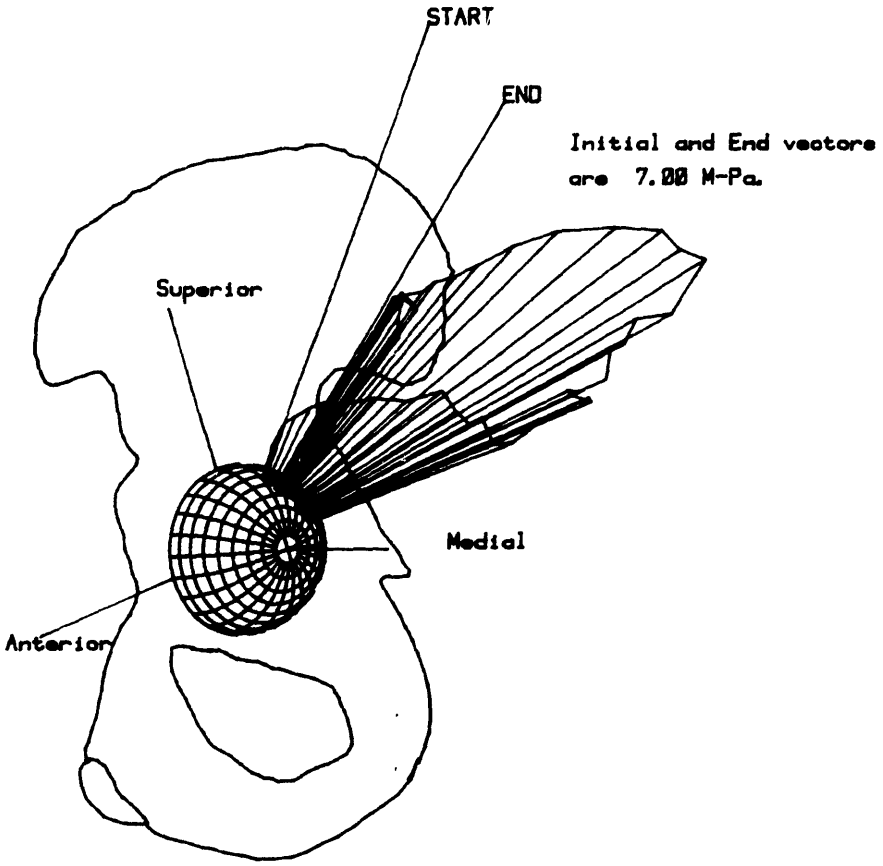

Figure V-24: Pressure measurements made at transducer 1 while stair-climbing 14 months after surgery. Every 8th frame of kinematic data presented.

Table V-14: Rates of Loading measured in vivo during stair-climbing

Test	Pressure Load Rate [M-Pa/sec]	Initial Position* Lat.	Long.	Degrees of Arc*	Flexion (Hip)	Ext. Force (Initial) [N]	Ext. Force Rate [N/sec]
6 months							
Tr. 1 +	15.0	47	173	12.2	67	370	1439
Tr. 2 +	23.3	59	157	6.5	53	509	616
Tr. 3 +	44.7	59	145	5.4	74	145	2800
Tr. 5 +	78.5	58	-165	6.5	59	479	474
Tr. 7 +	25.1	50	84	9.7	65	389	1158
11 months							
Test 1							
Tr. 1 +	45.8	44	175	7.2	71	200	1012
Tr. 2 +	59.1	68	148	4.3	48	602	223
Tr. 3 +	58.9	62	143	5.0	72	202	501
Tr. 5 -	48.1	55	170	2.9	43	590	-483
Test 2							
Tr. 2 +	49.9	61	151	4.7	50	580	568
Tr. 5 +	67.0	57	-173	9.4	54	561	415
Tr. 1 -	48.1	43	167	9.0	65	430	955
14 months							
Test 1							
Tr. 2 +	15.7	62	136	7.2	37	94	1893
Test 2							
Tr. 2 +	29.7	59	137	2.5	38	173	2377

* Latitude and Longitude are presented as initial value
change in position is given as percentage of acetabular circumference

of maximum pressures for the various test dates.

In general, more transducers were subjected to pressures between 4 and 10 M-Pa in stair-climbing than in walking. Some femoral locations, such as the position of transducers 4, 8, 9, and 10 did not experience high pressures in either level walking or stair climbing. Transducers 9 and 10 were in the inferior portion of the socket at the time maximum pressures were measured in both sitting-to-standing and stair-climbing tests. Transducers 8 and 4 were in the medial-anterior portion of the acetabulum.

The rate of loading at the hip was comparable for stair-climbing and level walking, Table V-14 contains some information on load rates, leg positions at which they occurred, and acetabular arc over which they occurred. In August the rate of loading for stair-climbing was slightly less than that for level walking, while in May it was greater.

E. Sitting-to-Standing

The highest pressures were recorded as the subject rose from a chair. Table V-15 contains the maximum pressures for all sitting to standing tests, the locations in acetabular coordinates and force measured at the forceplate at the time that the maximums occurred. The maximum pressures in rising from a chair were always recorded by transducer 1 while it was in the posterior region of the acetabulum. This behavior was observed during all tests from December 1984 to August 1985 and in tests for rising from all chair heights. The magnitude and location of the maximum pressure varied with test date and chair heights. Table V-15 also notes the chair

Table V-15: Results from data taken as subject rose from a chair. Maximum pressures presented with associated kinematic and forceplate data

Test Date (theta) Post-op	Chair ht.[cm.]	Max. Pressure [M-Pa]	Force-plate Force [N] (*)	Hip Flexion	Lat. (phi)	Long.
6 months	45.7	7.7	300	81	48	-150
11 months						
Test 1	45.7	17.8	387	93	44	-145
Test 2	45.7	18.0	365	101		
14 months						
Test 1	45.7	13.1	797	81	55	180
Test 2	45.7	11.5	757	83	57	180
Test 3	38.4	15.0	705	83	60	177
Test 4	56.2	9.2	607	74	52	171

* Note -- Subject rose with more difficulty in Dec and May than in August, thus her body weight was transferred to the forceplate more slowly.

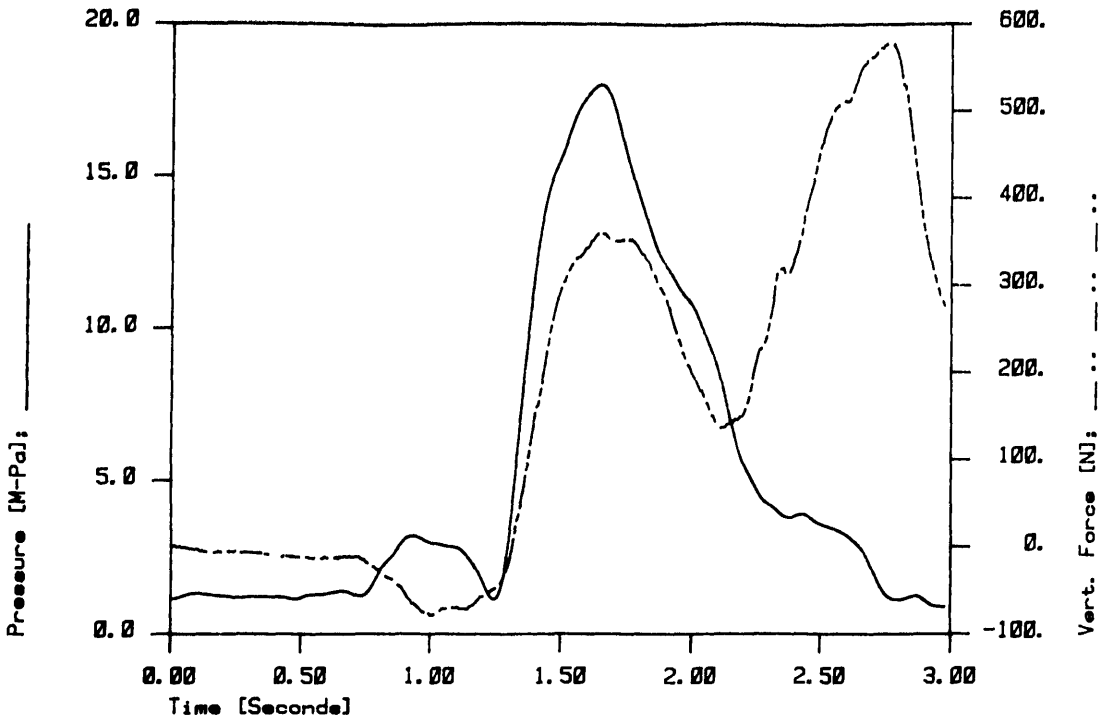

Figure V-25: Forceplate data and pressure at transducer that recorded maximum pressure during sitting-to-standing test 11 months after implantation.

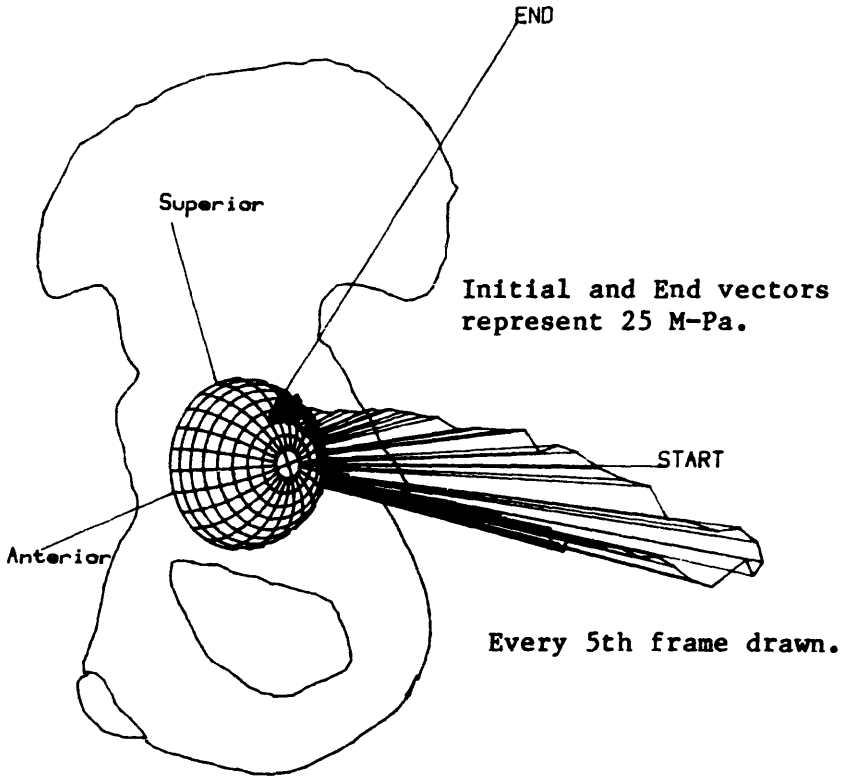

Figure V-26: Hemisphere display of pressure during sitting-to-standing test performed in May 1985.

height and date for test maximums.

Other transducers also produced high pressures during sitting to standing tests, however, all other transducers measured higher pressures in other types of tests. The time during the action at which transducers measured their maximum pressure varied more from transducer to transducer in sitting to standing tests than in some other dynamic tests, such as jogging.

Display of pressure vs. time data for the test from May 1985 in which the maximum pressure was recorded is shown in Figure V-25. This figure also contains the forceplate data for the same test. The locations and pressures for transducer 1 during the other May test are displayed in hemispherical form in Figure V-26. The pressures at all transducers at the time that the maximum pressure was measured are displayed in Figure V-27.

Rising from different height chairs altered the loading environment as measured at the hip. Figure V-28 presents pressure vs. time data for transducer 1 over sections of tests in which the subject rose from different chair heights. All data presented in Figure V-28 is from the same day, in August 1985. The test sections selected for Figure V-28 all cover the same length of time, although the speed at which the subject rose varied between the tests; all test segments displayed start with the subject seated and end after she is standing upright. The height of the chair used in most sitting-to-standing tests was 45.7 cm. This was an armless, mass-produced chair with a back-support. The lowest seated position from which the subject could rise was 38.4 cm. There was no back on this seat. The subject was able to rise from this height only if she

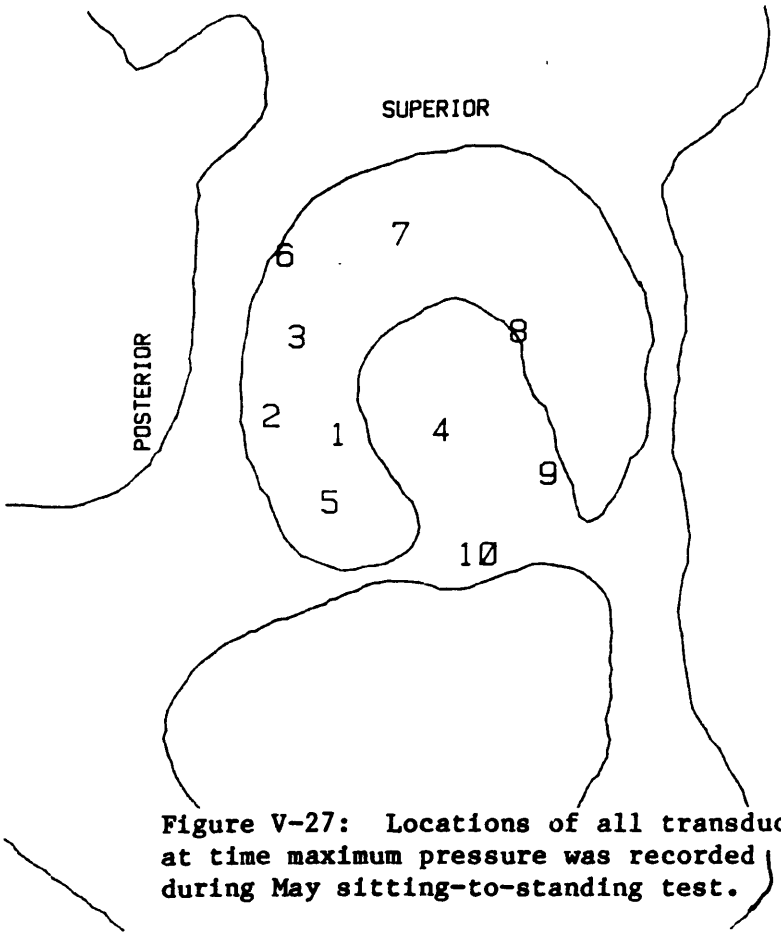

Pressure in Mega-Pascals:

1	17.81
2	1.07
3	5.57
4	0.00
5	1.41
6	-0.29
7	-1.65
8	0.83
9	0.17
10	-0.27

Figure V-27: Locations of all transducers at time maximum pressure was recorded during May sitting-to-standing test.

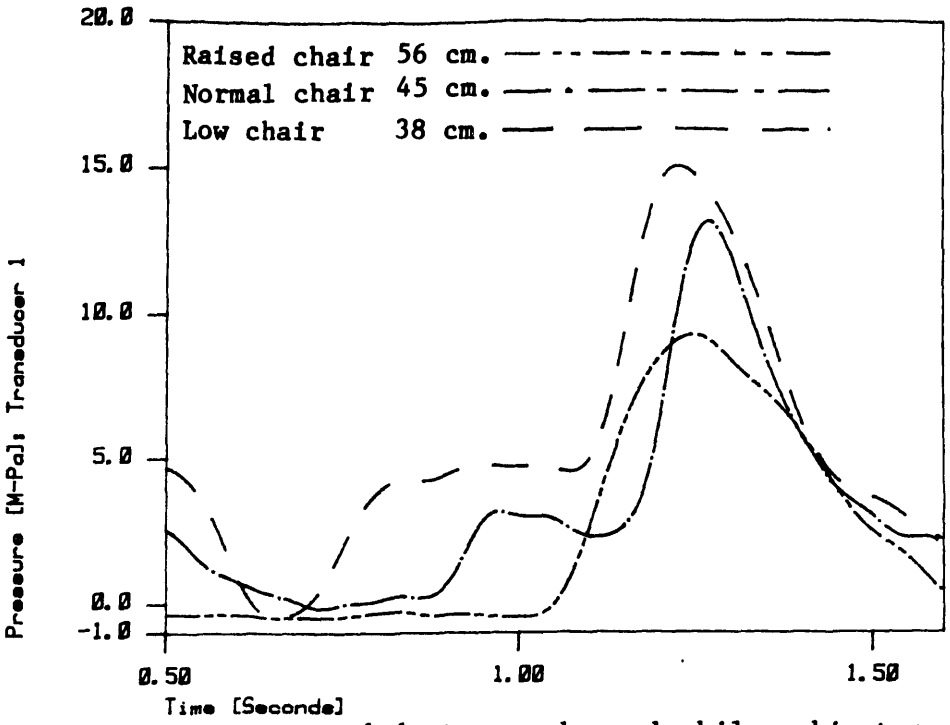

Figure V-28: Pressure recorded at transducer 1 while subject rose from different height chairs in August 1985. (Transducer 1 measured maximum pressure in all cases.) All sets of data presented start as force initially applied to forceplate. All cover same length of time.

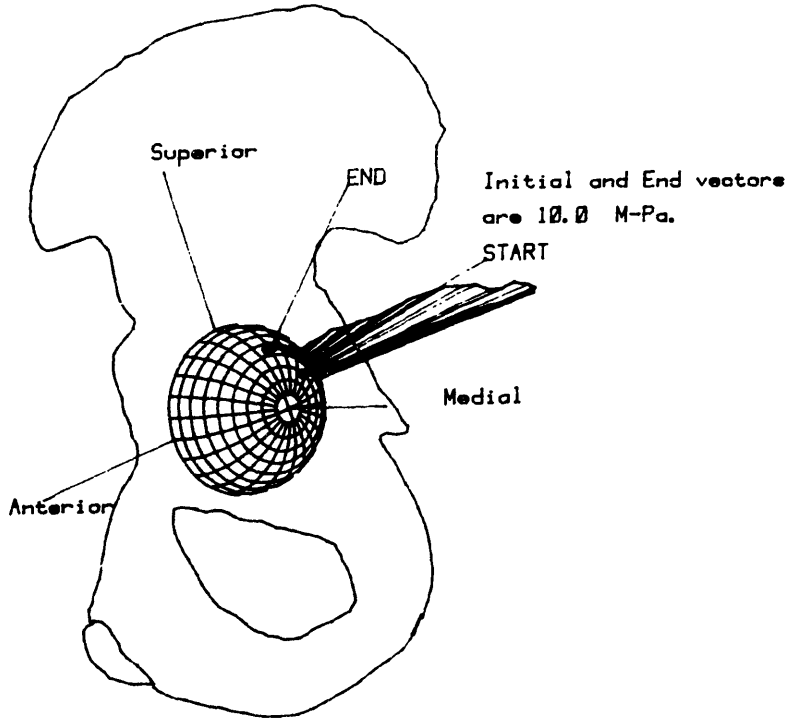

Figure V-29: Pressure measurements made at transducer 1 as subject rose from a seat 56 cm high. Data taken 14 months post-operative.

Figure V-30: Pressure measurements made at transducer 1 as subject rose from a seat 45 cm high. Data taken 14 months post-operative.

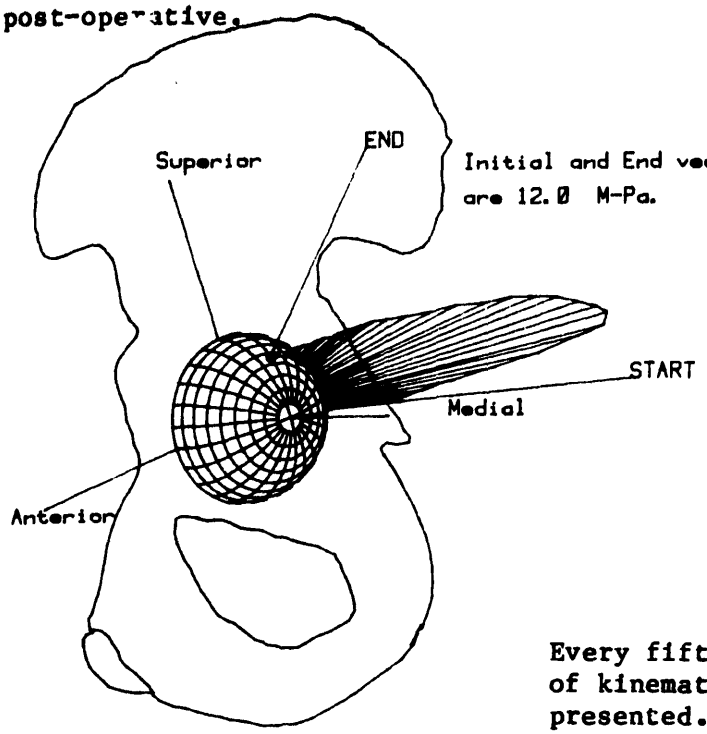

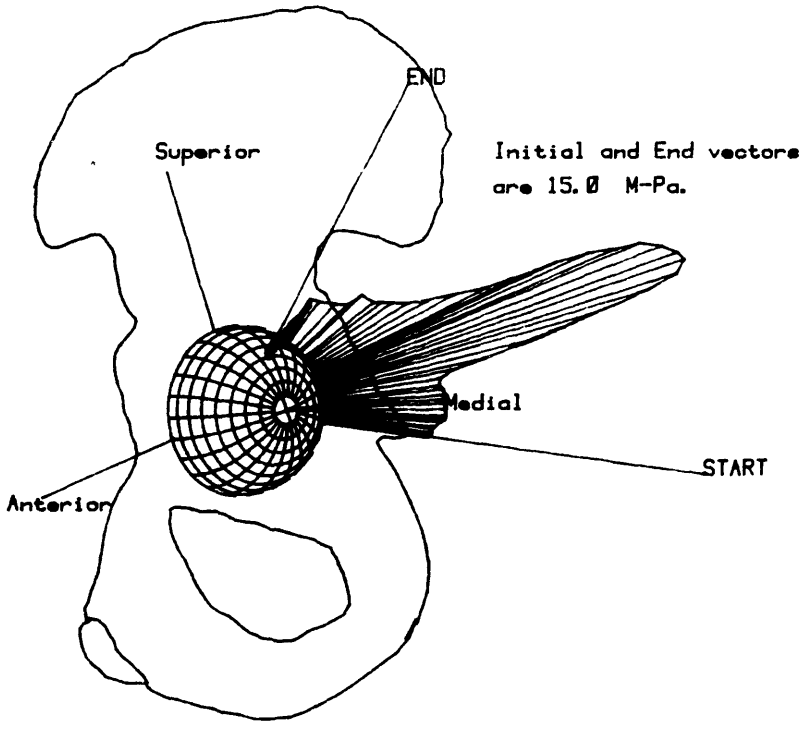

Figure V-31: Pressure measurements made at transducer 1 as subject rose from a seat 38 cm high. Data taken 14 months post-operative.

rocked back to gain some momentum. A seat 56.2 cm above the ground was used when the subject rose from a higher chair. Pressure data for rising from different height chairs is displayed in hemispherical format in Figures V-29 to V-31. These diagrams have all been scaled so that 1 M-Pa is the same distance. Vectors have been drawn for every fifth frame of data; there are 2 one-hundredths of a second between each vector on all three plots.

The highest load rates found at the hip also occurred as the subject rose from a chair. Maximum load rates, location and the arc over which they occurred are listed in Table V-16. The rate of loading increased between 6 months and 15 months post-operative; the greatest rate of loading found in August 1985 was 107 M-Pa/sec. This may be due to continued gains in muscular strength by the subject. The load rate at the hip was not higher when the subject rose from a very low chair than when she stood up from a "normal" seated position (86 degrees of knee flexion). This may be due partly to her difficulty in rising from a very low seat. Figure V-32 presents the hemispherical display for the maximum rate of loading observed at the hip.

F. Heel Bounce

The heel bounce test, in which the subject stood barefoot on the forceplate, rose on her toes, then dropped abruptly onto her heels was expected to generate high pressures and high rates of loading at the hip. Neither occurred. Initially the pressures in the hip joint were higher than for stationary stance as she plantarflexed and stood on her toes, as

Table V-16: Rates of loading while rising from a chair. Location and magnitude of maximum rates of loading and concurrent external load rate are presented.

Test	Pressure Load Rate [M-Pa/sec]	Forceplate Initial Value [N]	Rate of Force Change [N/sec]	Initial Position Lat.	Initial Position Long.	Degrees of Arc
6 months						
1	+ 38.0	112	994	51	-159	8.3
5	+ 14.7	236	-36	54	-154	8.6
11 months						
Test 1						
1	+ 47.2	129	1553	44	-148	7.2
1	- 46.0	346	207	40	-154	6.8
5	+ 38.9	252	-489	46	-163	8.6
Test 2						
1	+ 85.3	39	876			
5	+ 85.4	223	782			
14 months						
Test 1						
1	+ 107.4	803	41	60	-173	6.1
Test 2						
1	+ 79.8	814	-547	58	-173	5.0
Test 3						
1	+ 102.7	744	-328	62	-178	4.0
1	- 71.8	659	397	58	-171	10.4
Test 4						
1	+ 68.6	55	2472	47	168	6.5

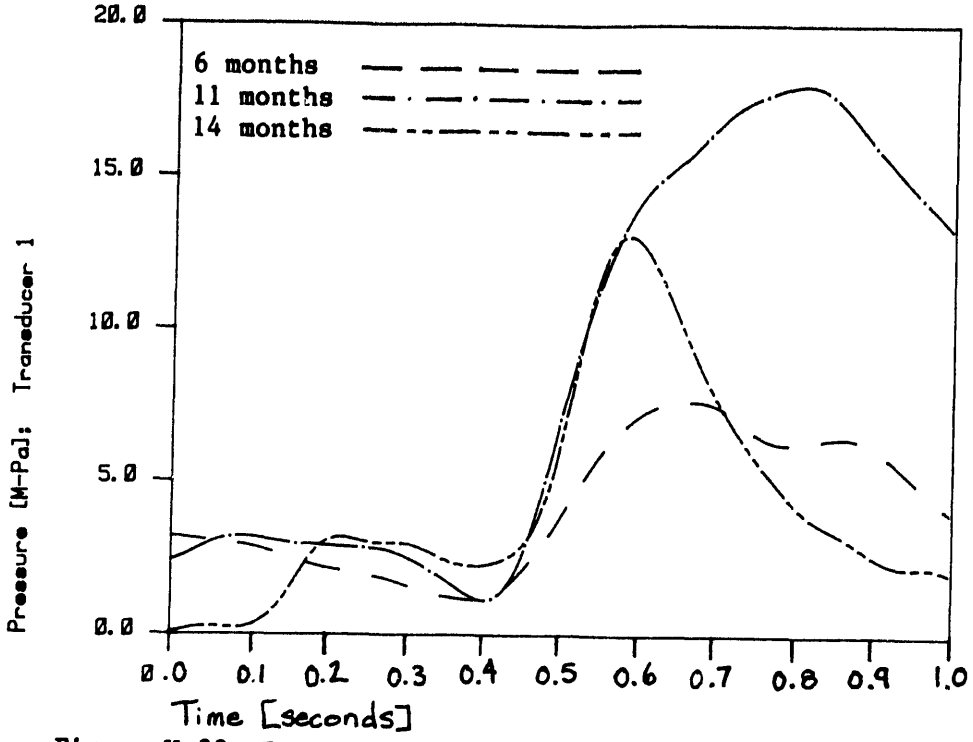

Figure V-32: Pressure measurements made during sitting-to-standing tests 6, 11, and 14 months after implantation. Chairs similar heights, movements made in rising varied.

Table V-17: Magnitude and acetabular location of maximium pressures in plantarflexion and normal two-legged stance.

	Plantarflexion	Normal Standing
Maximum Pressure:		
Test 1	6.02	2.13
Test 2	3.24	1.73
Acetabulum Location:[*]		
Latitude		
Test 1	71	49
Test 2	70	37
Longitude		
Test 1	83	139
Test 2	75	128

* Maximums occurred at different transducers in the two different positions.

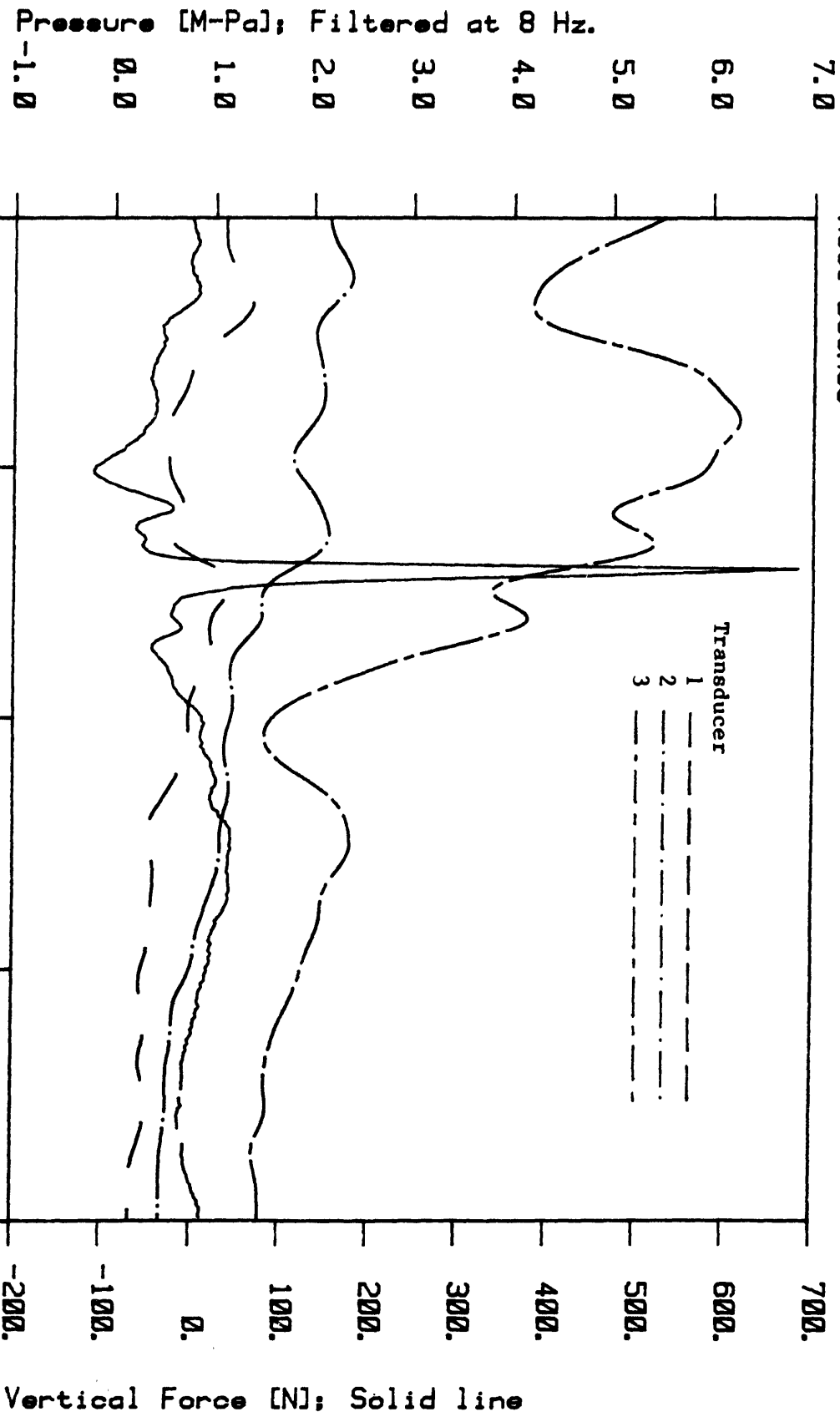

Figure V-33: Pressure and forceplate data recorded during a "heel bounce" test. Measurements from these transducers representative of recordings from all transducers.

shown in Table V-17. All data presented in Table V-17 was taken in May 1985. The maximums listed for plantarflexion and standing data were taken from the same tests, but maximums occurred at different transducers in the two different positions. In the second test, the maximum pressure during plantarflexion was probably higher before data acquisition began. The heel bounce occurred very shortly after the start of the data set.

Most transducers measured a gradual decrease in pressure as the subject moved from standing on her toes to a normal stance. Some transducers seemed to indicate a slight increase in pressure at the time of heel impact, however the change was of very low amplitude (.1-.8 M-Pa) and occurred slowly. In almost all cases, transducers measuring pressure rises at the time of heel-strike indicated an overall decrease in pressure of a larger magnitude than the peak at heel-strike. In one test a pressure peak similar to the foot-floor interaction forces was detected at one transducer, number 6. The position of this transducer was on the upper edge of the acetabulum at the time that its peak pressure was measured.

The vertical force measured at the forceplate and the corresponding pressure at three transducers in a typical heel-bounce test is shown in Figure V-33. This particular test was done barefoot and with no cushion between the floor and the subject's foot. The transducers showing relatively large variations in this test have been presented; the pressure measured at any other transducer was similar to one of the three records shown, but with less marked behavior. At no location in the joint did the pressure increase overall in this test.

The acetabular locations of the transducers are shown in Figure V-34. These positions varied little over the course of any test and were the same for all heel bounce tests.

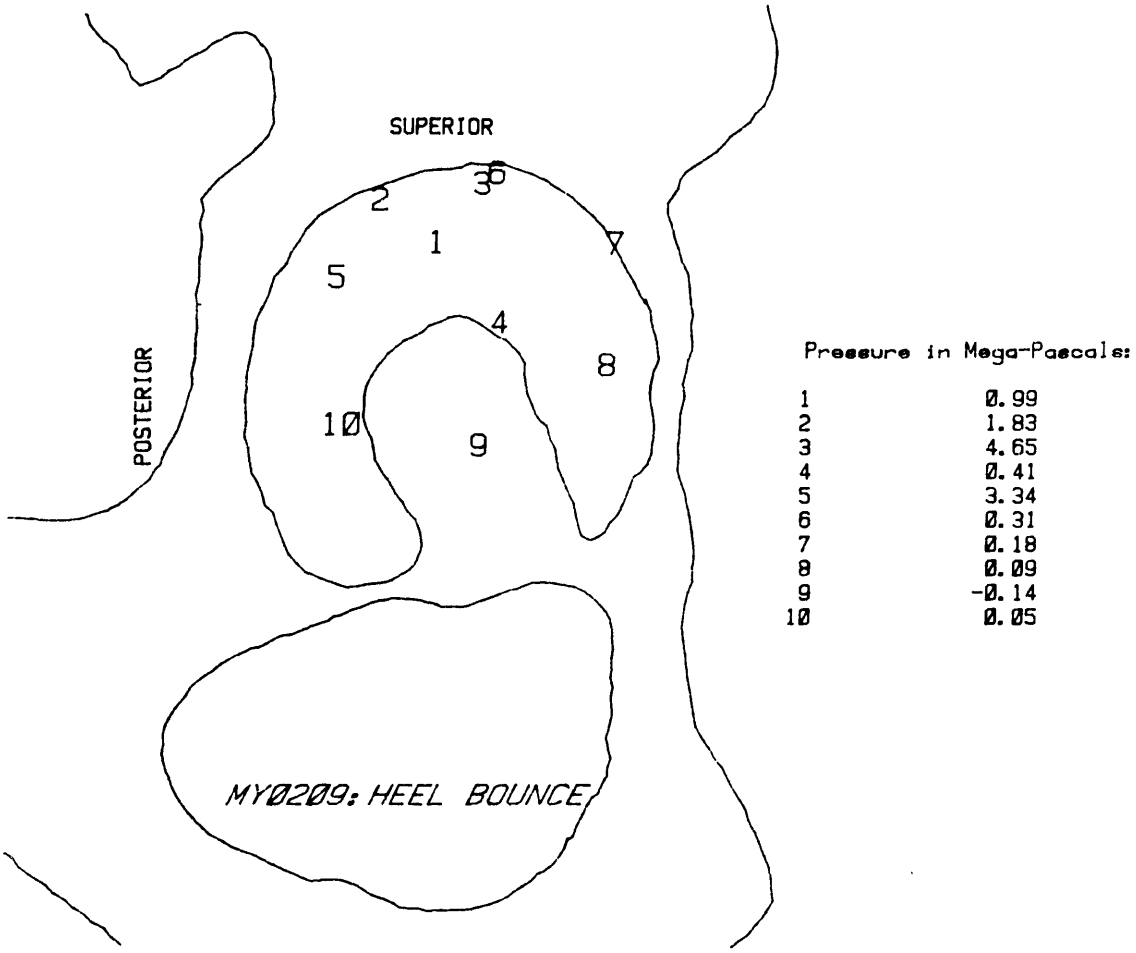

Figure V-34: Positions of transducers in hip socket during heel bounce test at time maximum force was measured at the forceplate.

VI. Discussion of Results

A. General Trends in Data

1. Comparison of Movements

a. Magnitude and Distribution of Pressures; The greatest pressures measured in vivo were approximately 18 M-Pa after filtering, located in the mid-posterior region of the acetabulum while the subject was in the process of rising from a chair. The location and magnitude of the maximum pressure in sitting-to-standing tests varied with the height of the chair. Higher chairs and consequently lower knee flexion angles produced less extreme loading environments at the hip, probably because the subject was closer to an upright position. The next highest pressures were found in stair-climbing tests; this motion produced relatively high pressures at more femoral locations than some sitting-to-standing tests. Jogging and hopping tests produced high pressures over a large portion of the joint simultaneuosly.

Pressure magnitudes produced as the subject walked varied with speed and her use of auxiliary support. In the initial period the subject walked very slowly and limped. Stance phase duration at that time was approximately twice as long as after 6 months of recovery. The maximum pressures and load rates seen in data taken at this time were about half of the corresponding values at a normal speed.

Walking with supports, a walker, crutches, or cane led to a reduction in the maximum pressure measured at the hip. Table VI-1 lists the data taken with supported walking and the maximum pressures after filtering. The use of crutches in some styles produced the greatest reduction in hip pressures. Use of a walker followed, and a cane reduced the pressures the least. Exerting 15 pounds of force on the cane lowered maximum hip joint pressures somewhat, and increasing the force on the cane to 30 pounds reduced the hip pressures more, but increasing the force on the cane to 50 pounds had no further effect on the hip joint pressures.

b. Location of Pressure Maximums; The maximum pressures in sitting-to-standing tests always occurred in the posterior region of the acetabulum. Maximum pressures were located in this region for some other actions as well, such as stair-climbing and walking assisted by crutches. In normal level walking tests the maximum pressures occurred in the dome of the acetabulum. This also was seen in cane-supported walking, independant of the force applied to the cane. Although there were other times when the highest pressure in the joint was located in an anterior region, the overall maximum for any movement was located toward the front of the body only in single-leg stance and heel bounce tests. In heel bounce tests the maximum pressures were measured as the subject plantarflexed.

Rising from a chair and climbing stairs are both actions in which the hip is flexed significantly. This probably affects the location of pressure maximums in the joint. Leg position during gait led to the expectation that the maximum pressures in normal gait would be nearer the zenith of the acetabulum, which did occur. Figure VI-1 presents overall pressure

Table VI-1; Typical maximum pressures measured while walking with various forms of assistance.

Test	Transducer	Maximum Pressure	Location	
			Lat.	Long.
Walker	5	3.8	52	152
Crutches:				
Foot off ground				
Knee Bent	7	2.4		
Knee Straight	5	4.1	78	171
Light Toe-Touch	2	2.3		
Partial weight-bearing	5	3.9	45	103
Cane:				
Light force	3	5.1	65	95
Medium force	3	4.8	66	93
Maximum force	3	4.8	67	93

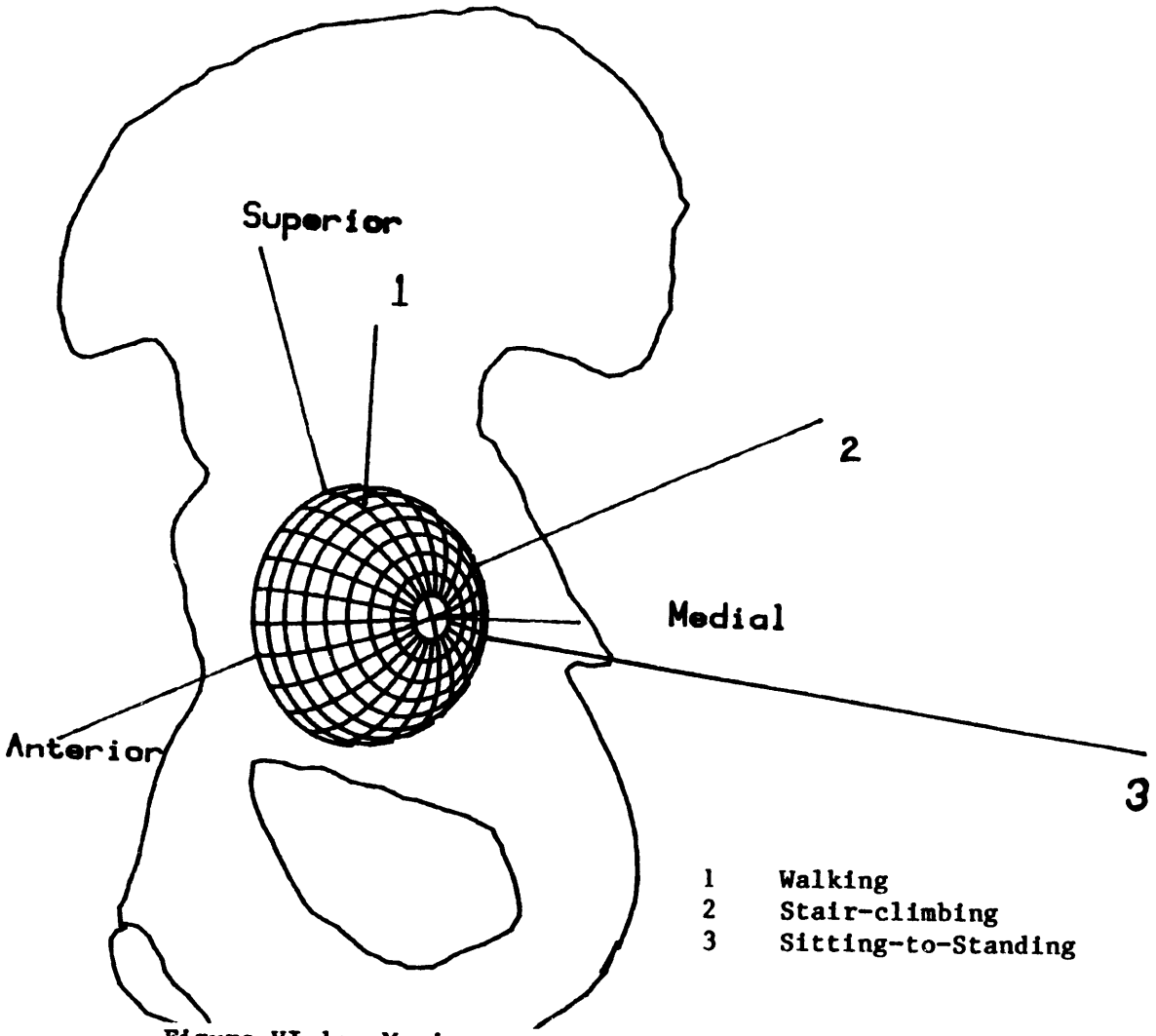

1	Walking	5.5 M-Pa
2	Stair-climbing	10.2 M-Pa
3	Sitting-to-Standing	17.8 M-Pa

Figure VI-1: Maximum pressures and location at which meaurements were made during some movements.

maximums for a few types of tests.

c. Rate of Loading at the Joint; The maximum loading rates found at the hip occurred during sitting-to-standing tests. All chair heights produced higher load rates than found in any other type of test. Four transducers recorded their fastest rates of loading during sitting-to-standing tests (transducers 1, 5, 3, and 2) The rate of loading was lower for a raised seat than for a normal or low seat. This was probably related to the production of lower maximum pressures in rising from an elevated seat; reduction in the severity of the loading environment at the hip when rising from a chair may be achieved by raising the chair height.

The next highest load rates were produced in stair-climbing and were only about half as large as those for rising from a normal seated position. The highest rate of change in pressures when jogging was not significantly greater than that for walking, although the change in force at the forceplate was faster in jogging tests.

One purpose of the heel bounce test described earlier was to generate high loading rates at the hip. However, maximum pressures in this test were found during plantarflexion, not on striking the floor. Though transducers in some locations measured peaks around the time heel strike occurred, the general trend was for the pressure in the joint to decrease, and decrease gradually, from plantarflexion to normal stance (Figure VI-2). At most transducers the change in pressure was not large, almost always less than 1 M-Pa. Noise in the transducer signals is between .1 and .35 M-Pa; this has made it difficult to draw firm conclusions about specific segments of

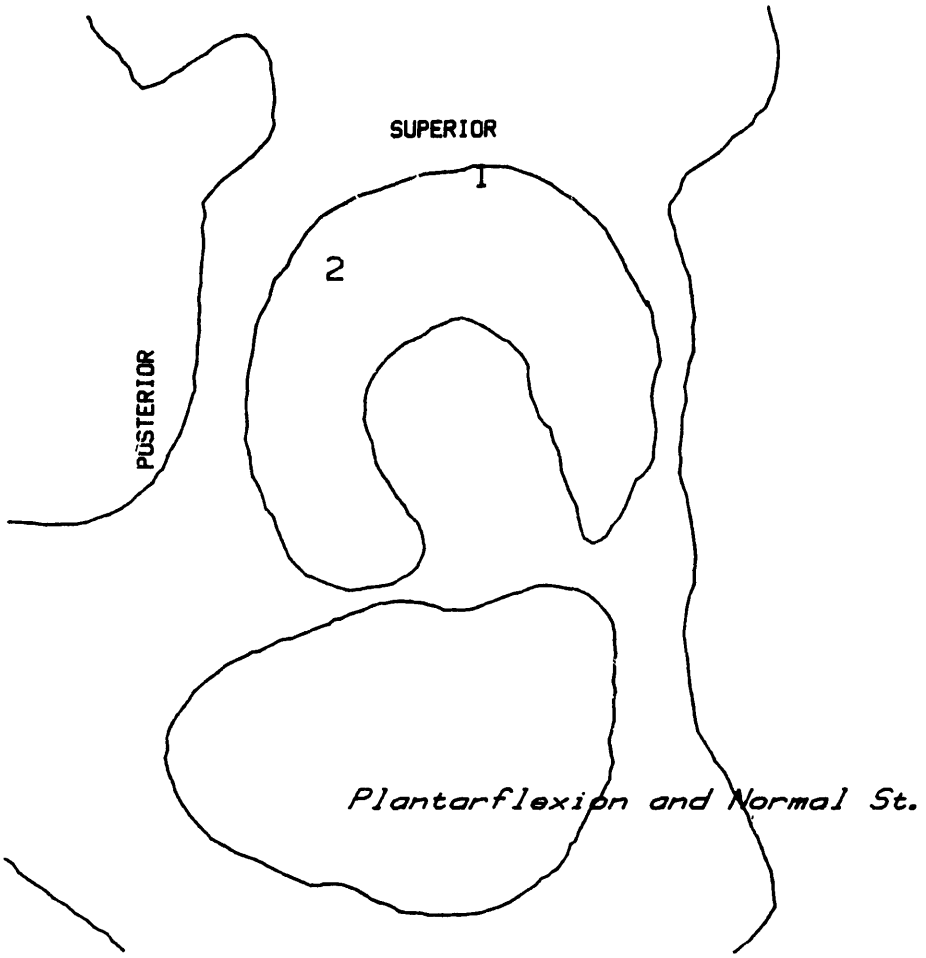

Figure VI-2: Positions of maximum pressures during plantarflexion and normal stance, taken from same test.

1 Plantarflexion	6 M-Pa
2 Normal, two-legged stance	2 M-Pa

heel bounce tests. However, the loading rates for heel bounce tests were compared to those observed at heel strike in level walking (Table VI-2). Heel bounce loading rates are presented from the time force was first applied to the floor to the peak force, which took place in less than one-fiftieth of a second. Rates of loading at heel strike in walking tests were calculated from the initial application of force over approximately the same period of time.

Muscle forces acting across the joint are the only possible cause of the results observed in heel bounce tests. Forces produced in co-contraction of the muscles surrounding the hip as the subject balances on her toes outshadow the later application of force at the foot. Much greater control of body placement is required in order to situate the center of gravity with more precision when the area of the support base is decreased by plantarflexion.

d. Locations of Maximum Load Rates; The maximum rates of loading were found in approximately the same acetabular region as the maximum pressures in sitting-to-standing tests. The same pattern was observed in stair-climbing. In level walking the highest rates of pressure increase occurred more posterior in the socket than the maximum pressures. This corresponds to the observation that the highest rates of pressure increase took place in the initial period of foot-floor contact, at which time the hip flexion angle is decreasing. Maximum rates of decrease in pressure occurred in the dome of the acetabulum in level gait. Maximum pressure increases during walking began before heel strike and preceded the largest increases in forceplate force.

Table VI-2: Comparison of Heel Strike and Heel Bounce Load Rates

	Heel Bounce Tests			Gait Data		
	11 mo.	11 mo.	14 mo.	11 mo.	11 mo.	14 mo.
Rate of change of force	26543	10996	14925	1660	4236	7474
Pressure Rate of Change						
Transducer						
1	9	5	10	3	11	9
2	-9	-2	0	22	14	23
3	-23	-4	-9	18	14	20
4	-4	2	-2	-2	2	-2
5	-12	3	-4	-1	10	17
6	-8	8	-1	-4	-3	-3
7	0	0	-1	4	1	5
8	1	2	1	1	1	2
9	0	2	0	0	-1	-1
10	-13	-4	1	-3	-3	-2

Maximum load rates were found at between 40 and 75 degrees in latitude, which is between the center and rim of the acetabulum. Longitudes at which maximum load rates were measured varied over a somewhat larger range, from approximately -140 (or 220) to 85 degrees in longitude. This arc extends from the lower posterior portion of the joint through the posterior and superior regions of the acetabulum.

The load rates were calculated over a finite period of time; however, times were chosen so that the slope of pressure with time was constant. The initial and final positions at which pressures were measured were identified (when kinematic data was available) and tables of load rates have included the degrees of arc in tha acetabulum over which calculations were made. From information in the Results section it can be seen that the locations at which pressures were measured did not change substantially during load rate calculations.

e. Relationship of Pressures and Foot-to-Floor Forces in Time: Maximum pressures often preceded or were simultaneous with the maximum force measured at the forceplate. The same order was observed between the maximum load rate at the hip and the greatest change of force on the forceplate. Decreases in pressure and force followed the same sequence; however, maximum pressure decreases typically occurred earlier in advance of maximum force decrease. The relative timing of pressures and external force may be due to muscular contraction in anticipation of external force changes. In some tests the greatest muscular forces may be required prior to the application of large foot-floor interaction forces. This seems particularly evident when rising from a chair.

In rising from a chair the highest pressures were typically generated when only a small part of the subject's body weight was supported by the floor, well before she had fully risen. Muscular contractions while rising contribute to the production of pressures greater than are measured in standing or walking. The subject begins the movement with her trunk, rotating forward about her hip joint; co-contraction of the muscles about her hip joint may occur to prevent further flexion at the hip. The momentum from the motion of her trunk then assists in continued movement forward as she rises.

Level walking and jogging produced completely different environments at the hip joint. Most notably, all transducers produced nearly the same profile of pressure vs. time for jogging tests, whereas in walking the shape of the pressure record with time varied widely among transducers. The load on the hip joint may be carried more completely by hydrostatic pressure in jogging than in walking. The timing of maximum pressures also differed; in jogging the overall maximum occurred at about 40 percent of the stance phase.

In some walking data the overall maximum occurred at between 30 and 40 percent of the stance phase, but in others it took place at about 20 percent of the stance phase. [*] More transducers measured pressures

---

[*] If stance phase is 60 percent of cycle in walking then the maximum pressure occurred at about 16 % of the gait cycle

close to the maximum in jogging than in walking, and transducer maximum readings occurred at more nearly the same time in jogging.

Heel bounce tests were expected to reveal information about the relationship between hip joint pressures and forceplate force without complicated kinematics. However, little could be said about the relative timing and magnitude of these two measurements on the basis of heel bounce data because the pressure variations associated with the movements were very low, of the same amplitude as noise.

2. Changes during Post-surgical Recovery

The subject was continuing to gain strength throughout the 15 months that data was taken. The most obvious gain occurred within the 6 months following implantation of the prosthesis. After that period of time she was walking normally, both in speed and the amount of force she placed on her instrumented leg. Changes in pressure maximums between 6 months and a year after prosthesis implantation cannot be entirely attributed to continued recovery because the subject's manner of performing actions varied. However, the speed of performance of motions demanding high exertion, such as rising from a chair and stair-climbing, continued to increase after 6 months, producing higher rates of loading at the joint. The maximum load rate measured at the hip increased from 38 M-Pa/sec at 6 months after implantation to 85 and 107 M-Pa/sec at 11 and 14 months. The increase in maximum load rate between 11 and 14 months post-operative occurred despite the measurement of lower maximum pressures 14 months into the subject's recovery.

B. Accuracy Issues

1. Error Bounds in Coordinate Transformations

Several sources of potential error are involved in transformation from prosthesis to acetabulum coordinates. These include estimation of the relationship between the externally mounted pelvis marker and the acetabulum and approximation of the acetabular surface by a sphere. These estimations introduced only a diminishingly small amount of error. Determination of the relationship between the pelvis and acetabulum was made on the basis of X-rays and surgical knowledge and is believed accurate. The acetabulum is known to be essentially spherical [99].

Estimation is involved in the display of transducer locations on the acetabulum, since the shape of the subject's pelvis and acetabulum could not be reproduced perfectly. The other source of error in locating pressures on the acetabulum is kinematic noise and error; these result in estimates of absolute physiological angles that are accurate to within +/- 2.5 degrees. However, changes in joint angle during a given test motion are accurate to within +/- 1 degree [32]. All three hip angles used in transformation to acetabular locations change both acetabular latitude and longitude, and do so in a manner which is dependant on latitude. A given linear distance on a hemisphere represents a greater change in longitude interval near zero degrees latitude than near 90 degrees latitude. The region within which pressures are known to have been measured is the same in area for all parts of the joint. Therefore, numerical error bounds and changes in location have been presented as a percentage of the

circumference of the sphere fitting the acetabular socket.

The absolute acetabular location of pressures can be considered accurate within +/- .7 % of the circumference of the sphere that fits the acetabulum. Error in the location of pressures at one time relative to that at another on the same test date is under +/- .3 % of the circumference of the joint-sphere. Calculations of the relative locations of two simultaneous pressure measurements are extremely accurate since the relative positions of transducers are fixed and known precisely. Area A in Figure VI-3 corresponds to the area within which the acetabular position of a pressure measurement may be known for a calculated location on the acetabulum and +/- 2.5 degree accuracy in hip angle measurements. Cross-hatched region B is a similar area for one degree of hip angle measurement error.

Thus, estimation of a given acetabular location cannot be made completely accurately. However, the relative placement of measurements in the acetabulum is much more accurate. Accuracy of changes in acetabular location is determined by kinematic accuracy alone; other sources of error affect all calculations of acetabular position equally.

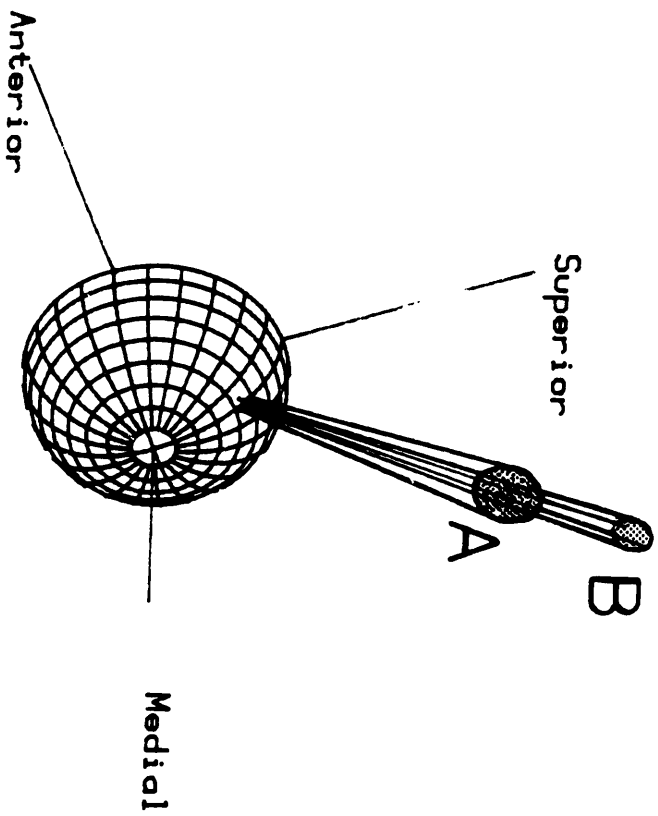

Figure VI-3: Error limits on location of pressure meaurements in acetabulum resulting from accuracy with which hip joint angles are known.

2. Noise

Transducer noise is about .2 to .35 M-Pa in amplitude (each transducer is slightly different). Transducers in the outer ring and transducer 4 rarely measured pressures above 1 M-Pa, thus the signal from these transducers is often of the same amplitude as noise, even in the 0 to 10 Hz range. Assessment of whether variations are the result of noise or pressure changes is difficult in tests where the range of pressures measured was close to the noise amplitude. Measurements at a single transducer which vary over a range larger than 0.5 M-Pa are clearly attributable to pressure changes but smaller measurement variations are less easily interpreted.

3. Transducer locations

Symmetrical arrangement of transducers is not equally optimal for pressure measurements in all femoral head positions. Ideally, in any action one would like to make all pressure measurements at areas which were likely to be load-bearing; there probably is no transducer arrangement that will accomplish this feat. For the current transducer arrangement, one or two transducers are sometimes facing the foveal notch or have rotated out of the acetabulum. Estimation of times at which this occurs can be made from the 2-D and hemispherical displays of the locations at which pressures are measured. Negative pressure measurements have been measured at transducers which may not be on the acetabulum. Relatively high pressures are also occasionally measured in non-acetabular regions, possibly from contact with the acetabulum labrum or other joint parts. In general, measurements made at transducers which are not thought to be opposite the acetabulum have

been discounted after their location is noted.

4. Rate of Data Acquisition

The early data acquired from the in vivo prosthesis has not been presented often in discussions of dynamic tests because this data was taken at a slow frame-rate, 10 frames per second. Data for a few tests in July 1984 was taken at 250 Hz; this has been presented when appropriate. A great deal of data was taken after recovery of the subject and the later kinematic data is probably more accurate due to increasingly accurate kinematic data acquisition. Most information presented in this thesis has been from data 6 months and more after implantation.

5. In Vivo Calibration

While applying unloading traction to the subject's leg is the most probable means of obtaining low pressures in all areas of the hip joint, some transducers are subjected to less pressure at other times. Although the determination of transducer output for zero pressure is thought to be reasonably accurate negative pressure values have sometimes been obtained. Pressure measurements which are negative mean only that a particular transducer has been loaded less than it was during the associated in vivo calibration test. the infrequence of negative pressure recordings justifies the use of unloading traction as an in vivo zero-pressure calibration technique.

C. Comparisons with Published Results

1. Rydell

The first human in vivo data to be reported on hip joint loading was published by Rydell in 1966. His strain-gauged femoral head apparatus measured force applied to a prosthetic femoral head. Table VI-3 summarizes the force vectors Rydell found in two subjects for various positions and actions. Although actual comparisons between Rydell's femoral head force vectors and MIT/MGH pressure measurements are not possible, transformation of the point of application of Rydell's force vectors from the femoral head coordinates in which he presents data to the corresponding acetabular locations in the coordinate system used throughout this thesis has been attempted. In order to do this, hip angles have had to be obtained from Rydell [90] or estimated on the basis of his description of his subjects' position. The algorithm used in coordinate transformations is presented in Appendix 4. The hip angle estimations that were made can be found in Table VI-4. Only results from static tests were used due to the lack of kinematic information for Rydell's dynamic data. Even for static data, the hip angles used for single-leg stance were taken from MIT/MGH kinematic data and may have little resemblance to the actual situation. For the flexion tests, only the flexion angle given in the test description was input for kinematic positioning. The resulting acetabular locations are also in Table VI-4. Figures VI-4 and VI-5 show Rydell's force vector measurements in hemispherical format for 90 degrees flexion and single-leg stance for both of his subjects. In addition to force vector measurement, Figures VI-4 and VI-5 present maximum pressure measurements from the

Table VI-3: Femoral locations taken from Rydell [66].

Test Description	% of Body Weight	Alpha	Gamma
30 degrees flexion			
Case 1	106	21.7	60
Case 2	101	27.7	32
90 degrees flexion *			
Case 1	65	29.3	58
Case 2	82	21	52
Single-limb support			
Case 1	230	40.2	7
Case 2	280	33	10

Table VI-4:
Rydell's results transformed to acetabular and femoral locations expressed in same latitude and longitude as MIT/MGH pressure-measuring in vivo results.

Test name	Hip Joint Angles			Femoral Head		Acetabulum	
	Flexion	Abduction	External Rotation	Lat.	Long.	Lat.	Long.
Flexion							
Case 1	30	0	0	41	-54	31	44
Case 2	30	0	0	32	-39	57	66
Case 1	90	0	0	44	-45	19	151
Case 2	90	0	0	39	-48	34	135
MIT/MGH	90	0	0	0	0	47	-142
Single-Leg Stance							
Case 1	15	5	0	23	-3	50	67
Case 2	15	5	0	22	-22	61	62
MIT/MGH	15	5	0	31	30	71	77

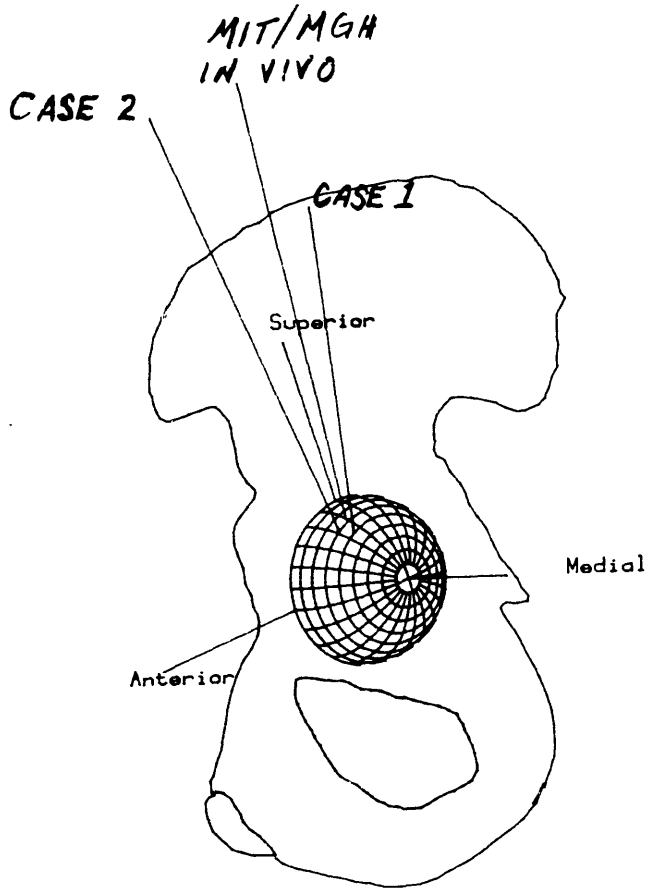

Figure VI-4: Comparison of Rydell's force vector meaurements with maximum pressure recorded from MIT/MGH instrumented prosthesis during single-leg stance. Hip angles for Rydell's data taken from kinematic data for MIT/MGH subject.

Case 1 2.3 x body-weight
Case 2 2.8 x body-weight
MIT/MGH 8 M-Pa

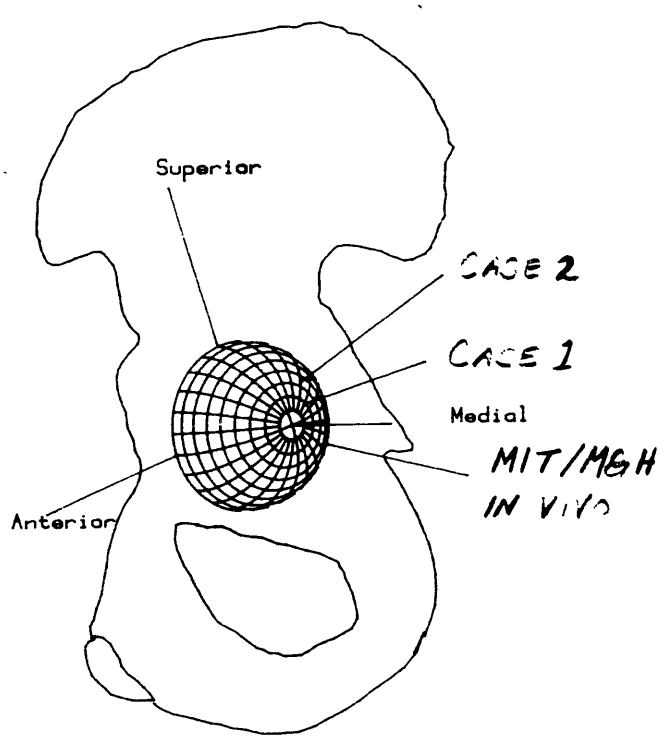

Figure VI-5: Comparison of Rydell's force vector meaurements with maximum pressure recorded from MIT/MGH instrumented prosthesis during 90 degree flexion.

Case 1 .65 x body-weight
Case 2 .82 x body-weight
MIT/MGH 2.1 M-Pa

MIT/MGH in vivo prosthesis for the same types of static tests. As can be seen, there are differences in the data. However, the point of application of the force vector determined by Rydell appears to fall in the general region in which the highest pressures have been found for comprable static tests.

2. Rushfeldt

Fewer assumptions were made in transferring data obtained from the hip simulator in the M.I.T. Lab. for Biomechanics to the format used previously in this thesis. Since results of tests done by Rushfeldt had already been arranged in acetabular locations, the coordinate system used by him had only to be changed to the one used in the hemispherical and 2-D display programs. This algorithm is presented in Appendix 5. Results from the hip simulator have been previously plotted in the form of pressure contours; in transformation to in vivo acetabular coordinates the boundary within which maximum pressure was measured has been outlined. Figure IV-21 is from Rushfeldt [86] and is of pressure contours in the acetabulum for a correctly fitting femoral head in a position similar to normal stance, with 2250 N of load applied. In Figure VI-6 the region of maximum pressure has been outlined on the hemispherical display. Figure VI-6 also presents the maximum pressures measured in vivo for static normal stance of the subject, in which approximately 350 N of force was measured at the forceplate. It is difficult to draw any conclusions regarding the comparison of the two sets of data though some similarity can be seen. The process of changing hip simulator data to this display format is somewhat laborious; very few sets of data have been transformed at this time.

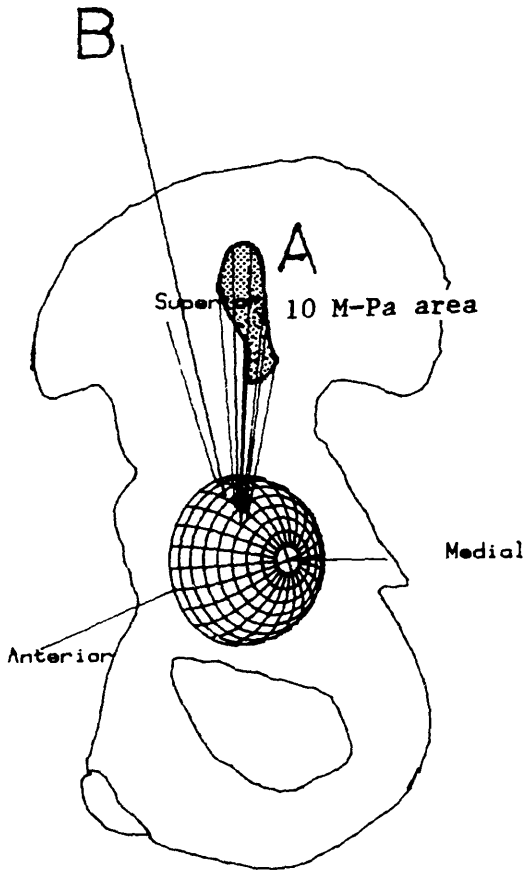

Figure VI-6: Comparison of region maximum pressure was measured in by Rushfeldt and maximum pressure in vivo for two-legged static stance.

A Rushfeldt 2250 N applied
B In vivo

3. Paul; Estimates of Maximum Force Vector

Paul [76,78] estimated that the maximum force at the hip joint during gait occurs at 7 and 47 percent of the gait cycle, as marked on the forceplate record in Figure VI-7. His estimate of maximum resultant force on the hip joint was 4.9 times body weight. Heel-strike was considered the start of a gait cycle; walking speeds were normalized by setting stance phase to 60 percent of a full cycle. Using the same standards the maximum pressure measured at the joint in vivo was found to occur at 16 to 30 percent of the cycle, as marked in Figure VI-7. The pressures recorded at all transducers at the time that the maximum pressure occurred have been shown in Figure VI-8. Figures VI-9 and VI-10 present the pressures at all transducers at 7 and 47 percent of a gait cycle (from data 11 months after implantation). Pressure vectors in these three figures have the same scaling. It seems very likely that the average pressure in the joint is higher at the time the maximum pressure was recorded than at either of the predicted times for pressure peaks.

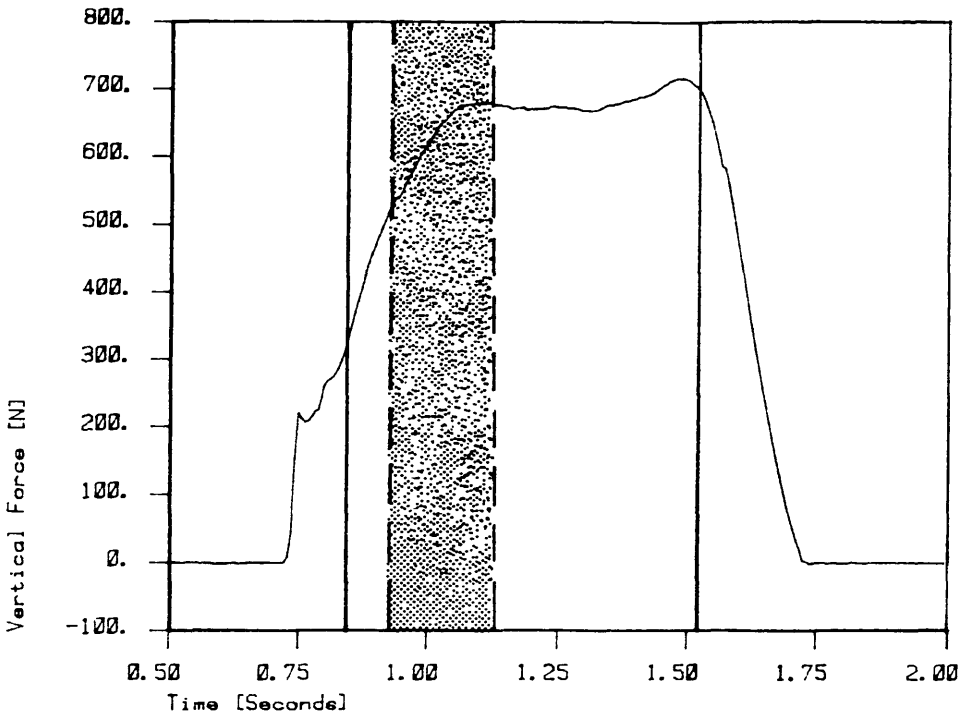

Figure VI-7: Times at which Paul [76] estimated peak hip joint forces (solid lines) and within which maximum pressures measured in vivo (dotted)

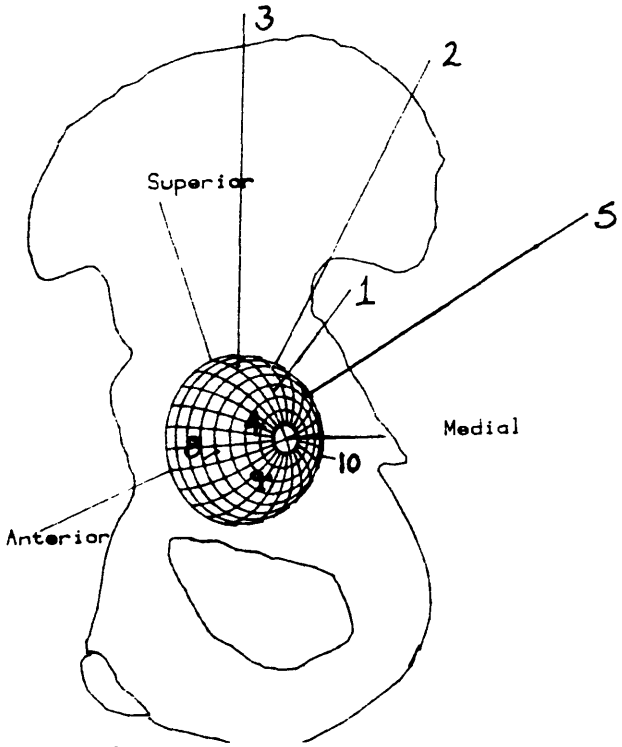

Figure VI-8: Hemisphere display of pressures at all transducers at time maximum pressure measured in level walking. Transducers 6 and 7 measured 0 M-Pa. Data from 11 months post-op.

Figure VI-9: Hemisphere display of pressures at all transducers at 7 % of gait cycle (as defined by Paul [76]). Transducers 6, 7, 8, 9, and 10 measured 0 M-Pa. Data from 11 months post-op.

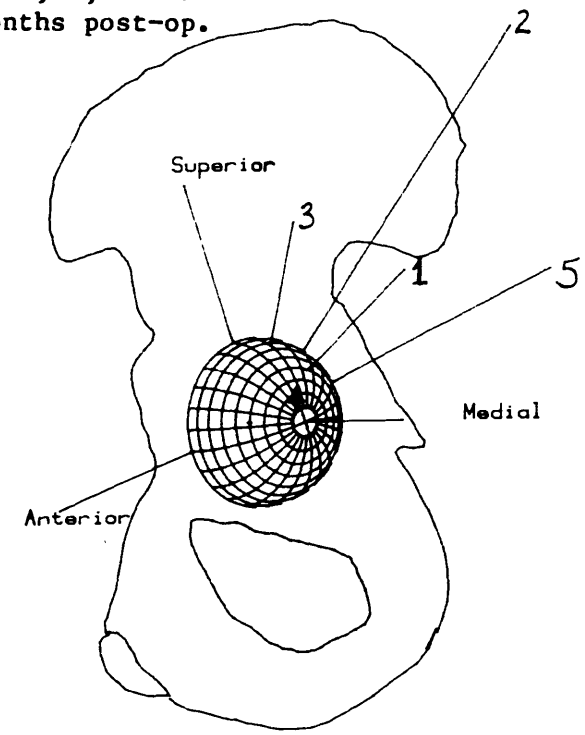

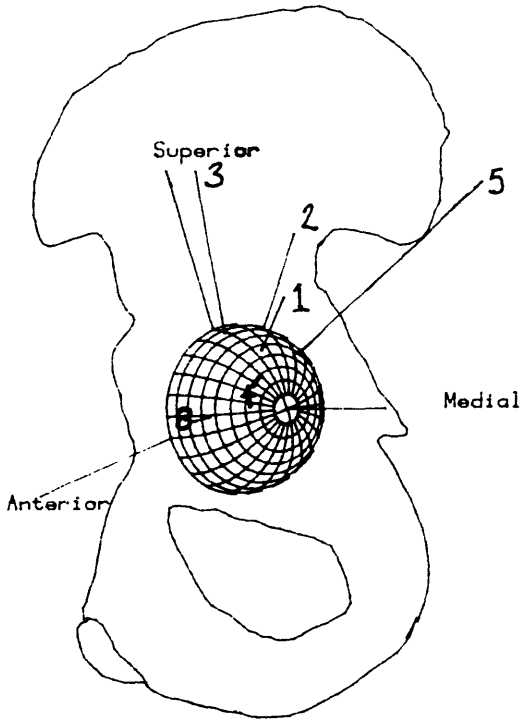

Figure VI-10: Hemisphere display of pressures at all transducers at 47 % of gait cycle. Transducers 6, 7, 9 and 10 measured 0 M-Pa. Data from 11 months post-op.

VII. Conclusions and Recommendations

A. Conclusions

Three points characterize the in vivo loading environment at the hip:

1. High pressures and rates of loading are found in the human hip joint during normal movements;

2. Measurement of non-uniform and irregularly varying pressures in vivo supports results obtained in vitro at MIT.

3. Muscle forces, including co-contraction forces, are significant in determination of the load experienced by joint cartilage.

The maximum pressure measured in vivo was 18 M-Pa. Pressures of this magnitude were not predicted by in vitro studies; the maximum measured by Rushfeldt was 14.3 M-Pa (2075 psi) which was measured when a 2250 N load was applied to an undersized prosthesis having very little contact with the acetabulum. Great care was exercised in ensuring a good fit between the in vivo instrumented prosthesis and the subject [108].

The rate at which pressures were found to increase in the hip joint was also unexpectedly high, although there is no previous data on which to base estimates of in vivo load rate. These new data must be reconciled with the

several extant joint lubrication mechanisms. Illumination of prosthesis failure and ways in which prosthesis designs may be improved will result from consideration of in vivo pressure data.

In spite of differences in the magnitude of pressures found in vivo and in vitro, the pressure data collected from the implanted prosthesis supports previous in vitro findings at MIT. In both situations the pressure distribution in the hip joint is non-uniform and contains regions of very high pressure. The in vivo pressure data suggests the presence of steep pressure gradients, as was also determined in vitro.

Probably the most important result from in vivo pressure data is establishment of the importance of muscle forces on loading at the hip. No analytic approach for determining the force at the hip joint has included muscle co-contraction forces. In some positions and motions co-contraction may be great enough to completely change the loading at the joint. This is particularly well demonstrated by results for the heel bounce and sitting-to-standing tests. Pressures in the heel bounce data were higher as the subject balanced on her toes than were pressures as her heels struck the floor (Table VI-2). Attenuation at the hip joint of the heel strike impact was expected from knee flexion and damping through the intervening body tissue. Beyond significant attenuation, the pressure actually drops over the course of the action as the muscles relax.

The effect of muscle forces is most apparent for those movements which produce severe conditions in the joint. Generation of high pressures, loading rates, or both occurred most frequently in motions which were

"high-demand" in terms of the muscle strength their performance required. The actions included in this group were rising from a chair, climbing stairs, jogging, and hopping. Rising from a chair led to the highest pressures and rates of joint loading. The hip also experienced high pressures and load rates when the subject climbed stairs. In jogging and hopping tests relatively high pressures were measured in many joint locations at the same time. Level walking did not lead to an extreme joint environment, but again demonstrated the effect of muscular contractions in the measurement of high loading rates and relatively high pressures prior to heel strike. Since the subject's ability to perform several types of movement still appears to be increasing 15 months post-operative; it is possible that even greater rates of loading will be measured in the future.

B. Directions for Further Work

Specific recommendations for future work and research fall into three broad categories. There are more possibilities to explore in display and manipulation of pressure and kinematic data. Acquisition of other types of data to augment that currently available is another line of work. The results thus far must also be examined more closely for correlation to joint function.

1. Data Manipulation

In three-dimensional pressure displays there is a need for user control of the angle from which the acetabulum is viewed. Use of a graphics terminal with the capability to perform 3-D hardware rotations of objects on display

(preferably one which can display objects in color and from which hardcopy can be obtained) would allow user selection of the acetabular view. This would make it possible to vary the region of the acetabulum displayed most advantageously. Other manners of displaying data would also be possible if color were available to convey information. Work is underway to extend displays in this fashion.

Undesirable restrictions on the use of data are presently imposed by the way in which data is stored. Currently, many types and formats of data must be available in order to fully assess the events that occur during a test. This means that much computer space must be allocated to the storage of data. Many tests are done on each test date and data has been acquired on several days making it impossible (with the currently available computer resources) to easily examine data from any test. Data must be transferred from storage on magnetic tape or multiple RL01 disk packs into available computer memory or onto one RL01. This is time-consuming and limits the inter-test comparisons that may be made. Compression of data into a format requiring less computer space would make assessment of the variations in hip load environment much easier.

No satisfactory numerical measure of the reproducibility of pressure data was developed. Comparisons of multiple data sets for a repeated action indicate approximately the same pressures in a given region of the joint under a given set of conditions. This is comforting, but such a statement is neither concise or precise. One relatively simple possibility that extends the idea of sample comparison is to make an assessment of variation in forceplate resultant force or vertical force at discrete times in a gait

cycle and compare this with the variations in transducer pressure magnitude and location in the acetabulum for the same points in a gait cycle.

Comparison of more published results with the in vivo data obtained from tne pressure-measuring prosthesis may be interesting. More of the results from the hip simulator at MIT should be compared with in vivo data. The peri-acetabular pressures obtained by Cristel et al [26] could also be compared to pressures evaulated at femoral locations.

Estimation of joint forces and moments is possible using kinematic and kinetic data alone; calculation of these quantities is possible with the kinematic and forceplate data acquired at MIT by using a software package labelled NEWTON. Although no force vector measurements are available from the in vivo prosthesis, comparison of estimates made by NEWTON with the actual instantaneous pressures may reveal information on the amount of co-contraction taking place.

2. More data possibilities

The importance of muscle forces in determining the loading environment at joints cannot be ignored. Knowledge of co-contraction forces is necessary for complete understanding of hip joint mechanics. More in vivo measurements of the pressures at the hip, and preferably forces as well, are required to obtain information on the magnitude and range of muscle forces applied in specific situations.

One direction to explore is the relationship between externally applied

force and the magnitude and rate of change of pressures at the hip. The hip simulator in the M.I.T. Biomechanics Lab. could be used with well-fitting acetabula and run in its force control mode. A means for controlling the rate at which force is applied through the hip simulator could also be devised. The force applied to the acetabulum could then be increased until pressures similar to those obtained in high-demand actions were measured. Different rates of external force application could be used in attempts to duplicate the joint load rates as well. This information may better illustrate the magnitude of muscle forces involved in the load transfers observed in vivo.

Redesign of an instrumented prosthesis to measure parameters in vivo could also be done. In the design of future prosthetic devices to be used in measuring pressure at the hip joint it may be desirable to relocate some of the transducers, and add more transducers if pressure alone is to be measured. The transducers enclosed in shaded hexagons in Figure VII-1 rarely gave useful results. The others registered relatively high pressures occasionally. Two other considerations in redesign of this pressure-measuring prosthesis include the addition of a means to measure force vector and temperature at the joint. Although pressure measurements are important to lubrication and osteoarthritis research, knowledge of the resultant force vector at the hip can more easily be interpreted to give the force with which muscles act across the joint. As a summary of the global environment of the joint, the force vector would more simply display the overall joint conditions.

The transducer zero-pressure value is known to change with temperature.

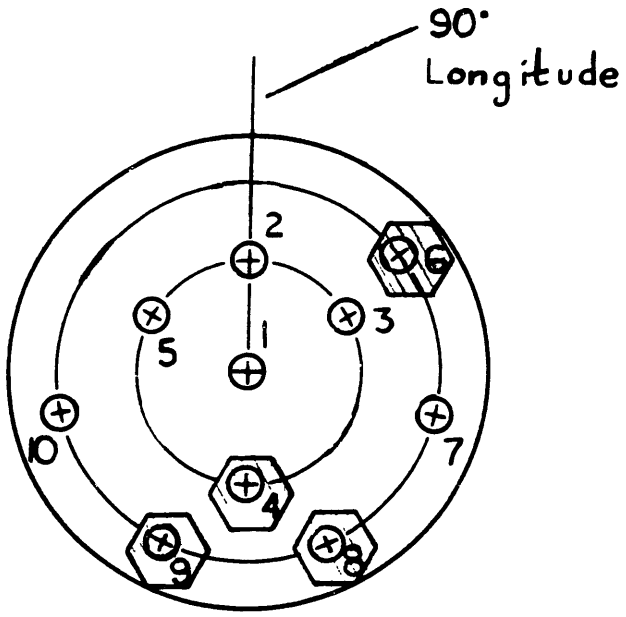

Figure VII-1: Femoral head measurement locations at which pressures greater than 1 M-Pa were rarely recorded. Marked locations are those which have been shaded.

The temperature of the joint may rise as much as 2 degrees C. during movement [109]. The prosthesis is also known to produce heat while it is powered. These difficulties were avoided as much as possible by taking in vivo calibration data and limiting the time the prosthesis was powered. Heat dissipation due to movement and prosthesis powering may have had the same affect on the calibration measurements and the other tests. However, a thermistor should be included in the design of future instrumented prostheses.

3. Interpretation of Results

Examination of the data obtained from the prosthesis has led to the development of a few guidelines for the interpretation of pressure data. Data should be filtered to eliminate electronic noise, or should be corrected for the peak-to-peak noise amplitude. Absolute location of transducers in the acetabulum can be considered approximately correct. Changes in transducer position in the joint are measured more precisely. The location of transducers in the hip joint should be taken into account when examining the pressures measured. Finally, and fortunately, pressure magnitude and position are similar in each data set from repeated motions; examination of a few sets of data for a given kinematic situation should be sufficient.

Use of these guidelines should allow other investigators to interpret the results obtained from the implanted instrumented prosthesis. The data presented is pertinent to several areas of research on human joint mechanics. Studies on osteoarthritis, joint lubrication, and prosthesis

failure mechanisms should incorporate information on the extreme loading environments found in vivo. Extending interpretation of results into these areas is beyond the scope of this thesis. The wealth of the data obtained from the instrumented prosthesis demands further attention from investigators in these fields. Results obtained in vivo should be compared to those obtained in vitro and from joint model simulations. The displays and processing techniques described and presented here should make information from the in vivo instrumented prosthesis accessible to investigators from a diverse range of backgrounds.

Appendix 1: Information on the TRACK data acquisition system

I. Introduction

Research on human and animal motion requires accurate information on the three-dimensional location of limb segments and the external forces applied to the limbs. Unlimited acquisition of this information is not possible. Historically, movement data has been very restricted in the region over which data can be taken, the constrictions to the subject from which data is taken, and the accuracy of the kinematic data. A motion analysis system was developed at the M.I.T. Eric P. and Evelyn E. Newman Laboratory for Biomechanics to increase the quality of kinematic data. This system makes use of both specialized hardware and software components to automatically acquire, process, and display kinematic and forceplate data. Relevant data can be acquired concurrently with pressures from the instrumented prosthesis.

Information on the kinematic data acquisition system can be found in references [3,32]

II. Components of the MIT motion analysis system

A. Hardware

Kinematic data at M.I.T. is acquired with two Selspot cameras. These cameras have lateral photo-effect diodes in their image planes. The

Selspot system time-multiplexes the serial illumination of 30 infra-red light-emitting-diodes (LEDs) at a maximum rate of 315 Hz for each LED. The LEDs used are small, omni-directional, and radiate only in the infra-red. The location on the image plane at which each LED light is centered is electronically registered and converted to an X-Y position in the viewing volume. This data is stored digitally in a PDP 11/60. Grouping of three or more LEDs at known spacing on a rigid structure allows reconstruction of the third dimension by comparison of the actual inter-LED distance with that recorded by the Selspot cameras. This ability is used in kinematic data acquisition by firmly attaching rigid LED arrays of precisely known dimensions to body segments of the subject. Calculation of the 3-D orientation of arrays is accomplished in software. The array structures are very light and care is taken not to restrict movement of the subject.

Another part of the hardware is a Kistler forceplate (two at the Mass. General Hospital gait lab) on level with the lab floor in a central region of the Selspot viewing volume. Data from the forceplate is acquired in synchrony with kinematic data.

B. Software

The TRACK (Telemetered Real-time Acquisition and Computation of Kinematics) software package primarily calculates and makes user-available the three-dimensional location and orientation of specific body segments. Initially the 3-D location of each LED is determined. The LEDs associated with each array are then grouped and the global position of the center of the array is calculated. This location is designated the origin of the array

coordinate system for the frame of data in question. Rotation of the array plane is then calculated and establishes the orientation and position of the associated body segment. Interpolation and filtering of kinematic data is also provided by TRACK.

Further programs have been written by Bob Fijan, while at the MIT and MGH gait labs, to obtain the joint center of rotation and calculated the relative angles between limb segments. Hip flexion, abduction and external rotation angles are used in the transformation from prosthesis to acetabular coordinates.

Many other TRACK programs and utility packages have been adapted for use with pressure data. Table 1-1 list the programs from TRACK.

Table 1-1: From [3].

TRACK III PROGRAMS	SECTION	(All are FORTRAN except where noted)
TRACK3.CMD	1.0	Batch Control
T3ASN.CMD	1.1	TRACK III logical device assignments
T3BFZD 2.0		Forceplate Zero collection
GTPHAD.MAC	2.1	Get Physical Address of an array
FPINIT	2.2	Initialize the FP Interface
FPINIM.MAC	2.3	Initialize the FP Interface
T3FPM1.MAC	2.4	Get one frame of FP data
T3BSFA 3.0		Selspot and Forceplate data acquire
T3SSFP	3.1	F4P to MAC arg translation SS and FP
T3SSM3.MAC	3.2	SS and FP DMA synchronous data collect
T3SFTM	3.3	Fortran to Macro argument translation
T3SSM2.MAC	3.4	Selspot Only DMA data collection
T3BBDI 4.0		Selspot Hardware Bad data interrogate
T3BFDT 5.0		FP data translate to canonical form
T3BRSV 6.0		Raw data save
T3BRDP 7.0		Reclaim for proces prev saved raw data
T3SPFC		
T3SPRD		
T3SPPR		
T3BWND 7.5		Data "Window" in Time
T3BCCR 8.0		Selspot camera correction
T3SCCR	8.1	Selspot camera correction
T3BRFT 9.0		Selspot Raw data l-p filter and interp
T3SFLD	9.1	Low-pass filter design
T3SIFR	9.2	Interpolate and filter
T3SFPI	9.3	First pass interpolator
T3SIIC	9.4	Interpolator Index Corrector
T3SSPI	9.5	Second pass interpolator
T3S2PF	9.6	Two pass filter
T3BFDR 9.8		Forceplate data reduction
T3BFFT 10.0		Forceplate data l-p filter
T3SLPF	10.1	Low-pass filter
T3S2PF		

TRACK III PROGRAMS	SECTION	(All are FORTRAN except where noted)
T3BACA	11.0	Selspot 3-D point calculate
T3SPIN	11.1	3-D process initialize
T3SPCA	11.2	3-D calculation process
T3BBAD	11.5	Prints of bad frame-channels for each LED
T3BPFT	12.0	Selspot 3-D data l-p filter
T3SFLD		
T3SIFR		
T3SFPI		
T3SIIC		
T3SSPI		
T3S2PF		
T3BPSV	12.3	3-D Point data save
T3BPEL	12.5	Selspot bad data eliminate
T3SPEL	12.6	Selspot bad data eliminate
T3BBAD		
T3BOCA	13.0	Orientation calculation
T3SOCA (T3SGSC)	13.1	Orientation calculation
T3BAPF	13.5	Result interpolate and filter (prior to deriv)
T3SFLD		
T3SIFR		
T3SFPI		
T3SIIC		
T3SSPI		
T3S2PF		
T3BACL	14.0	Velocity and acceleration calculation
T3BAFL	14.5	Velocity and acceleration filtering
T3SLPF		
T3S2PF		
T3BDSV	15.0	Result data save

T3 DATA DISPLAY SECTION

```
T3RFGF          16.0  Raw data graph
   T3SPRD
   T3SPPR
   SVGRAF

T3DFGR          17.0  Result data file graph (VT640)


T3DFGF          17.0  Result data file graph (VT11/NETWORK)
   T3SDFG             17.1  Result data file graph
      T3SPRD
      T3SPPR
      T3SPPP
   VGRAPH
```

T3 UTILITIES SECTION

```
T3PFCG          18.0  Parameter change
   T3SPFC             18.1  Parameter file change
      T3SPRD          18.2  Parameter file read
      T3SPPR          18.3  Parameter print

T3PHEX          18.5  Parameter Header Examine
   T3SPRD
   T3SPPR
   T3SPPP             18.6  Post Processing Parameter print

T3PSEL          19.0  Print Selspot data

T3PFCP          20.0  Print Forceplate data

T3DDIR          21.0  Print and change data directory

T3LFMP          22.0  LED file manipulate

T3POSN          23.0  Position the Selspot cameras
   T3SSM1.MAC         23.1  Selspot single cycle macro routine

STOP                  24.0  Routine to ABORT: TRACK3 and AT.
```

T3 DATA PARTITIONS SECTION

T3 CANONICAL DATA COMMON AND DATA FILE HEADER

UTILITY SUBROUTINES SECTION

FCS disk I/O and directory manipulation routines

FREQUENCY DOMAIN ANALYSIS

TRACK III LOGICAL DEVICE ASSIGNMENTS

TK0: (DR0:) Selspot raw data
TK1: (DL0:) Forceplate raw data

N.B. TK0: and TK1: MUST be different physical devices
w/ DIFFERENT CONTROLLERS!

TK2: (DR0:) Experimental parameters
TK3: (DR0:) LED files and directory
TK4: (DR0:) Results, manipulated data, scratch files, data directories, saved canonical form raw data.
TK5: (DR1:) Camera correction matricies
TK7: (DR1:) Track III Tasks

2 CHARACTER MONTH ABBREVIATIONS

JA	January
FB	February
MR	March
AP	April
MY	May
JE	June
JL	July
AG	August
SP	September
OC	October
NV	November
DC	December

The standard data file names are of the form:

MNDY

Where:
MN is a 2 character abbreviation for the current month
DY is the day of the month
is the number of the experiment on that day (00 to 99)

Appendix 2: Transducer Characteristics

Conversion of transducer outputs to pressure values requires knowledge of transducer measurement produced at zero-pressure and the slope of transducer reading to pressure changes. The relationship between changes in pressure and changes in transducer output is known to be linear and invariant for 10 of the transducers in the prosthesis. The other four transducers have not been used for any purpose, though their output data has been saved. Transducer output with no applied pressure changes over months, over the period the prosthesis is powered, and with temperature. Zero-pressure calibration has been done on each test date, as described in section IV. Calibration specific to a test date will include the effect of any slight variations in subject body temperature that occur. Thus, with current data only the slopes and zero-pressure outputs for a particular test date need be known.

The slope [mv/psi] of transducer ouput signal with pressure is presented in Table 2-1 for each of the 10 linear transducers. In all cases the transducer ouput increases with increasing applied pressure.

Table 2-1: Change in transducer output signal [mv] for a psi change in pressure

Transducer	Slope [mv/psi]
1	0.49834
2	0.79550
3	0.61685
4	0.65058
5	0.62767
6	0.59583
7	0.78429
8	0.94738
9	0.91537
10	0.74245

Table 2-2 is identical to Table IV-1 and lists the output signal value for zero pressure on each transducer. These numbers have been termed millivolts because the transducer signals are scaled by the calibration outputs sent at the start of each frame of transducer samples. The calibration signals correspond to telemetry outputs of one and zero volts.

Table 2-2; In Vivo Zero-Pressure Calibration Measurements

Values are average transducer reading over lowest 1 - 2 seconds of each unloading test.

Date	July 84	Dec 84	May 85	Aug 85	Sept 85
Transducer					
1	153.25	170.95	136.91	160.98	89.33
2	981.19	1016.27	1009.36	1049.28	949.64
3	1127.99	1129.01	1133.94	1121.23	1046.93
4	640.73	641.74	669.34	666.75	617.01
5	1127.99	1429.19	1509.91	1557.13	1508.62
6	-914.37	-983.40	-990.4	-1042.18	-1077.79
7	760.98	714.94	777.63	639.94	683.85
8	732.99	832.42	847.44	903.11	810.36
9	-121.99	-129.5	-86.25	-102.86	-138.28
10	-358.8	-401.0	-403.67	-455.75	-522.31

Table 2-2; Mean In Vivo zero-pressure values

Transducer	Mean	Std. Dev.
1	142.3	32.1
2	1001.1	37.6
3	1111.8	36.6
4	647.1	21.5
5	1426.6	173.1
6	-1001.6	62.3
7	715.5	56.2
8	825.3	61.9
9	-115.8	21.0
10	-428.3	62.8

Appendix 3: Transformation of Coordinates

A. Transformation from prosthesis to acetabulum coodinates

Pressure measurements obtained from the instrumented prosthesis are fixed in location on the prosthesis. The prosthesis surface on which pressures are measured is one-half of the spherical interface forming the joint. The other half of the joint is the acetabulum, formed of natural cartilage. Understanding of the performance of cartilage is enhanced by expression of measurements on the cartilage surface rather than the metallic prosthesis surface. Thus the location of measurements on the acetabulum has been found. The information used to change coordinate systems includes: (1) transducer location on the prosthesis; (2) prosthesis orientation relative to the femur;(3) instantaneous femur-thigh position with respect to the pelvis; and (4) acetabulum orientation relative to the pelvis. The use of these articles of information will be described briefly with words and figures, the programs used to accomplish the task have been included in Appendix 4.

Figure 3-1 contains a flowchart of the steps followed in changing coordinates. The first stage is to obtain the vector from the center of the prosthesis head to a given transducer. The transducer locations on the prosthetic femoral head are defined by their relationship to the femoral head center and transducer 1, as shown in Figure II-13. Description of the direction of the vector from the center of the prosthesis to the measurement location

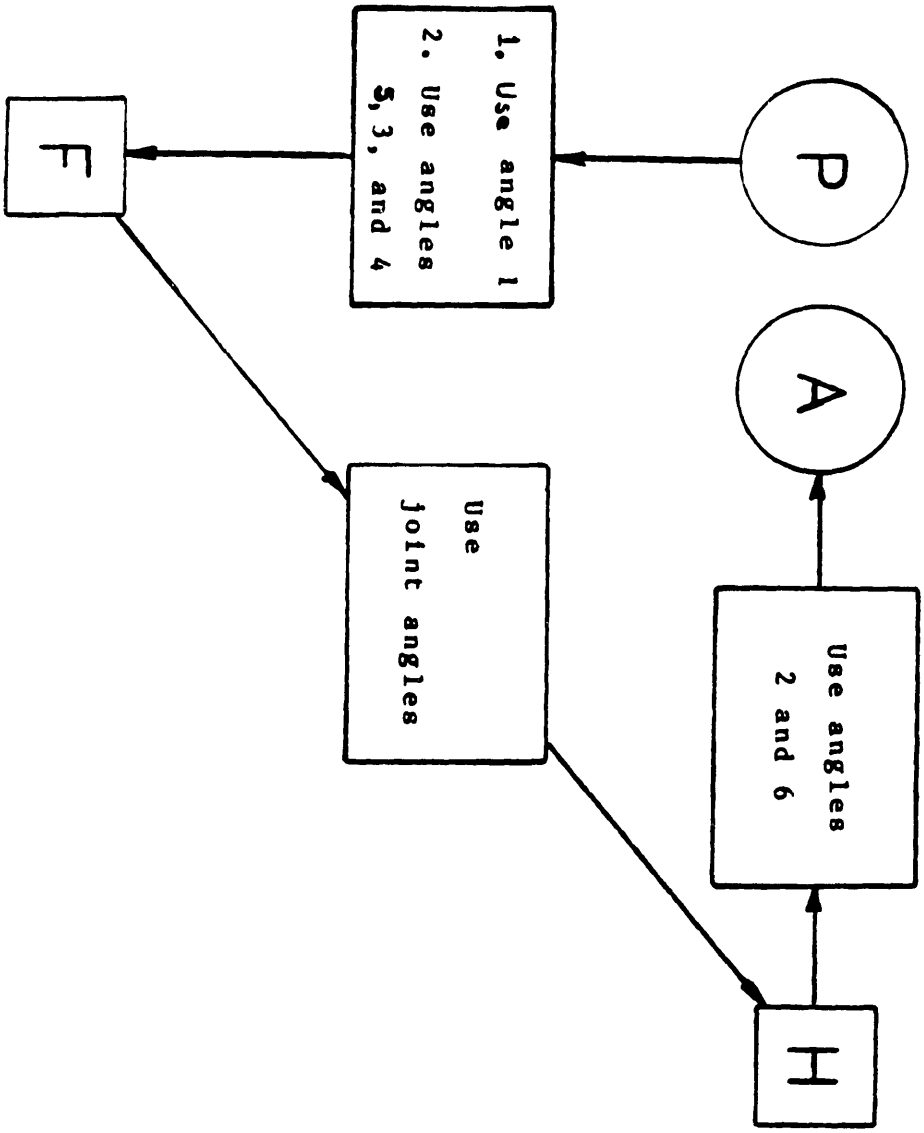

Figure 3-1: Outline of coordinate transformation procedure.

is changed to orthogonal coordinates by calculating:

$$u1 = \sin \phi \cos \theta$$

$$u2 = \sin \phi \sin \theta$$

$$u3 = -\cos \phi$$

where phi is latitude and theta is longitude as defined in Fig. II-13. After this vector has been determined it may be represented in other coordinate systems if the rotational relationship between coordinate systems is known. The first set of intermediate coordinates used are fixed on the stem as shown in Figure 3-2. The angle between the long axis of the prosthesis and the vector between the center of the femoral head and transducer 1 is used to specify rotation of coordinates. This angle, alpha, is 25 degrees. The formulas used are:

$$ua = u1$$

$$ub = u2 \sin \alpha - u3 \cos \alpha$$

$$uc = u3 \cos \alpha + u3 \sin \alpha$$

The stem of the prosthesis is related to the femur by angles determined in implantation and estimated by Dr. A. Hodge, from X-rays and experience in implantation of the prosthesis. The relationship between the stem coordinate system and that defined for the femur is shown in Figure 3-3, which also defines the angles used in the transformation of coordinates. Angle β 1 is that between the stem and vertical direction in the frontal plane. Beta(β2 is defined by the vector from the greater trochanter to the femoral head center and the medial-lateral direction while in a neutral

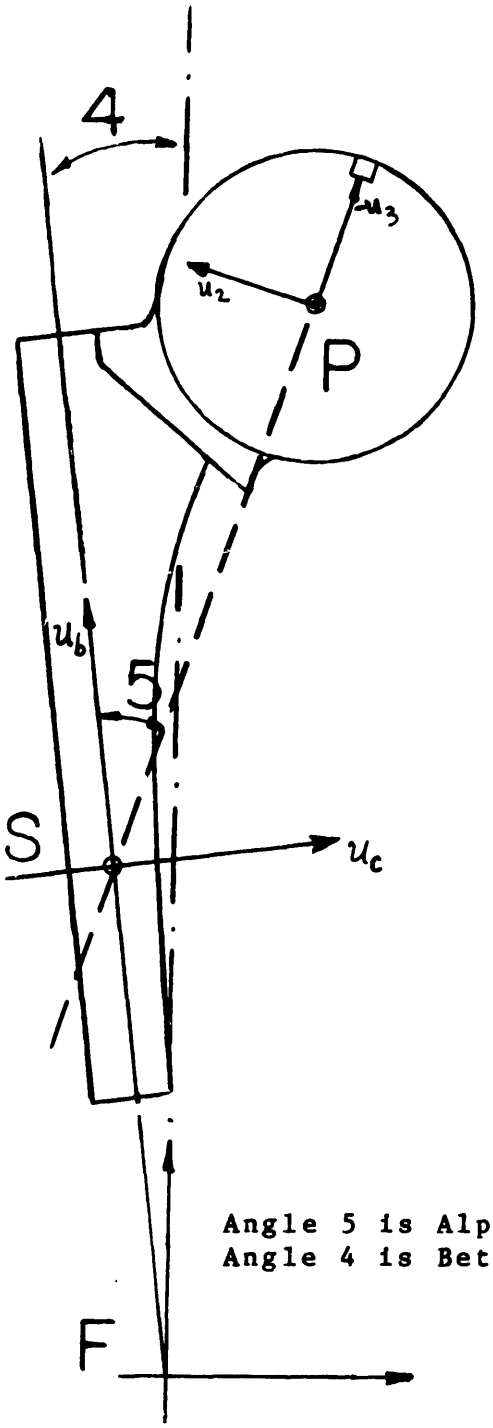

Figure 3-2: Prosthesis and Stem coordinates

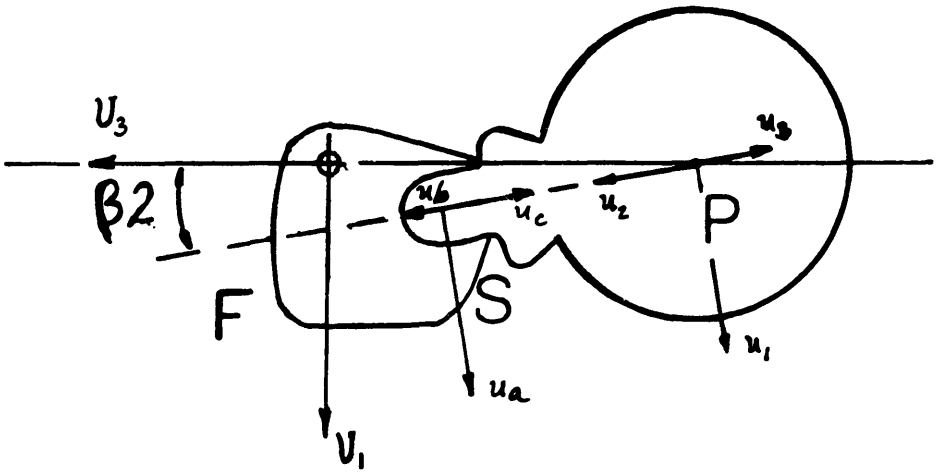

Figure 3-3: Prosthesis, Stem, and Femur coordinates

position. Beta (β)3 is the angle in the saggital plane between the stem and vertical while in a neutral position. The values of the angles used were:

$\beta 1 = 7$ degrees

$\beta 2 = 10$ degrees

$\beta 3 = 0$ degrees

These are used in calculating the components of the rotation matrix that describes the differences in orientation between the stem coordinate system and that of the femur. Rotation matrices are used extensively in dynamics and kinematics, Crandall et al [27] is the text that has been used for reference. A vector can be transformed from the set of coordinates in which it is known to its components in another system by multiplying it with the rotation matrix. Each element of the three by three rotation matrix is the cosine of the angle between Ui and ui where i refers to one of the three components of the
u or U coordinate systems.

$$\{U\} = [C]\{u\}$$

Calculation of the direction cosines needed for the rotation matrix is accomplished through geometric and trignometric use of the angles $\beta 1$ through $\beta 3$. The precise fomulas used can be found in the subroutine HTRANS.FTN included in Appendix 4. After calculation this rotation matrix is multiplied with the vector describing transducer location in stem coordinates to obtain the transducer location in femoral coordinates.

Once the transducer location is known in femoral coordinates the relationship between femoral and pelvic coordinates may be used. This information is acquired and made available by the TRACK system and kinematics programs [*] in the form of three hip angles, flexion, abduction, and rotation, as defined in Figure IV-15. These angles are used to obtain the rotation matrix between the two coordinate systems shown in Figure 3-4.

The final stage involves transformation from the new, pelvic, coordinates to acetabular coordinates. The orthogonal acetabular coordinate system used in this process is shown in Figure 3-5, in which the medial "horizontal" defines the x direction and z is defined by the acetabular outward normal. These directions are determined by angles $\gamma 1$ and $\gamma 2$ which are pictured in Figure 3-5. Angle $\gamma 1$ is the angle in the transverse plane between the medial-lateral (global Z) and the acetabular outward normal. Angle $\gamma 2$ is in the frontal plane between the medial-lateral direction and the acetabular outward normal. These angles are used to determine another rotation matrix.

In order to store two numbers rather than three, the transducer location in the orthogonal acetabular coordinate system shown in Figure 3-5 is changed to its representation in latitude and longitude on the spherical acetabulum surface. Definition of latitude and longitude angles is shown in Figure II-18 and is based on the acetabular outward normal. The acetabular

---

[*] Developed by Bob Fijan and Pete Loan.

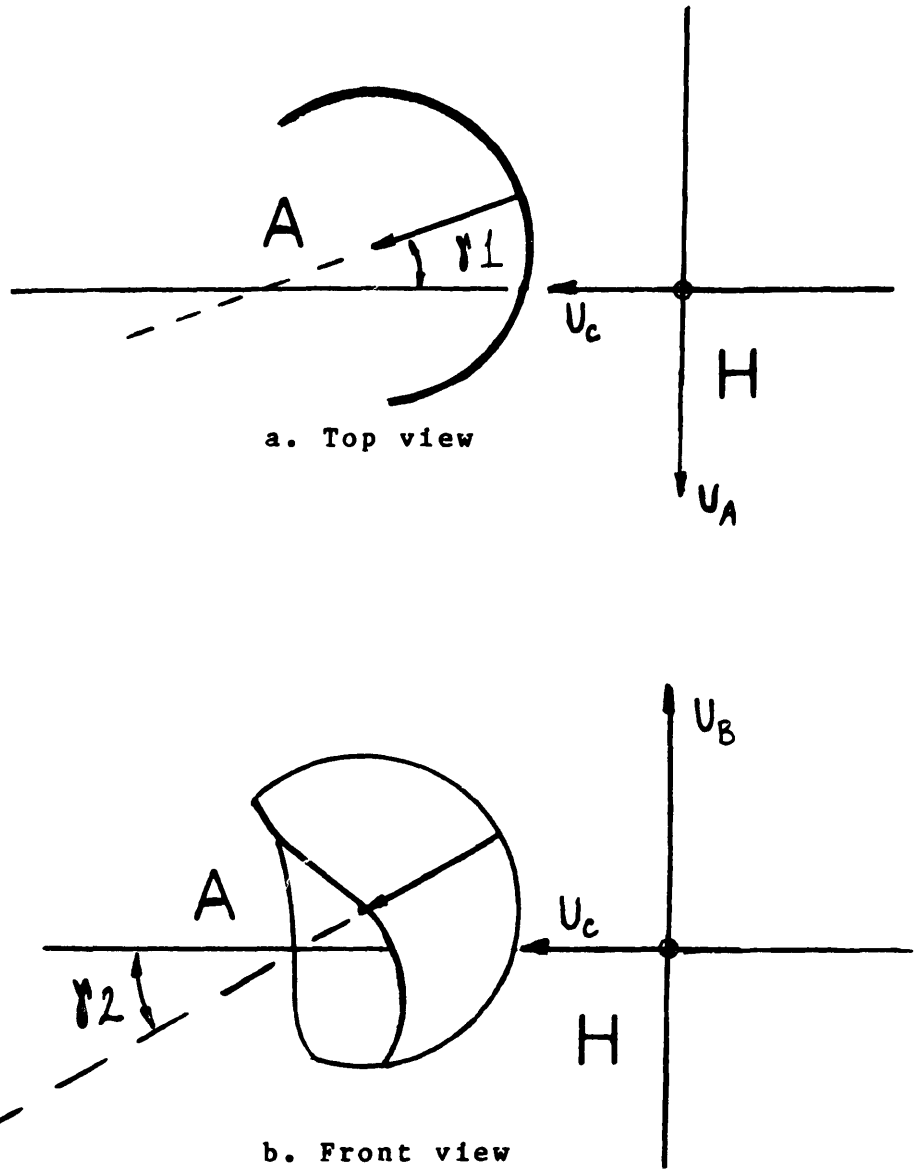

Figure 3-4: Pelvis (H) and Acetabulum (A) coordinate system relationship

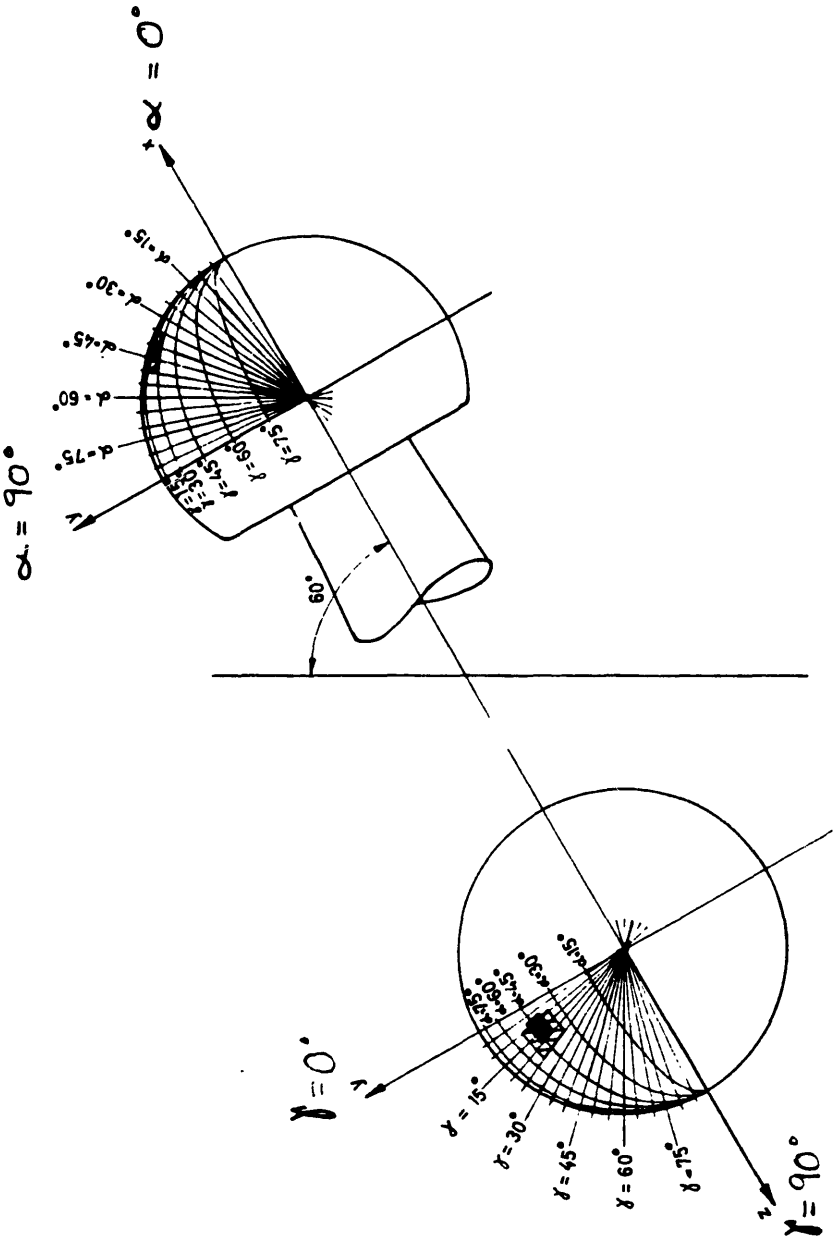

Figure 3-5: Rydell's femoral head coordinate system. [Rydell 66]

latitude and longitude at which measurements were recorded are stored in a data file and recalled when needed for display or computation.

B. Transformation from Acetabular to "Screen" coordinates

A relationship between acetabular latitude and longitude and the graphics terminal screen must currently be defined for display. In the future, using a graphics terminal with the capability to perform 3-D hardware rotations, this will not be necessary. Two separate procedures are presently employed for the two display formats.

The orientation of the 2-D display of the acetabulum surface is such that the normal from the screen at the acetabulum center is the same as the acetabulum outward normal. This simplifies the display of measurement locations, since these positions have been defined with respect to the acetabulum outward normal. Positions of transducers are shown as their projections onto a surface orthogonal to the z axis. Zero longitude corresponds to the anterior direction or the X direction in screen coordinates. Ninety degrees of longitude is in line with the screen Y axis. The latitude and longitude at which measurements were recorded are changed into X-Y positions by calculating:

$$X = \sin \text{phi} \cos \text{theta}$$

$$Y = \sin \text{phi} \sin \text{theta}$$

where phi is latitude and theta is longitude. The transducer numbers are then displayed on the screen at these X-Y locations, with appropriate

scaling. Transducers occasionally appear to overlap; this indicates that one is at a latitude greater than 90 degrees.

Simulation of three-dimensions on a two-dimensional surface is more complicated. The hemispherical display presented in this thesis is a view of the spherical joint surface looking through the pelvic bone and acetabulum. The acetabular outward normal is directed into and to the left on the display surface. Looking into the screen is equivalent to looking from an anterior position on the saggital plane in a posterior and slightly downward direction through the pelvic bone. A sense of the spherical surface is imparted by displaying lines of longitude at every 15 degrees and latitude to 90 degrees in 10 degree increments. This is accomplished by initially defining the lines of latitude and longitude in the acetabular coordinate system then rotating them using Euler angle formulas (as will be described in a sentence or two). Pressure locations are known in acetabular coordinates and the pressure magnitude at each location is known. A line with length scaled to a given pressure measurement is defined normal to the acetabular hemisphere at the position where that pressure measurement was obtained. The pressure "vectors" defined in this manner undergo Euler rotations identical to those imposed on the hemisphere. After determing the display coordinates for all objects (hemisphere, pressure "vectors", pelvis outline) graphics programs are given the location information to use in displays. Information on the programs and subroutines is given in Appendix 4.

Instead of direction cosines, the rotation of the acetabular coordinate system to screen coordinates has been done using Euler angle formulas [27].

The formulas used are printed in Figure 3-6. The angles used for the current display are -20, -35, and -90 degrees. Acetabular locations are first changed to components in an orthogonal coordinate system for which the Y axis corresponds to 0 degrees longitude, X is 90 degrees longitude, and Z is defined by the vector from the center of the sphere to 0 degrees latitude. The relationship between the acetabular coordinate system and the screen coordinate system is then used to determine where a point in the acetabular coordinate system will appear on the screen by employing the Euler angle rotations. Points defining objects may then be displayed on the terminal. Currently, using the VT100 terminal with a VT640 graphics board, or an H-P digital plotter, hidden line removal is accomplished by restricting display to points with a positive Z component.

C. Transformation of Previously Published Results to Hemispherical Display

Almost all reported estimates and measurements of pressures or forces at the hip joint have been presented in different coordinate systems. This makes comparison of results difficult. Results from a few investigators have been shown in the coordinate system used for display of results from the in vivo prosthesis. Separate programs were written for translation of each set of published results. The method used for the two sets of comparisons included in the Discussion section will be outlined.

1. Rydell's results

The directions of resultant force vectors at the hip determined by Rydell

$$\begin{Bmatrix} X \\ Y \\ Z \end{Bmatrix} = \begin{bmatrix} (\cos\psi \cos\varphi - \sin\psi \cos\theta \sin\varphi) & (\cos\psi \sin\varphi + \sin\psi \cos\theta \cos\varphi) & (\sin\psi \sin\theta) \\ (-\sin\psi \cos\varphi - \cos\psi \cos\theta \sin\varphi) & (-\sin\psi \cos\varphi + \cos\psi \cos\theta \sin\varphi) & (\cos\psi \sin\theta) \\ (\sin\theta \sin\varphi) & (-\sin\theta \cos\varphi) & \cos\theta \end{bmatrix} \begin{Bmatrix} x \\ y \\ z \end{Bmatrix}$$

Figure 3-6: Euler equations

were presented in the angular coordinates shown in Figure 3-7 (reproduced from [90]). These coordinates are fixed to the femoral head, some information on hip angles was included in the published report. Transformation from Rydell's angles α and γ to acetabular latitude and longitude defined from the acetabular outward normal is complex. A set of orthogonal coordinates fixed in the femoral head is initially defined. Angles α and γ are then translated to components in the orthogonal coordinate system assuming a sphere of unit radius. The femoral coordinate system, defined so that α and γ may be easily transformed to x, y, and z components, is rotated to an orientation identical to that of the prosthetic femoral head coordinates used for pressure data. The same programs used to determine acetabular locations for MIT/MGH data perform the required calculations for transformation of Rydell's results. Hip angles have been obtained from descriptions of leg position in Rydell [90] or by the use of kinematic data for the instrumented subject. These are nowhere near as accurate as kinematic data taken in conjunction with MIT/MGH pressure data. However, this process gives an idea of the direction of the measured resultant force vector with respect to the acetabulum.

2. MIT Hip simulator; Rushfeldt's results

Transformation of Rushfeldt's results to the coordinate system used with in vivo pressure data is less complex. Results from the MIT hip simulator are presented on the acetabulum. The coordinate system fixed on the acetabulum coincides with the prosthesis femoral head axes when the prosthesis is in a neutral position (0 degrees in all hip joint angles). Subroutines had been

written to perform coordinate transformations from femoral head locations to acetabular locations. These programs were used to change from hip simulator to in vivo coordinates by specifying a femoral position setting hip joint angles to 0 degrees. Results from left hips are first changed to the corresponding positions in right hip coordinates.

Changing Rushfeldt's results to appear in an orientation similar to that used for in vivo data is not difficult, but obtaining input points for pressure contours involved some guesswork. Tabulated data on the coordinates for pressure contours was not available. Thus, these coordinates had to be estimated from graphs and figures in Rushfeldt [86].

Appendix 4: Programs used in data analysis and display

The names of some of the programs used to obtain results are listed in Table 4-1. Table 4-1 is organized by the task performed by programs or a series of programs. Only the main programs and most important subroutines have been included here.

Table 4-1: Programs used in processing pressure data

Program	Subroutines	Description
Initial Processing		
GAP		Eliminates spaces in raw data
PROSTH		Initial processing of raw data
3DOLD		Processes static kinematic data to get body segment parameters
AQPATH		Uses kinematic data to locate
	TRANS	transducers in acetabulum
	ANGGET	automatic processing- writes file of transducer locations corresponding to kinematic data file
Filtering (PRFILT.CMD)		
PRSFFT		Finds Fourier series coefficients
	FFT	
FFTPLT		Plots Magnitude of Fourier Transform
PREFIL OR PR2FIL		Readies pressure data for filtering with Butterworth filter
T3BAPF		Butterworth filter from TRACK system
POSTFL		Puts filtered data from Butterworth filter in final form
PR3FLT		Finite Impulse filter
	T3FLTR	
PRDWRT		Puts filtered data from FIDR filter in final form
Initial Data Manipulation		
FILETAB		Finds Maximums, Minimums, Averages, and frame number for maximums for a series of filtered or unfiltered data files.
POSITAB		Finds positions of transducers for an input set of files and frame numbers

HPPRFP		Displays pressure and forceplate data vs. time.
	CHOOSE	
	READFP	
	SREAD	
	NGRAPH	
STANCEPH		Estimates time of heel-strike and toe-off from forceplate data
CPERCENT		Given heel-strike and toe-off times and a pressure frame of a time, calculates percentage of gait cycle and stance phase for that frame or time.

Acetabular plot (HIPP.CMD)

ACETANG		Gets Filtered pressure data and locations
A1		Gets unfiltered pressure data and locations
A1PLOT		Plots pressures at specified locations on acetabulum plot.
APPLOT		Draws acetabulum and plots user-specified points on it.
PTHDRW		Draws position of transducer(s) on the acetabular display over a period of time

Pressure Vector/Pelvis Display

	SHADESOC		Draws a hemisphere and lines of lat. and
*		SOCPLT	longitude
	3DPATH		Draws pressure vectors of the hemisphere
*		REAPTH	surface
		SOCPLT	Performs Euler rotations
*		VECDRW	Draws vectors and pelvis
		SCLPTH	Draws scaled path
		SILICO	Creates version of data to output to Silicon Graphics terminal
	RYPATH		Gets user-input in Rydell's femoral
		RYDPTH	angles and transforms to acetabular
*		RYDELL	lat. and long.
*		HTRANS	
		SOCPLT	
		LEGEND	
		VECDRW	
	RFELDT		Gets user-input in Rushfeldt's hip
		RFLPTH	simulator coordinates and
		RUSHFL	transforms
		HTRANS	

SOCPLT
RFLDRW

Repeatablity - final method

CYCLEC		Allows selection of time interval
	CHOOSG	for a series of data files
	PRFPLS	Plots all on same graph.
	CGRAPH	Will plot one set of data vs. another

Rate of Loading (LOAD.CMD)

LOAD1	Obtains rate of pressure increase
LOAD2	Obtains rate of increase in forceplate resultant force
DELTAC	Finds change in location on acetabulum as a percentage of joint great circle

---

* Programs which have been included.

```
C           SOCPLT
C                 Kjirste Carlson
C                 30-Aug-85
C           Subroutine to convert an array
C           A(I,3)from
C                 A(i,1) = r to A(i,1) = x(screen)
C                 A(i,2) = phi to A(i,2) = y(screen)
C                 A(i,3) = theta to A(i,3) = z(screen) = 0
C           where phi and theta are
C           as defined with respect to acetabular origin or w.r.t.
C           transducer 1.
C
C           ASSUMES PHI AND THETA ARE IN RADIANS
C
            SUBROUTINE SOCPLT(A,IPNT)
            DIMENSION B(3),C(3),A(1000,3)
            PI = 3.1415927
            DTR = PI/180.
            RTD = 180./PI
C                 Calculate Euler angle sins & cosines
            PHIE = -20. * DTR
            THETE = -35. * DTR
            PSIE = -90. * DTR
            SPH = SIN(PHIE)
            CPH = COS(PHIE)
            STH = SIN(THETE)
            CTH = COS(THETE)
            SPS = SIN(PSIE)
            CPS = COS(PSIE)
            DO 1000 II = 1,IPNT
C              Into femoral-head  or acetabular
C              orthogonal axes, Z along acet, normal, X
C              lined up with transducers 2 & 8
C              Y anterior.Or, Z medial, X superior,Y anterior
                  B(1) = A(II,1) * SIN(A(II,2)) * SIN(A(II,3))
                  B(2) = A(II,1) * SIN(A(II,2)) * COS(A(II,3))
                  B(3) = A(II,1) * COS(A(II,2))
C              Into Screen/Global coord., X horizontal, Z out of screen
                  C(1) = (CPS*CPH - SPS*CTH*SPH)*B(1) + (SPS*STH)*B(3)
                  C(1) = C(1) + (CPS*SPH + SPS*CTH*CPH)*B(2)
                  C(2) = (-SPS*CPH - CPS*CTH*SPH)*B(1) + (CPS*STH)*B(3)
                  C(2) = C(2) + (-SPS*SPH + CPS*CTH*CPH)*B(2)
                  C(3) = STH*SPH*B(1) - STH*CPH*B(2) + CTH*B(3)
C                       Important thing about C(3) is the sign
                  A(II,1) = C(1)
                  A(II,2) = C(2)
                  A(II,3) = C(3)
1000        CONTINUE
C
            RETURN
            END
```

```
C           REAPTH.FTN
C                 Kjirste Carlson
C           31-Aug-85
C                 Program to read pressure and
C           path files, get data to subroutine to
C           compile list of vectors for pressure
C           path plotting
            SUBROUTINE REAPTH(IFR,NFR,NSKIP)
            BYTE REPLY
            COMMON /BLKCHO/NAMPRD(8),NDATE(3),NFREQP,NPFRME,NDESCR(15)
            COMMON /BLKPRS/ RIBX(1,500),IND,IQI,RMAX
            COMMON /DATABK/ A(1000,3),IPNT,RIBMAX
            COMMON /PATHBK/ B(500,2),J2FR
            LUO = 5
            LUI = 5
            WRITE(LUO,1050)
1050        FORMAT('$Enter transducer number to plot: ')
            READ(LUI,1051) IQI
1051        FORMAT(I3)
            NFREQT = 204
            IF(NDATE(1) .GE. 5 .AND. NDATE(3) .GE. 85) NFREQT = 153
            CALL SREAD(IFR,NFR,NSKIP,JFR)
            IPNT = JFR
            CALL PTREAD(IFR,NFR,NSKIP,NFREQT,JTFR)
            JT = JTFR
            IF (JT.NE.IPNT) WRITE(LUO,45)IPNT,JT
45          FORMAT(I4,' PRESSURE FRAMES',/,I4,' TRACK FRAMES')
C               Now, need to scale vectors
C               Auto-scale by allowing Scale vector to be 6. units long
881         WRITE(LUO,888)
888         FORMAT('$Do you wish to scale vectors automatically? [D:Y] ')
            READ(LUI,889) REPLY
889         FORMAT(A1)
            IF( REPLY .NE. 'N' .AND. REPLY .NE. 'n') GOTO 887
            WRITE(LUO,886) RMAX
886         FORMAT(' The largest pressure is ',F5.2,' M-Pa')
            WRITE(LUO,1000)
1000        FORMAT('$Make 1.0 M-Pa what distance? ')
            READ(LUI,2000) SCAVEC
2000        FORMAT(F7.4)
            WRITE(LUO,885)
885         FORMAT('$What pressure should the scale vectors represent?
                  [INT]')
            READ(LUI,884) IBMAX
884         FORMAT(I4)
            RIBMAX = FLOAT(IBMAX)
            GOTO 883
887         RIBMAX = RMAX + 1.0
            SCAVEC = 6.0 / RIBMAX
883         IC = -1
            DO 100 I =1,JFR
                  IF( IC .GE. 995) GOTO 101
                  IC = IC + 2
```

```
            A(IC,1) = 1.0
            A(IC+1,1) = 1.0 + (RIBX(1,I) * SCAVEC)
100         CONTINUE
101         IREC = IC
            DO 110 I = 1,2
                  IC = IC+2
                  A(IC,1) = 1.0
                  A(IC+1,1) = 1.0+(RIBMAX*SCAVEC)
110         CONTINUE
            IC = IC-2
            DO 115 I = 1,2
                  A(IC,2) = A(1,2)
                  A(IC,3) = A(1,3)
                  IC = IC+1
115         CONTINUE
            DO 116 I = 1,2
                  A(IC,2) = A(IREC,2)
                  A(IC,3) = A(IREC,3)
                  IC=IC+1
116         CONTINUE
            IPNT = IC-1
            CALL SOCPLT(A,IPNT)
            RETURN
            END
```

```
C
C          VECDRW
C               Kjirste Carlson
C          31- Aug - 85
C               Subroutine to plot sphere
C               ( SOCKET) and pressure "vectors"
C
           SUBROUTINE VECDRW(ITIMES,ITRACE,ILEGEN,IPELV,IBPATH,NHVEC)
           BYTE REPLY
           COMMON /DATABK/ A(1000,3),IPNT,RIBMAX
           COMMON /PATHBK/ B(500,2)
           COMMON /BLKSCL/ XMIN,XMAX,YMIN,YMAX,IDEV
           COMMON /LABELS/TXST(2),IT1(25),IT2(25),IT3(25),IT4(25),NFD(30),
     *IRM(25),IFM(25),NDE2(30)
           DIMENSION NAMSOC(8),NAMTMP(3),NAMACE(8)
           DIMENSION NDESCR(15)
           DATA NAMSOC/'PL','1:','SO','CK','ET','.D','AT',"0/
           DATA NAMACE/'PL','1:','PE','LV','IS','.D','AT',"0/
           LUI = 5
           LUO = 5
           IDEV = 0
           NSKPV = 1
486        IF (IPELV.NE.1) GOTO 87
           WRITE(LUO,1003)(NAMACE(K),K=3,5),"7
1003       FORMAT('$Enter the name of the file to display: [D:',
     *          3A2,'] ',A1)
           READ(LUI,1001)(NAMTMP(IQ),IQ=1,3)
1001       FORMAT(3A2)
           IF (NAMTMP(1) .EQ. '  ') GOTO 87
           NAMACE(3) = NAMTMP(1)
           NAMACE(4) = NAMTMP(2)
           NAMACE(5) = NAMTMP(3)
87         WRITE(LUO,90)
90         FORMAT('$Draw all of the vectors? [D:Y] ')
           READ(LUI,91) REPLY
91         FORMAT(A1)
           IF( REPLY .NE.'N'.AND.REPLY.NE.'n') GOTO 249
           WRITE(LUO,92)
92         FORMAT('$Number of vectors to skip? ')
           READ(LUI,93) NSKPV
           NSKPV=NSKPV+1
93         FORMAT(I3)
249        IF (IPELV .NE. 1) GOTO 66
           IF(NAMACE(3) .EQ. 'PE'.AND.NAMACE(5) .EQ. 'TO')GOTO 233
           XMAX = 1.65 !Scaling worked out for PELVIS.DAT
           XMIN = -1.45      !created 5-oct-85
           YMAX = .94
           YMIN = -.54
           GOTO 234
233        XMAX = 1.3  !Scaling worked out for PELVTO.DAT
           XMIN = -1.21      !created 5-OCT-85
           YMAX = .6
           YMIN = -.55
234        WRITE(LUO,244)
```

```
244         FORMAT('$Do you wish to change scaling now? ')
            READ(LUI,245)REPLY
245         FORMAT(A1)
            IF(REPLY .NE. 'Y' .AND. REPLY .NE. 'y')GOTO 66
            WRITE(LUO,247)
247         FORMAT('$Enter XMAX,XMIN,YMAX,YMIN: ')
            READ(LUI,248)XMAX,XMIN,YMAX,YMIN
248         FORMAT(4F6.2)
66          CALL INIT(IDEV)
96          IF (IDEV.EQ.1) CALL SPEN(1)
            IF(IPELV.NE.1) GOTO 65
            CALL READVT(NAMACE)
65          XMIN=-7.0
            XMAX= 8.
            YMIN= -5.5* 8.0/10.5
            YMAX=  9.5 * 8.0/10.5
            CALL READVT(NAMSOC)
            XT = -2.7
            YT = -1.17
            CALL APNT(XT,YT,L,-1,F,0)
            CALL TEXT('Anterior',0)
            XT = 2.275
            YT = .011
            CALL APNT(XT,YT,L,-1,F,0)
            CALL TEXT(' Medial',0)
            XT = -.964
            YT = 2.98
            CALL APNT(XT,YT,L,-1,F,0)
            CALL TEXT('Superior',0)
C                 Plot the vectors, including reference vectors at
C                 start and finish.
999         IPN = (IPNT/2)-(2*ITRACE)
            IC = -1
            DO 400 IV = 1,IPN,NSKPV
                  IF(IV.EQ.1)IC = IC+2
                  IF(IV.NE.1)IC = IC+ (NSKPV*2)
                  IF(IV.GT.(IPN-NSKPV))IC = IPNT-1-(4*ITRACE)
                  X1 = A(IC,1)
                  X2 = A(IC+1,1)
                  Y1 = A(IC,2)
                  Y2 = A(IC+1,2)
                  Z1 = A(IC,3)
                  Z2 = A(IC+1,3)
                  IF( Z1 .GE. (-0.09)) GOTO 960
                  Z3 = Z2
                  X3 = X2
                  Y3 = Y2
C                       Calculate X2 and Y2
C                       fo circle intercept based
C                       on equations for radius and slope
                  SLOPE = (Y3-Y1)/(X3-X1)
                  AQ = 1. + SLOPE**2
                  BQ = -(2.*SLOPE * (X1 * SLOPE - Y1))
                  CQ = ((SLOPE*X1)**2 - (2.*Y1*SLOPE*X1) + Y1**2 - 1.)
```

```
                S1 = (-BQ + SQRT(BQ**2 - 4.*AQ*CQ)) / (2.*AQ)
                S2 = (-BQ - SQRT(BQ**2 - 4.*AQ*CQ)) / (2.*AQ)
                X2 = AMAX1(S1,S2)
                IF(X3 .LT. X1)X2 = AMIN1(S1,S2)
                Y2 = SLOPE*(X2-X1) + Y1
                IPP = -1
                IF(NHVEC .EQ. 1) GOTO 901
                IF(IDEV .EQ.1)CALL SPEN(2)
                CALL APNT(X1,Y1,L,-1,F,-1)
                IPP = 0
901             CALL APNT(X2,Y2,L,IPP,F,6)
                IF( IDEV.EQ.1)CALL SPEN(1)
                CALL APNT(X2,Y2,L,-1,F,-1)
                CALL APNT(X3,Y3,L,0,F,-1)
                GOTO 400
960             CALL APNT(X1,Y1,L,-1,F,-1)
                CALL APNT(X2,Y2,L,0,F,-1)
400         CONTINUE
            IF(ITRACE.NE.1)GOTO 465
            IF(IDEV.EQ.1)CALL SPEN(3)
            IC = IPNT-3
            DO 690 IV = 1,2
                  X1 = A(IC,1)
                  X2 = A(IC+1,1)
                  Y1 = A(IC,2)
                  Y2 = A(IC+1,2)
                  Z1 = A(IC,3)
                  Z2 = A(IC+1,3)
                  CALL APNT(X1,Y1,L,-1,F,-1)
                  CALL APNT(X2,Y2,L,0,F,-1)
                  IF(IV.EQ.1) CALL TEXT('START',0)
                  IF(IV.EQ.2) CALL TEXT('END',0)
                  IC = IC+2
690         CONTINUE
C                 Plot a line along tops of vectors
            IF (IDEV.EQ.1) CALL SPEN(2)
            IPN = ((IPNT-4)/2)-1
            DO 440 IC=1,2
                  IC2 = IC
                  CALL APNT(A(IC2,1),A(IC2,2),L,-1,F,-1)
                  DO 420 IV = 1,IPN
                        IC2=IC2+2
                        X2 = A(IC2,1)
                        Y2 = A(IC2,2)
                        Z2 = A(IC2,3)
                        CALL APNT(X2,Y2,L,0,F,-1)
420               CONTINUE
440         CONTINUE
C                 Option added to draw a scaled path
            IF(IBPATH .NE. 1) GOTO 465
            IF (IDEV.EQ.1) CALL SPEN(3)
            IPP = -1
            DO 421 IC2 = 1,IPN
                  X2 = B(IC2,1)
```

```
                Y2 = B(IC2,2)
                CALL APNT(X2,Y2,L,IPP,F,-1)
                IF( IC2 .EQ. 1) IPP = 0
421         CONTINUE
C
465         IF(ILEGEN .EQ. 0) GOTO 455
            CALL CHDF
            CALL SPEN(1)
            STOT = (XMAX-XMIN) * 8./10.5
            YP = TXST(2) * 8. /10.5
            XP = TXST(1)
            CALL APNT(XP,YP,L,-1,F,-1)
            CALL TEXT(NFD,0)
            YP = YP-(STOT/28.)
            CALL APNT(XP,YP,L,-1,F,-1)
            CALL TEXT(NDE2,0)
            YP = YP-(STOT/18.)
            CALL APNT(XP,YP,L,-1,F,-1)
            CALL TEXT(IT1,0)
            YP = YP - (STOT/28.)
            CALL APNT(XP,YP,L,-1,F,-1)
            CALL TEXT(IT2,0)
            YP = YP - (STOT/20.)
            CALL APNT(XP,YP,L,-1,F,-1)
            CALL TEXT(IT3,0)
            YP = YP - (STOT/28.)
            CALL APNT(XP,YP,L,-1,F,-1)
            CALL TEXT(IT4,0)
            YP = YP - (STOT/18.)
            CALL APNT(XP,YP,L,-1,F,-1)
            CALL TEXT(IRM,0)
            YP = YP-(STOT/28.)
            CALL APNT(XP,YP,L,-1,F,-1)
            CALL TEXT(IFM,0)
455         CONTINUE
            CALL ENDP
            IF( IDEV .EQ. 1) GOTO 500
            WRITE(LUO,1000)
1000        FORMAT('$Would you like a hard copy? [D:N] ')
            READ(LUI,2000) REPLY
2000        FORMAT(A1)
            IF( REPLY .NE. 'Y' .AND. REPLY .NE. 'y') GOTO 500
            IDEV = 1
            GOTO 486
500         RETURN
            END
```

```
C           RYDELL   27 - AUG - 85
C                 by Kjirste Carlson
C           program to convert from Rydell's
C           femoral head angles to those used
C           in MIT/MGH programs.
C                 That is: given Rydell's alpha
C           and gamma, get our phi and theta.
C
            SUBROUTINE RYDELL
            COMMON /MITANG/ PHI,THETA,PHIR,THETAR
            LUO = 5
            LUI = 5
            PI = 3.1415927
            DTR = PI / 180.
            RTD = 180./ PI
            PHI1 = 125.
            THET1 = 90.
669         WRITE(LUO,1000)
1000        FORMAT(' Enter angles on femoral head
     & as defined by Rydell, 1966')
            WRITE(LUO,1001)
1001        FORMAT('$Enter alpha [REAL:DEGREES]: ')
            READ(LUI,1002) ALPH
1002        FORMAT(F6.2)
            WRITE(LUO,1003)
1003        FORMAT('$Enter gamma [REAL:DEGREES]: ')
            READ(LUI,1002) GAM
            IF( ALPH .EQ. 0. .OR. GAM .EQ. 90.) GOTO 666
            GOTO 777
666         IF(ALPH .EQ. 0. )GOTO 667
            IF(GAM .EQ. 90. .AND. ALPH .NE. 90.)GOTO 667
            GOTO 777
667         WRITE(LUO,668)
668         FORMAT(' ERROR illegal angle specifications! ')
            GOTO 669
777         WRITE(LUO,1004)
1004        FORMAT('$Enter radius [REAL]: ')
            READ(LUI,1002) RADI
C
            ALPH = ALPH * DTR
            GAM = GAM * DTR
C                 Components in Rydell system
C                 Note that, due to his odd angle
C                 definitions, some combinations
C                 of alpha and gamma are illegal.
            IF( GAM .EQ. 0.) GOTO 778
            IF(ALPH .EQ. (90. * DTR)) GOTO 779
            XR = RADI * COS(ALPH)
            YR = RADI * SIN(ALPH) * COS(GAM)
            ZR = RADI * SIN(ALPH) * SIN(GAM)
            GOTO 800
778         ZR = 0.
            YR = RADI * SIN(ALPH)
```

```
          XR = RADI * COS(ALPH)
          GOTO 800
779       XR = 0.
          YR = RADI * COS(GAM)
          ZR = RADI * SIN(GAM)
C               Convert to our coord. system,
C               Takes two steps:
C               1) Rotation of -30 degrees about XR axis
C                     get y,z, and x from known relationships
C               then
C               2) Rotation of 60 +. degrees about new
C                     ZR axis, gets XR axis in place
C                     AND rotation of 90. degrees about
C                     X axis, brings ZR into place as Z
C               3) Get new relationships for phi and
C                  theta
800       R1 = SQRT(3.)/2.
          Y1 = R1 * YR - .5 * ZR
          Z1 = .5 * YR + R1 * ZR
          X1 = XR
C               Now; step 2; Use Euler angle relationships
          PHI1 = PHI1 * DTR
          THET1 = THET1 * DTR
          PSI1 = 0.
          SPH = SIN(PHI1)
          CPH = COS(PHI1)
          STH = SIN(THET1)
          CTH = COS(THET1)
          SPS = SIN(PSI1)
          CPS = COS(PSI1)
          X = (CPS*CPH - SPS*CTH*SPH)*X1 + (SPS*STH)*Z1
          X = X + (CPS*SPH + SPS*CTH*CPH)*Y1
          Y = (-SPS*CPH - CPS*CTH*SPH)*X1 + (CPS*STH)*Z1
          Y = Y + (-SPS*SPH + CPS*CTH*CPH)*Y1
          Z = STH*SPH*X1 - STH*CPH*Y1 + CTH*Z1
          IF (Y .NE. 0.) GOTO 790
          THETA = ASIN(X/ABS(X))
          GOTO 791
790       THETA = ATAN( X /Y )
791       R2 = SQRT( X**2 + Y**2)
          PHI = ACOS( Z / RADI)
          THETA = THETA * RTD
          IF(Y.LT.0.)THETA = THETA+180.
          PHI = ABS( PHI * RTD)
          WRITE(LUO,1006) PHI
1006      FORMAT(' And the latitude (phi) is ',F6.2)
          WRITE(LUO,1005) THETA
1005      FORMAT(' The longitude (theta) is ',F6.2)
          RETURN
          END
```

```
C
C          HTRANS
C          FROM TRANS
C                BY BOB FIJAN      18-JUL-84
C          Editted 5-JAN-85  Bob Fijan, Kjirste Carlson
C Editted 27-Aug-85 Kjirste Carlson - for Rydell Cases 1 & 2
C
C THIS SUBROUTINE TRANSFORMS ANGLES WRT PROSTHESIS (PHI & THETA)
C INTO ANGLES WRT ACETABULUM (PHIR & THETAR) GIVEN THE INPUT
C ANGLES FLEX, ABD, AND EXTROT.
C
C SUBROUTINE HTRANS(PHI,THETA,FLEX,ABD,EXTROT,PHIR,THETAR,ICASE)
C*************************************************************************
C
C  VERSION TO WORK WITH RYDELL'S DATA,
C  CONVERT HIS ANGLES TO ACETABULAR LOCATIONS.
C  First six numbers are Rydell case 1. Second
C  six are Rydell case 2. ( in RYCASE)
C*************************************************************************
 SUBROUTINE HTRANS(ICASE)
 COMMON /HIPANG/ FLEX,ABD,EXTROT
 COMMON /MITANG/ PHI,THETA,PHIR,THETAR
 DIMENSION VECT(3),R(3,3)
 DIMENSION RYCASE(12)
 DATA RYCASE/25.0,7.0,8.0,0.0,20.0,30.0,25.0,7.0,
     *       35.0,0.0,20.0,30.0/
 ANGLE0 = 25.0
 ANGLE1 =  7.0
 ANGLE2 = 10.0
 ANGLE3 = 0.0
 ANGLE4 = 20.0
 ANGLE5 = 30.0
 IF (ICASE .LT. 1 .OR. ICASE .GT. 2) GOTO 2
 INDEX = (ICASE-1) * 6
 ANGLE0 = RYCASE(1 + INDEX)
 ANGLE1 = RYCASE(2 + INDEX)
 ANGLE2 = RYCASE(3 + INDEX)
 ANGLE3 = RYCASE(4 + INDEX)
 ANGLE4 = RYCASE(5 + INDEX)
 ANGLE5 = RYCASE(6 + INDEX)
2 PI = 3.1415927
 RTD = 180.0/PI
 DTR = PI/180.0
 PHI = PHI * DTR
 THETA = THETA * DTR
 IF (FLEX.LT.89.9) GOTO 99
 IF (FLEX.GT.90.1) GOTO 99
 FLEX = 89.90
99 FLEX = FLEX * DTR
 ABD = ABD * DTR
 EXTROT = EXTROT * DTR
 ANGLE0 = ANGLE0 * DTR
 ANGLE1 = ANGLE1 * DTR
```

```
      ANGLE2 = ANGLE2 * DTR
      ANGLE3 = ANGLE3 * DTR
      ANGLE4 = ANGLE4 * DTR
      ANGLE5 = ANGLE5 * DTR
C FIRST,
C DEFINE A VECTOR FROM THE CENTER OF THE PROSTHESIS HEAD TO THE POINT
C IN QUESTION IN "PROSTHESIS" COORDINATES.
C  (LET THETA = 0 DEFINE THE X-DIRECTION AND THETA = 90
C  DEFINE THE Y-DIRECTION.)
      VECT(1) = SIN(PHI) * COS(THETA)
      VECT(2) = SIN(PHI) * SIN(THETA)
      VECT(3) = - COS(PHI)
C NEXT,
C TRANSFORM THE VECTOR INTO "STEM" COORDINATES
C BY USING THE ANGLE ANGLE0.
C  (LET THE VECTOR POINTING PROXIMALLY UP THE STEM DEFINE
C  THE Y-DIRECTION AND KEEP THE SAME X-DIRECTION)
      TEMP1 = VECT(1)
      TEMP2 = VECT(2)*SIN(ANGLE0) - VECT(3)*COS(ANGLE0)
      TEMP3 = VECT(2)*COS(ANGLE0) + VECT(3)*SIN(ANGLE0)
      VECT(1) = TEMP1
      VECT(2) = TEMP2
      VECT(3) = TEMP3
C NEXT,
C TRANSFORM THE VECTOR INTO "FEMUR" COORDINATES BY USING
C THE ANGLES ANGLE1, ANGLE2, AND ANGLE3.
C  (LET THE LOCAL LATERAL DIRECTION DEFINE THE Z-DIRECTION
C  AND LOCAL ANTERIOR DEFINE THE X-DIRECTION)
      DENOM = SQRT(1.0 + TAN(ANGLE3)**2 + TAN(ANGLE1)**2 )
      R(2,2) = 1.0 / DENOM
      IF (ANGLE3.GT.PI/2.0) R(2,2) = -R(2,2)
      R(2,1) = -TAN(ANGLE3)*R(2,2)
      R(2,3) = TAN(ANGLE1)*R(2,2)
      DENOM=( ( R(2,3)-R(2,1)*TAN(ANGLE2) ) / R(2,2) )**2
      DENOM=SQRT( 1.0 + TAN(ANGLE2)**2 + DENOM )
      R(3,3) = 1.0 / DENOM
      R(3,1) = -TAN(ANGLE2)*R(3,3)
      R(3,2) = ( R(2,1)*TAN(ANGLE2)-R(2,3) ) * R(3,3)/R(2,2)
      R(1,1)=R(2,2)*R(3,3)-R(2,3)*R(3,2)
      R(1,2)=R(2,3)*R(3,1)-R(2,1)*R(3,3)
      R(1,3)=R(2,1)*R(3,2)-R(2,2)*R(3,1)
      TEMP1=R(1,1)*VECT(1)+R(2,1)*VECT(2)+R(3,1)*VECT(3)
      TEMP2=R(1,2)*VECT(1)+R(2,2)*VECT(2)+R(3,2)*VECT(3)
      TEMP3=R(1,3)*VECT(1)+R(2,3)*VECT(2)+R(3,3)*VECT(3)
      VECT(1)=-TEMP1
      VECT(2)= TEMP2
      VECT(3)=-TEMP3
C NEXT,
C TRANSFORM THE VECTOR INTO "PELVIS" COORDINATES BY USING
C THE ANGLES FLEX, ABD, AND EXTROT.
C  (LET THE GLOBAL LATERAL DIRECTION DEFINE THE Z-DIRECTION
C  AND GLOBAL ANTERIOR (I.E. WRT PELVIS) DEFINE THE X-DIRECTION)
      R(2,1) = SIN(FLEX)*COS(ABD)
      R(2,2) = COS(FLEX)*COS(ABD)
```

```
      R(2,3) = SIN(ABD)
      R(1,3) = SIN(EXTROT)*SQRT(1.0 - R(2,3)**2 )
      A5 = R(2,2)**2 + R(2,1)**2
      B5 = 2.0*R(1,3)*R(2,3)*R(2,1)
      C5 = -R(2,2)**2 + R(1,3)**2 * (R(2,2)**2+R(2,3)**2)
      TEMP = B5**2 - 4.0*A5*C5
      R11A = ( -B5 + SQRT(TEMP) )/(2.0*A5)
      R11B = ( -B5 - SQRT(TEMP) )/(2.0*A5)
      R(1,1) = R11A
      IF ( (R(1,1)**2+R(1,3)**2) .GT. 1.01 ) R(1,1) = R11B
      R(1,2) = -( R(1,3)*R(2,3) + R(1,1)*R(2,1) )/R(2,2)
      R(3,1) = R(1,2)*R(2,3) - R(2,2)*R(1,3)
      R(3,2) = R(1,3)*R(2,1) - R(2,3)*R(1,1)
      R(3,3) = R(1,1)*R(2,2) - R(2,1)*R(1,2)
      R33TMP = COS(EXTROT)*SQRT(1.0 - R(2,3)**2 )
      IF ( R33TMP*R(3,3) .GE. 0.0 ) GOTO 111
      R(1,1) = R11B
      R(1,2) = -( R(1,3)*R(2,3) + R(1,1)*R(2,1) )/R(2,2)
      R(3,1) = R(1,2)*R(2,3) - R(2,2)*R(1,3)
      R(3,2) = R(1,3)*R(2,1) - R(2,3)*R(1,1)
      R(3,3) = R(1,1)*R(2,2) - R(2,1)*R(1,2)
  111 TEMP1=R(1,1)*VECT(1)+R(2,1)*VECT(2)+R(3,1)*VECT(3)
      TEMP2=R(1,2)*VECT(1)+R(2,2)*VECT(2)+R(3,2)*VECT(3)
      TEMP3=R(1,3)*VECT(1)+R(2,3)*VECT(2)+R(3,3)*VECT(3)
      VECT(1)= -TEMP1
      VECT(2)=  TEMP2
      VECT(3)= -TEMP3
C FINALLY,
C TRANSFORM THE VECTOR INTO "ACETABULAR" COORDINATES BY USING
C THE ANGLES ANGLE4 AND ANGLE5.
C  (LET THE MEDIAL "HORIZONTAL" DIRECTION DEFINE THE X-DIRECTION
C  AND THE OUTWARD NORMAL DEFINE THE Z-DIRECTION)
      DENOM=SQRT( 1.0 + TAN(ANGLE4)**2 + TAN(ANGLE5)**2 )
      R(3,3)=1.0/DENOM
      R(3,1) = TAN(ANGLE4) * R(3,3)
      R(3,2) = -TAN(ANGLE5) * R(3,3)
      DENOM = SQRT( 1.0 + (R(3,3)/R(3,1))**2 )
      R(1,3) = - 1.0/DENOM
      R(1,2) = 0.0
      R(1,1) = -R(3,3)/R(3,1)*R(1,3)
      R(2,1)=R(3,2)*R(1,3)-R(3,3)*R(1,2)
      R(2,2)=R(3,3)*R(1,1)-R(3,1)*R(1,3)
      R(2,3)=R(3,1)*R(1,2)-R(3,2)*R(1,1)
      TEMP1=R(1,1)*VECT(1)+R(1,2)*VECT(2)+R(1,3)*VECT(3)
      TEMP2=R(2,1)*VECT(1)+R(2,2)*VECT(2)+R(2,3)*VECT(3)
      TEMP3=R(3,1)*VECT(1)+R(3,2)*VECT(2)+R(3,3)*VECT(3)
      VECT(1)=TEMP1
      VECT(2)=TEMP2
      VECT(3)=TEMP3
C NOW, CONVERT THE FINAL UNIT VECTOR INTO ACETABULAR ANGLES
C  THETAR AND PHIR.
      THETAR = ATAN2( VECT(2),VECT(1) )
      PHIR = ACOS( -1.0 * VECT(3) )
      THETA = THETA * RTD
```

```
PHI = PHI * RTD
FLEX = FLEX * RTD
ABD = ABD * RTD
EXTROT = EXTROT * RTD
THETAR = THETAR * RTD
PHIR = PHIR * RTD
RETURN
END
```

REFERENCES

1. Ahmed, A.H., D.L. Burke, A. Tencer, and J.W. Stachiewicz, "A method for the in vitro measurement of pressure distribution at articular interfaces in synovial joints", Trans. 23rd Orthop. Res. Soc., Las Vegas, 1977

2. Anacona, M.G., W.M. Lai, and V.C. Mow,"Visualization of the Fluid Film Formation at the Acetabular Surface", 25th Annual ORS, San Francisco, Ca. Feb. 1979

3. Antonsson, E.K., A Three-Dimensional Kinematic Acquisition and Intersegmental Dynamic Analysis System for Human Motion, Ph.D. Thesis, M.I.T., 1982.

4. Antonsson, E.K. and R.W. Mann,"Frequency Content of Gait", J. Biomech. Vol. 18, No. 1, 1985

5. Armstrong, C.G., "Ageing Human Articular Cartilage: A Biomechanical Study of the Human Hip Joint", Ph.D. thesis, The Queen's University of Belfast, May 1977

6. Armstrong, C.G., A.S. Bahrani, and D.L. Gardner,"In Vitro Measurement of Articular Cartilage Deformations in the Intact Human Hip Joint under Load", JBJS Vol. 61-A, No. 5, July 1979

7. Barnett, C.H., D.V. Davies, and M.A. MacConaill, Synovial Joints: Their Structure and Mechanics, C.H. Thomas, Springfield, IL, 1961

8. Beckwith, Buck, and Marangoni, Mechanical Measurements, 3rd ed., Addison-Wesley, Reading, MA., 1982

9. Bennett, A. and G.R. Higginson, "Hydrodynamic Lubrication of Soft Solids", Journal of Mechanical Engineering Sciences, Vol. 12, 3, 1970

10. Bergmann, G., J. Siraky, R. Kolbel, and A. Rohlmann, "Measurement of Joint Forces with Implants, A new Method of Instrumentation and its Application in Sheep"

11. Bergmann, G., J. Siraky, R. Kolbel, and A. Rohlmann, "A Comparison of Joint Forces in Sheep, Dog, and Man", J. Biomechanics, Vol 17, No 12, 1984

12. Berme, N. and J.P. Paul, "Load Actions Transmitted by Implants", J. Biomedical Engineering, Vol 1, Oct. 1979

13. Bert, J.L., and I. Fatt, "Water Transport in Cartilage-A Comparitive Study", Life Sciences, Vol. 8, Part I, pp 343-346, 1969

14. Blount, W.P., "Don't throw away the cane", JBJS, 38 A(3): 695-708, 1956

15. Bourne, R.B., Landesberg, R.P., J.B. Finlay, and P. Andreage,"In Vitro Acetabular Strain-Patterns Following Endoprosthetic Femoral Head Replacement", Proc. of 30th Annual ORS, Atlanta Georgia, 1984

16. Brinckmann, P., W. Frobin, and E. Heirholzer,"Stress on the Articular Surface of the Hip Joint in Healthy Adults and Persons with Idiopathic Osteoarthritis of the Hip Joint", J. Biomechanics, Vol 14, no. 3, 1981

17. Brown, T.D., and A.B. Ferguson Jr.,"The Effects of Hip Contact Aberrations on Stress Patterns within the Human Femoral Head", Annals of Bio. Eng., Vol. 8, 1980

18. Brown, T.D., and A.M. DiGioma III, "A Contact-Coupled Finite Element Analysis of the Natural Adult Hip", J. Biomechanics, Vol. 17, 6, 1984, pp 437-448

19. Bullough, P., J. Goodfellow, A.S. Greenwald, and J. O'Connor,"Incongruent Surfaces in the Human Hip Joint", Nature, Vol 217, March 30 1968

20. Bullough, P., J. Goodfellow, "The Relationship between Degenerative Changes and Load-Bearing in the Human Hip", JBJS, Vol. 55:B, No. 4, Nov. 1973

21. Carlson, C.E.,"An Instrumented Prosthesis for Measuring the Cartilage Surface Pressure Distribution in the Human Hip", M.I.T., Sc. D Thesis, June 1972

22. Carlson, C.E., R.W. Mann, and W.H. Harris,"A Radio Telemetry Device for Monitoring Cartilage Surface Pressures in the Human Hip", IEEE Trans. on Biomedical Eng., Vol. BME-21, No. 4, July 1974

23. Cathcart, R.F.,"The shape of the femoral head and preliminary results of clinical use of a non-spherical hip prosthesis", JBJS, 53a(2):397, 1971

24. Cathcart, R.F., "The shape of the normal femoral head and results from clinical use of more normally shaped non-spherical hip replacement prostheses", Orthop. Rev. 2(3):15-22, 1972

25. Charnley, J., "The lubrication of animal joints",Symposium on Biomechanics, I.M.Eng, London, 12-22, 1959

26. Christel, P., P. Derethe, and L. Sedel,"Peri-Acetabular Pressure Recording, Using A Hip Simulator", Acta Orthop. Belg. 42 (Suppl. 1), 1976

27. Crandall, S.H., D.C. Karnopp, E.F. Kurtz, Jr., and D.C. Pridmore-Brown, Dynamics of Mechanical and Electromechanical Systems, Robert E. Krieger Publishing Co., Malabar, FL, 1982

28. Crowninshield R.D., R.C. Johnston, J.G. Andrews, and R.A. Brand. "A Biomechanical Investigation of the Human Hip", J.Biomechanics, Vol 11, 1978, pp 75-85

29. Day, W.H., S.A.V.Swanson, and M.A.R.Freeman,"Contact Pressures in the Loaded Human Cadaver Hip", J.B.J.S. , Vol. 57-B, No. 3, August 1975

30. Dowson. D. and W. Wright, "Introduction to the Biomechanics of Joints and Joint Replacements", Mechanical Eng. Publications LTD, London, 1981

31. Fijan, R.S., Calibration of the In Vivo Prosthesis, Lab memo, 1983

32. Fijan, R.S.,"Joint Axes of Rotation for the Lower Extremity", M.I.T., M.S. Thesis, Feb. 1985

33. Fijan, R.S.,W.A. Hodge, W.H. Harris, and R.W. Mann, "A Clinically Useful Three-Dimensional Dynamic Display for Human Gait Kinematics", 32nd ORS, poster session, New Orleans, Louisiana, Jan. 1986

34. Finlay J.B., R.B. Bourne, R.P. Landesberg, and P. Andreage,"Pelvic Stresses In Vitro, Part I, Malsizing of Endoprostheses", Orth. Res. Lab, Univ. of Western Ontario, London, Ontario, Canada,Oct. 1984

35. Finlay J.B., R.B. Bourne, R.P. Landesberg, and P. Andreage,"Pelvic Stresses In Vitro, Part II, A Study of the Efficiacy of Metal-Backed Acetabular Prostheses", Orth. Res. Lab, Univ. of Western Ontario, London, Ontario, Canada, Oct. 1984

36. Freeman, M.A.R. in Adult Articular Cartilage, 2nd ed., Pitman Med. Pub., Kent, England, 1979

37. Goel V.,K., and N.,L. Svensson, "Forces on the Pelvis", Journal of Biomechanics, Vol. 10, 1977, pp. 195-200

38. Gofton, J.P., "Studies in Osteoarthritis of the Hip", Canadian Medical Assoc. Journal, Vol. 104, 8, April 1971

39. Gore, T.A., G.R. Higginson, and R.E. Kornberg, "Some Evidence of Squeeze-Film Lubrication in Hip Prostheses", Engineering in Medicine, MEP Ltd., Vol 10, No. 2, 1981

40. Greenwald A.S., and O'Connor J.J., "The Transmission of Load through the Human Hip Joint", J. Biomechanics Vol. 4, 1971

41. Greenwald, A.S., and D.W. Haynes, "Weight-Bearing Areas in the Human Hip Joint", JBJS, Vol. 54B, 1, Feb. 1972

42. Greenwald, A.S., "Joint Congruence-a Dynamic Concept", Hip Society Proceedings, 1974

43. Greenwald, A.S, C.L. Nelson,"Relationship of Degenerative Arthritis to Weight-Bearing Areas in the Human Hip Joint",Surgical Forum, Orthopedic Surgery

44. Halcomb, F.J., "Pressure Distribution on the Human Hip Joint In Vivo and Selection of Hemiarthroplasty", M.I.T. M.S. thesis, Aug. 1980

45. Hammond, B.T., and J. Charnley,"The Sphericity if the Femoral Head", Med. and Bio. Engng., Vol 5, 1967

46. Hardt, D.E.,"Determining Muscle Fores in the Leg During Normal Human Walking - An Application and Evaluation of Optimization Methods", Transactions of A.S.M.E., Vol. 100, May 1978

47. Harrigan, T.P.,"Bone Compliance and its Effects in Human Hip Joint Lubrication", M.I.T. Sc.D thesis, June 1985

48. Harris, W.H., P.D. Rushfeldt, C.E. Carlson, J.Scholler, and R.W. Mann, "Pressure Distribution in the hip and selection of hemiarthroplasty", Proceedings of the Third Annual Open Scientific Meeting of the Hip Society, San Franscisco, 1975

49. Harrison M.H.M., F. Schajowicz, and J. Trueta,"Osteoarthritis of the Hip: A Study of the Nature and Evolution of the Disease", JBJS Vol. 35-B, No. 4, Nov. 1953

50. Hayes, W.C., "Abnormal Joint Biomechanics in Osteoarthritis", Human Joints in Disease, Ch. 17

51. Hayes, W.C. and L.E. Mockros,"Viscoelastic properties of Human Acetabular Cartilage",Journal of Applied Physiology, Vol.31, 4, Oct. 1971

52. Higginson, G.R. and R. Norman, "The Lubrication of Porous Elastic Solis with Reference to the Functioning of Human Joints", J. M. Eng. Sci. Vol. 16, No. 4, 1974

53. Higginson, G.R. and R. Norman, "A Model Investigation of Squeeze-film Lubrication in Animal Joints", Phys. Med. Biol., Vol 19, No. 6, 1974

54. Higginson, G.R., "Elastohydrodynamic Lubrication in Human Joints",

Proc. I.M.E. Vol. 191, 1977

55. Inman, V.T., "Functional aspects of the abductor muscles of the hip", J.B.J.S. 29A(3), 1947

56. Kempson, G.E., M.A.R. Freeman, and S.A.V. Swanson. "The determination of a creep modulus for articular cartilage from indentation tests on the human femoral head", J. Biomech. 4(4):239-50, 1971

57. Kempson, G.E., "Mechanical properties of articular cartilage", Adult Articular Cartilage, M.A.R. Freeman (ed.) 333-414, 1979

58. Kenyon, D.E. "A model for surface flow in cartilage", J Biomech. 13(2), 1980

59. Kilvington, M., and R.M.F. Goodman,"In vivo hip joint forces recorded on a strain gauged 'English' prosthesis using an implanted transmitter", M.E.P. Vol 10, No. 4, 1981

60. Linn, F.C. and L. Sokoloff, "Movement and Composition of Interstitial Fluid in Cartilage Joints", Arth. Rheum. 8(4), 1965

61. Linn, F.C., "Lubrication of Animal Joints", Journal of Lubrication Technology, April 1969, p329-339

62. Longfield, M.D.,D. Dowson, P.S. Walker, and V. Wright,"Boosted Lubrication of Human Joints by Fluid Enrichment and Entrapment", Bio-medical Engineering, Nov. 1969

63. Macirowski, T., Stress in the Cartilage of the Human Hip Joint, Sc.D. thesis, M.I.T., Feb. 1983

64. Mankin, H.J., and L. Lippiello. "The turnover of adult rabbit articular cartilage", J.B.J.S. 51A(8): 1591-1600, 1969

65. Mann, R.W., "The M.I.T.-M.G.H. Endoprosthesis for measuring the Pressure Distribution on Acetabular Cartilage in Life", N.I.H. Workshop on Instrumented Prostheses for In Vivo measurement of Joint Mechanics, Sept. 16, 1981

66. Maroudas, A., "Distribution and diffusion of solutes in articular cartilage", Biophys. J., 10(5):365-79, 1970

67. Maroudas, A., "Physicochemical properties of articular cartilage", Adult Articular Cartilage, M.A.R. Freeman (ed.) 215-90, 1979

68. McCall J.G.,"Stereoscan Studies on Load Deformantion in Articular Cartilage", 8th ICMBE, Chicago, Ill. 1969

69. McConaill, M.A., "The Movements of Bones and Joints - Mechanical Structure of Articulating Cartilage", J.B.J.S., Vol 33 B, 2, May 1951.

70. McCutcheon, C.W., "Mechanisms of animal joints:sponge-hydrostatic and weeping bearings", Nature 184:1284-5, 1959

71. McCutcheon, C.W., "The Frictional Properties of Animal Joints", Wear 5, 1962

72. McCutcheon, C.W.,"Cartilage is Poroelastic, not Viscoelastic.....", J. Biomechanics, Vol. 15, No. 4, 1982

73. McMurray, T.P.,"Osteoarthritis of the Hip Joint",British Journal of Surgery, Vol XXII, 88, 1935, pp 716-727

74. Meachim, G. and R.A. Stockwell, "The matrix", Adult Articular Cartilage, M.A.R. Freeman (ed.), 1979

75. Patriarco,A.G., R.W. Mann, S.R. Simon, and J.M. Mansour,"An Evaluation of the Approaches of Optimization Models in the Prediction of Muscle Forces during Human Gait", J. Biomech., Vol. 14, no. 8, 1981

76. Paul, J.P., "The Patterns of Hip Joint Force during Walking", Dig. of 7th Intl. Conf. on Med. and Biological Eng., Stockholm, 1967

77. Paul, J.P., "Forces Transmitted by Joints in the Human Body", Proceedings, Institute of Mechanical Engineering, Vol 181, 8 1967

78. Paul J.P., "Approaches to Design", Proceedings Royal Society of London, Britian, Vol. 192, 1976, pp. 163-172

79. Pauwels, F., Biomechanics of the Normal and Diseased Hip, 1975

80. Radin, E.L., D.A. Swann, and P.A. Weisser, "Separation of a Hyaluronate- free Lubrication Fraction from Synovial Fluid", Nature, 228:337-378, 1970

81. Radin,E.L., I.L. Paul, and M. Lowy, "A Comparison of the Dynamic Force Transmitting Properties of Subchondral Bone and Articular Cartilage", JBJS, Vol. 52-A, 3, April 1970

82. Radin, E.L., and I.L. Paul, "A Consolidated Concept of Joint Lubrication", J.B.J.S., Vol 54-A, 3, April 1972

83. Radin, E.L., I.L. Paul, and R.M. Rose,"Role of Mechanicl Factors in the Pathogenesis of Primary Osteoarthritis", The Lancet, March 4, 1972

84. Radin, E.L., M.G.Ehrlich, R.S.Chernack, I.L.Paul, and R.M. Rose,"Effect of Repetitive Impulse Loading on the Metabolism of Rabbit Articular Cartilage and its Relationship to Bone Stiffness", Proceedings 23rd O.R.S., Las Vegas, Nev., Feb. 1977

85. Rosenberg, L., "Structure of Cartilage Proteoglycans", Human Joints in Health, W.H. Simon (ed.), 1978

86. Rushfeldt, P.D.,"Human Hip Joint Geometry and the Resulting Pressure Distributions", M.I.T. Sc.D. thesis, April, 1978

87. Rushfeldt, P.D., R.W. Mann, and W.H. Harris, "Improved Techniques for Measuring In Vitro the Geometry and Pressure Distribution in the Human Acetabulum - II. Instrumented Endoprosthesis Measurement of Articular Surface Pressure Distribution", J. Biomechanics, Vol. 14, No. 5, 1981

88. Rushfeldt, P.D., R.W. Mann, and W.H. Harris, "Pressure Contours over the Human Acetabulum", Biosigma conference proceedings, April 1978

89. Rushfeldt, P.D., R.W. Mann, and W.H. Harris, "Influence of Cartilage Geometry on the Pressure Distribution in the Human Hip Joint", Science April 27, 1979

90. Rydell, N.W., Forces Acting on the Femoral-Head Prosthesis, 1966

91. Sanjeevi, R., "A Viscoelastic Model for the Mechanical Properties of Biological Materials", J. Biomechanics, Vol. 15, No. 2, 1982

92. Sedel, L.,P. Cristel, and P. Derethe, "Pressure Transmission through the Acetabulum Using an Animated Cadaver Pelvis", 25th O.R. S., Feb 20-22, 1979

93. Seireg A., and R.J. Arvikar, "The Prediction of Muscular Load Sharing and Joint Forces in the Lower Extremities During Walking", Journal of Biomechanics, Vol. 8, 1975, pp.89-102

94. Simon, S.R., E.L. Radin, I.L.Paul, and R.M. Rose,"The Response of Joints to Impact Loading: I. In Vivo Behavior of Subchondral Bone", 1972, J. Biomech. 5(3):267-72

95. Simon, S.R., E.L. Radin, and I.L.Paul,"The Response of Joints to Impact Loading: II. In Vivo Wear",1972, J. Biomech.

96. Sokoloff, L., The Biology of Degenerative Joint Diseases, 1969, University of Chicago Press, Chicago

97. Sokoloff, L., "The pathology and pathogenesis of osteoarthritis". Arthritis and Allied Cond.: a textbook of Rheumatology,1979

98. Tanner, R.I., "An alternative mechanism for lubrication of synovial joints", Phys. Med. Biol. 11:119-27, 1966

99. Tepic, S., Congruency in the Human Hip Joint, M.S. Thesis, M.I.T. 1980

100. Tepic, S., R.W. Mann, and W.H. Harris, "Ultrasonic Measurement of Femoral Head Geometry", 27th O.R.S., 1980

101. Trueta, J., "Studies on the Etiopathy of Osteoarthritis of the Hip", Joint Cartilage, Ch. 2, 1963

102. Vasu, R., D.R. Carter, and W.H. Harris,"Stress Distribution in the Acetabular Region - I. Before and After Total Joint Replacement", J. Biomechanics, Vol. 15, No. 3, 1982

103. Williams, J.F. and N.L. Svensson. "A force analysis of the hip joint", Biomed. Engr. 3(8): 365-70, 1968

104. Zarek, J.M.,and J. Edwards,"The Stress-Structure Relationship in Articular Cartilage", Med. Electron. Biol. Eng. , Vol 1,1963

105. Zarek, J.M.,and J. Edwards,"Dynamic Considerations of the Human Skeletal System", Symposium on Biomechanics and Related Bio-Eng. Topics, Univ. of Strathclyde, Pergamon Press, Oxford, 1964

106. Carvajal, T., "In Vivo Pressure Distribution Data in the Human Hip Joint", M.I.T., M.S. thesis, Feb. 1985

107. English, T.A., and M. Kilvington, "In vivo records of hip loads using a femoral implant with telemetric output (a preliminary report)", J. Biomed. Eng., 1(2):111-5, 1979

108. Hodge, W.A.,R.S. Fijan,K.L. Carlson,R.G. Burgess,W.H. Harris, and R.W. Mann, "In vivo measurement of Human Hip Joint Contact Pressures", June 1985, in press.

109. Tepic, S.,"Dynamics and Entropy Production in the Cartilage Layers of the Synovial Joint", M.I.T., Sc.D. thesis, May 1982

110. Weightman, B., "Tensile Fatigue of Human Articular Cartilage", J. Biomech., 9(4): 193-200, 1976

111. Brown, R.H., A.H. Burstein, and V.H. Frankel,"Telemetering in vivo loads from nail plate implants", J. Biomech., Vol. 15, no. 11, 1982

112. Stearns, S.D., Digital Signal Analysis, Hayden Book Co. Inc., New Rochelle, N.J., 1975